

# POLITECNICO DI TORINO

Corso di Laurea Magistrale  
in Ingegneria Civile

Master Thesis

## **Energy tunnels: recommendations for investigation and parameter assessing**



### **Supervisors**

Prof. Ing. Marco Barla  
Ing. Alessandra Insana  
Politecnico di Torino

### **External Supervisor**

Ing. Iulia Prodan  
Technical University of Cluj-Napoca

**Candidate**

Sofia Cairo

April 2019



*To my family*



# TABLE OF CONTENTS

|  |             |
|--|-------------|
| <b>LIST OF FIGURES .....</b>                                     | <b>V</b>    |
| <b>LIST OF TABLES .....</b>                                      | <b>XIII</b> |
| <b>INTRODUCTION.....</b>   | <b>XV</b>   |
| <b>INTRODUZIONE.....</b>   | <b>XIX</b>  |
| <b>1 GEOTHERMAL ENERGY .....</b>                                 | <b>1</b>    |
| <b>1.1 Classification of geothermal energy.....</b>              | <b>4</b>    |
| 1.1.1 Low enthalpy geothermal resources.....                     | 4           |
| <b>1.2 Ground Source Heat Pumps (GSHP).....</b>                  | <b>6</b>    |
| 1.2.1 Classification of GSHP systems.....                        | 7           |
| 1.2.1.1 Open loop systems .....                                  | 8           |
| 1.2.1.2 Closed loop systems .....                                | 8           |
| <b>1.3 Energy geostructures .....</b>                            | <b>10</b>   |
| 1.3.1 Energy tunnels.....  | 14          |
| 1.3.1.1 Technologies .....                                       | 15          |
| 1.3.1.2 Examples of application .....                            | 18          |
| <b>1.4 Sustainability .....</b>                                  | <b>29</b>   |
| <b>2 INVESTIGATION AND PARAMETERS ASSESSING.....</b>             | <b>31</b>   |
| <b>2.1 Geotechnical investigation and parameters.....</b>        | <b>33</b>   |
| 2.1.1 Geotechnical investigation .....                           | 33          |
| 2.1.2 Geotechnical parameters .....                              | 35          |
| 2.1.2.1 Outcomes.....  | 39          |
| 2.1.3 THM behaviour of soils .....                               | 40          |
| 2.1.3.1 THM investigation .....                                  | 42          |
| 2.1.3.2 Influence of temperature on geotechnical parameters..... | 45          |

|            |   |           |
|------------|---|-----------|
| 2.1.3.3    | Outcomes.....                                       | 53        |
| <b>2.2</b> | <b>Thermal investigation and parameters .....</b>   | <b>54</b> |
| 2.2.1      | Thermal parameters.....                             | 54        |
| 2.2.2      | Thermal investigation.....                          | 56        |
| 2.2.2.1    | Laboratory tests .....                              | 56        |
| 2.2.2.2    | In situ tests.....                                  | 59        |
| 2.2.3      | Outcomes.....                                       | 64        |
| 2.2.4      | Future for thermal investigation in situ: TCT ..... | 66        |
| <b>3</b>   | <b>ENERGY TUNNELS DESIGN PROCESS .....</b>          | <b>71</b> |
| <b>3.1</b> | <b>Tunnel design aspects.....</b>                   | <b>74</b> |
| 3.1.1      | Structure .....                                     | 75        |
| 3.1.1.1    | Shape of the tunnel.....                            | 75        |
| 3.1.1.2    | Vertical loads.....                                 | 75        |
| 3.1.1.3    | Convergence-confined method .....                   | 77        |
| 3.1.1.4    | Tunnels technologies in soils .....                 | 79        |
| 3.1.1.5    | Key parameters – structure.....                     | 85        |
| 3.1.2      | Ground.....   | 86        |
| 3.1.2.1    | Stability conditions.....                           | 86        |
| 3.1.2.2    | Surface settlement trough.....                      | 88        |
| 3.1.2.3    | Key parameters – ground .....                       | 90        |
| 3.1.3      | Soil-structure interaction .....                    | 91        |
| 3.1.3.1    | Key parameters – soil-structure interaction .....   | 92        |
| 3.1.4      | Numerical simulations.....                          | 93        |
| 3.1.4.1    | The model.....                                      | 93        |
| 3.1.4.2    | Constitutive laws .....                             | 95        |

|            |   |            |
|------------|---|------------|
| 3.1.4.3    | Soil-structure interaction in a FE model .....                | 96         |
| <b>3.2</b> | <b>Thermal design of tunnels .....</b>                        | <b>98</b>  |
| 3.2.1      | Analytical models.....  | 99         |
| 3.2.2      | TH design .....   | 101        |
| 3.2.2.1    | Quantification of heat transfer.....                          | 102        |
| 3.2.3      | Key parameters – efficiency of the system .....               | 106        |
| <b>3.3</b> | <b>Structural design of a segmental lining.....</b>           | <b>107</b> |
| 3.3.1      | Features of segments .....                                    | 107        |
| 3.3.1.1    | Materials.....  | 107        |
| 3.3.1.2    | Geometry.....   | 107        |
| 3.3.1.3    | Connections.....  | 109        |
| 3.3.1.4    | Sealing.....  | 109        |
| 3.3.1.5    | Legal framework .....   | 109        |
| 3.3.1.6    | Design process.....   | 110        |
| 3.3.2      | TM design .....   | 112        |
| 3.3.2.1    | Background experience .....                                   | 113        |
| 3.3.2.2    | Energy tunnels.....   | 118        |
| 3.3.3      | Key parameters – TM design of segments .....                  | 119        |
| <b>3.4</b> | <b>Outcomes.....</b>  | <b>120</b> |
| <b>4</b>   | <b>NUMERICAL ASSESSMENT OF THE ROLE OF THERMAL PARAMETERS</b> | <b>123</b> |
| <b>4.1</b> | <b>Introduction .....</b>                                     | <b>123</b> |
| <b>4.2</b> | <b>FLAC – Fast Lagrangian Analysis of Continua .....</b>      | <b>124</b> |
| 4.2.1      | General information .....                                     | 124        |
| 4.2.2      | Finite Difference Method .....                                | 125        |
| 4.2.3      | Thermo-Mechanical governing equations.....                    | 126        |

|            |   |            |
|------------|---|------------|
| 4.2.3.1    | Conduction .....                          | 126        |
| <b>4.3</b> | <b>The numerical model .....</b>          | <b>130</b> |
| 4.3.1      | Geometry .....                            | 130        |
| 4.3.2      | Phase 1: Tunnel construction .....        | 133        |
| 4.3.2.1    | Material properties .....                 | 133        |
| 4.3.2.2    | Initial and boundary conditions .....     | 134        |
| 4.3.2.3    | Solving .....                             | 135        |
| 4.3.2.4    | Model validation .....                    | 139        |
| 4.3.2.5    | Surface settlements .....                 | 140        |
| 4.3.3      | Phase 2: Thermo-Mechanical analysis ..... | 143        |
| 4.3.3.1    | Material properties .....                 | 144        |
| 4.3.3.2    | Initial and boundary conditions .....     | 144        |
| 4.3.3.3    | Solving .....                             | 149        |
| 4.3.3.4    | Parametric analysis – results .....       | 153        |
| <b>5</b>   | <b>CONCLUSIONS.....</b>                   | <b>179</b> |
|            | <i>Acknowledgements</i> .....             | <b>183</b> |
|            | <i>Ringraziamenti</i> .....               | <b>185</b> |
|            | <b>REFERENCES .....</b>                   | <b>187</b> |

# LIST OF FIGURES

|  |    |
|--|----|
| Figure 1.1. Structure of the Earth, showing the percentage of heat derived from the core, mantle and crust, compared with their volume. (Banks, 2012).....   | 2  |
| Figure 1.2. Example of the trend of temperature in the ground (Martin et al., 2010) .....  | 5  |
| Figure 1.3. An example of a GSHP system (Banks, 2012) .....  | 7  |
| Figure 1.4. Scheme of shallow geothermal systems that are closed (a) and open (b). (Hecht-Méndez et al., 2009).....  | 7  |
| Figure 1.5. Different configurations for GSHP systems. (a) Open loop GSHP with a-heat exchanger, b-abstraction well, c-injection ..... well. (b) Closed loop GSHP, vertical. (c) Closed loop GSHP, horizontal. (d) Closed loop GSHP, basket system. (Manzella, 2017) ..... | 9  |
| Figure 1.6. Scheme of heat flux balance for heating in an energy piles plant (Brandl, 2006) .....  | 11 |
| Figure 1.7. Examples of energy geostructures. a) Energy pile (Olgun et al., 2015) b) Energy wall (Kovačević et al., 2013).....   | 11 |
| Figure 1.8. Number of energy piles installed in Austria; since 2005 more than 7000 energy piles per year (Brandl, 2016).....   | 12 |
| Figure 1.9. Energy geotextile installed in an energy tunnel - conventional tunnelling method – Lainzer Tunnel Vienna (Adam & Markiewicz, 2009).....  | 15 |
| Figure 1.10. Energy tunnel with precast segments – mechanized tunnelling method (Barla & Perino, 2014).....  | 16 |
| Figure 1.11. 3D-CAD view of one energy lining segments with absorber pipes and reinforcement cage – Jenbach tunnel, Austria (Frodl, Franzius & Bartl, 2010).....   | 16 |
| Figure 1.12. Configurations of the ENERTUN segmental lining: a) ground&air, b) ground, c) air. (Barla and Di Donna, 2018).....   | 17 |
| Figure 1.13. Cross-section LT24, one side wall of cut and cover tunnel used as energy wall (Brandl, 2016).....   | 20 |
| Figure 1.14. Longitudinal section through the energy tunnel wall. The pile S-07-20 is a thermo-activated pile with also measurement devices (Brandl, 2016).....  | 20 |
| Figure 1.15. Energy membrane in a NATM excavated tunnel (Brandl, 2016) .....   | 22 |
| Figure 1.16 CAD view of the energy system (Frodl et al., 2010) .....   | 22 |

|  |    |
|--|----|
| Figure 1.17. Layout of demonstrator project in Jenbach, Austria (Franzius and Pralle, 2011).....   | 23 |
| Figure 1.18. Torino Metro Line 1 layout with highlighted South Extension (Barla, Insana, 2018).....  | 25 |
| Figure 1.19. Experimental site location (Barla and Insana,2018) .....  | 27 |
| Figure 2.1. Mohr-Coulomb strength envelop, cohesion and friction angle are represented (Basic mechanics of soils, 2000) .....  | 36 |
| Figure 2.2. Mohr-Coulomb strength envelope for undrained conditions, it is horizontal. ....  | 36 |
| Figure 2.3. Simple representation of the coefficient of earth pressure at rest .....   | 36 |
| Figure 2.4. Coefficient of Earth Pressure at rest, real data from Hoek & Brown (1978) and recent integrations (Barla, 2011) .....  | 38 |
| Figure 2.5. Different dilatant behaviour of dense and loose soils .....  | 38 |
| Figure 2.6. Schematic representation of relevant couplings in SGE system .....   | 41 |
| Figure 2.7. Heat transfer processes in soils (Vieria et al., 2017).....  | 41 |
| Figure 2.8. Triaxial device with controlled temperature (Cekerevac, 2003).....   | 43 |
| Figure 2.9. Direct shear apparatus with temperature control system (Vieira et al., 2017) .....   | 43 |
| Figure 2.10. Oedometer with vapour equilibrium technique: vertical load and temperature application system (EPFL website).....   | 44 |
| Figure 2.11. Results from a temperature-controlled TX test. Volumetric strain (a) and pore pressure change (b) in undrained conditions for saturated illite under a constant total stress of 200 kPa as a function of temperature. (Vieria et al., 2017) ..... | 47 |
| Figure 2.12. Thermal deformation of Boom clay under different initial conditions (data from Laloui & Di Donna, 2013) .....   | 48 |
| Figure 2.13. Influence of temperature on preconsolidation pressure (Laloui & Di Donna, 2013).....  | 49 |
| Figure 2.14. Shear strength at difference constant temperature of OC and NC clays (data from Laloui & Di Donna, 2013) .....  | 49 |
| Figure 2.15. Thermal cyclic effect on an illite (Laloui & Di Donna, 2013).....   | 50 |
| Figure 2.16. Thermal cyclic effects on a) consolidation of NC Bangkok Clay and b) undrained shear resistance of NC Tody clay (Laloui and Di Donna, 2013) .....   | 51 |
| Figure 2.17. Sand-concrete interface tests at 20°C and 60°C (Di Donna et al., 2015).....   | 51 |

|  |    |
|--|----|
| Figure 2.18. Schematic representation of a laboratory test run with the absolute technique - steady state method (Vieira et al., 2017).....  | 56 |
| Figure 2.19. Schematic representation of a laboratory test run with the comparative technique - steady state method (Vieira et al., 2017).....   | 57 |
| Figure 2.20. Principle of optical scanning method. V: velocity of scanning; O: area of the heat spot; S: detection area of the radiometer; A, B, C: main axes of thermal conductivity with angles $\alpha$ , $\beta$ , $\gamma$ to the line of scanning, respectively. (Vieira et al., 2017) ..... | 59 |
| Figure 2.21. Schematic figure of a TRT rig (Vieira, Prodan et al., 2017).....  | 60 |
| Figure 2.22. Example of output from a TRT, linear time scale (Banks, 2012).....  | 61 |
| Figure 2.23. Average ground thermal conductivity by TRT, DTRT and ETRT (Vieira et al., 2017)...  | 63 |
| Figure 2.24. Some schematic representations of CPT with different sensors: a) piezometric cone, b) seismic cone and c) thermal cone. ....  | 67 |
| Figure 2.25. Cone temperature increase against con friction (Akrouch et al., 2016).....  | 68 |
| Figure 3.1. Overview on the integrated design of an energy tunnel.....   | 73 |
| Figure 3.2. Tunnel design aspects- reference to the chapters in which they are discussed. ....   | 74 |
| Figure 3.3. Schematic representation of the shape of tunnels: circular, ovoid, vertical ovoid and horseshoe .....  | 75 |
| Figure 3.4. Terzaghi's (a) and Protodiaconov's(b) methods for vertical loads (Moldovan, 2013) .....  | 76 |
| Figure 3.5. Convergence-confinement curves for a) elastic behaviour and b) elasto-plastic behaviour (Panet, 1982).....   | 77 |
| Figure 3.6. Convergence confinement curve of soil and support (Panet, 1982) .....  | 79 |
| Figure 3.7. Some of the possible excavation sequences (Steffan, 2017).....   | 80 |
| Figure 3.8. Cross sectional diagram of an Earth Pressure Balance (EPB) TBM (herrenknecht.com) ..   | 83 |
| Figure 3.9. Suggested ranges for conditioning soils for EPB machines. (Peila, Tunneling Classes 2017) .....  | 85 |
| Figure 3.10. Example of 2D numerical model along a longitudinal section (Guglielminetti, 2008) ....  | 86 |
| Figure 3.11. Surface, crown and face displacements for different N values (Cesarin & Mair, 1981) ..  | 88 |
| Figure 3.12. Transverse settlement trough .....  | 89 |

|  |     |
|--|-----|
| Figure 3.13. Soil-structure interface in FEM: a) continuum interface, b) springs, c) zero thickness element.....   | 97  |
| Figure 3.14. Thermal design for an energy tunnel .....   | 98  |
| Figure 3.15. Effects of undisturbed ground temperature on the exchanged heat in a) winter and b) summer. (Di Donna & Barla, 2015) .....  | 103 |
| Figure 3.16. Effects of the groundwater rate on the exchanged heat in a) winter and b) summer (Di Donna & Barla, 2015) .....   | 104 |
| Figure 3.17. Effects of the thermal conductivity on the exchanged heat in a) winter and b) summer (Di Donna & Barla, 2015) .....   | 104 |
| Figure 3.18. Design charts for the heat exchange (extracted and injected heat in $W/m^2$ ), function of the groundwater flow, the ground temperature and the thermal conductivity. (Di Donna & Barla, 2015)..... | 105 |
| Figure 3.19. Geometry of different types of ring .....   | 108 |
| Figure 3.20. Secondary elements in the geometry of a segment .....   | 109 |
| Figure 3.21. (a)Thermal surface displacements, (b) thermal vertical displacements of the pile (Suryatriyastuti, Mroueha and Burlon, 2012).....   | 115 |
| Figure 3.22. Pile under thermal loading (a) temperature induced normal forces in the pile, (b) temperature-induced frictions mobilised at interface soil–pile. (Suryatriyastuti, Mroueha and Burlon, 2012).....  | 115 |
| Figure 3.23 (a) Lateral earth pressures in two periods of the year; (b) Variation of the displacements at the wall top over the year ( $x=1.2m$ ), (Coletti, Sterpi, 2016).....                                  | 117 |
| Figure 3.24. Axial load within the wall in two periods of the year and in three cross sections (Coletti, Sterpi, 2016) .....   | 117 |
| Figure 3.25. Bending moment within the wall in two periods of the year and in three cross sections (Coletti, Sterpi, 2016) .....   | 118 |
| Figure 3.26. Horizontal (xx) and vertical (yy) stresses versus temperature variations computed by the TM analysis (Barla, Di Donna, 2018) .....  | 119 |
| Figure 4.1. Basic explicit calculation cycle (FLAC User’s Manual) .....  | 125 |
| Figure 4.2. Geometry of the model .....  | 131 |
| Figure 4.3. Detail of the mesh in the tunnel spot.....   | 131 |

|  |     |
|--|-----|
| Figure 4.4. ENERTUN - Ring 179 - Extension of Turin Metro Line 1 (Barla & Insana, 2018).....                             | 132 |
| Figure 4.5. Boundary conditions - phase 1.....   | 135 |
| Figure 4.6. Total stresses along yy – initial condition.....   | 136 |
| Figure 4.7. Fictitious tractions on the tunnel boundary to simulate the excavation process – R.F.=0%<br>.....            | 137 |
| Figure 4.8. Fictitious tractions on the tunnel boundary to simulate the excavation process – R.F.=70%<br>.....           | 137 |
| Figure 4.9. Total stresses along yy – Excavation, R.F.=70%.....  | 138 |
| Figure 4.10. Lining installation – detail .....  | 138 |
| Figure 4.11. Total stresses along yy – Lining installed, R.F.=100%.....  | 139 |
| Figure 4.12. Finite Element model of the tunnel in RS2.....  | 139 |
| Figure 4.13. Surface settlements – Excavation R.F.=70% - FLAC vs. RS2 results.....                                       | 140 |
| Figure 4.14. Surface settlements - Installed lining R.F.=100% - FLAC vs. RS2 results .....                               | 141 |
| Figure 4.15. Surface settlements – R.F.=70% vs. R.F.=100% - FLAC .....   | 142 |
| Figure 4.16. Autocad view - Positions of the ground configuration pipes - ring 179 extension Turin<br>Metro Line 1 ..... | 143 |
| Figure 4.17. Marked points corresponding to the pipes’ configuration - FLAC.....   | 143 |
| Figure 4.18. Turin air temperature trends - data from Torino Caselle station (ilmeteo.it).....                           | 145 |
| Figure 4.19. Monitored tunnel internal temperature in the Metro (Barla et al.,2016).....                                 | 146 |
| Figure 4.20. Mean season values of the tunnel air temperature, derived from Barla et al. (2016).....                     | 147 |
| Figure 4.21. Winter - temperature distribution before activation of the lining - CS1 .....                               | 148 |
| Figure 4.22. Mid-season - temperature distribution before activation of the lining - CS1.....                            | 148 |
| Figure 4.23. Summer - temperature distribution before activation of the lining - CS1.....                                | 149 |
| Figure 4.24. Winter - temperature distribution after thermal activation of the lining - CS1 .....                        | 150 |
| Figure 4.25. Winter - DETAIL - temperature distribution after thermal activation of the lining - CS1<br>.....            | 150 |
| Figure 4.26. Mid-season - temperature distribution after thermal activation of the lining - CS1 .....                    | 151 |

|   |     |
|---|-----|
| Figure 4.27. Mid-season - DETAIL - temperature distribution after thermal activation of the lining - CS1 .....  | 151 |
| Figure 4.28. Summer - temperature distribution after thermal activation of the lining - CS1 .....               | 152 |
| Figure 4.29. Summer - DETAIL- temperature distribution after thermal activation of the lining - CS1 .....       | 152 |
| Figure 4.30. Winter - Surface settlements - CS1 .....   | 154 |
| Figure 4.31. Displacements history of the surface point corresponding to the tunnel axis – Winter CS1 .....     | 154 |
| Figure 4.32. Mid-season - Surface settlements - CS1 .....   | 155 |
| Figure 4.33. Displacements history of the surface point corresponding to the tunnel axis – Mid-season CS1 ..... | 155 |
| Figure 4.34. Summer - Surface settlements - CS1 .....   | 156 |
| Figure 4.35. Displacements history of the surface point corresponding to the tunnel axis – Summer CS1 .....     | 156 |
| Figure 4.36. CS1 - Surface settlements during the year .....  | 157 |
| Figure 4.37. Winter - Surface settlements - CS2.....  | 158 |
| Figure 4.38. Displacements history of the surface point corresponding to the tunnel axis – Winter CS2 .....     | 158 |
| Figure 4.39. Summer - Surface settlements - CS2 .....   | 159 |
| Figure 4.40. Displacements history of the surface point corresponding to the tunnel axis – Summer CS2 .....     | 159 |
| Figure 4.41. CS2 - Surface settlements during the year .....  | 160 |
| Figure 4.42. Winter - Surface settlements - CS3.....  | 161 |
| Figure 4.43. Displacements history of the surface point corresponding to the tunnel axis – Winter CS3 .....     | 161 |
| Figure 4.44. Summer - Surface settlements - CS3 .....   | 162 |
| Figure 4.45. Displacements history of the surface point corresponding to the tunnel axis – Summer CS3 .....     | 162 |
| Figure 4.46. CS3 - Surface settlements during the year .....  | 163 |

|   |     |
|---|-----|
| Figure 4.47. Comparison between surface settlements ( $x=0$ ) after the activation of the lining .....                                | 164 |
| Figure 4.48. Variation of the seasonal settlements (winter and summer) with the expansion coefficient .....                           | 165 |
| Figure 4.49. Improved temperature boundary conditions .....   | 166 |
| Figure 4.50. Temperatures distribution - before activation of the lining - Winter CS1 .....   | 167 |
| Figure 4.51. Temperatures distribution - after activation of the lining - Winter CS1 .....  | 167 |
| Figure 4.52. Temperatures distribution - before activation of the lining - Summer CS1 .....   | 168 |
| Figure 4.53. Temperatures distribution - after activation of the lining - Summer CS1 .....  | 168 |
| Figure 4.54. Displacements history of the surface point corresponding to the tunnel axis – Summer CS1 .....                           | 169 |
| Figure 4.55. Surface settlements after lining activation - in winter and summer conditions with new temperature conditions- CS1 ..... | 169 |
| Figure 4.56. Comparisons of the surface settlements between the two analyses - CS1 .....  | 170 |
| Figure 4.57. Displacements vectors - Winter CS1 .....   | 170 |
| Figure 4.58. Displacements vectors - Summer CS1 .....   | 171 |
| Figure 4.59. Winter conditions CS1 - 1 month of simulation - before the activation of the lining.....                                 | 172 |
| Figure 4.60. Winter conditions CS1 - 1 month of simulation - before the activation of the lining – detail .....                       | 172 |
| Figure 4.61. Winter conditions CS1 - 1 month of simulation - after the activation of the lining.....                                  | 173 |
| Figure 4.62. Winter conditions CS1 - 1 month of simulation - after the activation of the lining – detail .....                        | 173 |
| Figure 4.63. Displacements history of the surface point corresponding to the tunnel axis – Winter CS1 .....                           | 174 |
| Figure 4.64. Summer conditions CS1 - 1 month of simulation - before the activation of the lining ..                                   | 174 |
| Figure 4.65. Summer conditions CS1 - 1 month of simulation - before the activation of the lining - detail .....                       | 175 |
| Figure 4.66. Summer conditions CS1 - 1 month of simulation - after the activation of the lining .....                                 | 175 |
| Figure 4.67. Summer conditions CS1 - 1 month of simulation - after the activation of the lining - detail .....                        | 176 |

Figure 4.68. Displacements history of the surface point corresponding to the tunnel axis – Summer  
CS1 ..... 176

Figure 4.69. Surface settlements - comparison between 1 month of activation vs. 70+ years of  
activation ..... 177

# LIST OF TABLES

|   |    |
|---|----|
| Table 1.1. Classification of geothermal resources (based on Dickson and Fanelli, 2004).....   | 4  |
| Table 1.2. Heat exchange comparison between two segmental lining with different configuration of the loops – winter season (Barla and Di Donna, 2018) ..... | 18 |
| Table 1.3. Technical data of the energy plant LT24 (Brandl, 2016) .....   | 21 |
| Table 1.4. Environmental and economic benefits LT24 plant (from Brandl, 2016) .....   | 21 |
| Table 1.5. Geometrical information of the Jenbach tunnel energy plant .....   | 23 |
| Table 1.6. Hydraulic and thermal average parameter of Turin subsoil (Barla et al., 2015) .....  | 25 |
| Table 1.7. Extracted/injected heat in winter and summer by modelling - Torino Metro line 1 (Barla and Di Donna, 2016) .....                                 | 26 |
| Table 1.8. Geometrical information of the Turin ML1 prototype energy plant .....  | 27 |
| Table 1.9. Timeline of the process - from casting to operating mode .....   | 28 |
| Table 2.1. Basic physical information from drilling in soils .....  | 34 |
| Table 2.2. Different formulations of $k_0$ available in literature.....   | 37 |
| Table 2.3. Typical values of $k_0$ for different types of soil, according to the Terzaghi's formulation (1944).....   | 37 |
| Table 2.4. Resume of laboratory and in situ tests for soils, useful to investigate parameters for tunnels design.....                                       | 39 |
| Table 2.5. Geotechnical parameters for tunnel design and their determination, with reference to Table 2.2 .....   | 39 |
| Table 2.6. Typical values of volumetric thermal expansion coefficient for some soils, water and concrete.....   | 46 |
| Table 2.7. Factors affecting TRT results.....   | 62 |
| Table 2.8. List of investigation methods for thermal properties .....   | 64 |
| Table 2.9. Thermal properties of soils and rocks and common ways of determination with respect to Table 2.7 .....   | 64 |
| Table 3.1. Some analytical method for estimation of the face-support pressure (Guglielminetti et al., 2008).....  | 87 |

|  |     |
|--|-----|
| Table 3.2. Values of the K coefficient for the calculation of settlement trough.....   | 89  |
| Table 3.3. Equations that govern the TH problem .....  | 101 |
| Table 3.4. Influencing parameters in the design of an energy tunnel - in bold letters the parameters for the parametric analysis ..... | 121 |
| Table 4.1. Geometry of the tunnel.....   | 130 |
| Table 4.2. Geotechnical parameters for the Geotechnical Unit 2 in Turin (Barla & Barla, 2012).....                                     | 133 |
| Table 4.3. Mohr-Coulomb input parameters for GU2 in FLAC .....   | 133 |
| Table 4.4. Mechanical parameters for reinforced concrete segments (Duretto, 2018).....   | 133 |
| Table 4.5. Elastic input parameters for concrete in FLAC.....  | 134 |
| Table 4.6. Maximum surface settlements - FLAC vs. RS2 results .....  | 141 |
| Table 4.7. Thermal properties for isotropic conductive materials (Duretto, 2018).....  | 144 |
| Table 4.8. Coefficients of linear thermal expansion - parametric analysis .....  | 144 |
| Table 4.9. Mean external air temperatures - Turin.....   | 145 |
| Table 4.10. Mean tunnel air temperatures – Metro Turin (from Barla et al., 2016).....  | 146 |
| Table 4.11. Winter - Temperature boundary conditions .....   | 147 |
| Table 4.12. Mid-season - Temperature boundary conditions.....  | 148 |
| Table 4.13. Summer - Temperature boundary conditions.....  | 149 |
| Table 4.14. Different fluid temperatures imposed in the analyses .....   | 149 |
| Table 4.15. Description of case studies.....   | 153 |
| Table 4.16. Values of surface settlements corresponding to the tunnel axis - CS1 (x=0).....  | 157 |
| Table 4.17. Values of surface settlements corresponding to the tunnel axis – CS2 (x=0) .....   | 160 |
| Table 4.18. Values of surface settlements corresponding to the tunnel axis – CS3 (x=0) .....   | 163 |
| Table 4.19. Comparison between surface settlements (x=0) after the activation of the lining .....                                      | 164 |

# INTRODUCTION

Energy resources management has become one of the most important issues with global interest in the past years. In this context, the exploration of new technologies for renewable energy with low impact on the environment is one of the aspects that needs to be investigated.

Considering the uncontrolled rising global temperature, mainly due to the overuse of fossil resources and the consequent pollution, the development of sustainable alternatives in the energy production is needed, today as never before. In this scenario, geothermal energy is an innovative solution for renewable energy that ensures low impact on the environment and also long-term financial savings. A relatively new way to exploit it are the so called “energy geostructures”: geotechnical structures that, besides their primary structural role, can be equipped with pipes systems and used as heat exchangers. *Energy piles*, thermo-activated foundation piles, are the most common and widely used energy geostructures. *Energy tunnels* are another example of this way of combining, in a single operation, structural and energy functions, on a large scale. Energy tunnels exploit shallow geothermal energy, involving larger volume of ground and surface for heat exchange than energy piles. In the modern set-up, where urban areas are getting more and more populated, there is high necessity of new metro lines for the future development. A few numerical and experimental assessment have been carried out to analyse the efficiency of this type of energy geostructures.

Energy tunnels is a type of energy geostructures that can be considered still at the beginning in comparison with energy piles even if the activation of tunnel linings can have more both environmental and economic benefits. The hydro-thermal-mechanical interaction between the activated structural elements and the ground is still under study, not enough information is available about this kind of behaviour. Therefore, there still is a high need for research on this topic.

It is important to meticulously assess all the geotechnical and thermal parameters in order to optimize the design process and have an accurate evaluation of the structural properties and the energy availability. The first and most important step is to obtain all the parameters that govern the behaviour of the ground interacting with the structure. The geometry of the problem must be carefully taken into account, as the depth, the dimension of

the excavated tunnel, etc. To define the geotechnical parameters that are used in the design process, in situ and laboratory tests are run. Data from tests can be then interpreted with one of the models or of the failure criteria that are available in literature. Some of the geotechnical parameters can be influenced by temperature, such as deformability parameters and permeability.

When the energy function is also given to the structure, additional thermal parameters need to be identified. Even in this case, field tests and laboratory tests are used. Thermal response test (TRT) is the most common in situ test: it measures ground thermal conductivity and undisturbed ground temperature, useful to assess the geothermal potential. As the use of energy geostructures is becoming more and more prominent, there is a high need to investigate the thermal properties of the ground in a rapid and easy way, an example is represented by the TCT (Thermal Cone dissipation Test). Laboratory test can be held in steady-state or transient conditions. They can lead to parameters as thermal conductivity, diffusivity, volumetric heat capacity and temperature of the sample, but not all techniques are suitable to all types of soils and rocks. Trends are to use steady-state methods for rocks and transient methods for soils, under any water condition (Vieira et al., 2017).

Factors as mineralogy, density, drainage conditions, moisture content, and above all Over Consolidation Ratio (OCR) influence soils thermo-mechanical behaviour (Vieira et al., 2017). One of the most influencing factors in the thermo-mechanical behaviour of the soil is the stress history: in a normally or slightly consolidated soil the heat process can induce irreversible deformations, while in over consolidated soil temperature effects are negligible, the expansion experienced during heating is recovered during cooling.

One of the real challenges is to determine what are the most important influencing factors that directly affect the behaviour of an energy tunnel and to accurately assess the most important parameters (geotechnical and thermal) in the first steps of the design of a tunnel.

Energy tunnels are a renewable new technology, with a high potential in the future development of urban areas for district heating and cooling. For this purpose, further and detailed research on thermo-hydro-mechanical behaviour of energy tunnels is necessary. Considering all the above, analyse of input parameters needed in the design is a topic that needs careful consideration, in order to have and reach successful implementations of the system.

In *Chapter 1*, a brief introduction on the geothermal energy is treated: it is classified with attention on the low enthalpy geothermal resources and the Ground Source Heat Pumps (GSHP). The concept of “energy geostructures” is introduced with a little discussion about the types of geostructures now available on the market and their intrinsic sustainability.

In *Chapter 2*, the geotechnical and thermal parameters needed in the design of an energy tunnel are the main characters. The traditional ways of geotechnical laboratory and in situ investigation are reported, followed by the relatively new THM tests, which consider the effects of temperature on the input parameters. Thermal parameters and their investigation are discussed with the addition of a brief paragraph about the future of thermal investigation in situ.

In *Chapter 3*, all the design process of an energy tunnel with reference to the needed input parameters is dealt. The first part of the chapter explains how the structural design and behaviour of a tunnel works, in terms of structure, ground and soil-structure interaction; the second part introduces the THM (Thermo-Hydro-Mechanical) problems related to the design of an energy tunnel; the last part deals with its thermal design and energy performances. Each subchapter has a little reference to the numerical models and analyses. Some examples of application in Austria and Turin are in the end reported.

In *Chapter 4* the numerical model is described, it is used to make a parametric analysis, studying missing aspects of an energy tunnel design. The varying parameters are the thermal linear expansion coefficient and temperatures, first of all the fluid temperature and consequently also the ground, the internal air and the external temperatures, in order to have more realistic seasonal simulations. The analysis is focused on the surface settlements, the way they vary with thermo-activation of the lining.

In the conclusive chapter, the outlines of the study are presented and recapped, and further developments are suggested.



# INTRODUZIONE

La gestione delle risorse energetiche risulta essere, negli ultimi anni, una delle più importanti questioni da affrontare a livello mondiale. In questo contesto, la ricerca di nuove tecnologie per lo sfruttamento di energie rinnovabili con basso impatto sull'ambiente è un aspetto che richiede di essere approfondito.

Considerando l'innalzamento incontrollato delle temperature terrestri, principalmente causato da uno sfruttamento eccessivo di risorse fossili, con conseguente inquinamento, lo sviluppo di alternative sostenibili per la produzione di energia è necessario, oggi come mai prima d'ora. È in questo scenario che l'energia geotermica trova spazio, una soluzione innovativa che garantisce basso impatto ambientale oltre ad un risparmio economico a lungo termine. Una modalità relativamente nuova di sfruttare l'energia geotermica è rappresentata dalle cosiddette "energy geostructures", geostrutture energetiche, ovvero strutture geotecniche, che, oltre al loro ruolo strutturale primario, possono essere equipaggiate con sistemi di tubature e usate come scambiatori di calore.

Gli *energy piles*, pali di fondazione termicamente attivati, sono le più comuni e diffuse geostrutture energetiche. Gli *energy tunnels* sono un altro esempio di questo modo di combinare, in un'unica opera, funzioni strutturali ed energetiche su larga scala. Sfruttano l'energia geotermica superficiale, coinvolgendo un volume di terreno e una superficie di scambio termico di gran lunga superiore rispetto agli *energy piles*. Nella società moderna, dove le aree urbane stanno diventando sempre più popolate, risulta esserci un'elevata necessità di nuove linee metropolitane che permettano di aumentare la qualità della vita delle città.

Al fine di valutare l'efficienza di questo tipo di opera, è stato condotto un numero molto ridotto di analisi numeriche e sperimentali. La galleria energetica è un tipo di geostruttura energetica che può essere considerata ancora agli inizi, rispetto ad altre tipologie di fondazioni termo-attivate, anche se l'attivazione termica di un tunnel può avere benefici ambientali ed economici maggiori.

L'interazione termo-idro-meccanica tra gli elementi strutturali termicamente attivati e il terreno è ancora oggetto di studio, non sono disponibili informazioni a sufficienza a

descrivere questo tipo di comportamento. Pertanto, è necessario un ulteriore approfondimento di questo comportamento.

Quando si progetta una galleria energetica, ai parametri geotecnici si affiancano quelli termici, ed è di fondamentale importanza valutare entrambi meticolosamente, al fine di ottimizzare il processo di progettazione e ottenere una stima accurata delle proprietà strutturali e dell'energia disponibile. Il primo passo risiede dunque nel derivare tutti i parametri che governano il comportamento del terreno interagente con la struttura. La definizione dei parametri geotecnici può avvenire tramite test di laboratorio o in sito; i risultati dei test vengono interpretati successivamente con l'ausilio di modelli e criteri di rottura disponibili in letteratura. La presa in considerazione delle condizioni di temperatura può portare ad influenzare alcuni dei parametri geotecnici, come i parametri di deformabilità e la permeabilità.

L'attivazione energetica richiede necessariamente l'identificazione di parametri termici. Test in laboratorio e test in sito sono utilizzati anche in questa circostanza. Il *Thermal Response Test* (TRT) è uno dei più comuni test in sito: misura la conducibilità termica e la temperatura non disturbata del terreno, utile per valutare il potenziale geotermico. Visto l'incremento di implementazione di geostrutture energetiche, in particolare per quanto riguarda i tunnel energetici che richiedono indagini in sito molto estese, è necessario individuare metodologie di indagine dei parametri termici che siano il più possibile rapide e semplici, un esempio può essere rappresentato dal TCT (*Thermal Cone dissipation Test*). Per quanto riguarda le indagini in laboratorio possono essere condotte in condizioni "steady-state" o "transient", ottenendo parametri come la conducibilità termica, la diffusività, la capacità termica volumetrica e la temperatura dei campioni, ma non tutte le metodologie sono adatte a tutti i tipi di terreno e roccia. In genere si utilizzano i metodi "steady-state" per le rocce e quelli "transient" per i terreni, in qualsiasi condizione idrica (Vieira et al., 2017).

Fattori come mineralogia, densità, condizioni di drenaggio, contenuto d'umidità e soprattutto OCR (Over Consolidation Ratio) influenzano il comportamento termo-meccanico dei terreni (Vieira et al., 2017). Uno dei fattori che più influisce è per l'appunto la storia tensionale: in un terreno poco o normal-consolidato il processo di riscaldamento può indurre deformazioni irreversibili, mentre in terreni sovra-consolidati gli effetti della temperatura sono trascurabili, l'espansione che avviene in fase di riscaldamento viene recuperata totalmente una volta che la fonte di calore viene sottratta.

Alcune delle numerose sfide in questo campo sono quella di determinare quali siano i fattori che influiscono direttamente sul comportamento di un tunnel energetico e di individuare accuratamente i parametri più importanti (geotecnici e termici) già dalle prime fasi di progettazione.

Le gallerie energetiche sono una nuova tecnologia rinnovabile, con un alto potenziale per lo sviluppo futuro di aree urbane, per il riscaldamento e il raffrescamento dei distretti. A questo scopo, ulteriori ricerche più dettagliate sul comportamento termo-idro-meccanico degli *energy tunnels* sono necessarie. Concludendo, l'analisi dei parametri di input per il progetto di una galleria energetica è un tema che richiede attenta considerazione, al fine di avere e raggiungere un'implementazione efficace del sistema.

Nel *Capitolo 1*, è riportata una breve introduzione sull'energia geotermica: è classificata e viene posta attenzione sulle risorse geotermiche a bassa entalpia e sugli impianti geotermici, noti come GSHP – Ground Source Heat Pump. Il concetto di geostruttura energetica viene introdotto, accostato a una breve descrizione dei tipi di energy geostructures disponibili sul mercato e la loro intrinseca eco-sostenibilità.

Il *Capitolo 2* riporta i parametri geotecnici e termici necessari nella progettazione di un energy tunnel: le metodologie tradizionali di indagine in laboratorio e in situ sono richiamate, seguite dalle relativamente nuove indagini termo-idro-meccaniche, che considerano l'effetto della temperatura sui parametri. Le caratteristiche termiche e le loro metodologie di indagine sono discusse, introducendo in coda un breve paragrafo sul futuro delle indagini termiche in situ.

Il *Capitolo 3* offre una panoramica sul processo di progettazione di un energy tunnel, con particolare attenzione, per ogni fase, ai parametri richiesti al fine di procedere con i calcoli. La prima parte del capitolo riporta una carrellata di aspetti di progettazione legati principalmente alla realizzazione di una galleria tradizionale; la seconda parte introduce le problematiche relative al comportamento termo-idro-meccanico collegate alla realizzazione di un energy tunnel; l'ultima sezione affronta la progettazione termica e le performance energetiche di una galleria termo attivata. Alla fine, qualche esempio di interesse viene riportato, specificatamente in Austria e a Torino.

Nel *Capitolo 4* è descritto il modello numerico creato al fine di svolgere un'analisi parametrica su aspetti non ancora investigati in letteratura. I parametri che vengono fatti

variare sono il coefficiente di espansione termica lineare del terreno e le temperature, in primis del fluido circolante nel sistema di tubature e, di conseguenza, anche dell'aria interna al tunnel o dell'aria esterna per simulare delle attivazioni stagionali. L'aspetto che si vuole indagare sono i cedimenti in superficie, come essi variano se seguito dell'attivazione termica dei conci, simulata mediante l'introduzione di veri e propri carichi termici.

Nel capitolo conclusivo sono presentate le discussioni finali inerenti ai risultati ottenuti e sono suggeriti ulteriori sviluppi.

# 1 GEOTHERMAL ENERGY

Geothermal energy is the thermal energy stored within the Earth and usually refers to that part of ground heat that can be extracted from the subsurface and converted into energy products. Considering the shallow portion of Earth, it is possible to say that heat is inexhaustible, and it derives from slow cooling of the primordial heat and mainly from the decay of radioactive isotopes that are in the crustal rock minerals. It was demonstrated that there is no equilibrium between the produced heat and the dissipated one: our globe is getting colder, but the cooling process is so slow that does not affect the definition of “inexhaustible” (Manzella, 2017).

It is well known, from the seventeenth century, that temperature increases with depth: the difference between the warmer deeper zones and the colder shallower zones gives rise to a heat flow from the inner part of the Earth to the upper part. Therefore, there is a geothermal gradient and typical values are 2.5 – 3.0 °C per 100 m, even if it can vary considerably between different locations (Dickson and Fanelli, 2004).

The internal structure of the Earth is divided into layers: a solid inner core, a molten outer core, a stiffer mantle and an outer silicate solid crust.

## Geothermal Energy

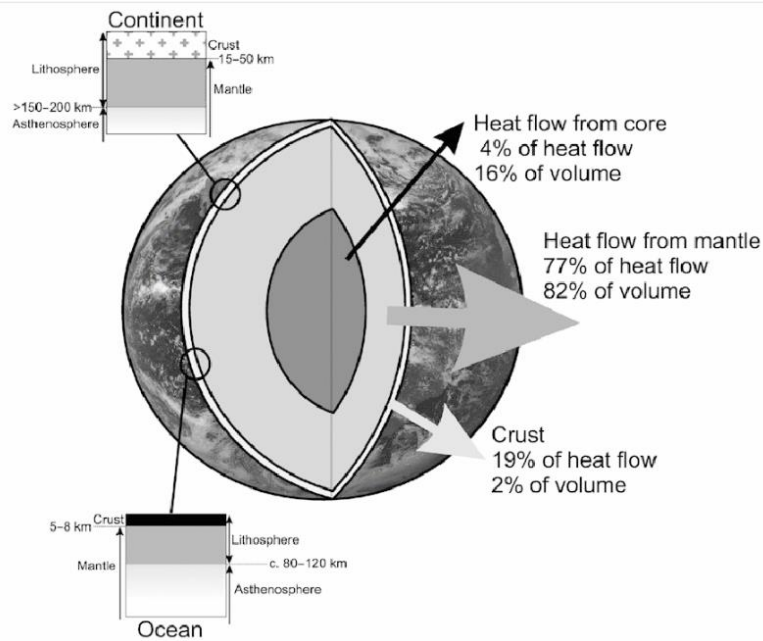


Figure 1.1. Structure of the Earth, showing the percentage of heat derived from the core, mantle and crust, compared with their volume. (Banks, 2012)

As shown in *Figure 1.1*, the crust only represents the 2% of the total volume of the planet, but almost the 19% of the heat comes from that portion, due to a substantial presence of radioactive isotopes (Banks, 2012).

Physical and chemical properties of the crust, mantle and core are different, for example the external part, also called lithosphere, can be considered as a rigid layer, floating on the mantle, where rocks behave more like fluids than solids. For that reason, it is possible to define Earth as a heterogeneous convecting sphere, with the outer shell, composed of six main tectonic plates, in constant slow motion: near tectonic plate boundaries are the hottest areas of the Earth's surface, often associated to volcanoes and seismic activities (Manzella, 2017).

This heterogeneity brings to convection movements in the fluids within the globe: they cross the hotter layers and stores heat, bringing it to the shallower layers, where heat is dissipated or used with energy purposes.

Convection's laws govern the geothermal systems: hot fluid, with less density, tends to move up and to be replaced by a cooler fluid, with higher density, coming from the shallow boundary of the system. This heat flow varies depending on the considered part of the Earth: on average, from the continental crust it is  $57 \text{ mW/m}^2$  and from the oceanic crust is  $99 \text{ mW/m}^2$ . The differences lie in thickness, composition and density of the two types of crust: the first one is thicker, with 15-50 km of crust and even more under mountains, and rich in

## Geothermal Energy

---

silicon, aluminium and minerals which are the constituents of the granites; the second one is very thin (5-8 km), denser than the continental crust, mainly composed of basic minerals and rocks (Manzella, 2017).

A geothermal system is made of three components: a heat source, a reservoir and a fluid, the heat carrier. The only one that must be natural is the source, it can be a magmatic intrusion at high temperature ( $>600$  °C) at relatively little depth (5-10 km) or the usual heat of the Earth.

The reservoir is made of hot permeable rocks in which fluids can flow, absorbing heat. It is usually between two impermeable layers of rock and connected to shallow recharge zones, from where meteoric waters can refill the fluids that were lost in a natural way or by artificial exploitation. This natural recharging can be also integrated with an artificial one: the geothermal fluids, after being used, can be introduced again in the reservoir through reinjection wells. The geothermal fluid is in most cases meteoric water, liquid or vapour, depending on the temperature and pressure of the system (Dickson and Fanelli, 2004).

## 1.1 Classification of geothermal energy

The most common way to classify the geothermal energy is based on fluids' enthalpy. Enthalpy is a thermodynamic quantity equivalent to the total heat content of a system that in this field of application is often associated to the fluid temperature responsible for the heat transport.

Resources are divided into low, medium and high enthalpy, depending on what temperature ranges they cover: it is important to notice that a standard classification is not available, so it changes between different authors, as it is shown in *Table 1.1*.

*Table 1.1. Classification of geothermal resources (based on Dickson and Fanelli, 2004)*

|                        | Muffler and Cataldi<br>1978 | Hochstein<br>1990 | Benderitter and Cormy<br>1990 | Nicholson<br>1993 | Axelsson and Gunnlaugsson<br>2000 |
|------------------------|-----------------------------|-------------------|-------------------------------|-------------------|-----------------------------------|
|                        | T [°C]                      | T [°C]            | T [°C]                        | T [°C]            | T [°C]                            |
| <b>Low enthalpy</b>    | < 90                        | < 125             | < 100                         | ≤ 150             | ≤ 190                             |
| <b>Medium enthalpy</b> | 90 – 150                    | 125 – 225         | 100 -200                      | -                 | -                                 |
| <b>High enthalpy</b>   | > 150                       | > 225             | > 200                         | > 150             | > 190                             |

High enthalpy resources allow the exploitation of the deep energy of the Earth at very high temperatures to mainly produce electrical power. On the contrary, it is possible to take advantages of the ground heat, even if temperatures are low: this refers to the low enthalpy resources, also known as shallow geothermal energy. They can be used, with a system of heat pumps, to exploit thermal energy to use in buildings' climate control (Dickson and Fanelli, 2004).

### 1.1.1 Low enthalpy geothermal resources

From the Earth's core heat spreads and reaches the surface: the shallower layer of the ground (almost the first 100 m) has a constant temperature of about 10–15 °C, according to the mean annual air temperature. The first few meters from the surface are not considered because they

## Geothermal Energy

are affected by seasonal and daily changes of the external temperature, as *Figure 1.2* shows (Martin et al., 2010).

As a logic consequence, the ground is warmer than the air in winter, and colder in summer; starting from this observation, it is possible to design a system that cools in summertime and heats during winter.

Hence, when talking about low-enthalpy geothermal plants, one refers to heat pumps that extract energy from the abovementioned portion of the ground at constant temperature and use it, for example, to heat or cool nearby residential buildings and public utilities, to produce domestic hot water or, more recently, there are some applications in the field of de-icing bridge decks and airport runways.

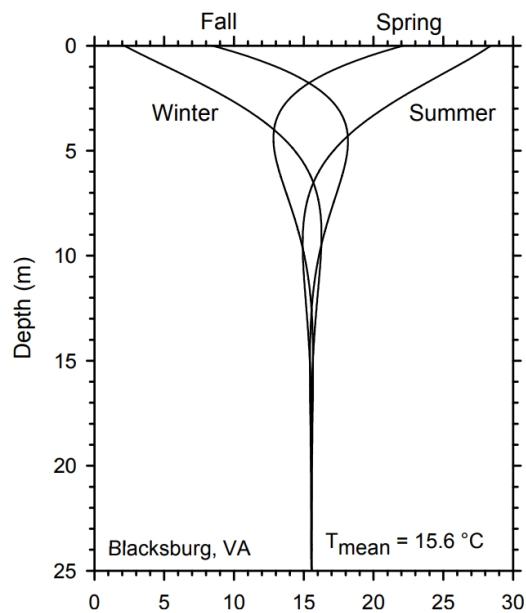


*Figure 1.2. Example of the trend of temperature in the ground (Martin et al., 2010)*

## 1.2 Ground Source Heat Pumps (GSHP)

Heat is extracted from the ground by heat pumps at a relatively low temperature and then converted to thermal energy at higher temperature exploiting the physical property of fluid to absorb or release heat when changing its state of matter, i.e. when vaporizing or condensing, respectively.

Briefly, a heat pump works as a refrigeration machinery, a device using mechanical energy to transfer heat from a lower temperature body to a higher temperature body, in order to keep the first cool. The mean that transfers heat is a refrigerant fluid, usually water or other fluids that do not compromise the environment. It circulates in the circuits and, depending on temperature and pressure conditions, it can be liquid or vapour.

A Ground Source Heat Pump (GSHP) system, as shown in *Figure 1.3*, is different from traditional heat pump systems because the source of energy is the ground (or the groundwater) instead of the external air. In this respect, many advantages arise in terms of efficiency: ground has a property that should not be underestimated, temperature is stable throughout the whole year. Higher COPs (Coefficient Of Performance) are obtained, in a range from 2.4 to 5.0 (*Market report 2013, European Geothermal Energy Council*), compared to traditional heating systems, i.e. boilers, that typically have a COP of 1.

$$COP = \frac{\text{heating output [kW]}}{\text{electricity input [kW]}} \quad (\text{Eq. 1.1})$$

The higher the COP, the more efficient is the technology and less electrical power is required. Considering an average COP value of 4 for a GHSP system, it means that for each kilowatt of electric power supplied to run the GSHP unit, around four kilowatts of heat energy are produced (Brandl, 2006).

There are reversible heat pumps that can both supply heating and cooling function, for the latter in summertime heat is extracted from buildings and injected into the ground. It is important to notice, that an accurate planning of resources exploitation is crucial: natural equilibria must be respected. Considering a year period, these technologies with “reverse mode” are the most environmentally friendly: heat extraction from the ground in winter and heat injection into the ground in summer result in energy balance.

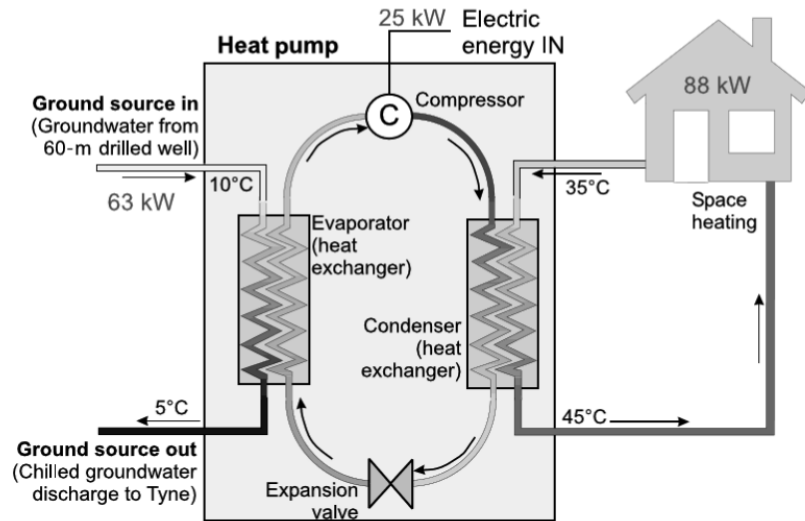


Figure 1.3. An example of a GSHP system (Banks, 2012)

### 1.2.1 Classification of GSHP systems

GSHP systems can be classified into two different categories, in Figure 1.4 an overview is reported:

- *Open loop systems*, where groundwater is used as heat carrier;
- *Closed loop systems*, in which heat is exchanged indirectly from the ground to the heat pump. The heat carrier medium circulates in heat exchangers located in the ground, transporting heat to the heat pump, without being in contact with the ground or rock.

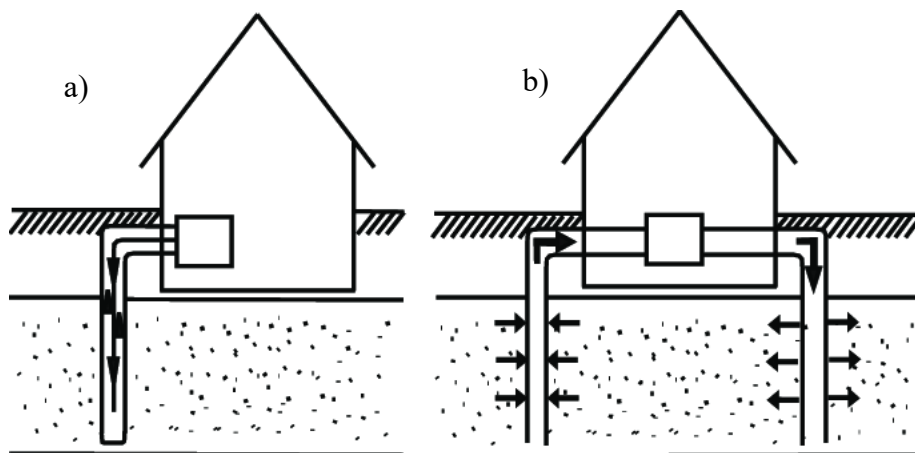


Figure 1.4. Scheme of shallow geothermal systems that are closed (a) and open (b). (Hecht-Méndez et al., 2009)

The choice for the right system depends on several factors:

- Geology and hydrogeology of the site, i.e. open systems need sufficient permeability to work;
- Available area on the surface, i.e. horizontal closed systems require a lot of space;
- Heating and cooling characteristics of the buildings that are going to be powered.

### ***1.2.1.1 Open loop systems***

This solution extracts water directly from the ground, water is usually pumped from springs, drilled boreholes or flooded mines. Fundamental requirements are to have an aquifer in the site of construction and adequate permeability, transmissivity and storage properties of the rock.

In the system there are generally two wells, abstraction and injection, and a heat exchanger (*Figure 1.5.a*). Re-injection is a fragile step of the mechanism, temperature and characteristics of water could change during the process; it could alter the groundwater. When there is no risk of reducing the groundwater in the aquifer, the injection well does not exist and the extracted water is released at the surface.

These solutions are suitable for large installations because of a higher efficiency at lower costs, however there are some requirements regarding the chemistry quality of the groundwater, in order to maintain the serviceability of the plant, that have to be observed.

### ***1.2.1.2 Closed loop systems***

Groundwater is not always available and the so called “closed loop” systems are used to get over this problem. No fluid exchange takes place: closed loop tubing made of high-density polyethylene are installed in the ground where a fluid (mixture of water and anti-freeze) circulates and extracts heat from the surrounding soil or rocks. This system avoids any risk due to the reinjection of the carrier fluid.

Several types of installation are used: horizontal, vertical or baskets loops (*Figure 1.5.d*), differences lie in depth at which probes are and in what is the main development direction.

Vertical exchangers (*Figure 1.5.b*) are the most common: they consist of one or several U-pipes or coaxial pipes in boreholes, spaced at least 5-6 m apart at a depth that varies with the geological and building characteristics, generally between 20 and 200 m. Ascending pipes, with the heated fluid, and descending pipes, with the cooled fluid, are separated in order not to chill the fluid before it reaches the heat pump. The boreholes drilling is one of the factor

## Geothermal Energy

that mostly affect the costs of installation of these systems, but they have lower cost of maintaining comparing to the traditional solutions: in 10 years the initial investment is recovered.

Horizontal loops (*Figure 1.5.c*) are installed in trenches at a depth of 1.2-2 m, they need a large surface available for their implementation. This depth allows to be practical during the excavation process, with low costs, and a modest thermal storage is always provided: it's deep enough to isolate the loop from the winter frosts but also shallow enough to be replenished in summer by solar and atmospheric heat (Manzella, 2017).

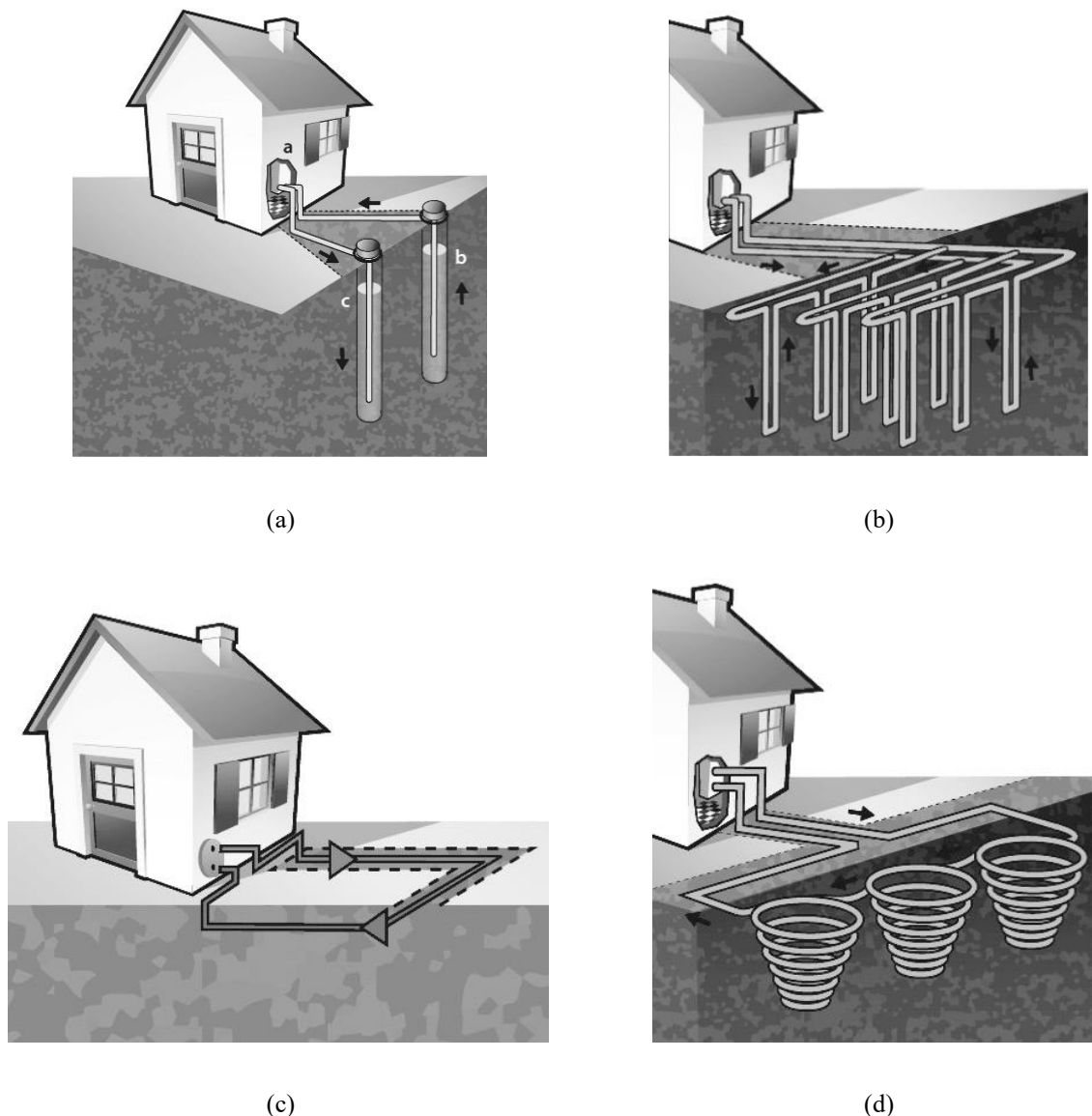


*Figure 1.5. Different configurations for GSHP systems. (a) Open loop GSHP with a-heat exchanger, b-abstraction well, c-injection well. (b) Closed loop GSHP, vertical. (c) Closed loop GSHP, horizontal. (d) Closed loop GSHP, basket system. (Manzella, 2017)*

### 1.3 Energy geostructures

A relatively new way to exploit the geothermal energy are the so-called *energy geostructures*: geotechnical structures that, besides their primary structural role of supporting buildings (i.e. foundations) or the ground itself (i.e. retaining walls, tunnels), can be equipped with pipes systems and used as heat exchangers. Where it is asked to build this kind of structures, a generally constant ground temperature over the year is required and it can be said that in most continental Europe, with temperate climate, this requirement is satisfied.

First applications took place in the 1980s in Austria and Switzerland, after which they reached other countries: this technology was initially implemented in shallow foundation elements, then bearing piles, diaphragm walls and tunnels followed (Bourne-Webb et al., 2016)

Energy geostructures use the closed loop technology in earth-contact structural elements: they contain a system of polyethylene absorber pipes in which a fluid flows transferring heat and concrete is in contact with the ground, it has a higher thermal conductivity and storage capacity than soil. The essential difference from conventional ground heat exchangers is that no additional element, such as boreholes or wells, is required: they provide the thermal performance of deep geothermal systems without the additional drilling costs, for that reason also economic benefits can be taken from these technologies.

These systems belong to the category of low enthalpy geothermal plants and are associated with heat pumps: they can work heating or cooling mode only, or in a reversible way. In the first case, efficiency is higher if there is a flow in the groundwater, otherwise, for seasonal operation (i.e. heating in winter and cooling in summer) steady state conditions with a low hydraulic gradient are preferable. As shown in *Figure 1.6*, heat pump represents the connection between the so called primary circuit, made of closed loops embedded in the earth-contact concrete elements, and the secondary circuit, namely the system that distributes heat inside buildings or infrastructures (Brandl, 2006).

The design procedure needs to consider not only the traditional structural design, but also the dimensioning of the geothermal equipment, paying particular attention to energy demand and the additional effects induced by temperature variations in terms of stresses and strains that affect the whole structure.

## Geothermal Energy

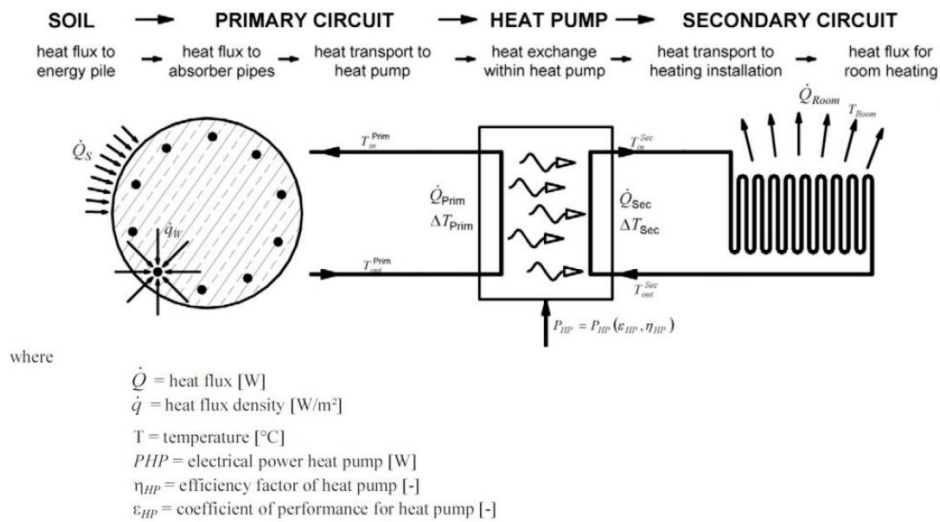


Figure 1.6. Scheme of heat flux balance for heating in an energy piles plant (Brandl, 2006)

Theoretically speaking, all kind of underground geotechnical structures can be used as energy geostructures with proper equipment, anyway the most common are the so-called *energy piles* (Figure 1.7.a), thermo-activated foundation piles. *Energy walls* (Figure 1.7.b) are thermo-activated retaining walls. *Energy tunnels* are another example of this way of combining, in a single operation, structural and energy functions, on a large scale; however, nowadays there are still limited implementation (see Chapter 3).

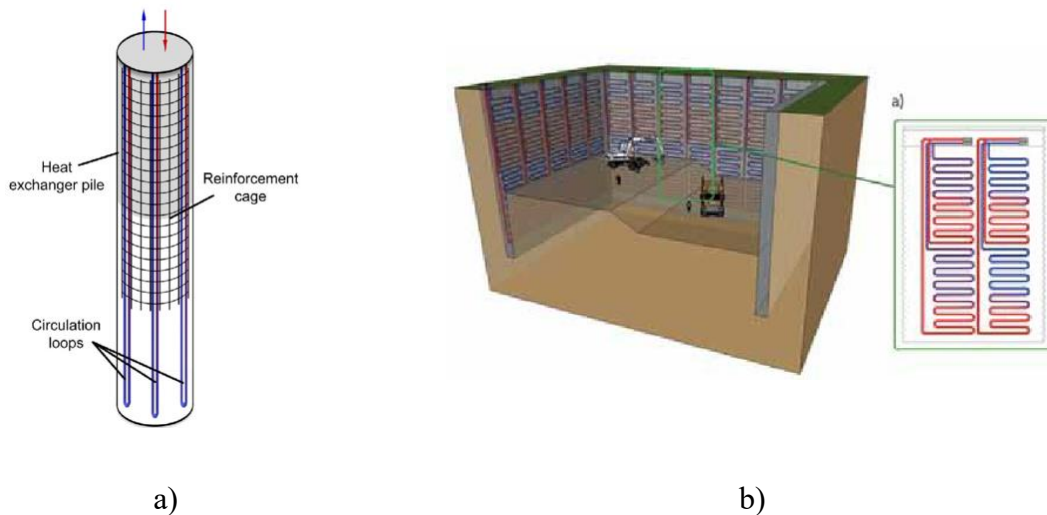


Figure 1.7. Examples of energy geostructures. a) Energy pile (Olgun et al., 2015) b) Energy wall (Kovačević et al., 2013)

*Energy piles* are foundation piles with cooling/heating elements: piles contain tubes through which a glycol-water fluid mixture is circulated via a heat pump system (primary circuit) between the piles and the heating/cooling system of the building (secondary circuit).

## Geothermal Energy

The mostly followed construction sequence is:

- a large-diameter hole (0.4 m to 1.5 m) is drilled in the ground, commonly up to 15-30 m depth;
- the steel reinforcement cage with the attached heat exchange loops, usually made of High Density Polyethylene (HDPE), are inserted in the hole;
- the hole is filled with concrete that can also be a thermally enhanced concrete.

Typical values of power outputs for energy piles range between 20 W and 100 W per meter of pile, depending on site-specific factors. When ground has a low quality, typically 25 W/m are extracted; with average quality 51 W/m; if ground has excellent qualities values can reach 80 W/m (Martin, 2017).

This kind of energy geostructure is the most common, used and modelled between the thermo-activated foundations: its implementation has rapidly increased over the last decades, especially in Europe, where it is possible to find many energy piles projects. Austria, UK, Switzerland and Germany can be regarded as the pioneering countries that have investigated the use of geostructures for decades. In *Figure 1.8*, it is possible to see how Austria had a pioneering role in this scenario, showing the increase of energy piles between 1984 and 2013. Since the year 2005 more than 7,000 energy piles have been installed per year (Brandl, 2016).

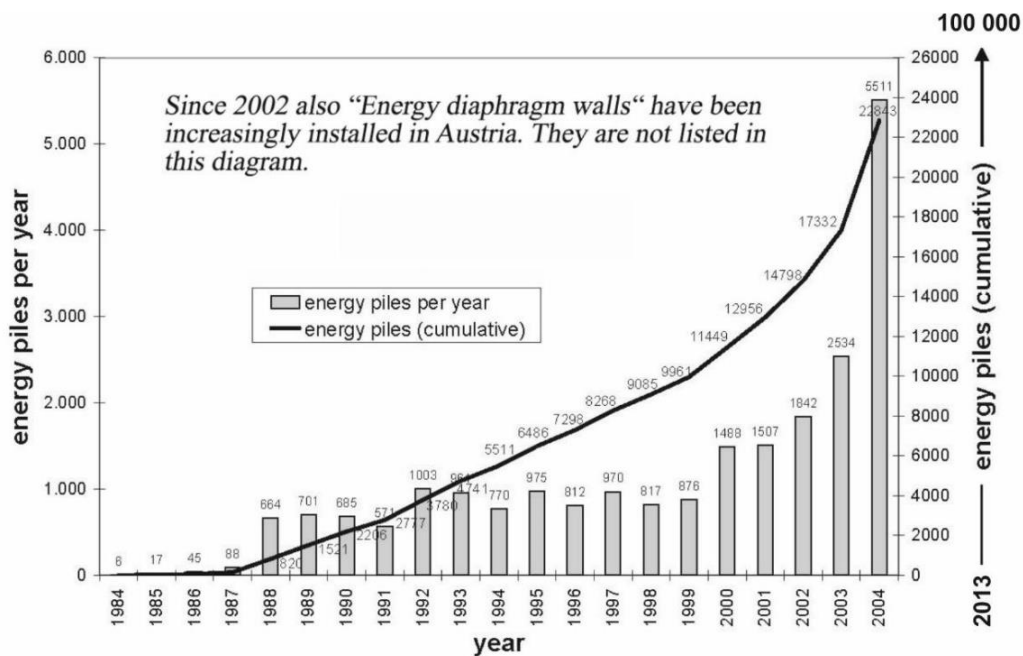


*Figure 1.8. Number of energy piles installed in Austria; since 2005 more than 7000 energy piles per year (Brandl, 2016)*

Several examples can be reported, one of them is the Dock Midfield at Zürich Airport, completed in 2003. It has been built on 440 foundation piles of 30m, about 300 piles have been equipped with 5 U-pipe fixed on the reinforcement cage to use them as heat exchangers with the ground. A measurement project started from the end of 2004, with the aim of determining the system thermal performances, checking the validity of the design procedure, optimizing the system operation. After 2 years of measurements, it has been observed that the annual heating and cooling demands were close to the design values, with a high global efficiency. This achievement has been possible thanks to a careful design procedure that included detailed investigations of both geotechnical and thermal material properties, including response test analysis, thermal dynamic simulations of the building and the energy piles system (Pahud et al., 2007). In Switzerland a lot of other examples took place, i.e. in schools and public or private buildings. In order to investigate the behaviour of this type of foundation, at the École Polytechnique Fédérale De Lausanne (EPFL) an experimental site has been implemented under its congress hall. Four test-piles, entirely equipped and instrumented, have been built: the aim is to study them under different thermal load configuration and acquire more knowledges in the investigation field for these energy geostructures. In Austria, important projects have been run in Vienna, like the Uniqa Tower and the Lainzer Tunnel, where heat is exchanged by lateral walls made of piles, approximately 17 m long with a diameter of 120 cm. In Germany, the Main Tower of Frankfurt is a 198 m high building, based on more than 300 piles and 262 of them are energy piles. Combined with other 130 energy piles in the lateral retaining walls, they form a geothermal system with a heating and cooling power of 1000 kW. In England, the One Change Building of London rests on more than 200 thermo-activated piles, with a heating power of 1638 kW and a cooling power of 1742 kW. (Di Donna and Laloui, 2012)

The main reasons why all those countries have successfully developed these technologies are related to the fact that they have national guidelines, government often offers incentives in an effort to promote their use and the aim is to reach the construction of zero carbon buildings within the next few years. Anyway, at the moment, no European guidelines, such as Eurocodes, are available on this topic, even if there are organizations working on providing them. Therefore, very few applications take place in Eastern Europe: a lack of knowledge and national guidelines for designing has brought to non satisfactory implementations, due to wrong choices of input parameters.

*Energy walls* are thermo-activated diaphragm walls, structures that are often used to support deep excavations where other techniques are unsuitable. They are typically 0.8 m to 1.2 m wide, with depths typically between 10 m and 40 m. One of the main differences from the energy piles is that it can happen that, on one side and for some portion of its depth, the diaphragm is in contact with air: this is to be considered since that part of the wall would be expected to experience different rates of heat transfer than the one in contact with soil (Mauri and Sterpi, 2015).

Other examples of energy geostructure under study are the *energy anchors* and *energy sewers*: anchors play an important role in structural support in retaining structures or tunnels, if thermally equipped they can also have a double function; sewers could be used for heating and cooling adjacent buildings depending on the filling level, sewage flow and sewage temperature (Brandl, 2006).

### 1.3.1 Energy tunnels

More recent applications of energy geostructures concern energy tunnels: like others, tunnels are thermo-activated by embedding polyethylene pipes within their concrete structure. Differences lie in the involved volume and surface in the heat exchange that in this case are larger, compared to building foundations, and in the heating source, heat comes from the ground but also from the traffic circulating inside the tunnel.

Nowadays, this technology has very limited real implementations, the main obstacle in the industrial development is the lack of analytical, physical or numerical tools to consider the complex interactions between thermal storage and the mechanical behaviour. There aren't standard guidelines that explain how to have an optimized design assuring an advantageous ratio between the initial cost of installation and the energy production in the operational phase, which strongly depend on the specific site.

Anyway, it is possible to make a simple classification based on the thermal conditions of the tunnels. There are *cold tunnels*, where air temperature is similar to that of the ground (15 °C) throughout the whole year and the passing trains have low frequency, so they don't affect the tunnel temperature. Typically, this kind of tunnel has an internal diameter of 10-12 m, road tunnels are an example. When temperatures are higher, approximately of 30 °C, it is the case of *hot tunnels*: they have smaller internal diameters (7 m). Urban tunnels can be classified as

hot tunnels: the air temperature in the tunnel is increased by the passage of trains at high frequency, in this sense it's important to pay attention to the temperature variations induced to the surrounding soil.

### 1.3.1.1 Technologies

To exploit the geothermal energy using tunnels, two methods are available depending on the tunnelling method adopted. If a conventional method is used, absorber pipes are attached to non-woven geosynthetics placed between the primary and secondary lining (*Figure 1.9*).



*Figure 1.9. Energy geotextile installed in an energy tunnel - conventional tunnelling method – Lainzer Tunnel Vienna (Adam & Markiewicz, 2009)*

On the other side, if mechanized tunnelling is used, segments are precast in factory, optimized for heat exchange by putting the geothermal equipment in the cast concrete, and then installed in an easier way in situ by the Tunnel Boring Machine (TBM), see *Figure 1.10*.

The geothermal equipment for these applications is fabricated in reticulated polyethylene (Pe-Xa) and generally composed by three concentric layers: the inner layer with high-density polyethylene, the intermediate layer in polymeric material and the outer layer formed by a barrier in ethylene vinyl alcohol (EVOH) which avoids permeability to oxygen. The pipes have external diameters of 15-35 mm and are 1.5-3 mm thick: they are able to withstand high pressures and temperatures, resist to chemical corrosion and guarantee high durability. The carrier fluid is a propylene glycol mixed with water that can work down to a temperature of  $-20\text{ }^{\circ}\text{C}$ . (Barla et al., 2016)

Hydraulic connections link adjacent segments, forming lining ring circuits, usually made of 6-7 segments. Each circuit is connected to the main conduit which directs the heat carrier fluid from them to the heat pump and vice versa. In order to reduce the number of connections on

the main conduit and the consequent significant head losses two or more rings can be hydraulically connected in parallel forming a sub circuit. Head losses can also be reduced by carefully designing the main conduit, optimizing its length in order to allow heat distribution only at the district scale.

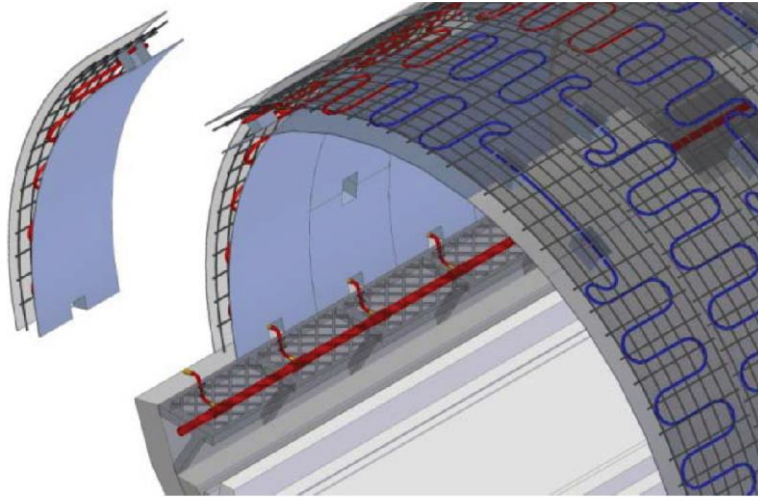


*Figure 1.10. Energy tunnel with precast segments – mechanized tunnelling method (Barla & Perino, 2014)*

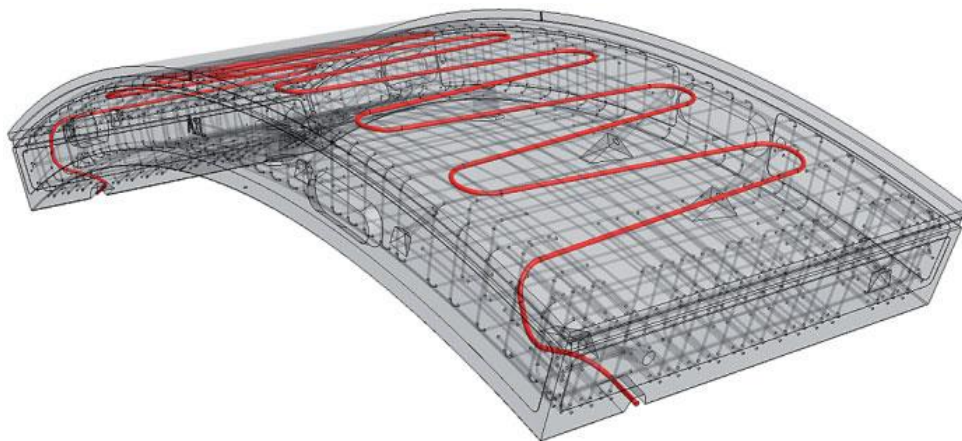


*Figure 1.11. 3D-CAD view of one energy lining segments with absorber pipes and reinforcement cage – Jenbach tunnel, Austria (Frodl, Franzius & Bartl, 2010)*

As shown in *Figure 1.10* and *1.11*, pipes are traditionally placed in the segments parallel to the tunnel axis.

An innovative way to implement these pipes, which leads to higher efficiencies of the geothermal plant, has been patented by a research group of Politecnico di Torino and is called Enertun (Barla & Di Donna, 2016). The innovation stands in the pipes' geometry: they are positioned so that their main direction is perpendicular to the tunnel axis. This change allows to reduce head losses and increases efficiency, particularly when the groundwater flows

perpendicular to the tunnel axis (*Table 1.2*). Distances between parallel tracks of tubes are in the order of 20-40 cm.

Segments in general are in the order of 30 to 50 cm thick, function of the geotechnical conditions of the ground and of the geometric characteristics of the tunnel: this variation in terms of thickness allows to place the pipes in different configurations. When pipes are only installed in the first external 5-15 cm of the segments, they promote the heat exchange with the ground and they constitute a *ground system* (*Figure 1.12.b*), it can be used for district heating and cooling; on the contrary, if pipes are installed in the first internal 5-15 cm of the segments, they mainly exchange heat with the air in the tunnel, constituting an *air system* (*Figure 1.12.c*), it can be used to cool hot tunnels in order to save on costs of ventilation and cooling systems; when both of the abovementioned configurations coexist, it means that heat is exchanged in a *ground & air system* (*Figure 1.12.a*).

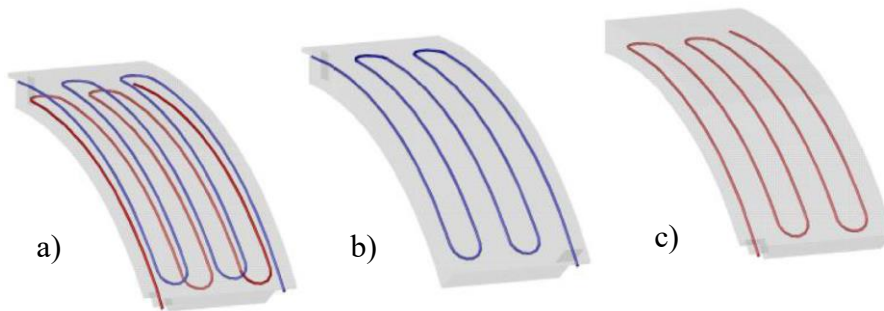


*Figure 1.12. Configurations of the ENERTUN segmental lining: a) ground&air, b) ground, c) air. (Barla and Di Donna, 2018)*

This system is suitable for heating and/or cooling neighbouring utilities: thermo-hydraulic and thermo-mechanical coupled analysis and simulations have been run, with all the related difficulties. Particular attention has been paid to the presence of air inside tunnels, compared to the other energy geostructures, new boundary conditions have been considered.

As reported in *Table 1.2*, when talking about the Enertun segmental lining, the increase in thermal exchange is in the order of 5% to 10% compared to the traditional configuration, in addition, the decrease in terms of heat losses is between 20% and 30% for each tunnel ring (Barla and Di Donna, 2018).

Table 1.2. Heat exchange comparison between two segmental lining with different configuration of the loops – winter season (Barla and Di Donna, 2018)

| <b>Pipes main direction with respect to tunnel axis</b> | <b>Total extracted power</b> | <b>Extracted power per square meter</b> | <b>Extracted power per meter of tunnel</b> |
|---|------------------------------|---|--|
|   | <b>Q [W]</b>                 | <b>q [W/m<sup>2</sup>]</b>              | <b>q [W/m]</b>                             |
| Parallel  | 1670.79                      | 52.76                                   | 1193.42                                    |
| Perpendicular (ENERTUN)                                 | 1773.49                      | 56.00                                   | 1266.78                                    |

### 1.3.1.2 Examples of application

There are few existing case studies of energy tunnels. The Vienna LT22 testing plant was the first geothermally activated sprayed concrete lining tunnel in Austria. The absorber pipes were attached to a geosynthetic and placed between the primary and secondary tunnel lining.

More recently, thermal structures have been built by using TBMs, enabling tunnel excavation in weak ground with a minimal risk of damage to existing surface structures. An example is the Jenbach twin track highspeed rail tunnel in Austria, which incorporated a 54 m long demonstration section with thermally activated segmental tunnel lining equipped with heat exchange pipes (Frodl et al., 2010; Franzius and Pralle, 2011). More recently, in 2016, some new energy segments, called ENERTUN, were installed in the Metro Line 1 of Turin (Barla & Di Donna, 2016).

#### Lainzer tunnel – Vienna (Austria)

The first thermo-active traffic tunnel took place in Vienna, Austria. It is known as the “Lainzer Tunnel”, and links the northern Vienna area with the Eastern Europe for 12.8 km. The activation involves a large quantity of geothermal energy, useful for heating/cooling railway stations, neighbouring buildings and for keeping platforms, bridges, passages etc. de-iced during winter.

In order to optimize the thermal design, understanding in a better way the thermal behaviour, some geothermal projects have been carried out in the Lainzer Tunnel, which has been built in several sections by two main methods:

1. *Cut and cover*, for example section LT24 (Hadersdorf-Weidlingau), which has been equipped with an *energy plant*;
2. *NATM*, for example section LT22 (Bierhäuslberg), which has been equipped with an *energy membrane*.

In addition, in the Hetzendorferstraße section of the tunnel, an *energy well* has been installed, in order to investigate its performances and to lower the groundwater level.

### *LT24, Hadersdorf-Weidlingau*

In the LT24 cross-section there are 59 bored energy-equipped piles, with a diameter of 1.2 m and an average pile length of about 17.1 m, one every three piles of the primary side wall lining (*Figure 1.10*). The energy piles are equipped with absorber pipes, situated behind reinforcement bars, connected to collector/distributors, easily accessible on top of the cut and cover tunnel. This section contains a lot of different measurement devices in order to investigate aspects of thermal behaviour in tunnels, because the project is part of a research initiative of the Austrian government. Between those devices there are temperature gauges and combined strain-temperature gauges, heat picture photographs were used to check the temperature differences between energy piles and standard piles and the groundwater temperature surrounding the energy plant was registered (Brandl, 2016).

The energy plant started working in February 2004, and the data obtained during the first testing phase were used to optimize the absorber system. Since autumn 2004 the energy system runs permanently for a school near the tunnel (*Figure 1.9*) and, if the external temperature is higher than  $-5\text{ }^{\circ}\text{C}$ , it is its only heating source.

## Geothermal Energy

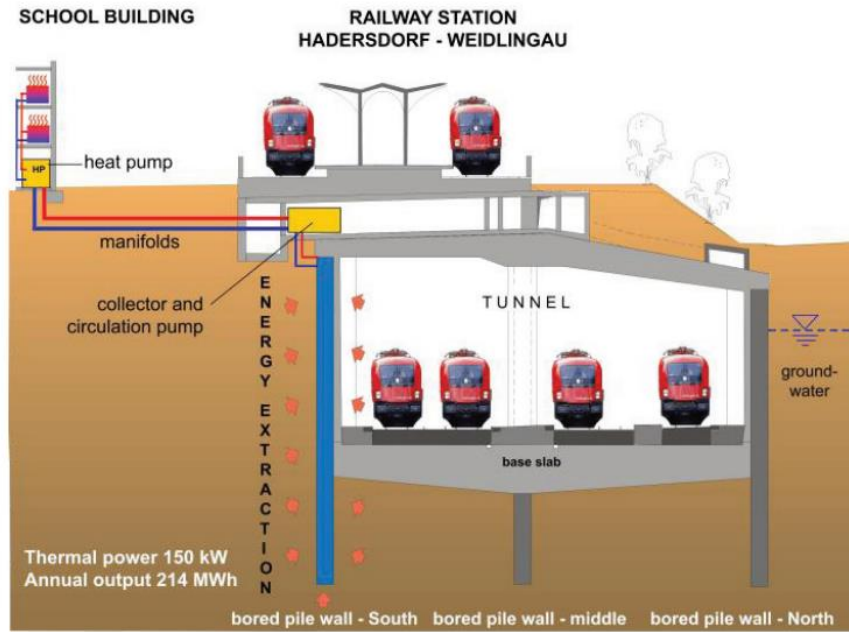


Figure 1.13. Cross-section LT24, one side wall of cut and cover tunnel used as energy wall (Brandl, 2016)

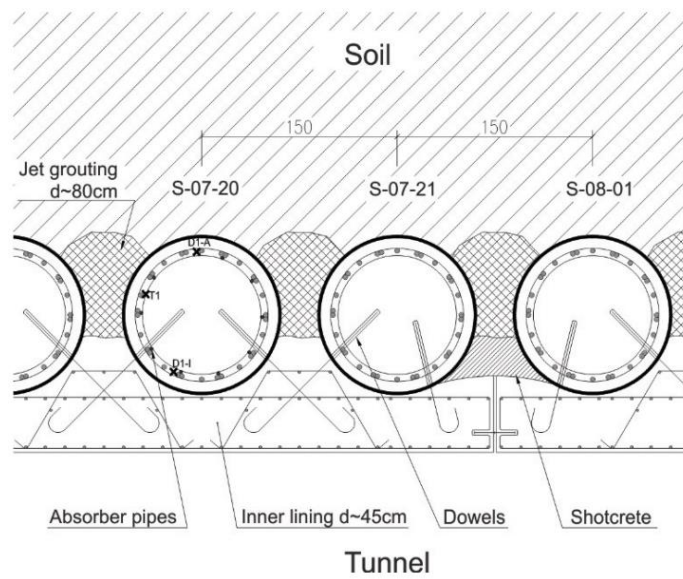


Figure 1.14. Longitudinal section through the energy tunnel wall. The pile S-07-20 is a thermo-activated pile with also measurement devices (Brandl, 2016)

Table 1.3 reports the most relevant technical data of the LT24 plant, while Table 1.4 demonstrates environmental and economic benefits of this plant.

## Geothermal Energy

*Table 1.3. Technical data of the energy plant LT24 (Brandl, 2016)*

|                                       |  |
|---------------------------------------|--|
| Annual heating output                 | 214 MWh  |
| Energy piles                          | 59 units   |
| Mean length                           | 17.1 m   |
| Heating piles                         | 150 kW   |
| Required antifreeze passage           | 51.6 m <sup>3</sup> /h                           |
| Absorber pipes HDPE                   | d <sub>o</sub> = 25 mm<br>d <sub>i</sub> = 20 mm |
| Absorber circuits                     | 80 units   |
| Absorber pipes in piles, total length | 9709 m   |
| Connecting lines, total length        | 13754 m  |

*Table 1.4. Environmental and economic benefits LT24 plant (from Brandl, 2016)*

|  |                             |
|--|-----------------------------|
| Reduction of natural gas   | 34,000 m <sup>3</sup> /year |
| Decrease of CO <sub>2</sub> emissions  | 30 t/year                   |
| Savings in operation costs (compared to the old natural gas heating system of the school building) | 10,000 €/year               |

### *LT22, Bierhäusberg*

In this section of the tunnel the NATM excavation method has been used, requiring special absorber elements for heat extraction/storage. An energy membrane is created, composed of three main structural elements (*Figure 1.11*):

1. Energy anchors;
2. Energy geosynthetics (non-woven geotextiles and geocomposites);
3. Thermo-active secondary lining.

All the above-mentioned elements allow to thermally activate a large volume of the surrounding ground, represented with the light blue thickness in *Figure 1.15*.

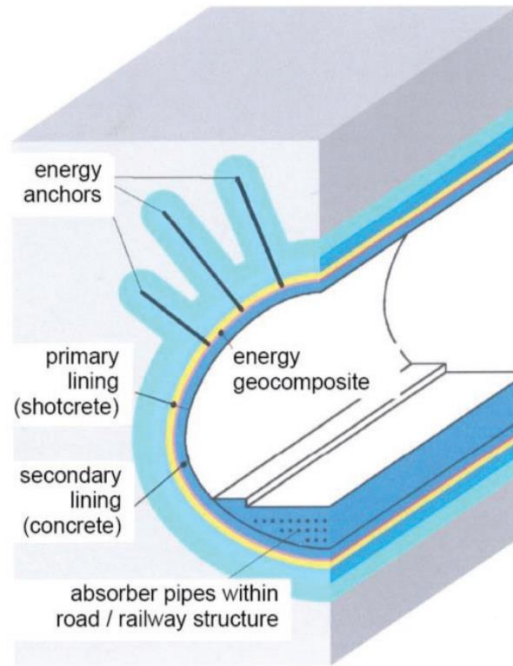


Figure 1.15. Energy membrane in a NATM excavated tunnel (Brandl, 2016)

### Jenbach tunnel

Tunnel Jenbach on the northern approach route to the Brenner Base Tunnel, is a section of the TEN axis 1 “Berlin-Palermo” tunnel equipped with energy lining segments, which enable the laying of absorber pipework in the TBM-driven tunnel. Such a system – the energy lining segment – has been developed to supply heat to a building on the surface, far less than 150 m from the access point to the tunnel (Figure 1.16 and 1.17).

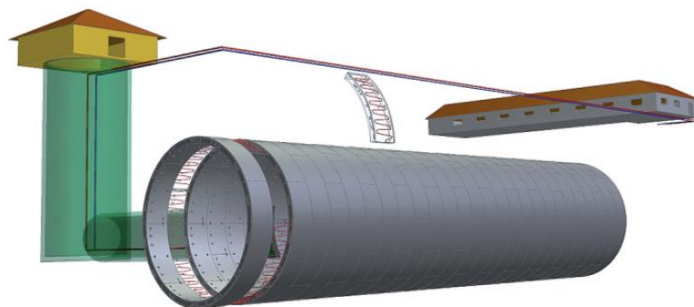
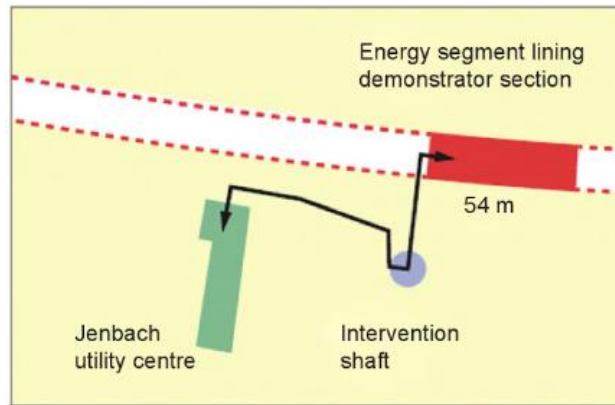


Figure 1.16 CAD view of the energy system (Frodl et al., 2010)

## Geothermal Energy



*Figure 1.17. Layout of demonstrator project in Jenbach, Austria (Franzius and Pralle. 2011)*

Energy lining segments contain absorber pipes of cross-linked polyethylene (PE-X) laid in loops to extract heat from the soil or deliver heat to the soil. The same reinforcement cages and formwork sets are used for making the energy segments as for conventional segments, ensuring that the production of the energy segments can be efficiently incorporated into standard production. The design of the energy segments and pipework had to be integrated into the existing design.

The tunnel is 12 m in diameter and situated 27 m below the surface. Each concrete segment that forms the tunnel lining is 2 m wide and 0.50 m thick. 27 rings of energy segments were installed in the tunnel, corresponding to a length of 54 m. The ring is formed with seven segments and a keystone. In each segment, there are about 25 m of absorber pipes, resulting in a total of about 175 m per ring. The geothermal system is designed to cover the basic demand of about 40 kW for a municipal building above the tunnel. The gas heat pump is designed for typical peak loads (around 80 kW at an outdoor temperature of  $-16^{\circ}\text{C}$ ).

*Table 1.5. Geometrical information of the Jenbach tunnel energy plant*

|                                   |               |
|-----------------------------------|---------------|
| Energy elements (7 segments/ring) | 27 rings      |
| Ring thickness                    | 0.50 m        |
| Ring width                        | 2.00 m        |
| Total activate length             | 54 m          |
| Absorber pipes PE-X               | $d_o = 20$ mm |
| Absorber pipes per segment        | 25 m          |
| Absorber pipes per ring           | 175 m         |

The project has been also equipped with a monitoring system, which allows the measurement of the temperature of the segments among other information. This data should permit the optimisation of future geothermal systems in tunnels.

### **Torino Metro Line 1**

A new South extension of the Metro Torino Line 1 (1.9 km and 2 stations) from Lingotto toward Piazza Bengasi is currently under construction. This portion has been considered as it provides a good opportunity to test the energy tunnel technology in the Torino subsoil (*Figure 1.14*). The tunnel has been excavated by four shielded EPB TBM (Earth Pressure Balance Tunnel Boring Machine) with a diameter of about 8 m (internal diameter 6.8 m and external diameter 7.4 m). The average cover of the tunnel is 21.5 m and excavation took place below the water table. The tunnel lining is made of precast concrete rings (thickness 30 cm), each constituted by 6 segments installed by the TBM itself, 1.4 m wide. The average rate of construction was about 10 m per day. Cement foam is injected to guarantee full contact with the ground and the segments are appropriately sealed in order to avoid groundwater incomings.

Under the thermal point of view, it is a cold tunnel as ventilation is guaranteed by several wells that inject external air into it. In order to allow easy inspection during the tunnel lifetime, with the metro system in service, the inflow pipe and the outflow pipe are located in the sidewalls of the tunnel, below the security pedestrian footpath.

Thanks to a large amount of data about the Turin subsoil properties and conditions (Bottino and Civita, 1986; Barla and Barla, 2005, 2012; Barla and Vai, 1999), it was possible to establish hydraulic and thermal average parameters, reported in *Table 1.6*. Turin subsoil is characterized by the presence of a sand and gravel deposit, from medium to highly dense; from a depth of 8-10 m lenses of cemented soil are often present. At the site, the water table surface is about 12 m below the ground level and the aquifer is 22-23 m thick, with an average temperature of 14 °C and it flows toward the Po River.

## Geothermal Energy

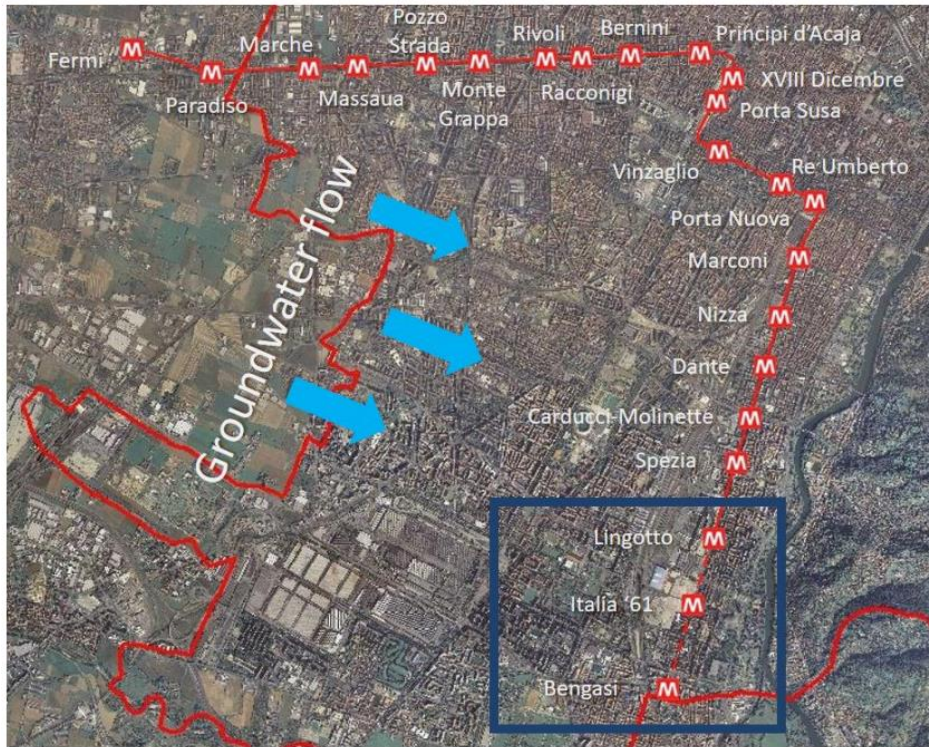


Figure 1.18. Torino Metro Line 1 layout with highlighted South Extension (Barla, Insana, 2018)

Table 1.6. Hydraulic and thermal average parameter of Turin subsoil (Barla et al., 2015)

|  |                                     |                              |
|--|-------------------------------------|------------------------------|
| Horizontal hydraulic conductivity                | $k_h$ [m/s]                         | $3.8 - 4.5 \cdot 10^{-3}$    |
| Vertical hydraulic conductivity                  | $k_v$ [m/s]                         | $0.19 - 0.225 \cdot 10^{-3}$ |
| Porosity   | $n$ [-]                             | 0.25                         |
| Heat capacity of the water                       | $\rho_w c_w$ [MJ/m <sup>3</sup> /K] | 4.20                         |
| Heat capacity of the solid                       | $\rho_s c_s$ [MJ/m <sup>3</sup> /K] | 2.00                         |
| Thermal conductivity of the water                | $\lambda_w$ [W/m/K]                 | 0.65                         |
| Thermal conductivity of the soil solid particles | $\lambda_s$ [W/m/K]                 | 2.80                         |
| Longitudinal dispersivity                        | $\alpha_L$ [m]                      | 3.10                         |
| Transversal dispersivity                         | $\alpha_T$ [m]                      | 0.30                         |

In this scenario a real-scale energy tunnel prototype was recently implemented.

## Geothermal Energy

First, a numerical model of the thermally activated tunnel ring has been computed in order to determine the exploitable heat, optimize the geothermal plant and assess the thermal activation consequences on the surrounding soil. A first 3D model was computed to study the efficiency of the system by reproducing a portion of the instrumented tunnel lining and a 2D large scale model of Turin aquifer was run to investigate the effects of the activated tunnel on the surrounding environment (Barla and Di Donna, 2016). All the material properties, such as pipes, ground, concrete, internal air, have been set up, in order to have a precise model, reproducing the real conditions of the system. During the simulation the inlet flux of the carrier fluid was fixed at 0.5 m<sup>3</sup>/h (inlet fluid rate of 0.4 m/s) and the inlet temperatures of 4 °C in winter (heating mode) and 28 °C in summer (cooling mode) were assumed. It has been possible to derive two main behaviours, one for winter seasons and one for summertime. Results are reported below, in *Table 1.7*.

*Table 1.7. Extracted/injected heat in winter and summer by modelling - Torino Metro line 1 (Barla and Di Donna, 2016)*

| Season | Total extracted/ injected power<br>Q [kW] | Extracted/injected power per square meter<br>q [W/m <sup>2</sup> ] | Extracted/injected power per meter of tunnel<br>q [W/m] |
|--------|---|--|---|
| Winter | 1.67                                      | 52.76  | 1193.42   |
| Summer | 2.34                                      | 73.87  | 1670.81   |

Analysing the effects of the energy tunnel on the surrounding ground, it resulted that the influence in terms of temperature variations of the groundwater flow is within 5 °C at 10 m distance from the tunnel contour and a full recovery takes place after the year-round cycle.

The aim of a real-scale energy tunnel prototype is to assess the thermal performance of the Enertun energy segment concept, patented by a research group of Politecnico di Torino (Barla & Di Donna, 2016), for its future implementation along the Metro Line 2, at present under design.

Under an economic point of view, the additional cost required to activate the tunnel lining was computed to be less than 1% of the total cost of the project. Compared to the use of vertical piles with ground source heat pumps, an energy tunnel that cover the same energy requirement, is 41% less expensive.

## Geothermal Energy

The experimental site has been installed near the Bengasi station, as shown in *Figure 1.15*. The real-scale prototype of energy tunnel consists of two rings (number 179 and 180 – ref to *Figure 1.19*) equipped with the *ground&air* configuration, for a total longitudinal length of 2.80 m. The heat pump and data acquisition system are in a “control room”, easy to reach without interfering with the TBM work.

In each segment, four special coupling pockets were included at the intrados, in order to connect the *ground&air* nets of pipes to the adjacent segments’ ones, once they are on site. There are two continuous circuits in each segment, one at the extrados and the other at the intrados (Barla and Insana, 2018).

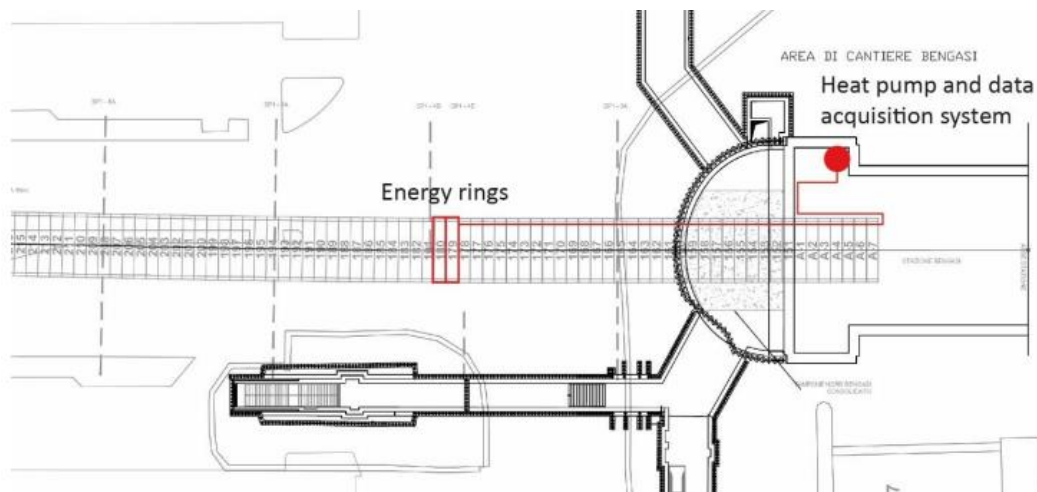


*Figure 1.19. Experimental site location (Barla and Insana,2018)*

*Table 1.8. Geometrical information of the Turin ML1 prototype energy plant*

|                                   |  |
|-----------------------------------|--|
| Energy elements (6 segments/ring) | 2 rings                                      |
| Ring thickness                    | 0.30 m                                       |
| Ring width                        | 1.40 m                                       |
| Total activate length             | 2.80 m                                       |
| Absorber pipes PE-Xa              | d <sub>o</sub> = 20 mm<br>thickness = 2.0 mm |
| Flow and returns pipes PE-Xa      | d <sub>o</sub> = 32 mm<br>thickness = 2.9 mm |

## Geothermal Energy

Table 1.9. Timeline of the process - from casting to operating mode

|   |                |
|---|----------------|
| Cast, curing and testing of the energy segments       | May 2017       |
| Implementation and connection of the segments on site | July 2017      |
| Monitoring (undisturbed conditions) from              | September 2017 |
| Heating mode tests                                    | October 2017   |

As reported in *Table 1.9*, from the end of October 2017 some heating mode tests started, one of them, for instance, carried out for the ground circuit (both rings 179 and 180) at a target temperature of 30 °C for slightly more than two days, resulted in a total extracted power of 1.59 kW, equivalent to 48.70 W/m<sup>2</sup> and 1132.25 W/m.

Preliminary experimental results are very promising and in line with existing thermo-hydro numerical models (i.e. *Table 1.6*); anyway, further study is needed to verify this trend under different operating conditions of the system, for example under the summer operational mode (Barla and Insana, 2018).

The prototype was also instrumented with a specifically designed monitoring system to monitor stresses, strains and temperatures in the lining (Barla and Insana, 2018). It is possible to find:

- pressure cells, to monitor radial, hoop and longitudinal stresses;
- intrados and extrados vibrating wire strain transducers, to monitor hoop and longitudinal strains;
- embedded thermistor, to provide local temperature measurements;
- a monitoring system based on single-mode fiber optics sensors, to measure strains and temperatures at various locations after a post-processing step;
- multimodal fibers, to return distributed measurements, all along the ring's length;
- a temperature probe located inside a piezometer well within the construction site, to monitor the upstream groundwater temperature;
- additional probes, to monitor tunnel air and segments surface temperature.

### 1.4 Sustainability

Considering the uncontrolled rising global temperature, mainly due to the overuse of fossil resources and the consequent pollution, the development of sustainable alternatives in the energy production is needed, today as never before.

Geothermal energy can be called a *green energy*, it is considered as an environmentally friendly, renewable and sustainable energy (Hähnlein et al., 2013).

Its renewability is because the heat flow coming from the centre of the Earth continuously heats the fluid circulating in the ground: after having been exploited, fluid enters again the reservoir from the recharge zones or from the injection wells. The circulation of heat and fluid can be considered constant.

A sustainable use of these resources means maintaining them with care, in order to have the possibility to use them in the present, but also to leave them available for future generations. Heat can be extracted at different rates: the idea is not to overexploit resources at high rates, so that the extracted energy can naturally be replenished and the resource can be considered inexhaustible and renewable. In other words, the rate of consumption should not exceed the rate of generation, so that the heat removed from the resource is replaced on a similar time scale. Considering sustainability under a technical point of view, a geothermal system be sustainable if long production ability is guaranteed (> 30 years).

Even the geothermal resources have environmental, technical and social consequences: they influence the biological, chemical and physical characteristics of the groundwater and the subsurface, so it is important to balance their exploitation with nature's needs. To make an example, an increase in temperature of a lake of just 2 or 3 °C can irreversibly damage its ecosystem.

The most economical and environmentally friendly is a seasonal operation with an energy balance throughout the year, hence heating in winter (i.e. heat extraction from the ground) and cooling in summer (i.e. heat sinking/recharging into the ground).

GSHP systems have very low emissions of CO<sub>2</sub> into the atmosphere, they can reduce energy consumption – and corresponding air pollution emissions – up to 44% compared to air source

heat pumps and up to 72% compared to electric resistance heating with standard air-conditioning equipment (Manzella, 2017).

Talking about energy geostructures, sustainability of such system lies in the use of the building elements which are already needed for structural reasons, exploiting the thermal storage capacity of the ground but above all of the concrete (it is higher than ground's) that can be used as an energy storage element. There are several advantages, from an energy point of view: first of all, CO<sub>2</sub> emissions can be reduced up to 50% for new buildings; the use of primary energy is reduced and renewable energy takes its place.

Energy foundations and thermo-active elements contain closed coils of plastic piping through which a heat carrier fluid is pumped that exchanges energy from a building with the ground. In this sense, closed systems avoid the chemical pollution of the groundwater and the surrounding soil, they do not use water from the aquifer.

To conclude with an economical-sustainable point of view, geothermal energy, if correctly exploited, can assume a significant role in the energy balance of the countries: it is a way to exploit local resources without the necessity to buy energy from other countries.

## **2 INVESTIGATION AND PARAMETERS ASSESSING**

The geotechnical and thermal characterization of soils and rocks is a determinant aspect when designing an energy geostructure: a competent analysis reduces the risk of unsuccessful results and allows the optimization of the economic resources available for the construction.

Investigation is the key step to understand the parameters that govern the system and it includes laboratory and in situ tests. An important aspect is to investigate a representative volume of ground (REV, Representative Elementary Volume), in order to have results that correspond to the real ground conditions.

Considering tunnelling, the aim of investigations is to obtain the information that is necessary to establish the alignment, the cross section, the excavation procedures, the design of appropriate supports and water sealing. This process is not only useful to get the soil and rock properties, but also the future configurations during excavation, by developing realistic models of the behaviour of the ground in contact with the structure.

However, it is important to be always conscious of not being able to completely define existing subsurface conditions or to fully predict ground behaviour during construction. Due to the variation in the geotechnical conditions, the design of an underground structure cannot

be compared to a structural design of other buildings, where the loads, the system, and above all the characteristics of the used materials are known.

The results from investigation are usually interpreted by geotechnical and thermal models, which have intrinsic uncertainties. An important aspect to be underlined is that the design is continuously updated during all the steps of construction, based on the findings on site. In underground structures, depending on the geotechnical conditions, different failure modes can be expected. Depending on the potential failure modes, it is important to choose specific construction measures to ensure stability.

Laboratory and in situ tests must be considered complementary and they are not alternatives. Investigations on site have the advantage to give with good accuracy and continuity a snapshot of the geostatic conditions. Laboratory tests are often the best way to study not only the short-term behaviour of the analysed soil/rock, but also the long term. The accuracy is function of the realisation of the samples, i.e. “degree of disturb”, type of sampler and boring, execution procedure, and so on.

To successfully plan, design and construct an energy tunnel, various types of investigative techniques are required. The extent of the investigation should be consistent with the project scope, objectives and constraints. Factors as location, size, and budget, risk tolerance, long-term performances, geometry, constructability, aesthetics and environmental impact have an impact on the choices related to the investigation plans (Balasubramanian, A., 2016).

Geotechnical parameters are essential for the mechanical design of the tunnel and attention must be paid to the influence on them by thermal loads, while the assessing of thermal parameters is important to model the energy performance of the system.

## 2.1 Geotechnical investigation and parameters

Designing in underground is challenging, projects have big uncertainties, geology dominates the involved costs and investigations are more demanding than other foundation engineering problems because they must take into account a regional behaviour. The abundant geotechnical uncertainty requires tunnel exploration to be redundant and iterative.

### 2.1.1 Geotechnical investigation

Insufficient investigation can result in misleading information and can substantially increase the risk of not finding hazards and unknown conditions that can seriously delay or stop construction, with costly consequences (Parker, 2004).

Geotechnical services, data collection, and evaluation should begin very early in the conceptual planning of any project and should continue through construction and even after construction to document the as-built conditions and the behaviour of the tunnel in service.

In general, four main phases of investigation can be planned, the planning of each phase should be based on the results of the previous one (Raines, 2016).

#### 1. *Planning Phase*

At the very beginning it is important to study all the geologic maps of the construction site, data from previous reports and case histories, data from aerial photos/LIDAR interpretation, in order to make a preliminary map with all the collected data (discontinuities, faults, alteration zones, etc.). Conceptual geologic and geotechnical models should be developed, taking into account possible constraints that could affect the design. Once this information is available, it is possible to plan a subsurface investigation program.

#### 2. *Preliminary Design – Initial field investigations*

This is the phase where the bulk of the site characterization effort is applied: field conventional drillings and tests are implemented, surface and down-hole geophysics are run, samples are taken and the laboratory testing program is planned.

Sampling can be performed in most soil types, difficult in gravel-cobbles (Raines, 2016). It provides information relating to relative density, strength, and applicability

of some ground improvement methods (e.g., soil mixing, jet grouting, chemical grouting).

In *Table 2* are reported all the results that can be obtained when boreholes are drilled in soils; these data are fundamental in the first steps of the design process of every type of structure, not only for energy tunnels.

### 3. *Final Design – Additional/Follow-Up Field Investigation*

The aim of this phase is to identify all the specific geotechnical parameters that may impact the design: field and laboratory tests are performed. From the results of the investigation, geotechnical reports are drawn up.

### 4. *Final Phase – Construction*

Even during the construction phase, it is required a continuous investigation and monitoring of the site conditions, in order to optimize the construction process if results do not match with the previously obtained.

In *Table 2.1* a resume of the different types of investigation is presented. Each test can lead to different types of parameters, function of what the designer needs. For example, a single test like the triaxial test can give different results depending on the cohesion or the drainage conditions.

*Table 2.1. Basic physical information from drilling in soils*

| <b>Soils</b>  |
|---|
| <ul style="list-style-type: none"><li>• Lithology</li><li>• Soil type, USCS (Unified Soil Classification System)</li><li>• Colour</li><li>• Consistency/Density</li><li>• Grain size distribution</li><li>• Moisture</li><li>• Cementation</li><li>• Plasticity (Clays)</li><li>• Roundness</li></ul> |

### 2.1.2 Geotechnical parameters

In order to have an accurate design of an energy tunnel, the first and most important thing is to obtain all the parameters that govern the mechanical behaviour of the ground interacting with the structure.

When referring to index parameter tests, they are meant to be that kind of tests, which are useful to determine the physical properties of the ground, such as the unit weight, the size of grains and their distribution, the water content, the density and the indexes and limits (i.e. the plastic limit, the liquid limit, the plasticity index, etc.).

All the other geotechnical parameters can be determined by the evaluation of the in situ or laboratory tests results, depending on the imposed initial conditions it is possible to have different type of parameters from the same kind of test.

A fundamental set of parameters that is always required for designing a tunnel is the one of the *deformability parameters*, such as the Young's Modulus and the Poisson's coefficient. The *Young's Modulus* of a soil, also known as the deformation modulus, measures soil stiffness. It is often used for estimation of ground settlements and deformation analysis. The *Poisson's coefficient* is a non-dimensional value that can be defined as the amount of transversal expansion divided by the amount of axial compression, some typical values for different types of soil are reported in *Table 2.3*.

Another set of parameters is related to *strength parameters*. They control the behaviour of the ground at failure. Cohesion and friction angle describe the shear strength in soils. Its definition is mainly derived from the Mohr-Coulomb failure criterion (*Figure 2.1*). In the stress plane of shear stress-effective normal stress, cohesion is the intercept on the shear axis of the Mohr-Coulomb shear resistance line. The soil cohesion depends strongly on the consistence, packing, and drainage condition. If the conditions are undrained, the *undrained shear strength* is considered (*Figure 2.2*), it is useful to analyse short term stability or quick loading conditions. The *friction angle* is a shear strength parameter of soils, it is the angle of inclination with respect to the horizontal axis of the Mohr-Coulomb shear resistance line.

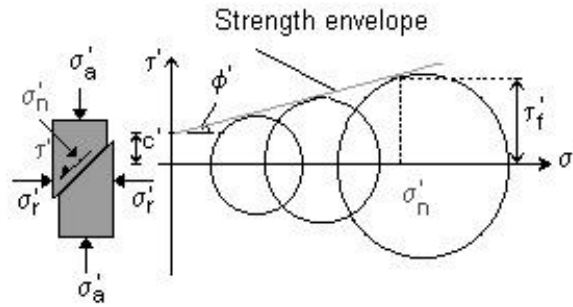


Figure 2.1. Mohr-Coulomb strength envelop, cohesion and friction angle are represented (Basic mechanics of soils, 2000)

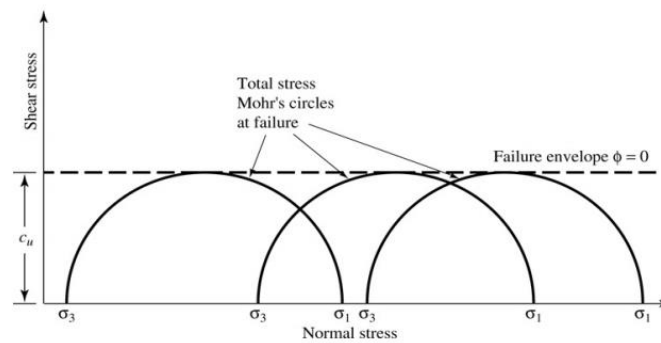


Figure 2.2. Mohr-Coulomb strength envelope for undrained conditions, it is horizontal.

The soil possesses resistance to shearing. The more the resistance to shearing, the less the horizontal pressure. In order to calculate the horizontal pressure, the *coefficient of Earth pressure at rest*, as coined by Terzaghi (1920), is used. In soils  $k_0$  can be defined as the horizontal-to-vertical stress ratio (Figure 2.3).

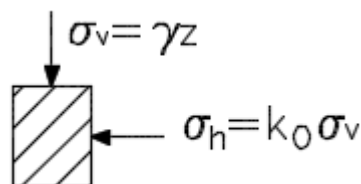


Figure 2.3. Simple representation of the coefficient of earth pressure at rest

There are several variants of its formulations in literature (Church, 2003), some of them are reported in Table 2.2, while in Table 2.3 some typical values for different types of soil are reported.

## Investigation and Parameters Assessing

*Table 2.2. Different formulations of  $k_0$  available in literature*

|   |  |           |
|---|--|-----------|
| Terzaghi's formulation for cohesive soils                               | $k_0 = \frac{\nu}{1 - \nu}$  | (Eq. 2.1) |
| Jaky's formulation for cohesionless soils (1944)                        | $k_0 = \left(1 + \frac{2}{3} \sin\phi'\right) \cdot \frac{1 - \sin\phi}{1 + \sin\phi} \approx 0.9(1 - \sin\phi)$ | (Eq. 2.2) |
| Jaky's simplified formulation for cohesionless soils (1948)             | $k_0 = (1 - \sin\phi')$  | (Eq. 2.3) |
| Schmertmann's formulation for overconsolidated soils                    | $k_0 = 0.5 \cdot (OCR)^{0.5}$  | (Eq. 2.4) |
| Moroto and Muramatsu (1987) formulation for overconsolidated clay soils | $k_0 = \sqrt{\frac{E_h}{E_v}}$   | (Eq. 2.5) |
| Mayne and Kulhawy (1982) formulation for overconsolidated soils         | $k_0 = (1 - \sin\phi')OCR^{\sin\phi}$  | (Eq. 2.6) |

*Table 2.3. Typical values of  $k_0$  for different types of soil, according to the Terzaghi's formulation (1944)*

| Soil type         | Typical value of Poisson's Ratio | K <sub>0</sub> |
|-------------------|----------------------------------|----------------|
| Clay, saturated   | 0.40 – 0.50                      | 0.67 – 1.00    |
| Clay, unsaturated | 0.10 – 0.30                      | 0.11 – 0.42    |
| Sandy Clay        | 0.20 – 0.30                      | 0.25 – 0.42    |
| Silt              | 0.30 – 0.35                      | 0.42 – 0.54    |
| Dense Sand        | 0.20 – 0.40                      | 0.25 – 0.67    |
| Coarse Sand       | 0.15                             | 0.18           |
| Fine-grained Sand | 0.25                             | 0.33           |

In *Figure 2.4*, some values of  $k_0$  from in-situ measurements are shown (Hoek & Brown data with recent integrations; Barla, 2011). Near the surface, values are scattered, while they assume a precise tendency with depth. Hoek & Brown proposed two equations, between

which most values are. At great depths, where soil is unable to deform laterally,  $k_0$  assume values between 0.3 and 0.5 and a good estimation of the coefficient is given by Eq. 2.1.

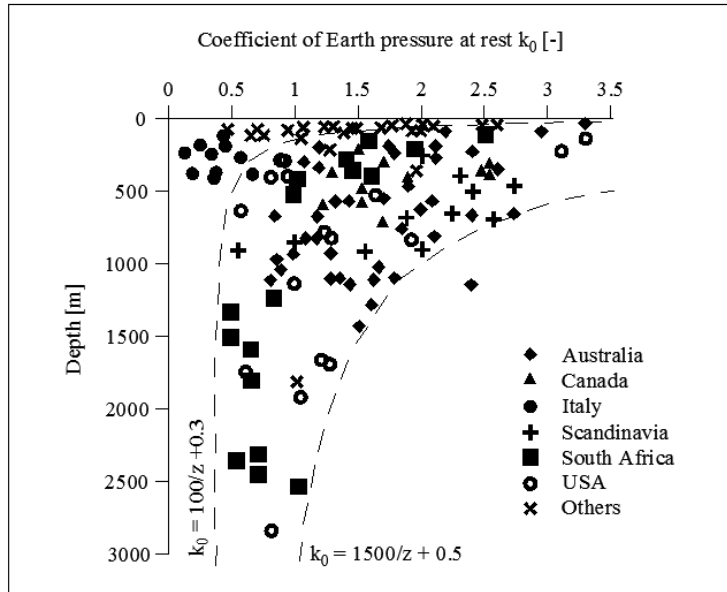


Figure 2.4. Coefficient of Earth Pressure at rest, real data from Hoek & Brown (1978) and recent integrations (Barla, 2011)

Another aspect that must be considered is the *dilatancy*, very important in soil behaviour, it can change the stress state around the tunnel. It manifests itself as a volumetric strain coupled to an applied shear strain. It is variable and mainly depends on soil density and stress level. In general, the denser the soil the greater the amount of volume expansion under shear (Figure 2.5). Because of dilatancy, the angle of friction increases as the confinement increases until it reaches a peak value. After the peak strength of the soil is mobilized the angle of friction abruptly decreases. As a result, slopes, footings, tunnels and piles in such soils could be subjected to a potential decrease in strength after the soil strength reaches this peak value.

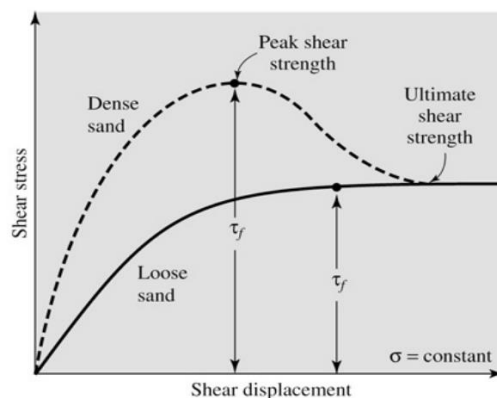


Figure 2.5. Different dilatant behaviour of dense and loose soils

### 2.1.2.1 Outcomes

Table 2.5 reports the geotechnical parameters considered in tunnelling, referred to the common investigation methods, contained in Table 2.4.

Table 2.4. Resume of laboratory and in situ tests for soils, useful to investigate parameters for tunnels design

| <b>Soils</b>         |   |
|----------------------|---|
| <b>Lab tests</b>     | 1 Eodometer Test  |
|                      | 2 Direct Shear Test   |
|                      | 3 Triaxial Compression Test   |
|                      | 4 Constant Head Permeability Test                                       |
|                      | 5 Falling Head Permeability Test  |
|                      | 6 Index Parameters Tests (Plasticity index, liquid limit, density, ...) |
| <b>In situ tests</b> | 7 SPT - Standard Penetration Test                                       |
|                      | 8 CPT - Cone Penetration Test   |
|                      | 9 HDP, MDP, LDP   |
|                      | 10 Marchetti Dilatometer Test   |
|                      | 11 Lugeon Test  |
|                      | 12 Geophysical Tests  |

Table 2.5. Geotechnical parameters for tunnel design and their determination, with reference to Table 2.2

| <b>Mechanical parameters</b>          | <b>Symbol</b>  | <b>Unit</b>       | <b>Determination</b> |                     |
|---------------------------------------|----------------|-------------------|----------------------|---------------------|
|                                       |                |                   | <b>Lab test</b>      | <b>In situ test</b> |
| Young's Modulus                       | E              | MPa               | 1, 3                 | 7, 8, 9, 10, 12     |
| Poisson's Coefficient                 | ν              | -                 | 1, 3                 | 12                  |
| Cohesion                              | c              | MPa               | 2, 3                 |                     |
| Undrained Cohesion                    | c <sub>u</sub> | MPa               | 3                    | 7, 8, 10            |
| Friction Angle                        | φ              | °                 | 2, 3                 | 7, 8, 9, 10         |
| Unit weight                           | γ              | kg/m <sup>3</sup> | 6                    |                     |
| Dilatancy                             | ψ              | °                 | 2, 3                 |                     |
| Coefficient of Earth pressure at rest | k <sub>0</sub> | -                 |                      | 10                  |
| Porosity                              | n              | -                 | 6                    |                     |
| Permeability                          | k              | m/s               | 1, 3, 4, 5           | 8, 11               |
| Over Consolidation Ratio              | OCR            | -                 | 1                    | 8, 10               |

### 2.1.3 THM behaviour of soils

Geotechnical parameters can be affected by the presence of thermal conduction, convection and radiation. Understanding the types of soils and conditions susceptible to these additional thermal processes is important, since their occurrence may lead to errors in property determination and, consequently, in the later system design.

Dealing with heat flux, often groundwater flow cannot be neglected and both thermal and hydraulic processes have impacts on the mechanical behaviour of the earth-structure system. This is the reason why a fully Thermo-Hydro-Mechanical (THM) coupled analysis should be adopted to study efficiency and integrity problems together; however, practically, a fully THM analysis is generally avoided due to its complexity and computational demand.

In general, it is possible to assume that the interaction between the thermal and the mechanical behaviour is only in one direction, temperature induces additional stresses and strain in the structure, but the mechanical actions on the temperature field are considered negligible. Between the thermal and hydraulic effects there is a mutual interaction: hydraulic conditions affect the thermal field and thermal loads induce changes in pore pressure and water flow regime. An example is the moisture migration in fine grained unsaturated soils. Considering an unsaturated soil means that water and air coexist in the pores of the solid phase: if a heating process occurs, it can cause pore water evaporation, as the water absorbs the energy associated with the latent heat of evaporation. The water vapour that arises from this process is susceptible to vapour pressure gradients and it migrates through the soil to an area of lower vapour pressure, where the temperature may also be lower, triggering the vapour condensation, which releases the latent heat in a new location. If the heat injection is too high, the soil may dry and a reduction of thermal conductivity can be a consequence. Mechanical and hydraulic effects are also combined, if pore pressure varies it induces effective stress on the structure, if mechanical loads change, they can induce a change in the porosity of the material. A brief representation is reported in *Figure 2.6*.

In *Figure 2.7* the main heat transfer processes in soils are reported, function of the degree of saturation and the effective size of grains, in soils and rocks, conduction is the dominant heat transfer process, even if convection and radiation can also occur. The thermal conductivity is the basic parameter that controls this phenomenon and mainly depends on density and

## Investigation and Parameters Assessing

moisture content of the material. System performances can be affected by free convection if the hydraulic conductivity of the soil is greater than around  $10^{-5}$  m/s in both vertical and horizontal directions, but usually, the presence of stratification in the ground reduces it, because less permeable layers can be present. When speaking of soils and rocks, it is better to consider the forced convection, a more significant phenomenon that occurs when there is a groundwater flow.

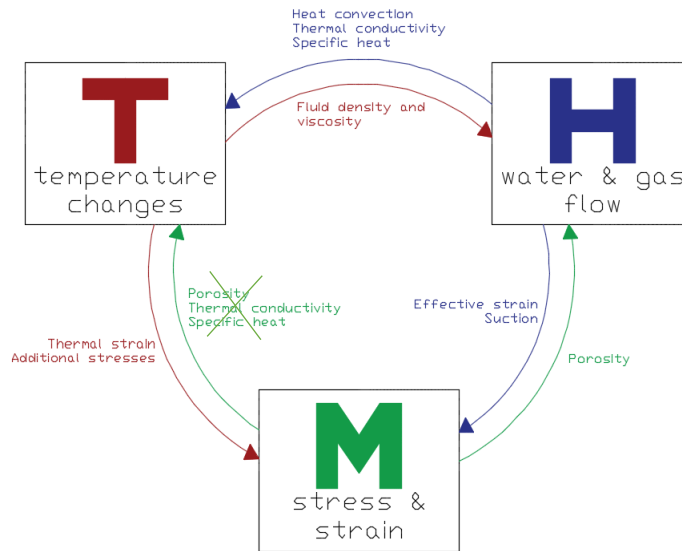


Figure 2.6. Schematic representation of relevant couplings in SGE system

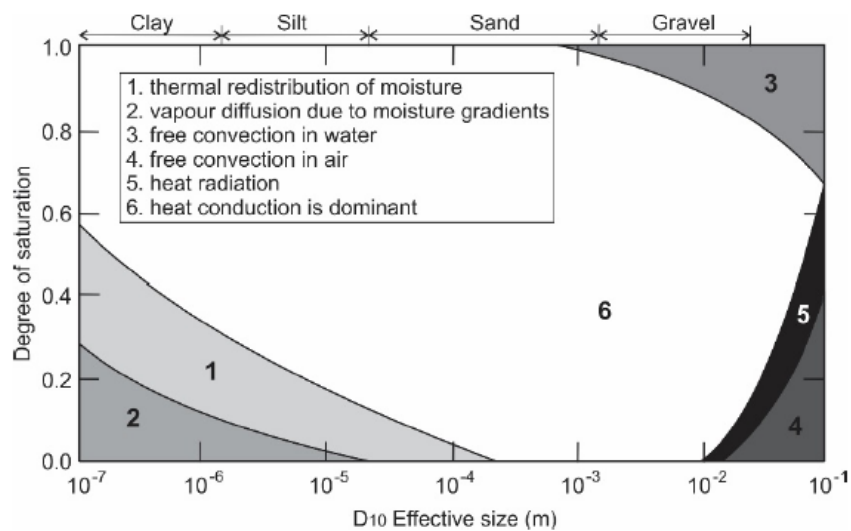


Figure 2.7. Heat transfer processes in soils (Vieria et al., 2017)

### 2.1.3.1 THM investigation

It has been proved that THM effects influence the energy geostructure design, anyway, there are no standardised tests for soil THM characterization. The THM response can be obtained using analytical solutions that evaluate an elastic thermal expansion coefficient, otherwise, a better way consists in typical soil mechanics laboratory tests, which can be properly equipped in order to control the temperature conditions.

Thermo-mechanical tests can be subdivided in three main groups, namely those involving heating by circulating fluid, heating with internal heaters, and heating with external heaters.

To characterise the THM behaviour, the best-established test is the temperature controlled triaxial test, because it is simple and key variables can be controlled, but also oedometers and direct/simple shear devices can be equipped to control the temperature. Shallow geothermal heat exchangers are subjected to seasonal temperature cycles, which can be reproduced in laboratory by applying to the samples cyclic thermal loads.

In *Figure 2.8*, the setup of a *triaxial test* with temperature control system is reported, it is possible to see the systems for control of stresses, strains, pore-water pressure and temperature. The heating system consists of the heater, the circulating device (pump), the insulation and the temperature controlling unit. Heating of the sample is obtained indirectly by circulating water inside a metal tube placed spirally around the sample. Temperature measurements are made by using two thermocouples.

The *direct shear test* apparatus used to estimate the THM behaviour of a material, has the traditional setup of a direct shear test apparatus, with some adaptations that allow to maintain constant temperature conditions during the test, for instance the addition of a copper tube connected to a heating/cooling circulator, thermocouples and some polystyrene sheets for insulating, as shown in *Figure 2.9*.

Its configuration is suitable to investigate the soil-structure interaction, both in monotonic and cyclic conditions, because one of the interfaces can be concrete and the other the soil, many investigations of this kind have been carried out for pile-soil interface. Results from these previous studies show that, when dealing with sand-concrete interface, temperature does not

affect the behaviour, on the contrary, if the soil is clay, it is sensitive to thermal variations, clay-pile interface strength increases with heating because of thermal consolidation.

However, recent studies do not present totally convergent conclusions on the results obtained by direct shear tests with monotonic or cyclic loading. Furthermore, this test is less reliable than others – due, for example, to the lack of information on the complete stress state of the tested specimen and the need to impose the orientation of the shear surface.

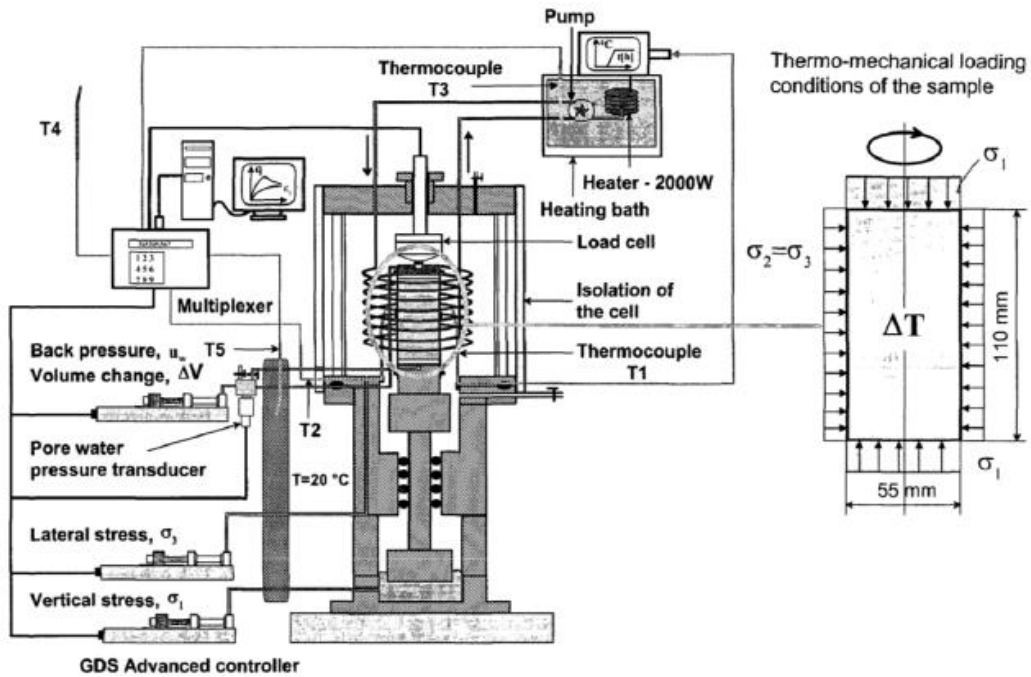


Figure 2.8. Triaxial device with controlled temperature (Cekerevac, 2003)

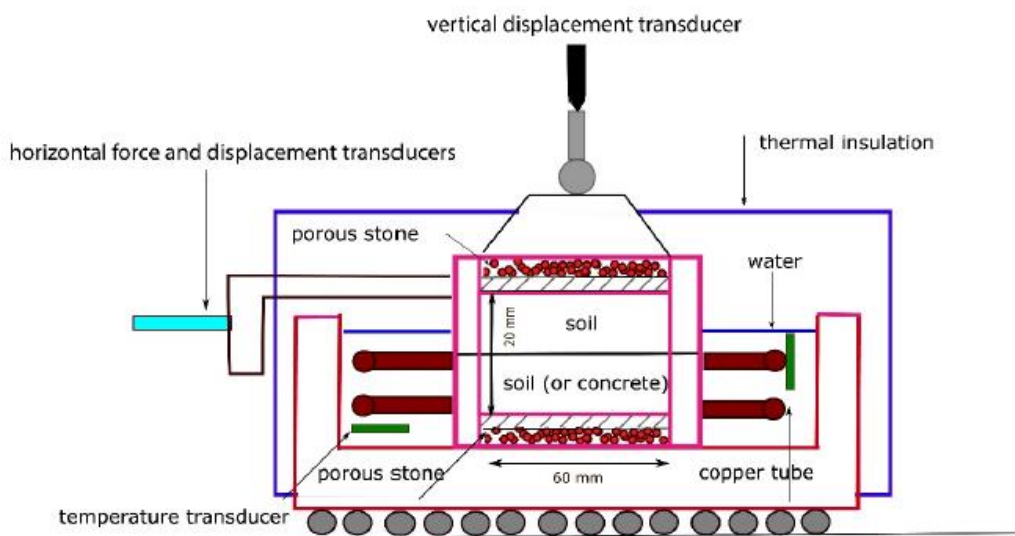
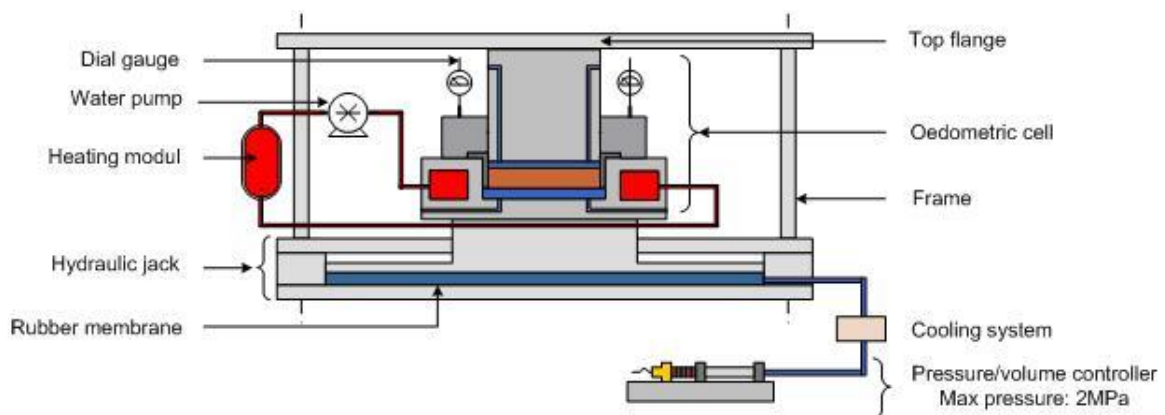


Figure 2.9. Direct shear apparatus with temperature control system (Vieira et al., 2017)

## Investigation and Parameters Assessing

The *THM Oedometer*, represented in *Figure 2.10*, is another advanced laboratory test and refers to an oedometer test with temperature and suction control. It allows characterizing the soil stress-strain behaviour during one-dimensional compression under controlled thermal and saturation condition. It allows testing of soil samples at different degrees of saturation and different temperatures. The temperature is usually controlled by means of a heating device consisting of a ring-shaped chamber surrounding the soil sample and filled with circulating heated water or oil. The liquid itself is heated to the desired temperature through an electric cryostat. An appropriate thermal insulation of the oedometer cell is required in order to avoid the influence of ambient room temperature. This can be done by placing the oedometer cell system in an insulated box or by using thermal insulating covers around the cell. The test is carried out on a cylindrical specimen of saturated or unsaturated soil. As in oedometer test, vertical static load is incrementally applied to the sample and the vertical displacement of the sample is measured at different loading steps. The difference is that the loading can be a combination of vertical stress, suction, and temperature variation. The results are then used to characterize the consolidation and the stress-strain behaviour of the soil under the influence of suction and temperature (François & Laloui, 2010).



*Figure 2.10. Oedometer with vapour equilibrium technique: vertical load and temperature application system (EPFL website)*

### 2.1.3.2 Influence of temperature on geotechnical parameters

Soil has a multiphase microstructure, which shows a complex THM behaviour, because each constituent's behaviour must be considered. The most influencing factors are the particle size, the degree of saturation, mineralogy and stress history.

The simplest way to analytically evaluate the thermo-mechanical soil response is to determine an elastic thermal expansion coefficient. It is possible to evaluate it, considering an elastic isotropic saturated soil element in free expansion conditions. The volumetric thermal expansion  $\epsilon_v^T$  and the excess pore pressure  $u$  are obtained by

$$\epsilon_v^T = -\beta T \quad (\text{Eq. 2.7})$$

$$u = \frac{(KK_f[n(\beta_w - \beta_g) - \zeta/T])}{K + K_f} T \quad (\text{Eq. 2.8})$$

Where:

- T applied temperature;
- $\beta$  volumetric free thermal expansion coefficient for any drainage condition,
- K,  $K_f$  bulk modulus of the soil skeleton and Biot's modulus, respectively. ( $K_f = 0$  for totally drained conditions);
- n porosity ( $K_f = K_w/n$ ,  $K_w$  the water's bulk modulus);
- $\zeta$  rate of water per unit volume flowing into or out of the soil voids ( $\zeta > 0$  for water flowing out of the voids,  $\zeta = 0$  in undrained conditions).

When thermal loads produce irreversible strains, it is not possible to refer to these formulations and elasto-plastic relationship would better describe the situation; to calculate thermo-plastically induced strain or stress, employing a critical state-type constitutive model it is typically necessary to numerically solve the equations.

It is useful to deepen the concept of volumetric free thermal expansion coefficient for any drainage condition,  $\beta_g$  and  $\beta_w$  are respectively for the soil particles and water,  $\beta$  is determined as reported in Eq. 2.9.

$$\beta = \frac{[K + (1 - n)K_f]\beta_g + K_f(n\beta_w - \zeta/T)}{K + K_f} \quad (\text{Eq. 2.9})$$

$\beta = \beta_g$  for totally drained conditions, consequently  $u = 0$ .

It is possible to correlate the volumetric thermal expansion coefficient to the linear thermal expansion coefficient  $\alpha$  with the following formulation:

$$\beta \cong 3 \cdot \alpha \quad (\text{Eq. 2.10})$$

In *Table 2.6*, typical values of volumetric thermal expansion coefficient for some soils, water at 22°C and concrete are reported.

*Table 2.6. Typical values of volumetric thermal expansion coefficient for some soils, water and concrete*

| Material     | $\beta$ [ $^{\circ}\text{C}^{-1}$ or $\text{K}^{-1}$ ] | Data from:                |
|--------------|--|---------------------------|
| Clay         | $4 - 6 \cdot 10^{-5}$                                  | Bodas Freitas et al. 2013 |
| Concrete     | $2 - 4 \cdot 10^{-5}$                                  |                           |
| Water (22°C) | $27 \cdot 10^{-5}$                                     |                           |

This parameter has been investigated with the above-mentioned laboratory THM tests by many authors among which Campanella & Mitchell (1967), Baldi et al. (1988), Cekerevac & Laloui (2004), Vieria et al. (2017); some results and considerations are described in the following pages.

In general, soils can be divided into two families with two different THM behaviour: granular (sand and gravel) and fine-grained (silt and clay) materials (Laloui & Di Donna, 2013).

When a THM triaxial test is run under isotropic conditions and heating/cooling process, behaviour is different if the sample is in drained or undrained conditions.

Heating a sandy soil in drained conditions results in an increase of volume directly related to the grains' thermal expansion coefficient. Since the water is free to flow away, it does not contribute to the volume variation of the material itself, even if it has a thermal expansion coefficient usually higher than that of grains.

In undrained conditions water is not able to freely expand, heating produces a pore pressure increase and, consequently, an effective stress decrease. As reported in *Figure 2.11*, the

general behaviour is such that an increase in temperature induces an increase in pore pressure (pressurisation) and a decrease in effective stress, if  $\beta_w > \beta_g$ , because the solid skeleton restrains water expansion. When temperature decreases, it occurs a decrease in pore pressure and an increase in effective stress.

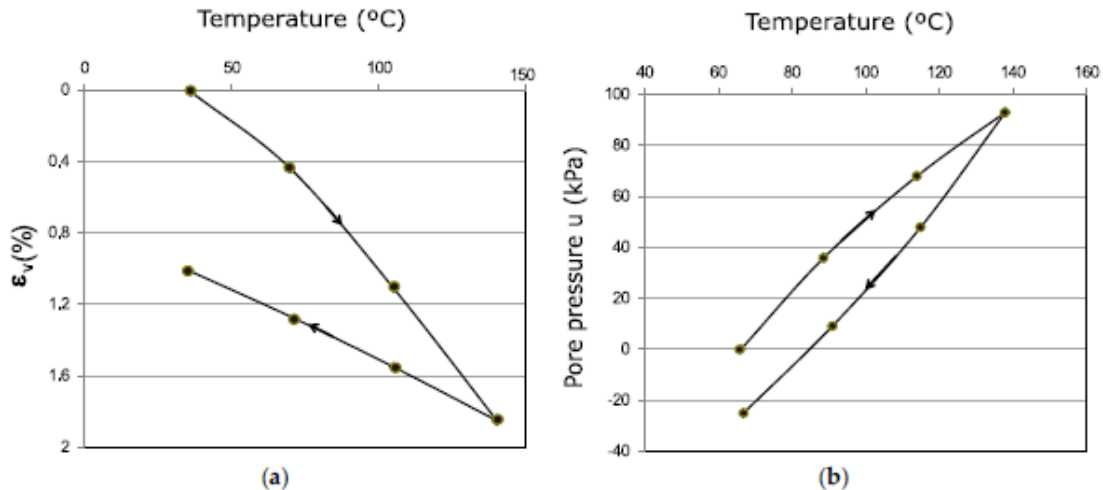


Figure 2.11. Results from a temperature-controlled TX test. Volumetric strain (a) and pore pressure change (b) in undrained conditions for saturated illite under a constant total stress of 200 kPa as a function of temperature. (Vieria et al., 2017)

Between the completely dry and fully saturated conditions, the partially saturated soil conditions introduce additional complexity, especially for fine grained soils, due to the presence of suction forces that are also temperature dependent.

During heating at constant mean effective stress, two plastic effects interact:

- Softening effect, due to a higher temperature;
- Hardening effect, void ratio reduces because of the thermal compaction.

The response of clayey samples varies in function of the Over Consolidation Ratio (OCR, the ratio between the preconsolidation stress and the current stress) and the soil type, in terms of clay activity. It has to be noticed that the potential for thermal volume change is proportional to the clay activity in the sample: the higher the activity, the higher the volumetric strain (Vieria et al., 2017).

If soils are normally or slightly over-consolidated, these effects cause an irreversible rearrangement in the soil particles and a density increase, which is not recovered during cooling and a residual strain remains. In highly over-consolidated samples, during drained heating, clayey soils initially show a dilatant behaviour, repulsive forces between clay

particles increase and make the interparticle spacing increasing (thermo-elastic dilation), possibly followed, for higher temperatures, by thermo-plastic volume reduction. During cooling, everything is recovered (Laloui & Di Donna, 2013)

This behaviour is clearly represented in *Figure 2.12*, where the path of the volumetric strain in function of the temperature is reported. For a NC clay, at the end of the heating/cooling process a high value of residual strain remains, while for the OC clay (OCR=6) heating and cooling follow almost the same path, showing a reversible behaviour. Between these two extreme cases, there is an intermediate case represented by slightly OC clays (OCR=2). In this case, the material shows initial dilation and subsequent contraction during heating, followed by contraction during cooling, thus representing a transition between the two main cases.

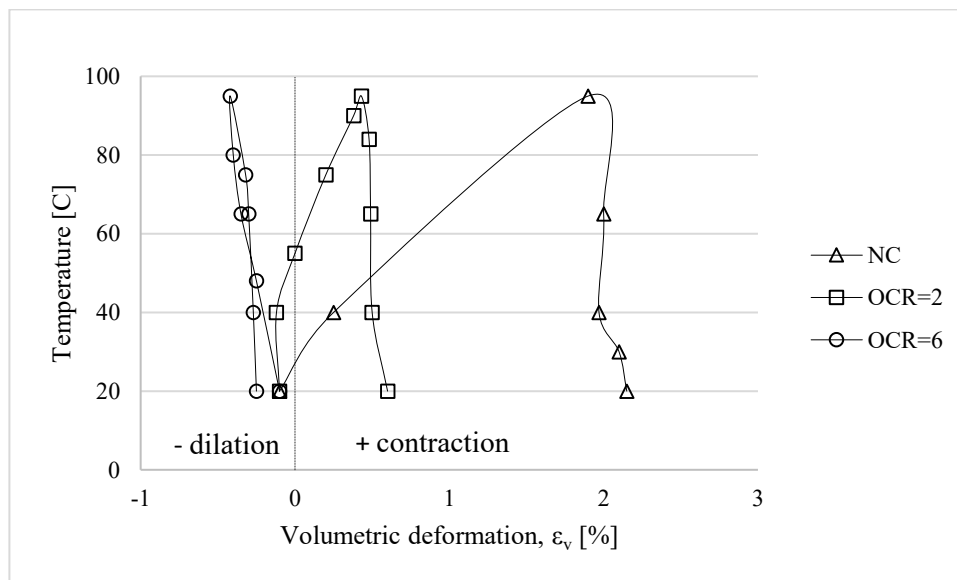


Figure 2.12. Thermal deformation of Boom clay under different initial conditions (data from Laloui & Di Donna, 2013)

In order to describe this phenomenon, several experimental studies on various clays have been performed. The conclusion is that the “apparent” preconsolidation stress decreases at constant void ratio with increasing temperature, as it is possible to see in *Figure 2.13*. “Apparent” means that the applied mechanical load does not change, so that the maximum load historically applied is always the same. This is called *thermal softening*.

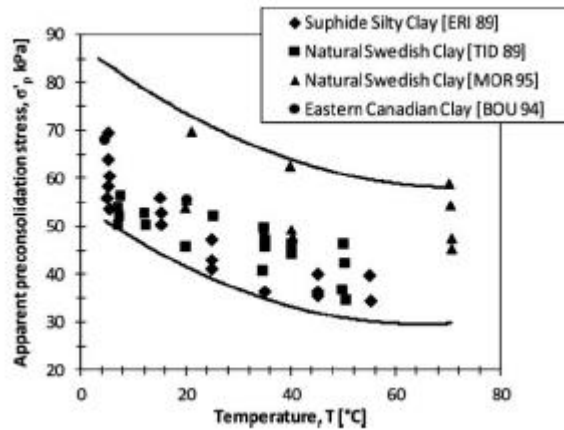


Figure 2.13. Influence of temperature on preconsolidation pressure (Laloui & Di Donna, 2013)

If a non-isotropic stress state is considered, when heated, an OC material undergoes plasticity earlier than in the isothermal case, while a NC or slightly OC material results in combination of thermal softening and hardening, as shown in Figure 2.14.

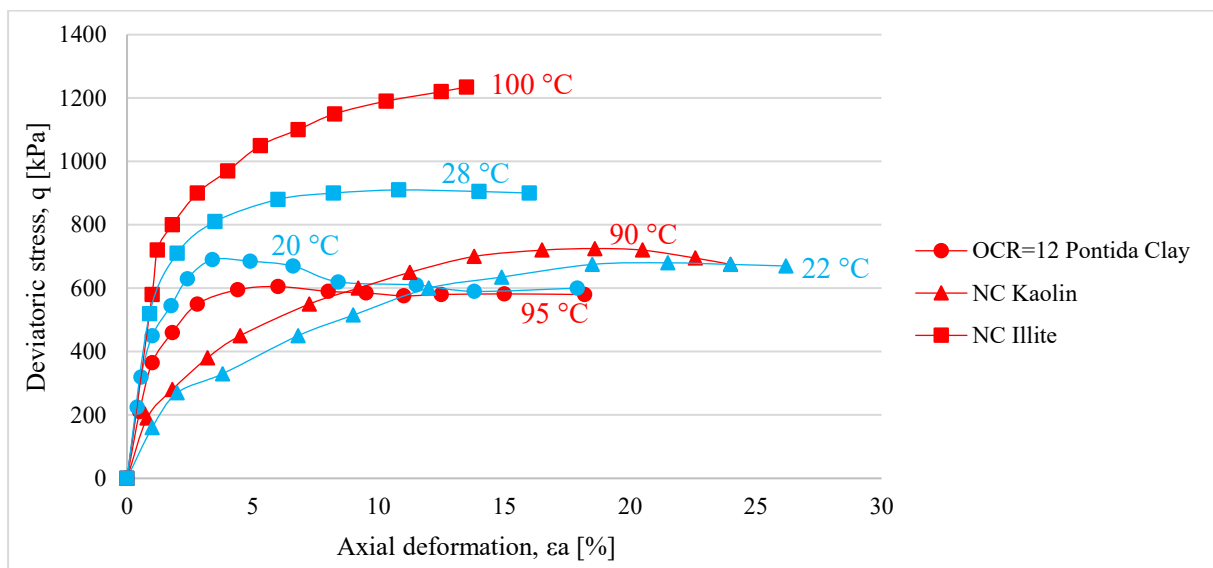


Figure 2.14. Shear strength at different constant temperature of OC and NC clays (data from Laloui & Di Donna, 2013)

When dealing with energy geostructures, the THM behaviour of the soil have to be investigated not only under a single monotonic heating process, but also under cyclic thermal loading, which reproduces the seasonal changes of temperature.

For NC materials it has been observed that during the first cycle the biggest irreversible volume change occurs, after that, an accommodation phenomenon takes place, because the subsequent cycles of the same magnitude produce only small increments of irreversible deformation (Figure 2.15).

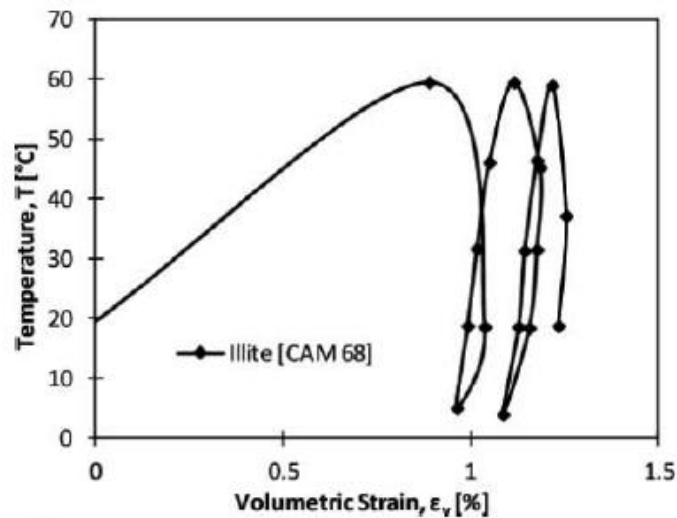


Figure 2.15. Thermal cyclic effect on an illite (Laloui & Di Donna, 2013)

It is expected that the initial OCR also influences the shear strength of the material at ambient temperature after the application of one or more thermal cycles. If the material is initially OC, a heating-cooling cycle does not produce any plastic deformation, so that the response under shearing is not affected because no permanent change is induced on the void ratio. Conversely, if an initially NC or slightly OC material is subjected to a heating-cooling cycle, strain hardening occurs as plastic deformation is produced. At an ambient temperature, the material ends up being thermally induced over consolidated and a higher stress is needed to plastify again (Laloui & Di Donna, 2013). The thermally induced consolidation also resulted in an increase in shear strength (*Figure 2.16a*).

For instance, if an NC sample is heated and then cooled in drained conditions and tested in a triaxial apparatus, its undrained shear strength is higher than that of an equivalent sample tested at constant ambient temperature, as shown in *Figure 2.16b*.

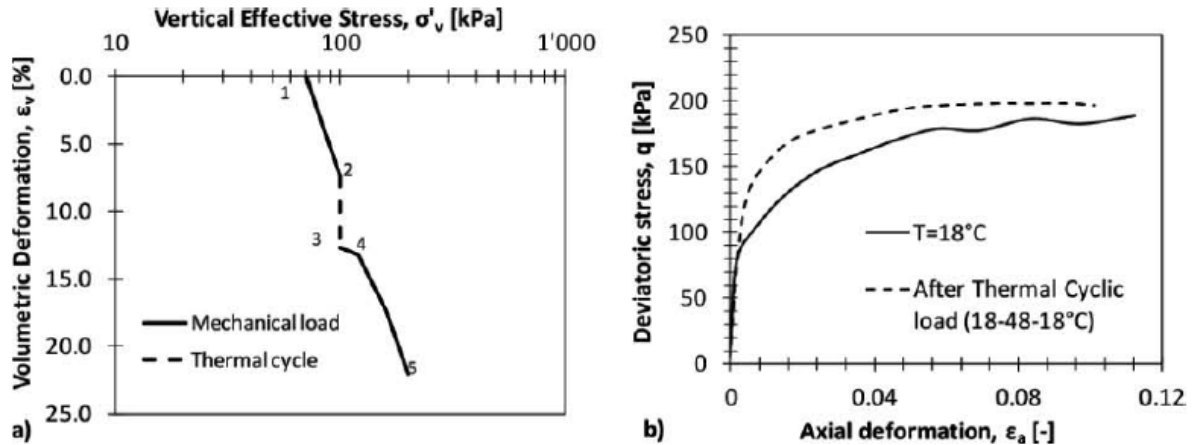


Figure 2.16. Thermal cyclic effects on a) consolidation of NC Bangkok Clay and b) undrained shear resistance of NC Tody clay (Laloui and Di Donna, 2013)

In addition to these statements, Di Donna, Ferrari and Laloui (2015) ran laboratory shear tests in order to study the sand-concrete and the clay-concrete interaction under different temperature conditions (20 and 60 °C). Results are different for the two type of soil.

In general, they concluded that for a *sand-concrete interface*, it has been possible to observe that no thermally induced effect occurred on the interface shear response and on the volumetric response, as it is possible to see in Figure 2.17. They could state that a change in temperature does not affect the shear strength parameters of the sandy soils in contact with concrete, and the internal friction angle is only function of the roughness.

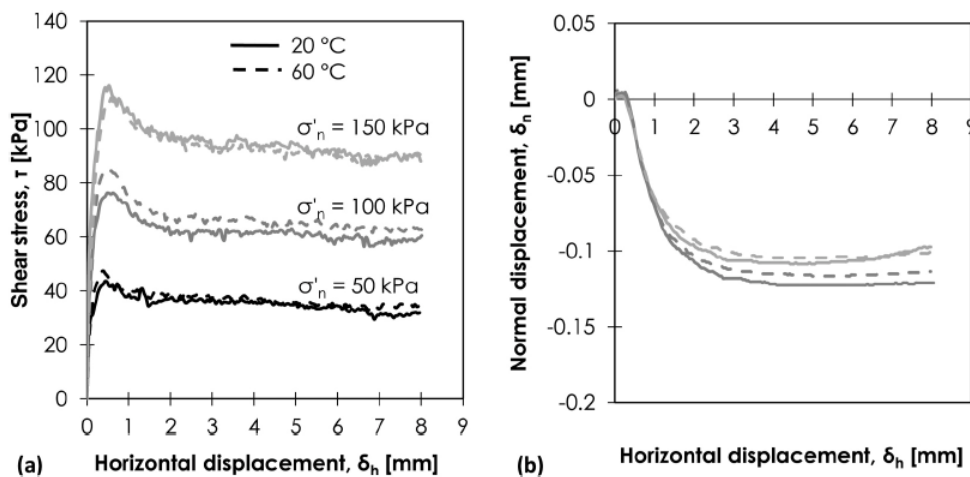


Figure 2.17. Sand-concrete interface tests at 20°C and 60°C (Di Donna et al., 2015)

When dealing with *clay-concrete interface* the situation is different and is a confirmation of the above-mentioned observation about the temperature effect on the geotechnical parameters. The response of clay-concrete interface changes at different temperatures shows an increase of strength with increasing temperature. The interface friction angle slightly reduces at high temperature, but the most significant thermal effect is found to be an increase in the adhesion between the two tested materials. This is related to the thermal consolidation of the clay, which results in an increase in the contact surface between the two materials (Di Donna et al., 2015).

### **2.1.3.3 Outcomes**

It is possible to say that the most influencing factors on the THM behaviour of soils are the Over Consolidation Ratio, the mineralogy and type of soil, the drainage and water conditions and the density.

Temperature affects the soil behaviour in three main ways: thermo-elastic expansion of soil particles and pore water, thermo-plastic bulk volume changes, and thermally induced modification of frictional strength. Irreversible thermal effects that are most relevant to energy geostructures are the thermally induced strength changes and the thermal consolidation.

When dealing with the THM soil-concrete interaction, studied with the direct shear test apparatus, it is possible to state that it is function of the roughness, the soil density, the volumetric response upon shearing (dilatancy), the grain size distribution of the soil and the normal stresses applied. Moreover, the contrast between the volumetric elastic thermal expansion coefficients of concrete and of the phases of the soil should be considered.

## 2.2 Thermal investigation and parameters

Energy tunnels must be designed not only under the mechanical point of view, but also under the energy performance point of view. The latter is dependent on several factors, among which thermal properties emerge. The best way is to acquire them by laboratory testing or with in situ field tests.

### 2.2.1 Thermal parameters

Thermal parameters must be meticulously assessed; otherwise energy availability might be over- or underestimated or the structural integrity may be threatened.

The thermal parameters of soils and rocks that could affect the performances of an energy tunnel are:

- Thermal conductivity  $\lambda$  [ $W \cdot m^{-1} \cdot K^{-1}$ ]
- Thermal diffusivity  $\alpha$  [ $m^2 \cdot s^{-1}$ ]
- Volumetric heat capacity  $\rho c_p$  [ $J \cdot m^{-3} \cdot K^{-1}$ ]
- Undisturbed ground temperature  $T_{ug}$  [ $^{\circ}C$  or  $K$ ]
- Thermal resistance of the GHE  $R_b$  [ $m \cdot K \cdot W^{-1}$ ]

*Thermal conductivity* is the property of the soil or rock to conduct heat and it is an anisotropic property, which implies that it changes if different directions are considered. A ground with high thermal conductivity not only yields large heat transfer rates but also recuperates rapidly from thermal depletions and thermal build-ups. The thermal conductivity of a soil may depend on temperature, dry density, moisture content, particle size, porosity and mineralogy. Measurement of soil and rock thermal conductivity can be undertaken by either laboratory or field methods.

The *thermal diffusivity* is defined as the thermal conductivity divided by the volumetric heat capacity  $\alpha = \lambda/\rho c_p$ , where  $\rho$  is the density of the soil/rock [ $kg/m^3$ ] and  $c_p$  its specific heat at constant pressure [ $J/(kg K)$ ]. It measures the rate of transfer of heat of a material from the hot side to the cold side.

The *volumetric heat capacity* of a soil is defined as the change in heat content of a unit bulk volume of soil per unit change in temperature. It depends on the composition of the solid phase (mineral and organic constituents) of the soil, on bulk density, and on soil wetness. Its value can be estimated by summing the heat capacities of the various constituents, weighted according to their volume fractions: solid, water and air.

The *undisturbed ground temperature* is a thermo-geological parameter that allows to assess the geothermal potential of an area and from which depend several factors, among which the sizing of the GHE, the extracted thermal power and the performance of the heat pump. The ground temperature can assume different values if the surface and shallow zones are considered, where diurnal and seasonal cycles affect its value, or the relatively-deep zone, where temperature increases slowly with depth due to the geothermal gradient. In order to have a single design value of temperature, an average is usually done and this is the undisturbed ground temperature. It is a parameter that suffers the effects of urbanisation and other anthropogenic activities: ground temperatures are usually higher in proximity of urban areas. The heat transfer between the GHE and the surrounding ground is function of the temperature difference between the undisturbed ground temperature and the fluid temperature circulating in the pipes. This parameter can be assessed with the downhole temperature logging and the fluid circulating method.

The *thermal resistance of the GHE*, often regarded as the inverse of thermal conductivity, is the effective thermal resistance between the heat carrier fluid in the ground heat exchanger and the surrounding ground. If  $R_b$  has low values, installation costs and size of GHE decreases, while performances improve.

## 2.2.2 Thermal investigation

Thermal properties are highly dependent on site-specific conditions, like groundwater flow, spatial heterogeneity and scale effects, so the best way to investigate them may be the in situ testing. However, laboratory methods are typically used as they are in general relatively less expensive, quick and allow for greater control over the boundary conditions compared to field methods.

### 2.2.2.1 Laboratory tests

Laboratory tests can be classified into two main categories: steady state methods and transient methods (frequency domain methods). The difference lies in how temperature within the sample is considered.

In *steady state methods* the temperature difference across the sample does not change with time, requiring a well-engineered experimental setup, in order to maintain the desired heat flow. It takes from hours to days to register single data points.

The steady-state *absolute technique* is a widely used and accurate technique for determining the thermal conductivity of insulation materials, however, when testing soils or rocks, lower accuracy is expected: moisture migration in unsaturated soils can occur when carrying out long duration steady-state tests, which can produce heat losses.

A heat source supplies a steady heat flow ( $Q$ ) at one surface of a sample that is transferred through the sample volume to its opposite side, where a heat sink is present. Ideally, a one-dimensional (1D) thermal heat flow in the test section is guaranteed because no heat leakage should occur from the source, the specimen, or the boundaries. The temperature ( $T_1$ ) of the heater and that of the heat sink ( $T_2$ ), after an initial stage, are constant and are monitored by a control system (Figure 2.18).

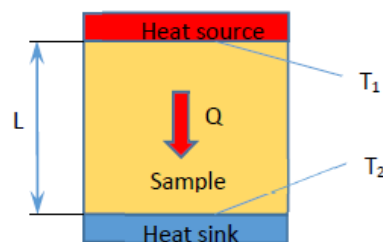


Figure 2.18. Schematic representation of a laboratory test run with the absolute technique - steady state method (Vieira et al., 2017)

Various devices exploit the absolute technique such as the guarded hot plate apparatus and the thermal cell.

In the *guarded hot plate apparatus*, the guards minimise lateral heat losses. The plates are made from highly conductive materials, in order to guarantee a uniform temperature across them. For this kind of test large circular or rectangular samples are required, it is preferable if they are dried. This apparatus gives the possibility to measure thermal conductivity at different temperatures without needing external chambers, but it is a long duration test. It is a standardised method for rocks but not for soils, nevertheless, the apparatus was also used to measure the thermal conductivity of sands and clays. However, when soil is saturated it could occur an overestimation of  $\lambda$  and moisture migration may occur in unsaturated soils.

The *thermal cell* is a method suitable for any soil, sample sizes and shape are suited to the routine site investigation practice. Some problems are related to the fact that it takes a long time to conclude the investigation, it overestimates the thermal conductivity due to uncontrolled heat losses and there is a potential for moisture migration in unsaturated soils.

An improvement of the absolute technique is the *comparative technique* (divided cut-bar method). The difference is that a standard material with known thermal conductivity is added in the system.

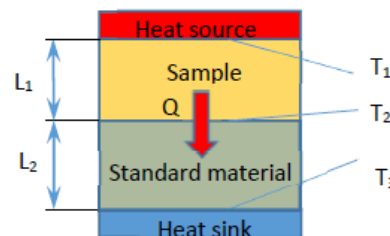


Figure 2.19. Schematic representation of a laboratory test run with the comparative technique - steady state method (Vieira et al., 2017)

The thermal conductivity of the sample can be derived by the thermal conductivity of the standard material and there is no need to measure the heat flow, the amount of heat flow through the standard material is equal to that of the testing sample.

$$\lambda_1 = \lambda_2 \frac{A_2 L_1 (T_2 - T_3)}{A_1 L_2 (T_1 - T_2)} \quad (\text{Eq. 2.11})$$

Where, with respect to *Figure 2.19*,  $L_i$  is the length of the material,  $A_i$  is the area normal to the direction of heat flow, and  $T_i$  represents the corresponding temperatures. It has the same

problems encountered in the absolute technique about the moisture migration and long duration. Good results come from rock samples, where moisture migration is negligible.

**Transient methods** measure the thermal conductivity during the modulated heating up process and they do not need the steady state to be reached, reducing the duration of tests. The heating source can be either electrical or optical, while temperature can be measured by contact (e.g., thermocouple) or without contact (infrared).

A body of known dimensions and thermal constants, the so called “probe”, contains a heating device and a temperature sensor embedded in a stainless-steel core and it is immersed in the soil whose constants are unknown. With the aid of suitable theoretical relations, these constants are then deduced from a record of probe temperature versus elapsed time. Different sizes and types of probes can be utilised. The probe can be inserted directly in soft soils or after a predrilling in rocks or harder soils, even if this latter aspect can lead to contact resistance errors.

The traditional application implies the use of the *single needle probe*, followed by the *dual thermal needle probe* but also multi-needle probes have been developed. The single needle probe is a standardised and rapid test, which allows the results not to be affected by the moisture migration. Function of the size of the samples, needle sizes change in order to adapt to it, however, samples must be large enough to avoid the effects of boundaries. Disadvantages are related to the fact that it is a local measurement, in a heterogeneous soil many investigations are needed to define the properties. The dual thermal needle probe is similar to the single one but has a different configuration: temperature is collected over time by a receptor needle that stands at a known distance from a line heat source placed in a parallel needle. The most important thing is that this distance remains unchanged over the testing time, otherwise results are wrong.

Between the transient methods, the *Transient Plane Source (TPS) Method* appears. It has a surface probe, used both as a heat source and a temperature sensor, usually insulated on one face in order to reproduce a 1D heat propagation. It allows to measure the thermal conductivity, the thermal diffusivity, the volumetric heat capacity and the temperature of all type of soil and rock samples. This kind of test is preferable to needle tests when dealing with hard soils or rocks, because no drilling is needed. The probe has to be in good contact with a flat and slightly polished surface of the sample and the contact is ensured by some applied

pressure, compressible materials should not be tested with this method. The transient heating signal has to be short enough that the sample can be considered an infinite or semi-infinite body.

Another technique that is well suited for rocks is the *Optical Laser Scanning Technique*, a noncontact optical method. The apparatus with the infrared radiometer and the heat source passes at a known rate and distance in front of the sample, following a line of scanning (*Figure 2.20*). The sample is covered with a black coat and can be cylindrical or plane, dried or saturated. With this technique it is possible to have thermal information about thermal conductivity in more than one direction, so that it is possible to study in a more accurate way this anisotropic property.

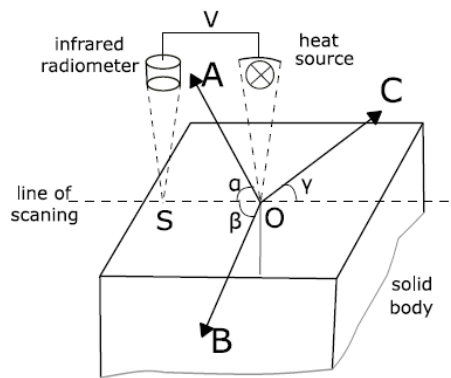


*Figure 2.20. Principle of optical scanning method. V: velocity of scanning; O: area of the heat spot; S: detection area of the radiometer; A, B, C: main axes of thermal conductivity with angles  $\alpha$ ,  $\beta$ ,  $\gamma$  to the line of scanning, respectively. (Vieira et al., 2017)*

To sum up, different laboratory techniques are available to determine the thermal properties of soil samples, but their use depends on the nature and on the preparation of specimens, so it is not so useful to make a direct comparison between them.

In general, measurements from transient and steady-state methods agree for dry soils and those with low moisture content, but for soils with high moisture content the situation changes. Due to the fact that a lack of standardization occurs in this field, there are only trends that suggest utilising steady-state methods for rocks and transient methods for soils.

### 2.2.2.2 *In situ tests*

It can be queried if the determinations made on samples of only few centimetres are representative. In reality, the volume of material that is involved is huge and it can be affected with discontinuities or fractures. A field test is necessary to study the real behaviour. The

most well-known and widely used for assessing thermal properties of the ground is the *Thermal Response Test (TRT)*.

It measures the undisturbed ground temperature, the ground thermal conductivity and the thermal resistance of the ground heat exchanger, which can be considered critical design parameters.

A thermal response test is usually performed to assist the sizing of ground heat exchanger fields. Its execution is recommended for installation capacities larger than 30 kW. It measures the temperature evolution of a GHE under a prescribed thermal load and evaluates ground and borehole thermal properties using a suitable heat transfer model.

As represented in *Figure 2.21*, to carry out a TRT the following is needed:

- A representative, completed, thermally equilibrated closed-loop borehole;
- A circulation pump and a flow meter for the carrier fluid;
- A source of constant heat input;
- Temperature sensors at the well head on the upflow and downflow shanks of the ground loop;
- Means of recording data.

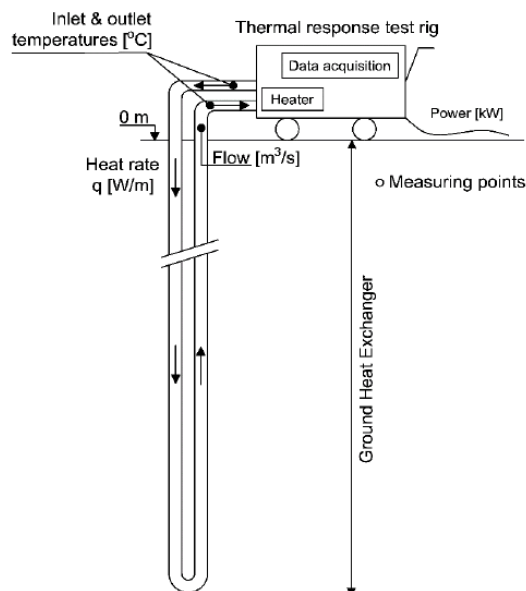


*Figure 2.21. Schematic figure of a TRT rig (Vieira, Prodan et al., 2017)*

The conventional approach to thermal response testing begins with measuring undisturbed ground temperature, followed by constant power heat injection or extraction for a period of 2–3 days. It is the preferred testing method for estimating ground and borehole thermal properties thanks to its simplicity of design, implementation, control, and evaluation.

Most often the testing is performed in heat injection mode to minimise the influence of external factors affecting the measurements. The heat carrier fluid is usually heated by an electric resistance at a constant power rate  $q$  of 50–80 W/m.

Measurements are taken at regular intervals of 1–10 min and include the temperature of the heat carrier fluid entering and leaving the borehole, the flow rate, ambient temperature, and input power to the electric heater and the circulation pump. An example of how the output of a TRT test are, is reported in *Figure 2.22*.

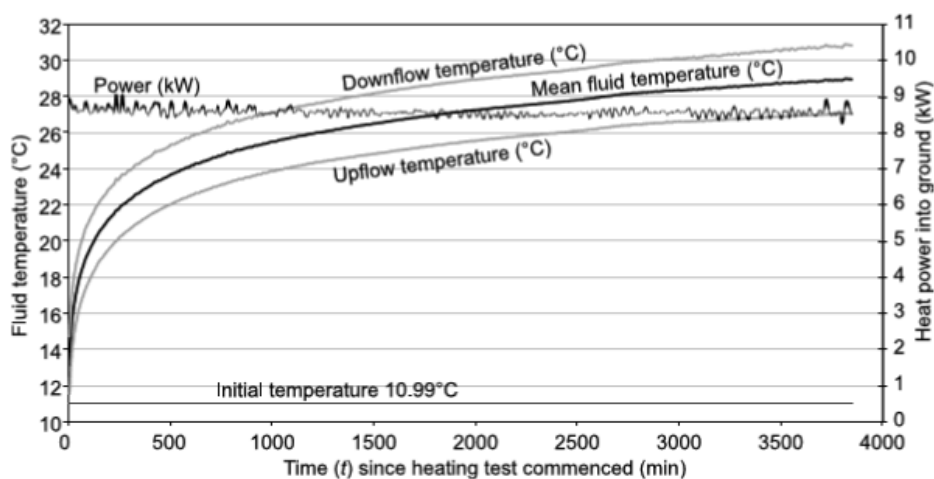


*Figure 2.22. Example of output from a TRT, linear time scale (Banks, 2012)*

At the end of the registration phase, results are analysed using a mathematical heat transfer model, i.e. the infinite line source and the cylindrical-source approximation, to evaluate ground thermal conductivity and borehole thermal resistance values.

It has been carried out that results can be affected by several factors such as climatic conditions, groundwater flow, input power variations, test duration and analysis method; in *Table 2.7* is a resume of the main factors.

## Investigation and Parameters Assessing

Table 2.7. Factors affecting TRT results

| Factors                    | Effects  |
|----------------------------|--|
| Climatic conditions        | Heat losses that arise from undesired heat exchange with the ambient outside the borehole cannot be neglected. If neglected, $\lambda$ can be affected by a factor of one third. A solution to avoid the heat losses is to thermally insulate all the connections of the system. |
| Hydrogeological conditions | The presence of a groundwater flow has a huge influence on the determination of thermal properties. If a significant groundwater flow is present, the heat transfer is enhanced and can lead to a higher but inaccurate estimation of the ground thermal conductivity.           |
| Duration of test           | It influences the accuracy of the estimated results: the longer the test, the more accurate the results. This is due to the fact that the behavior of the system tends to reach a steady-state condition.  |

Thermal response tests are also subjected to possible errors caused by:

- Uncertainties in measurements, factors such as imprecise location, calibration, or limitations of the measuring instruments;
- Uncertainties in (input) design parameters, inaccessible, incomplete, or inaccurate data on material properties, geometrical dimensions, and boundary and input conditions;
- Uncertainties in the analysis method, limitations of mathematical models used to determine ground conductivity and borehole resistance values.

When running a conventional TRT, average values of thermal properties are derived, without taking into account the stratigraphy of the site, which implies different values for each type of soil/rock. In order to analyse this with the aim of optimizing the thermal design of the structure, two alternative configurations of TRT exist.

*Distributed and Enhanced Thermal Response Tests* (DTRTs and ETRTs) measure variations in ground thermal conductivity along the entire length of the borehole heat exchangers, taking measurements at multiple depths. They exploit the fiber optics technology to acquire a high-resolution temperature along the borehole, each fiber sends information to a Distributed

Temperature Sensing (DTS) equipment, which allows spatial resolution of 0.2–5 m, temporal resolution of 1–10 min, and temperature resolution of 0.1–0.5 K. However, the disadvantage is that this technique requires continuous in situ calibration.

The analysis of the results is based on a discretization of the borehole, divided into several smaller zones, and for each zone the parameter determination process of the conventional TRT is run. However, analysing literature results, it is possible to say that differences from conventional method and enhanced/distributed method are less than 10% (*Figure 2.23*).

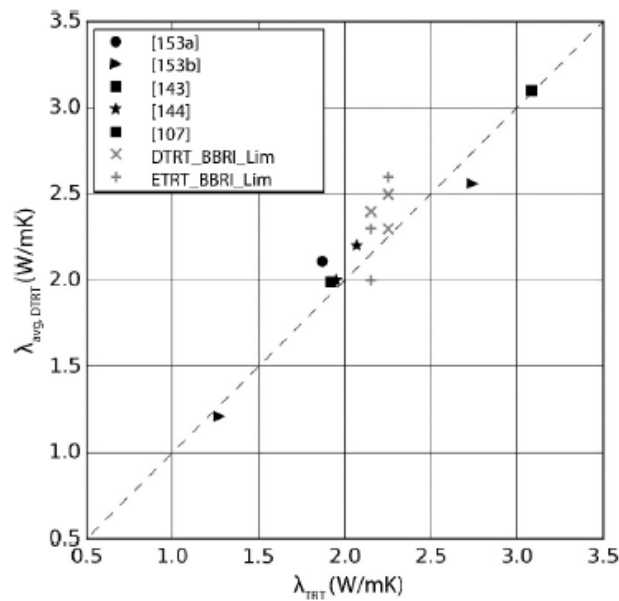


Figure 2.23. Average ground thermal conductivity by TRT, DTRT and ETRT (Vieira et al., 2017)

### 2.2.3 Outcomes

To conclude, two tables are reported regarding the thermal parameters affecting the thermal behaviour of an energy tunnel and the investigation methods used to assess them.

*Table 2.8. List of investigation methods for thermal properties*

| <b>Thermal investigation methods</b> |  |
|--------------------------------------|--|
| <b>Ref.</b>                          | <b>Lab tests</b>                                     |
|                                      | <i>1 Steady state methods</i>                        |
| 1a                                   | Guarded Hot Plate - Absolute technique               |
| 1b                                   | Thermal Cell - Absolute Technique                    |
| 1c                                   | Comparative cut-bar technique                        |
|                                      | <i>2 Transient methods (frequency domain method)</i> |
| 2a                                   | Needle-Probe Method                                  |
| 2b                                   | Twin heat probe method                               |
| 2c                                   | Dual thermal needle probe                            |
| 2d                                   | Transient Plane Source (TPS) method                  |
| 2e                                   | Optical scanning technique                           |
| <b>Ref.</b>                          | <b>In situ tests</b>                                 |
| 3                                    | Thermal Response Test (TRT)                          |
| 4                                    | Downhole Temperature Logging                         |
| 5                                    | Fluid Circulation Method                             |
| 6                                    | Distributed TRT (DTRT)                               |
| 7                                    | Enhanced TRT (ETRT)                                  |

*Table 2.9. Thermal properties of soils and rocks and common ways of determination with respect to Table 2.7*

| Thermal parameters of the ground | Symbol          | Unit               | Determination                     |                   |
|----------------------------------|-----------------|--------------------|-----------------------------------|-------------------|
|                                  |                 |                    | Lab test                          | In situ test      |
| Temperature                      | T               | °C or K            | 2d, 2e                            | 6, 7 (with depth) |
| Thermal Conductivity             | $\lambda$       | W/mK               | 1a, 1b, 1c, 2a, 2b,<br>2c, 2d, 2e | 3, 6, 7           |
| Thermal diffusivity              | $\alpha$        | m <sup>2</sup> /s  | 2c, 2d                            | /                 |
| Volumetric heat capacity         | $\rho c_p$      | J/m <sup>3</sup> K | 2d                                | /                 |
| Undisturbed ground temperature   | T <sub>ug</sub> | °C or K            | /                                 | 3, 4, 5           |
| Thermal resistance of the GHE    | R <sub>b</sub>  | mK/W               | /                                 | 3                 |

There are few case studies where high-quality testing, both in situ and at the laboratory scale, has been carried out on the same materials from the same locations. It has been evaluated that in most cases the field scale tests present higher values of thermal properties, this is due to several factors, between them the true scale effects, groundwater effects and sampling issues. Without any doubt, laboratory tests involve smaller volumes of soil and rock, compared to the in situ tests, and they do not take into account several large-scale features, which with the heat flow direction can highly affect the value of the thermal conductivity. The groundwater movement plays the main role in laboratory/field discrepancies: on site, groundwater flow is the major cause that modifies the values of the conductivity. In addition, as for the geotechnical investigation, also the sampling procedure can affect the results: for granular soils, samples have to be reconstituted at voids ratio or moisture content not entirely representative of field conditions; for clays, the structure and the moisture content can locally vary due to the shearing induced by sampling; for rocks, there are many difficulties related to the reconstitution of the samples. Thermal properties can be largely affected if samples dry over time.

### 2.2.4 Future for thermal investigation in situ: TCT

As the use of energy geostructures is becoming more and more prominent, there is a high need to investigate the thermal properties of the ground in a rapid and easy way. Referring to energy tunnels, it arises from the previous observations that laboratory tests are suitable to investigate the thermal parameters, but samples must be representative of the in situ conditions and, concerning this aspect, it is not always possible to assure it, in particular, laboratory tests do not take into account the effects of the borehole made to carry the samples out.

The state-of-the-art in situ methods, as reported in *Chapter 2.2.2.2*, include the TRT, which presents some limitations. It takes a long time to be concluded, requires a constant power over the test duration, involves large costs and is a local/punctual investigation system, very appropriate when testing soil for example for energy piles, but when considering the construction of a tunnel, the involved volume of soil is huge. This implies that TRT is not practicable for large scale investigations.

In this scenario, it would be advantageous to identify an economic, fast and effective way to determine the in situ thermal properties on a large scale. Due to the fact that the drill of boreholes is in any case requested during the construction of such a project (for the stratigraphy, geomechanical and hydraulic parameters, sampling, etc.), traditional in situ geotechnical devices could be properly equipped with sensors in order to investigate also the thermal behaviour of the soil.

It could be possible, for instance, to introduce some thermal sensors in the CPT cone, where currently other types of sensors for different purposes (i.e. seismic waves sensors) are already added. Other approaches could involve the use of the in situ needle probe, paying attention to choose the best and representative sections where to run the measurements.

In *Figure 2.24* there is a schematic representation of different types of cones available for a CPT device.

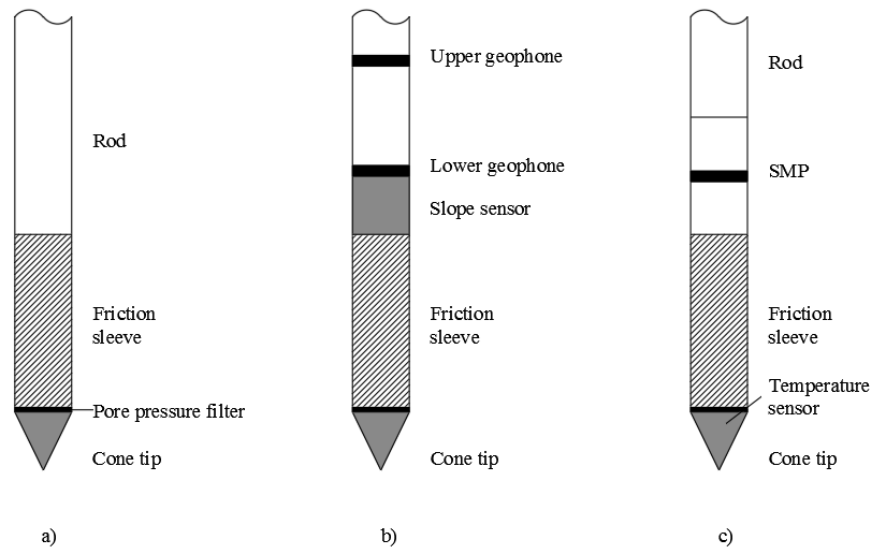


*Figure 2.24. Some schematic representations of CPT with different sensors: a) piezometric cone, b) seismic cone and c) thermal cone.*

In the last few years, some authors proposed and studied the Thermal Cone dissipation Test (TCT). It is an expansion of the CPT, in particular the cone penetration test with pre-pressure measurements, CPTu. The device is thought to overcome to some drawbacks of the current in situ methods to measure thermal properties, in that it is rapid and less expensive (Lines et al., 2017).

In this test, the temperature is variable with time during the measurements, so it can be classified as a transient method: the idea is to extrapolate the thermal properties with the temperature decay. A thermocouple is attached to the CPT device to measure the temperature at the contact between the rod and the surrounding soil (Akrouch et al., 2016).

At the very beginning, a heater element was also added to the apparatus in order to first generate a heat pulse to the ground and then analyse the way temperature decreases. However, during the experimental campaign, it was observed that the penetration process, during the CPT, resulted in a sufficient increase in the cone temperature. The increase is induced by the heat generated by the friction between the soil and the cone, as reported in *Figure 2.25* (Akrouch et al., 2016).

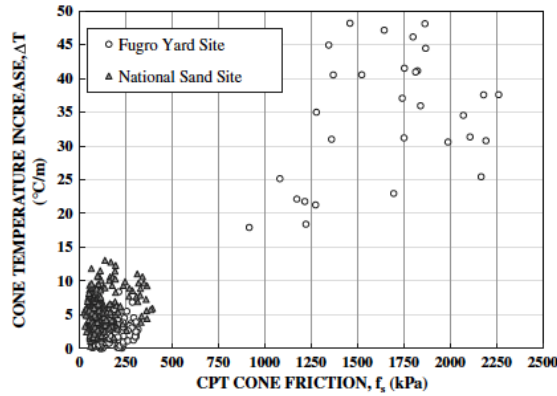


Figure 2.25. Cone temperature increase against con friction (Akrouch et al., 2016)

The measured dissipation of heat is then used to determine the thermal parameters of the soil over the test interval. The cone temperature decay against time is recorded for at least 30 minutes and from it, with proper empirical curves, it is possible to derive the thermal properties. The empirical equations proposed by Akrouch et al. (2016) to estimate the thermal conductivity and diffusivity derive from the similarity of the thermal physical process with the hydraulic one. The calibration of the above-mentioned curves of temperature decay is based on in-situ experiment results, laboratory investigations and numerical simulations.

$$\lambda \approx \frac{1}{(A \cdot t_{50})^B} \quad (\text{Eq. 2.12})$$

$$\alpha \approx \frac{T_{50} a^2 \chi}{t_{50}} \quad (\text{Eq. 2.13})$$

Where:

- $\lambda \left[ \frac{W}{mK} \right]$  is the thermal conductivity;
- $\alpha \left[ \frac{m^2}{s} \right]$  is the thermal diffusivity;
- $A, B$  and  $\chi [-]$  are parameters from the calibration of the TCT results;
- $t_{50} [s]$  is the recorded time from the TCT;
- $T_{50}$  is the time factor, normalized against the soil thermal diffusivity and cone diameter, required to dissipate half of the initial increase in temperature.

Nowadays, there are few TCT data available, in the future the amount will increase and also the calibration will be more precise and for a larger range of soils. Vardon et al. (2018) proposed a more theoretical approach.

To sum up, the proposed procedure is:

1. Locate the area and depths where thermal information is needed;
2. Prepare the TCT apparatus in the testing location;
3. Push the thermal cone to the desired depth (standard penetration rate 20 mm/s);
4. Record the cone friction and tip resistance during the pushing process;
5. Stop the cone at the desired depth;
6. Record the cone temperature decay against time for at least 30 minutes – the initial 5 minutes are the most important, since this is when by far the largest dissipation occurs (Lines et al., 2017);
7. Reduce the measured data and evaluate  $t_{50}$  from the temperature decay curve;
8. Repeat from 3 to 7 for the other depths.

This method has many advantages:

- Shorter duration compared to other types of test, it is a useful tool to have a quick estimate of the thermal properties of the ground;
- No need of additional heating sources, friction is sufficient;
- The test equipment is more robust than, for example, needle probe type tests, when pushed into the ground it is possible to reach large depths without tools being swapped;
- TCT is simultaneous with the traditional CPT, thermal properties, soil stratigraphy, hydraulic and mechanical properties are all derived from a single test.

All those advantages have an implicit one: under the economic point of view, it is a less expensive procedure of obtaining soil thermal parameters for the initial design stage with respect to other in situ methods (i.e. TRT).

Referring to the needle probe, it is a more fragile device due to the fact that it is very thin; however, it can be used in very soft, close-to-surface soils and the other kind of soil can be tested by the TCT (Vardon et al., 2017).



### **3 ENERGY TUNNELS DESIGN PROCESS**

The aim of this chapter is to make a discussion on the design of an energy tunnel. With reference to the traditional design, there are several differences to be highlighted. In the design of a traditional tunnel, the geomechanical parameters, the in-situ state of stress and the in-situ water conditions are required to assess the geomechanical model, which is the starting point of the structural design.

When dealing with an energy tunnel, the THM behaviour plays a major role and other aspects must be considered to design a performant system. It is necessary to design both the structural and the thermal aspects.

In this chapter, after a general introduction on a wide range of technologies available for the implementation of a tunnel, the segmental lining design is deepened.

Two main aspects must be taken into account in designing thermo-activated segmental linings: the quantification of the exploitable heat (i.e. efficiency) and the evaluation of the thermal effects on the structural elements, integrity has to be guaranteed for the long-term behaviour.

Under the thermal point of view, intended as the efficiency of the heat exchanger, the heat exchange mechanisms must be considered, the most significant are the conduction and convection. A Thermo-Hydro (TH) numerical model can be built in order to evaluate the extracted/injected power of the thermal plant and the environmental impact on the surrounding ground, as Barla and Di Donna (2016) reported in their article on “Underground Space” journal.

Since pipes are present in the lining, temperature effects on the structural behaviour must be studied. The thermal activation results in a variation of the stress state inside the lining, with consequent implication on the structural dimensioning. Temperature can be considered as an additional load on the structure. The best way to analyse this kind of influences is to implement a Thermo-Mechanical (TM) numerical model, which couples the structural aspect and the temperature effects.

In the following pages, a study both on the structural and thermal design is reported, with particular attention to the most influencing parameters for each design stage. In *Figure 3.1* is a comparison between the design steps of a traditional tunnel and an energy tunnel.

## Energy Tunnels design process

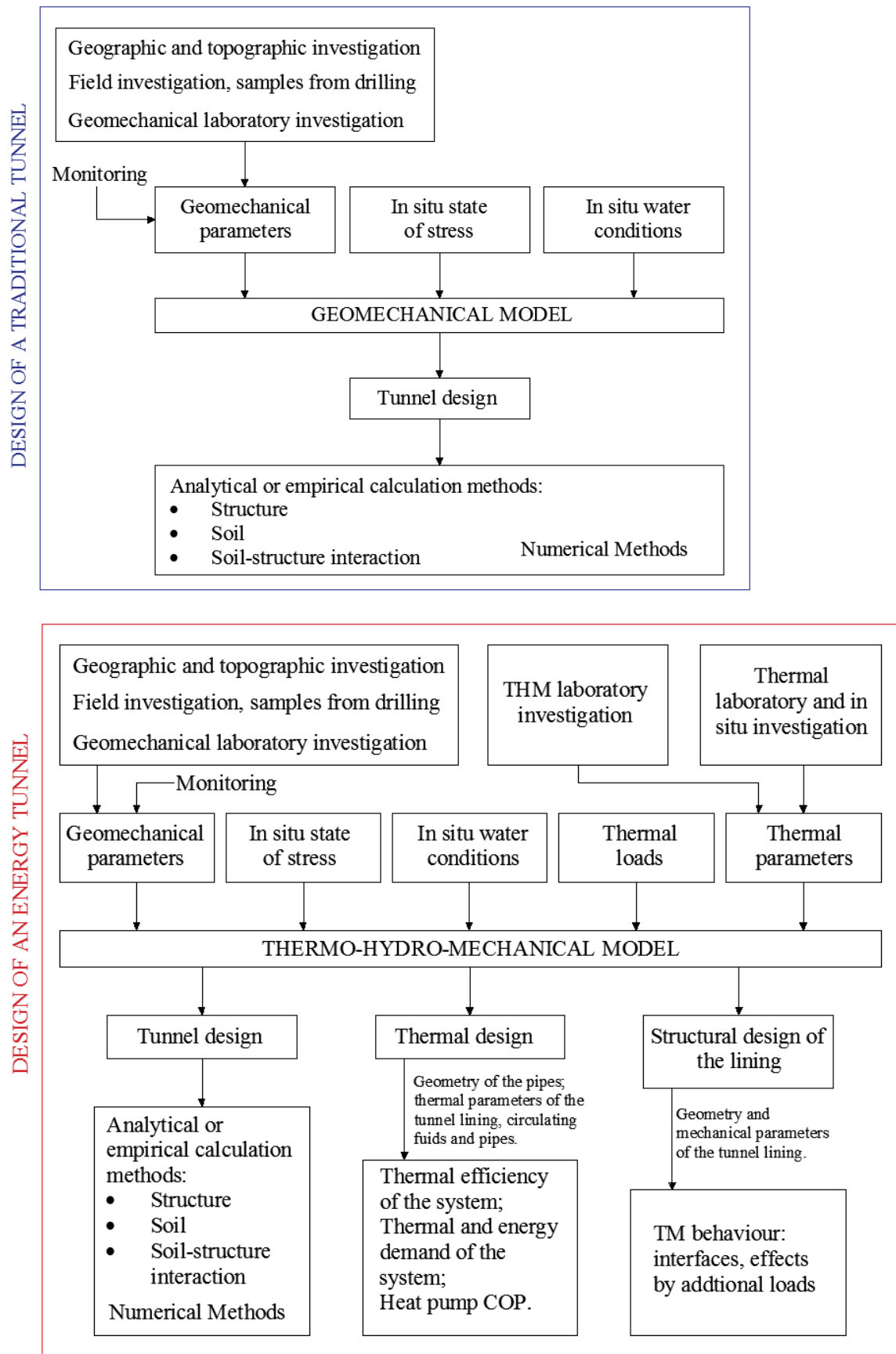


Figure 3.1. Overview on the integrated design of an energy tunnel

### 3.1 Tunnel design aspects

In order to make a very general introduction, when designing a tunnel, typical stages from conception to completion are planning, feasibility study, corridor and alignment study, environmental impact studies, conceptual design, preliminary design, final design and construction.

Reality must be considered as precise as possible, i.e. initial state of stress of the ground, physical-chemical characteristics, behaviour of the ground, and properties of the cross-section and execution phases of work. It is possible to start with a series of empirical and structural “hand” calculations and then results can be compared to the Finite Element simulations, which can confirm and follow the previous results or can give a warning of some mistakes in the process. It is important, when simplifications are to be introduced into the design, that the simplified approach is conservative and that deformation results are in a realistic order of magnitude.

The aspects that need to be carefully considered in designing an underground structure are mainly three (*Figure 3.2*): the structure itself, the surrounding soil and their interaction. Input parameters play the main role: they are chosen based on the type of model and failure criteria that is used in the design process to describe the ground conditions and results closely depend on them.

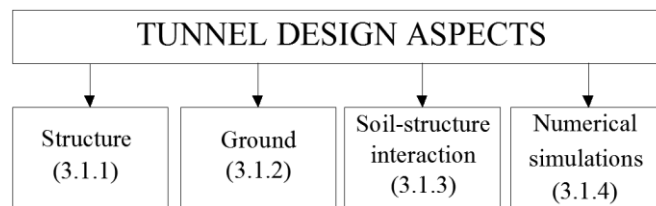


*Figure 3.2. Tunnel design aspects- reference to the chapters in which they are discussed.*

### 3.1.1 Structure

#### 3.1.1.1 Shape of the tunnel

Once that the tunnel envelope is provided, the shape of the tunnel can be defined: most common are circular, ovoid, vertical ovoid and horseshoe, in *Figure 3.3* a schematic representation. The choice of the shape must take into account the  $k_0$  value, i.e. the coefficient of earth pressure at rest, which relates vertical and horizontal stresses in the ground,  $\sigma_v$  and  $\sigma_h$  respectively.

$$\sigma_h = k_0 \cdot \sigma_v \quad (\text{Eq. 3.1})$$

If  $k_0 = 0.5$ , vertical stresses are twice the horizontal, minimum pressures are registered with a circular or vertical ovoid shape. If  $k_0 = 1.0$ , stresses are equal in the two directions, the best shape to have smallest compressions is the vertical ovoid section (Moldovan, chapter 9, ???).

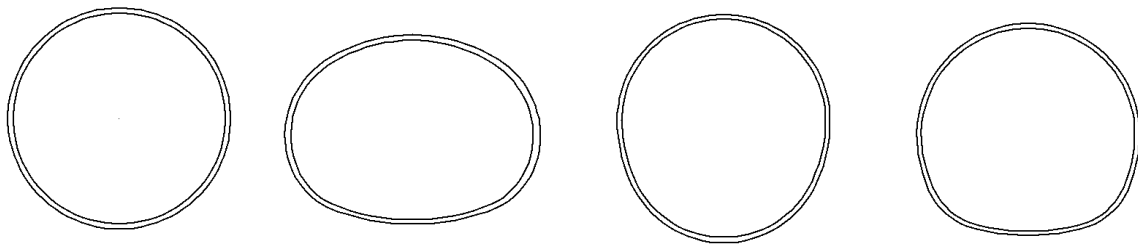


*Figure 3.3. Schematic representation of the shape of tunnels: circular, ovoid, vertical ovoid and horseshoe*

#### 3.1.1.2 Vertical loads

Next step is to determine the vertical loads, there are several calculation methods, between them Terzaghi and Protodiaconov are two examples. They use two different ways to consider the cover above the tunnel, their representation is given in *Figure 3.4* with the correspondent relationships.

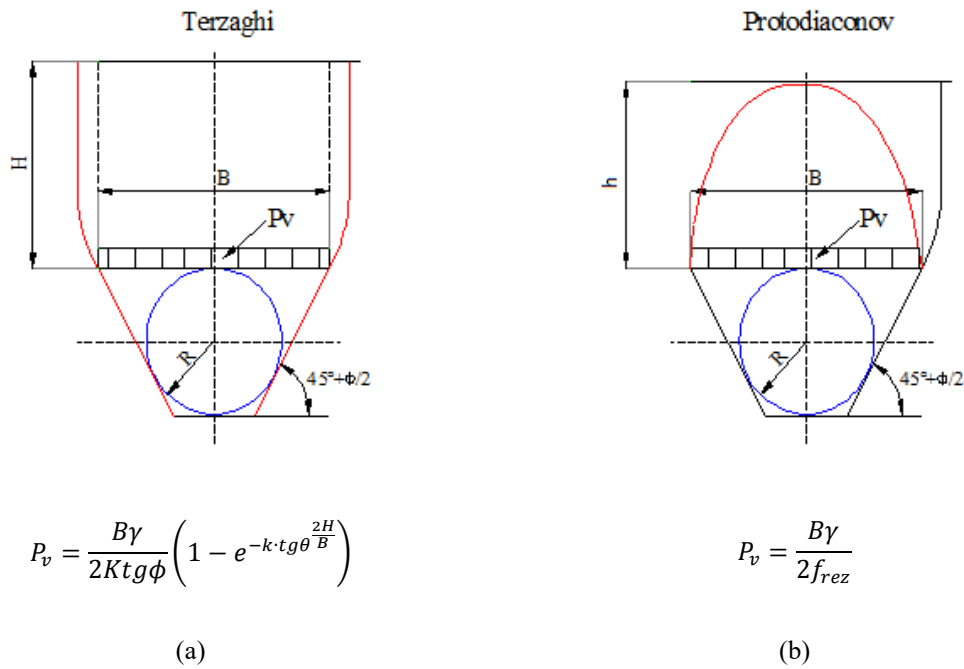


Figure 3.4. Terzaghi's (a) and Protodjaconov's(b) methods for vertical loads (Moldovan, 2013)

Where:

- B is the width between the failure surfaces and can be calculated as

$$B = 2R \cdot tg \left( \frac{45^\circ}{2} + \frac{\phi}{2} \right);$$

- $\gamma$  is the specific weight of the ground;
- $\phi$  is the internal friction angle;
- $f_{rez}$  is the strength, it depends on the cohesion;

$$\circ f_{rez} = \begin{cases} \frac{\tau}{\sigma} = tg\phi & \text{with low cohesion} \\ \frac{\tau}{\sigma} = tg\phi + \frac{c}{\sigma_0} & \text{with high cohesion} \\ \frac{c_p}{100} & \text{for rocky or semi - rocky rocks} \end{cases}$$

- H and h are the cover above the tunnel.

There can be different configurations, functions of the ratio between the width of influence of vertical loads and the height of the cover, i.e. the distance from the surface.

Speaking about the horizontal stresses, they arise with the excavation, due to the fact that ground tends to move towards the centre of the tunnel. Anyway, they are smaller than the vertical pressures.

### 3.1.1.3 Convergence-confined method

In order to preliminary design and size a proper support system, the convergence-confined method can be used, based on the evaluation of the radial displacements of the tunnel contour, but some simplifications have to be done: the cross-section is circular and the initial state of stress is isotropic and constant.

The convergence-confinement method basically consists of the definition of the internal pressure (radial stress) – radial displacement (in absolute values) ( $p-|u|$ ) relationships on the boundary of the tunnel. This relationship is called the convergence-confinement curve. In this phase, the constitutive laws chosen to describe the ground behaviour come into play.

For an internal pressure equal to  $p_0$  (lithostatic stress) there is no change in the initial stress and strain state around the tunnel and therefore the radial displacement of the wall is nil. With a diminishing of the internal pressure  $p$ , the radial displacement of the wall begins to appear. Initially this increases linearly, at a certain point (for pressures lower than  $p_{cr}$ ), the trend can result to be of a curvilinear type. In the simplest case of rock behaviour of an elastic type, the convergence-confinement curve is represented by a linear segment (*Figure 3.5a*).

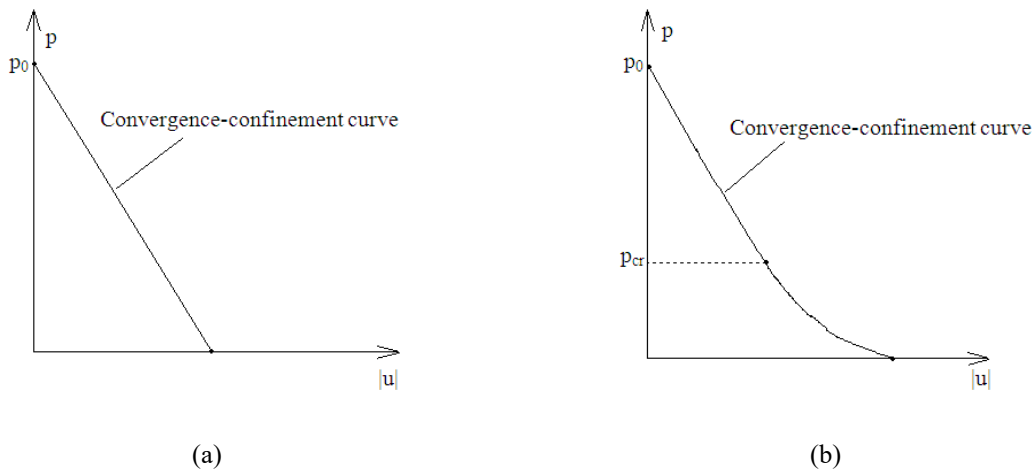


Figure 3.5. Convergence-confinement curves for a) elastic behaviour and b) elasto-plastic behaviour (Panet, 1982)

In the more general case of elastic-plastic behaviour, for a certain internal pressure  $p$  and with the decreasing of  $r$ , the elastic limit is reached when the stress state reaches the limit conditions defined by the strength criterion (*Figure 3.5b*). Such a value of  $r$  is called the plastic radius  $R_{pl}$ . The radial pressure on the plastic radius is called the critical pressure  $p_{cr}$ , which is only a function of the peak strength parameters of the soil. When  $p_{cr} \leq 0$ , the convergence-confinement curve continues to appear as a linear segment, which means that the

elastic limit is not reached in any point and the material remains in the elastic field throughout. Instead if  $p_{cr} > 0$ , a zone of thickness  $(R_{pl} - R)$  under plastic behaviour appears for  $p < p_{cr}$  around the tunnel, called the plastic zone. The material continues to remain in elastic conditions for any distance greater than  $R_{pl}$ .

The abovementioned convergence-confinement only considers a generic internal pressure which, varying, provokes a different tunnel response both in terms of convergence and extension of the plastic zone, without taking the presence of a support into consideration. In order to consider it, its own reaction line and the concept of fictitious internal pressure are introduced.

The fictitious internal pressure allows to face a three-dimensional problem (due to the presence of the excavation face) with a simplified bi-dimensional scheme. After having identified a precise section to study along the tunnel axis, the following different situations take place:

- a) Excavation face very far from the studied section, the excavation works do not produce any stress perturbation at the studied section, and the internal pressure is equal to the lithostatic one.
- b) Excavation face closer to the studied section, even if it is still not excavated, radial displacements on the perimeter of the future tunnel appears. The tunnel face is near and it causes a progressive stress release.
- c) Studied section passed by the excavation face, the consequences for the presence of the tunnel are considered through the fictitious internal pressure concept which diminishes, until it disappears, in function of the distance from the tunnel face.

Supports are required when the displacements are too high and make the excavation unstable and dangerous for workers. With the convergence-confinement method, it is possible to overlap the convergence-confinement curve of the tunnel with the reaction line of the support (*Figure 3.6*). The overlapping point represents the balance point between the convergent tunnel and the support, which gives a pressure to the contour in order to minimize the radial displacements of the tunnel towards its centre. The supports are installed close to the excavation face where the tunnel wall has already shown a certain radial displacement, any further development would provoke the loading of the supports, according to a usually linear relation characterised by support stiffness  $k$ .

Usual supports are spritz-beton (5-20 cm thick), anchors and bolts. If one support is not enough to bear the pressures, several supports can be combined.

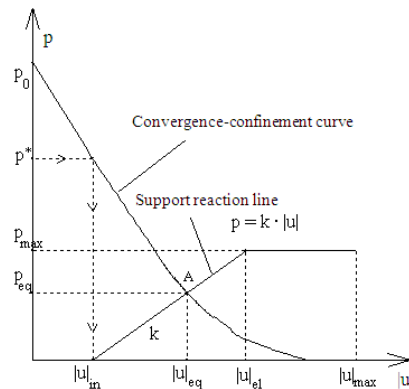


Figure 3.6. Convergence confinement curve of soil and support (Panet, 1982)

### 3.1.1.4 Tunnels technologies in soils

In order to have an adequate design of the type of geothermal system to implement in the tunnel, attention must be paid to the excavation method. Excavation is function of the geological conditions of the site and material properties. In this chapter excavation in soils will be treated. The only way to get this information is a careful preliminary investigation of the site conditions. Once they are determined, tunnel can be excavated using conventional or mechanized methods.

The excavation of a tunnel causes a redistribution of the natural stresses inside the rock mass. It is necessary to understand the ground behaviour and its answer to tunnelling operation. The stability conditions of a tunnel are controlled by the ground geotechnical properties, the natural state of stress, the shape and size of the tunnel section, the underground water and the construction methods. Tunnel design and construction are strictly linked. The link is monitoring.

There are other aspects to consider when excavating: the disturbance of the nearby structures and buildings must be minimized, and the health and safety of the workers must be guaranteed.

#### 3.1.1.4.1 Conventional methods

Talking about conventional methods of excavation, some example can be the drill and blast method and the punctual machines method. The constructive process is cyclic and follows three main steps: excavation, removal of debris, installation of the preliminary support

system. It is advantageous in sites where there is a high variability of the geotechnical and geological characteristics, being the cheapest solution. It fits into short tunnels, with particular geometries different from the circular one or into tunnels with difficult access. Using these methods, during excavation it is possible to continue the investigations and if they bring to a change in the parameters it is possible to adapt the work in progress, being these operations very flexible.

If the tunnel is to be excavated in a rock mass with great mechanical characteristics, the drill and blast method is to be preferred. The first step is to design a “blasting scheme”, with the positions of the explosive charges, in function of the geometry that is to be obtained, the properties of rock, presence of water and the consequences of the blast developed vibrations. During the drilling operation, an adequate ventilation plant is needed, in order to remove dust derived from rock fragmentation.

When the ground is softer and weaker, punctual machines can be used. They excavate the tunnel with a simpler dust management, there is no need of a ventilation plant but water is used to treat dust. Since no blasting is required, the problem linked to the vibrations does not exist.

The stability of the excavations is a fundamental aspect to take into account: there are self-supporting and non-self-supporting grounds. In the first case, there is no need of special support elements and excavation can be done using a full-face system; in the second case the situation is more critical. It is possible to take some remedial measures such as subdividing the excavation section into smaller portions that are excavated at different times (*Figure 3.7*).

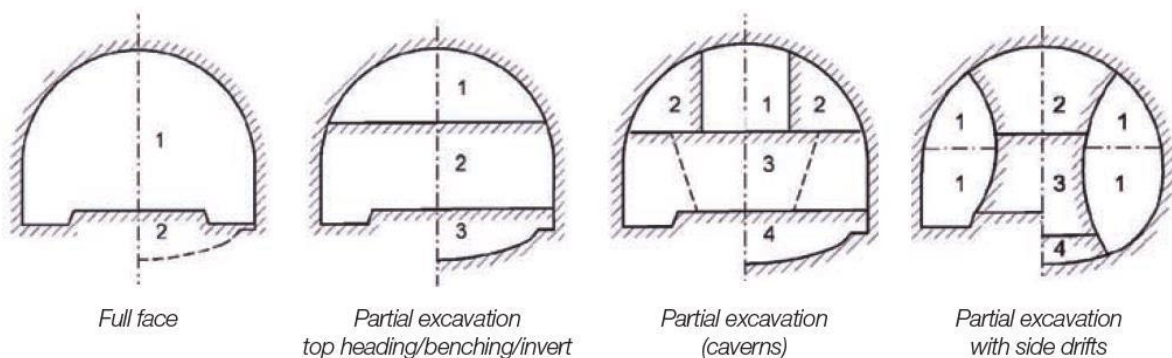


Figure 3.7. Some of the possible excavation sequences (Steffan, 2017)

Ground properties can be improved under the mechanical point of view, for example injecting fluids or freezing the fluids already present in the ground and/or inserting structural elements, with one dimension prevalent, such as fully grouted bolts, cables, pattern of micro-piles. It is also useful to drain water far from the tunnel in order to reduce its pressure on the excavated tunnel and to create a pre-support before the excavation, using insertion of structural concrete or steel elements ahead the tunnel face.

After having excavated and consolidated the ground, it can be needed a preliminary support in order to give stability to the excavation and keep the workers safe. It will be followed by a final lining. The choice is mainly based on the geological characteristics of the site and on ground properties. The most common structural elements used are bolts, steel ribs, mesh and shotcrete, and they can be used separately or combined.

Steel ribs are curved steel elements that follow the tunnel profile and there are several geometries available; they can be subdivided into rigid and deformable steel ribs, the first ones do not allow deformations and the structure has a high strength.

### **3.1.1.4.2 New Austrian Tunneling Method**

Many modern tunnels have used as excavation technique the *New Austrian Tunneling Method* (NATM). It started to be considered in the 1960s, after a work run in Austria by Ladislaus von Rabcewicz, Leopold Müller and Franz Pacher. Compared to the earlier approaches for tunnelling, there are differences related to economic advantages born by exploiting the inherent geological strength available in the surrounding ground to stabilize the tunnel.

It is a “design as you monitor” approach, very flexible, during construction ground conditions are continuously observed and monitored in order to optimize the support technologies. It can be used in several geotechnical conditions and for different cross-section geometries.

Loosening and excessive ground deformation must be minimized. During the excavation process, it could happen that some materials fail, falling down and causing the section to be over excavated, this can be avoided by applying for example a thin layer of shotcrete immediately after face advance. In order to monitor potential deformations of the excavation, the installation of sophisticated measurement instrumentation embedded in lining, ground, and boreholes is required. The real-time comparison of the evaluated and assumed deformations forms a core element of this technology: if the actual ground conditions do not match those predicted, it is possible to react in real time and change the design of the tunnels.

Additional supports are installed only when needed, it is possible to add active supports to strengthen the tunnel and the combination of them can be very flexible and linked to the site conditions, with a resultant overall economy to the total cost of the project.

Especially crucial in soft ground, the quick closing of the invert, which produces the ring closure that gives the static effect to the structure, is important. This can be made by using shotcrete, which has a lot of properties, ideal for tunnelling: it can be used as a durable concrete inner shell; it acts as a thin, pliable shell and minimizes bending stress; it can be used for all types of cross sections and soil types.

The final lining is function of the outbreak type, outbreak method and of the future use of the tunnel. The most used variants are the single-shell tunnel lining and the two-shell tunnel lining. For single-shell constructions, a shotcrete with structural concrete quality is required, a shotcrete reinforced by steel fibers is often used. These single-shell constructions can be produced in multiple layers, whereby a bond between the individual layers must be ensured. For two-shell constructions, the two layers are usually separated by a protective layer of geotextile and a sealing film.

The sealing film is one of the waterproofing systems that can be used for tunnels: these systems are usually designed individually for each project. The main distinction is made between pressure-free sealing system, which allows the drainage of water, and a pressurized water sealing system.

### **3.1.1.4.3 Mechanized methods**

Talking about mechanized methods of excavation, the main characters are the Tunnel Boring Machines, better known as TBMs, open or mono/double shield. This technology allows to excavate tunnels with different diameters, ranging from 400 mm for microtunnels to more than 17 m. The TBM is equipped with a cutter head that is used to mine the ground. The excavation is continuously supported by installing precast concrete segments. When tunnelling with a mechanized method the excavation, the support and the removal of debris take place simultaneously and continuously.

This kind of technology has many advantages with respect to the conventional one: the ambient is safer and healthier for workers; costs and times of excavation are reduced; it allows to handle sections with difficult excavation conditions; the final quality of the lining varies less since precast concrete segments are better checked than the in situ-cast supports.

Once the type of TBM is chosen and the excavation has started, it is no more possible to make changes in the technology. The excavation has to be finished without modifications because could be very difficult and expensive. This is one of the disadvantages of the TBM technology, it is not flexible and needs a very detailed previous analysis of the geology of the site.

There are different types of TBMs, they vary in function of the type of ground to be excavated. The selection of the excavation type depends on the geometrical configurations, the ground conditions, the type of crossing, and environmental requirements. When dealing with soils (soft ground), which have worst mechanical characteristics than rocks, there are three main type of TBM currently used: the Earth Pressure Balance Machine (EPB), the Slurry Shield Machine (SS) and the open face machine.

A section of the Earth Pressure Balance Machine is reported in *Figure 3.8*. The EPB exploits the excavated material to balance the pressure on the tunnel face. This technology can be used in homogeneous and heterogeneous ground conditions. In the latter case, the TBM is designed for the overall optimum, not only for the optimum of a specific geology.

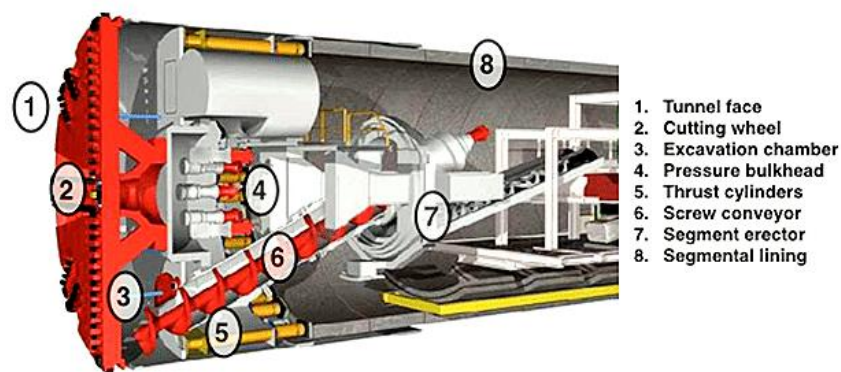


*Figure 3.8. Cross sectional diagram of an Earth Pressure Balance (EPB) TBM (herrenknecht.com)*

The factors that mostly affect the soft ground tunnelling are (Langmaack & Feng, 2005):

- *Soil permeability.*

It is a very variable value, it can go from  $k = 10^{-3} \text{ m/s}$  for the most porous soils (Turin), coming down to practically impermeable clays. In the first case, the tunnel face could be very instable, uncontrolled soil can be faced and there could be water income as well as loss of face pressure through the soil. Otherwise, the TBM in clayey soils could face clogging and adhesion problems.

- *Ground water pressure.*

The ground water level, respectively the ground water pressure, highly influences the EPB excavation process. The higher the water pressure, the more difficult uncontrolled water income and settlement risks can be avoided.

- *Risk of clogging and adhesion problems.*

In clay formations easily the cutter head openings and tools can be closed and turned ineffective. This phenomenon can lead to difficulties in TBM guiding and extensive cleaning and the advance rates could decrease.

The common solution that can help avoiding all the above-mentioned problems is conditioning the soil with some additives. Only the use of soil conditioning additives enables to fill the TBM working chamber, to reduce the TBM torque and to reduce the abrasion. When excavating in instable ground and sensitive surface areas, the most suitable way to advance is filling the TBM excavation chamber completely with a homogeneous and impermeable soil treated with conditioning agents, like foams or/and polymers. Their role is to give to the ground a plastic behaviour with pulpy consistency; the aim is to obtain the suitable rheology of the soil in order to build up and to maintain the necessary support pressure in the working chamber and to prevent high pressure variations. They have effect on the strength parameters of the soil, additives reduce the internal friction angle and the cohesion (Langmaack & Feng, 2005).

An important aspect for the choice of soil conditioning additives is their possible impact on the surrounding environment (emission into ground water, working place concentrations, emissions from the land filling of the treated soil).

To sum up, the use of the right soil conditioning additives is vital, for very permeable soil under groundwater table as well as for clay soil with high clogging and adhesion potential. In order to investigate which is the best conditioning additive, laboratory tests can be run on conditioned soils, such as the slump test, the permeability test, the wear test and the screw driver extraction test. For example, in the slump test the assessment of the quality of the conditioning is carried out measuring the cone fall height and observing the final consistency of the mix. In *Figure 3.9* there are the suggested additives in function of the soil type.

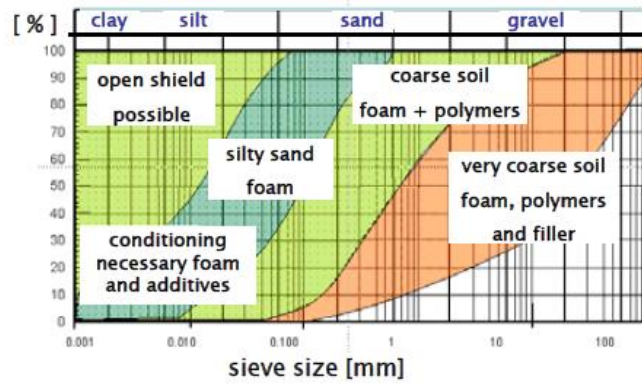


Figure 3.9. Suggested ranges for conditioning soils for EPB machines. (Peila, Tunneling Classes 2017)

### 3.1.1.5 Key parameters – structure

The geotechnical parameters and factors that mostly affect the design and the construction of the structure of the tunnel are:

- The strength parameters, important in the determination of the influence width of the vertical loads on the tunnel and therefore the vertical loads themselves.
- The coefficient of earth pressure at rest, which determines the value of the horizontal stresses acting on the tunnel, in function of the vertical stresses, and consequently influences the shape of the tunnel.
- The site conditions, in terms of type of soil and presence of buildings on the surface areas, influence the choice of the excavation method to be used.
- The permeability, the groundwater level and the percentage of clay, they influence the conditioning of the soil when excavating with a mechanized method.

### 3.1.2 Ground

#### 3.1.2.1 Stability conditions

In the presence of shallow tunnel in urban areas, the stability of the tunnel face is a problem that must be faced, since is one of the factors that influences the choice of the type of excavation.

The evaluation of the face-support pressure is a critical aspect during the design and construction phase, however no standardised guidelines are available to face this feature. In current practice, the estimation of the design value of the face-support pressure is needed to evaluate the stability conditions of the excavation. The face-support design follows two main steps:

1. Verification of the equilibrium conditions of the excavation face;
2. Identification of the consequent stabilizing measures for a complete control of the development of deformations and water inflows.

The methods for analysis of face stability include *analytical methods*, based on the Limit Equilibrium Method or on the earth pressure theory, and *numerical methods*, 2D or 3D. The interaction between excavation and soil is very complex, to supply complete results the best procedure should be a 3D numerical analysis; however, 2D analyses, along the longitudinal sections, simulate with reasonable approximation the strain behaviour at the tunnel face and evaluate the applied pressure effects.

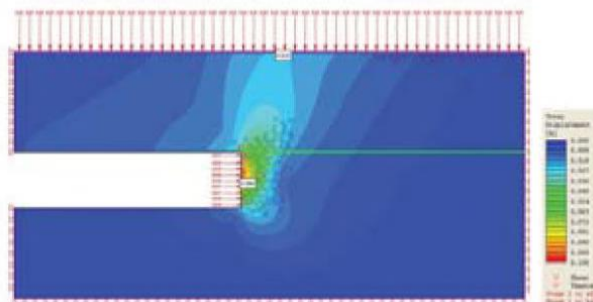


Figure 3.10. Example of 2D numerical model along a longitudinal section (Guglielminetti, 2008)

Analytical methods are applied for their relative simplicity especially in the initial design phase for rapid simulations of the conditions to be excavated; however, they are not sufficient for a complete assessment of the long-term stress-strain behaviour of the ground, around the

tunnel and on the ground surface. They could be useful to validate the results of the numerical analyses (Guglielminetti et al., 2008). In *Table 3.1*, a selection of analytical methods is reported.

*Table 3.1. Some analytical method for estimation of the face-support pressure (Guglielminetti et al., 2008)*

| <i>Modell/method</i>   | <i>Analysis type*</i> |       | <i>Failure surface</i>           | <i>Failure criterion</i> |
|--|-----------------------|-------|----------------------------------|--------------------------|
| 1. Horn model (Horn, 1961)   | GE                    | 3D    | Linear (Wedge + silo)            | –                        |
| 2. Murayama method (Murayama, 1966)  | GE                    | 2D    | Spiral logarithmic               | MC                       |
| 3. Broms & Bennemark method (Broms et al., 1967)   | GE                    | 2D    | Not defined                      | TR                       |
| 4. Atkinson & Potts method (Atkinson et al., 1977)   | St                    | 2D    | Not defined                      | MC                       |
| 5. Davis et al. method (Davis et al., 1980)  | St                    | 2D    | Not defined                      | TR                       |
| 6. Krause method (Krause et al., 1987)   | GE                    | 2D–3D | Circular                         | MC                       |
| 7. Mohkam method (Mohkam et al., 1984, 1985, 1989)   | GE                    | 2D–3D | Spiral logarithmic + Cylindrical | MC                       |
| 8. Leca & Dormieux method (Leca et al., 1990)  | St                    | 3D    | Not defined                      | MC                       |
| 9. Jancsecz & Steiner method (Jancsecz et al., 1994)                                       | GE                    | 3D    | Linear (Wedge + silo)            | MC                       |
| 10. Anagnostou & Kovari method (Anagnostou et al., 1994, 1996)                             | GE                    | 3D    | Linear (Wedge + silo)            | MC                       |
| 11. W. Broere method (Broere, 2001)  | GE                    | 3D    | Linear (Wedge + silo)            | MC                       |
| 12. Caquot method (Caquot, 1956) implemented by C. Carranza-Torres (Carranza-Torres, 2004) | St                    | 3D    | Not defined                      | MC–HB                    |

\* GE = Global equilibrium, St = Stress method; 2D, 3D = analytical formulation derived from 2-dimensional, 3-dimensional numerical analyses. MC = Mohr-Coulomb; TR = Tresca; HB = Hoek-Brown.

To mention few of the analytical methods of *Table 3.1*, a distinction between drained and undrained conditions must be made. In soils where permeability is low, the undrained stability plays an important role during the excavation. Broms & Bennemark (1967) defined a *stability ratio*  $N$ , as the ratio between stresses and strains on the tunnel and, based on it, Cesarin and Mair (1981) gave a set of curves to compute the displacements at the surface, crown and face (*Figure 3.11*).

$$N = \frac{\sigma_s + \gamma \cdot \left(C + \frac{D}{2}\right) - \sigma_t}{c_u} \quad (\text{Eq. 3.2})$$

Where:

- $\sigma_s$  surface surcharge pressure (if any);
- $\gamma$  unit weight of soil, considering all homogeneous;
- $C$  cover above the tunnel;
- $D$  diameter of the tunnel;
- $\sigma_t$  tunnel support pressure (if any);
- $c_u$  undrained shear strength at tunnel axis level.

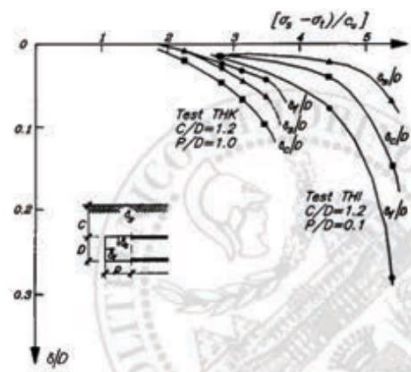


Figure 3.11. Surface, crown and face displacements for different  $N$  values (Cesarin & Mair, 1981)

When dealing with drained stability conditions, cohesion and friction angle influence the behaviour, and it is possible to refer to the Leca & Dormieux formulation (1990) to evaluate the face-support pressure.

### 3.1.2.2 Surface settlement trough

When excavating a shallow tunnel, especially in urban areas, not only the stability of the tunnel itself has to be considered, but also its influence on the buildings on the surface, it leads to stress redistribution and deformation in the subsoil as well as surface settlements in the surrounding area. They must be little enough in order to guarantee the serviceability of all the shallow infrastructures and utilities.

The surface settlement trough immediately following the tunnel construction develops above and ahead of the advancing heading; it is function of the geological condition of the site and it is well described by a Gaussian distribution curve (Figure 3.9). The maximum value of settlements is above the tunnel axis.

$$s(y) = s_{max} \cdot \exp \left[ -\frac{y^2}{2i^2} \right] \quad (\text{Eq. 3.3})$$

Where:

- $s(y)$  is the settlement of ground in one point;
- $y$  is the horizontal distance from the tunnel axis;
- $s_{max}$  is the maximum settlement;
- $i$  is the horizontal distance between the tunnel axis and the point of inflection.

It is also possible to calculate the volume of surface settlement trough, per metre length of tunnel, integrating the abovementioned equation. The results are:

$$V_s = \sqrt{2\pi} i s_{max} = 2.5 i s_{max} \quad (\text{Eq. 3.4})$$

Where  $i = Kz_0$  is a parameter function of the depth of tunnel ( $z_0$ ) and the ground conditions (K).

Typical values of the coefficient K are reported in *Table 3.2*.

*Table 3.2. Values of the K coefficient for the calculation of settlement trough*

| Ground conditions                          | K         |
|--|-----------|
| Soils with no cohesion (sands and gravels) | 0.2 – 0.3 |
| Normally consolidated clay                 | 0.5       |
| Overconsolidated clay                      | 0.6 – 0.7 |
| Rocks                                      | 0.8 – 0.9 |

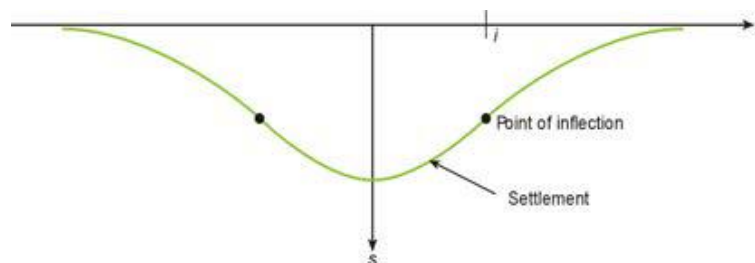


*Figure 3.12. Transverse settlement trough*

Several methods in order to evaluate the surface settlements are available.

The *Volume Loss* method is an empirical method that evaluates the amount of ground lost in the region close to the tunnel, primarily due to one or more of the following components: deformation of the ground towards the face resulting from stress relief; passage of the shield (overcutting edge); tail void (gap between the tailskin of the shield and the lining); deflection of the lining, consolidation.

It can be expressed as a percentage of the notional excavated volume of the tunnel (D=diameter):

$$V_L = \frac{V_s}{\pi D^2/4} [\%] \quad (\text{Eq. 3.5})$$

The volume loss also depends on the adopted excavation method, when a conventional method is used, the percentage ranges from 0.8 to 1.5%, if the TBM method is used values are lower, 0.5 – 1%.

Another method follows the *Herzog's theory* (1985) that says that the maximum settlement is given by

$$s_{max} = 0.785 \cdot (\gamma \cdot Z_0 + P_s) \cdot \left( \frac{D^2}{i \cdot E} \right) \quad (\text{Eq. 3.6})$$

Where:

- $\gamma$  is the unit weight of soil;
- $Z_0$  is the tunnel depth;
- $P_s$  is the total surface load;
- $D$  is the diameter of the tunnel;
- $I$  is the distance between the tunnel axis and the point of inflection;
- $E$  is the Young Modulus.

A lot of other empirical formulations for the calculation of the maximum surface settlement are available in literature, such as Schmidt (1969), Verruijt and Booker (1996), Loganathan and Poulos (1998) and many others (Chakeri and Unver, 2013).

### **3.1.2.3 Key parameters – ground**

Considering all the above, there are several parameters that can be considered in the prediction of the maximum surface settlement value and stability conditions. They include cohesion, angle of internal friction, tunnel depth, tunnel diameter, Poisson's ratio, Young's modulus, unit weight, face support pressure and surface surcharge.

Focusing on the deformability parameters, the Young's Modulus is the parameter that gives the amount of the deformations, once stresses are settled. The excavation process produces in the ground a redistribution of stresses, in order to evaluate the new strain state, the link is the Young's Modulus. For instance, it permits to evaluate the surface settlements that take place after the excavation of the tunnel in underground.

### 3.1.3 Soil-structure interaction

The term “soil-structure interaction” refers to all analytical models where the behaviour of the ground and the behaviour of a structural member are closely linked and interact significantly.

Since the 1980s, a lot of studies have been carried out on the behaviour of the soil-structure interface: most of them take into account isothermal conditions and do not consider the possible effects of temperature variations. According to these research studies, the soil-structure interface is defined as a thin zone of soil that can be subjected to different boundary conditions with respect to the surrounding soil. Its thickness depends on soil and structure properties but is generally considered to vary from 5 to 10 times the average particles diameter.

The ground behaviour is characterized by the reactive soil stresses, their distribution and the associated ground deformation: a tunnel lining is a typical structure with a dominant soil-structure interaction.

The crucial factor in the soil-structure interaction is the determination of a realistic ground-structure stiffness ratio, especially if non-linear characteristics are to be considered.

The *stiffness ratio*  $\beta$  is the ratio between the ground stiffness and the flexural rigidity of the structural members. For tunnels, it is defined as follows (ITA guidelines for tunnelling):

$$\beta = \frac{E_g \cdot R^3}{E_c \cdot I_c} \quad (\text{Eq. 3.7})$$

Where:

- $E_g$  [MPa] is the deformation modulus of the ground;
- $R$  [m] is the radius measured on the centre line of the tunnel;
- $E_c$  [MPa] is the deformation modulus of concrete (lining);
- $I_c$  [ $\frac{m^4}{m}$ ] is the moment of inertia of the lining;
- $E_c \cdot I_c$  is the flexural rigidity of the tunnel lining.

When  $\beta \rightarrow 0$  it refers to a rigid non-deformable structure and/or to an extremely soft ground; when  $\beta \rightarrow \infty$  it refers to a very flexible structure and/or a very stiff ground.

The stiffness and interaction parameters determine the reaction forces and the distribution of the load portions to be carried by the tunnel lining and the supporting ground. The stiffness ratio  $\beta$  is the main influencing factor determining the load sharing between ground and tunnel lining when elastic behaviour is prevalent.

- $5 \leq \beta \leq 50$  Soft soils;
- $\beta > 1000$  Hard rocks;
- $\beta \leq 120$  The lining is stiff in comparison with the ground;
- $\beta > 120$  Considerable load sharing between ground and lining, and the lining can be considered a relatively flexible structure.

Analytical methods to evaluate the interaction are available in literature, Schwartz and Einstein (1980) defined a simplified analysis for ground-structure interaction in tunnelling, with the aim of making it an accessible and effective tool in the design procedure. The “simplified analysis method” includes the effects of three major variables: the stiffness of the support; the spatial delay of support construction behind the tunnel face; the yielding of the ground mass surrounding the support.

More recently, other methods appeared, among them the bedded-beam spring model (Barpi et al., 2011), which describes the tunnel lining as a series of beams connected at their nodes to a series of radial and tangential springs that are designed to model the ground reactions.

### ***3.1.3.1 Key parameters – soil-structure interaction***

It has been observed that the most influencing geotechnical parameter in the soil-structure interaction is the deformation modulus of the ground, its stiffness. Compared to the one of the lining, it gives the stiffness ratio that governs the interaction behaviour.

### **3.1.4 Numerical simulations**

Analytical models have been developed to allow the evaluation of the stresses and displacements in the lining and in the ground with simplifications, but it is practically impossible to take all the influences, parameters and boundary conditions that are dependent on the geology and construction phases into account in a simple calculation.

Since the analytical methods give simplified results and they are unable to model the full complexity of a tunnel during construction, nowadays building a numerical model in a Finite Element method is the most widely used numerical technique.

A numerical model allows to consider all the aspects presented in the previous chapters at the same time, structure, soil and soil-structure interaction, with the advantage of having the possibility to take into account complex geometries and configurations.

When considering a soil, it can be treated as a continuum: Finite Element (FE), hybrid Finite Element/Boundary Element (FE/BE) or Finite Difference (FD) methods can be applied. On the contrary, if it is considered as a discontinuum, which means that every single component behaves separately, the Distinct Element Method (DEM) can be used. If there is the need to combine the discontinuum and the continuum model the Finite Discrete Element Method (FDEM) is the chosen method.

An important step before modelling an unknown problem is always the validation of the software, because it is not to be trusted a priori. This is usually done by simulating problems for which analytical or closed form solutions are available: numerical and analytical results are then compared.

#### ***3.1.4.1 The model***

It is important to build a model that has right input parameters, according to the chosen constitutive law, geometry must reflect as much as possible the real conditions and also the computational stages must be accurate, in order to reproduce the exact excavation/construction sequence.

There is a very clear sequence to follow to build a FEM model:

1. *Model the geometry of the tunnel and of the underground stratigraphy.* A high influence on the behaviour of the model is given by the geometry that is imposed. Once that the dimension of the tunnel is set, the model built around it has to be big enough, so that the boundary conditions do not affect the behaviour of the model.
2. *Discretize* to create the FE mesh. The software is usually an automatic generator, which, given some indications, builds the mesh. The accuracy of the results depends on the number of points where the analysis are made and the precision of the outcome: the more the points, the better the quality.
3. *Define the boundary conditions*, in terms of constraints on the boundary, such as rollers and/or hinges, and in terms of external applied loads (also thermal), groundwater table, etc.
4. *Choose a soil model and assign the material properties* to the ground and to each element.
5. *Assign the initial stress state to the nodes.*
6. *Define the computational stages*, in order to reproduce construction sequence. The first stage must always be representative of the in situ state of stress before excavation, with zero displacements set, because the model is in equilibrium and does not move under the action of its weight. After that, each step will include a progressive modification of the conditions, until the last step is reached, which represents the concluded tunnel.
7. *Compute.*
8. *Interpret the results.* This analysis is run in order to calculate as exact as possible settlements and deformations as a result of the tunnel work and to size the shotcreting tunnel shell, with the ability to take into account complex geometry

The stress redistribution that takes place while excavating a tunnel, particularly at the advancing face, is three-dimensional: the best practice would be modelling in three-dimensions. Otherwise, 3D models are complex to construct, time-consuming to analyse and difficult to interpret. Frequently the tunnel is represented as a two dimensional model assuming transverse plain strain. There are some practices that allow to simulate the third dimension: for example, the 3D behaviour of excavation can be simulated by the progressive decrease of the stiffness of the ground inside the excavation area, in order to simulate settlements before the installation of supports.

To simulate structural supports in a FE model there are two methods available: the first one consists of considering the real geometry of the structural elements in contact with the ground and model them with continuum 2D elements, however, sometimes the dimensions of the structural elements are small compared to the overall geometry and therefore, to model them would result in either a very large number of elements, or elements with unacceptable aspect ratios. To overcome these shortcomings, special FE have been developed (method 2), formulated by essentially collapsing one, or more, dimensions of the structural component to zero. The element is formulated directly in terms of bending moments, axial and shear forces and their associated strains so that the quantities of engineering interest come directly from the finite element analysis.

The most widely used special FE are the beam element, the cable element, the pile element. For a tunnel the beam elements are used, they represent a structural member in which bending resistance and limited bending moments are important. They may be used to model a wide variety of supports, including support struts in an open-cut excavation and concrete or shotcrete linings in a tunnel.

### ***3.1.4.2 Constitutive laws***

When talking about soils, many models that describe the ground behaviour are available at various degree of accuracy, from the linear elastic model to the advanced HHSsmall model (Hardening Soil with Small strains). The linear elastic model is not suitable to reproduce the highly non-linear and irreversible soil behaviour: it only takes into account two elastic parameters, the Young's Modulus  $E$  and the Poisson's ratio  $\nu$ , it is too simplistic to capture all the essential features of soil and rock behaviour. However, advanced models should be used only when all the parameters needed for the computation are well-established, on the contrary, advanced tools with bad input parameters could bring to unreliable results.

The best "first approximation" of soil and rock behaviour is the linear elastic perfectly-plastic Mohr-Coulomb model. For each layer a constant average stiffness or a stiffness that increases linearly with depth can be evaluated, making computations relatively fast with a first estimate of deformations. The model requires few parameters:

- Young's Modulus  $E$  [MPa]
- Poisson's coefficient  $\nu$  [-]
- Cohesion  $c$  [MPa]

- |  |                  |
|--|------------------|
| • Friction angle                       | $\varphi$ [°]    |
| • Dilatancy angle                      | $\psi$ [°]       |
| • Cut-off tension and tensile strength | $\sigma_t$ [MPa] |

Very similar to the Mohr Coulomb model, there is the Drucker-Prager plasticity model, which takes into account the same parameters. It is an approximation of the Mohr-Coulomb failure criterion.

The *Hardening Soil* model is an advanced model for the simulation of soil behaviour. As for the Mohr-Coulomb model, limiting states of stress are described by means of the friction angle, the cohesion and the dilatancy angle. However, soil stiffness is described much more accurately by using three different input stiffnesses: the triaxial loading stiffness, the triaxial unloading stiffness and the oedometer loading stiffness. A basic feature of the Hardening Soil model is the stress dependency of soil stiffness: it increases with pressure, resulting in longer calculation times. It is suitable both for soft and stiff soils.

Even more accurate is the *Hardening Soil with Small-strain stiffness* model. The original Hardening Soil model assumes elastic material behaviour during unloading and reloading. However, the strain range in which soils can be considered truly elastic, i.e. where they recover from applied straining almost completely, is very small. With increasing strain amplitude, soil stiffness decays nonlinearly

### **3.1.4.3 Soil-structure interaction in a FE model**

With a finite element analysis, it is possible to evaluate the ground-structure interaction in a realistic manner. Complex non-linear ground or time-dependent behaviour (e.g. due to construction phases) or detailed deformations can be realistically evaluated. When modelling with continuum elements, they do not allow relative movements at the soil-structure interface, but, in reality, they occur and they are of great importance in the behaviour of the structure. Joint elements or interfaces can be used to model soil-structure interaction. It is possible to vary the constitutive behaviour of the soil-structure interface: differential movements, slip and separation are allowed. Many methods have been proposed to model discontinuous behaviour at the soil-structure interaction:

- The use of a continuum element to reproduce the interface, with different constitutive behaviour with respect to the soil (*Figure 3.13.a*);

- The use of springs to model interfaces, springs with an elasto-plastic interaction model (*Figure 3.13.b*);
- The use of special interface elements with zero thickness (*Figure 3.13.c*).

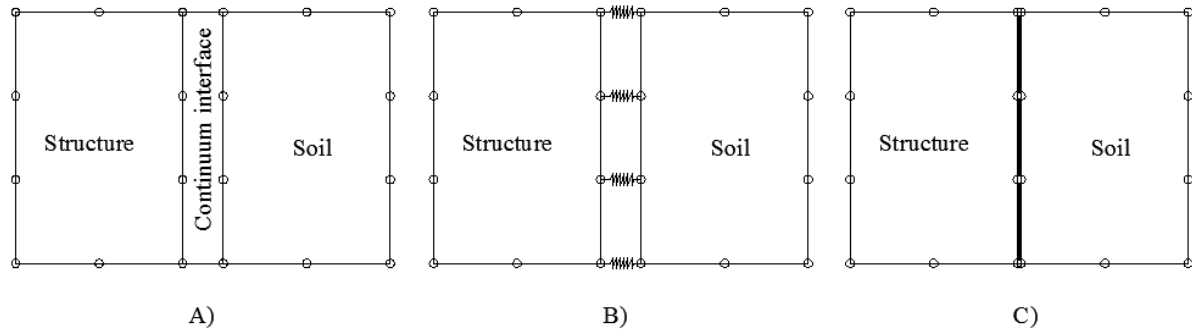


*Figure 3.13. Soil-structure interface in FEM: a) continuum interface, b) springs, c) zero thickness element*

For example, in a tunnel where the lining is reproduced by beam elements, if they are attached to a sub-grid by interface elements, the frictional interaction of the structure with the soil or the effect of geotextiles can be simulated.

### 3.2 Thermal design of tunnels

In this chapter the thermal design is tackled: the aim is to determine how the thermal parameters of the system affect the energy performances of the energy tunnel.

The energy efficiency of an energy tunnel is function of:

- Thermal properties;
- Thermal behaviour of surrounding ground;
- Thermal demand;
- THM behaviour of the ground, in terms of temperature changes.

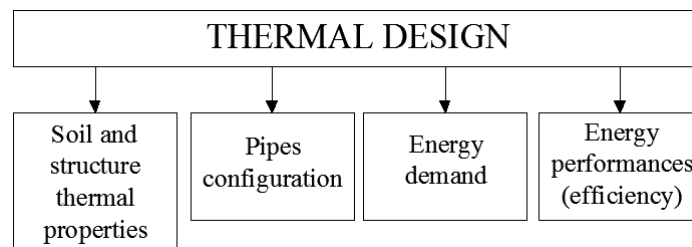


Figure 3.14. Thermal design for an energy tunnel

### 3.2.1 Analytical models

Analytical models commonly used for designing and analysing Boreholes Heat Exchangers include the line-source and cylindrical-source solutions, the ASHRAE handbook method, the Superposition Borehole Model, etc. (Bourne-Webb et al., 2016). However, for energy tunnels very much simplified model exists.

Brandl (2006) showed the solutions of diffusion equations for the cases of a semi-infinite body, an infinite body with cylindrical gap and an infinite body with a spherical gap. They could be applied also for the computation of an energy tunnel, however, due to the complexity of the whole system, alternative procedures are usually adopted.

Analytical solutions assume that conduction is the only mechanism for heat flow in the soil and within the heat exchangers. Some solutions solve the diffusion equations directly, others use the thermal resistance, which is a parameter influenced also by the geometry of the heat exchanger. In the absorber pipes, there is heat conduction in the pipe walls and convection in the fluid inside the pipes, where conduction can be neglected due to the high flow rate.

A simple thermal resistance model was developed for an energy tunnel for determining the energy potential for the tunnel projects of “Stuttgart21”. In this model, heat transfer in the soil is based on conduction only, so no groundwater flow could be considered (Schlosser et al., 2007). Another conduction only model for tunnel lining ground heat exchangers was developed by Zhang et al. (2013) and verified using the results of a thermal response test carried out in the Lichang tunnel, China.

The difficulties of applying an analytical method lie in the consideration of all those factors that affect the heat exchange, such as the air inside the tunnel and the energy released by the circulation of the traffic. While the determination of the surrounding soil temperature is approximately possible with the aid of the geothermal gradient, the determination of a corresponding tunnel air temperature is comparatively difficult. References could not be found on this topic. Simple arithmetical estimates sometimes led to implausible results. The air temperature in the tunnel depends on several parameters. These are the outdoor air temperature, the flow through the tunnel, the length of the tunnel, the wall or ground temperature, the internal heat sources and the location in the tunnel. The influence of the

outside air temperature decreases with long tunnels, the larger the distance to the tunnel portal. Short tunnels are mainly influenced by the outside air (Schlosser et al., 2007).

The above-mentioned observations are some of the reasons why numerical analyses are preferable when dealing with the thermal design of an energy tunnel.

### 3.2.2 TH design

Numerical analyses have the aim to quantify the efficiency of the energy tunnel system as well as to assess its sustainability in the long term. Most of the numerical methods are based on heat conduction. Temperature and flux boundary conditions can be applied, a TH analysis is usually done, it simulates the thermal exchange between the fluid circulating through the pipes, installed in the tunnel concrete lining, and the surrounding soil, submerged under the ground water table.

The TH problem is governed by mass conservation, energy conservation equations, and Darcy's velocity law (*Table 3.3*).

*Table 3.3. Equations that govern the TH problem*

|  |  | <i>Involved parameters</i>   |
|--|--|--|
| <p><i>Mass conservation equation</i><br/>(Eq. 3.7)</p>   | $S \cdot \partial_t p - n\beta_w \partial_t T + \nabla \cdot (nv_{w,i}) - nv_{w,i}\beta_w \nabla T = 0$                  | Porosity, pressure, water and solid compressibility, water thermal expansion coefficient, temperature, water velocity.                                     |
| <p><i>Energy conservation equation</i><br/>(Eq. 3.8)</p> | $[n\rho_w c_w + (1-n)\rho_s c_s] \partial_t T + n\rho_w c_w v_{w,i} \nabla T - \nabla \cdot (\lambda_{ij} \nabla T) = 0$ | Hydraulic conductivity, water density and dynamic viscosity, hydraulic head.   |
| <p><i>Darcy's velocity law</i><br/>(Eq. 3.9)</p>         | $v_{f,i} = nv_{w,i} = -\frac{k_{ij}\rho_w g_i}{\mu} \nabla h = -k_{ij} \nabla h$   | Water and solid phase heat capacity, soil particles density, water and solid phase thermal conductivity, longitudinal and transverse thermal dispersivity. |

When building a TH model, it is important to reproduce accurately the geometry of the problem and the groundwater condition.

In the TH softwares, the absorber pipes inside the tunnel lining can be modelled as one-dimensional discrete feature elements, widely validated and with good agreement with analytical solutions (Diersch, 2009): the conservation of mass and energy is satisfied and the fluid inside them flows following the Hagen-Poiseuille law.

### 3.2.2.1 *Quantification of heat transfer*

In the model, after having set all the initial conditions up, an initial inlet temperature and velocity of the carrier fluid is imposed, the analysis is run and the results include the outlet temperature at equilibrium, from which is it possible to quantify the extracted or injected heat ( $Q$ ).

$$Q = m \cdot c \cdot \Delta T \quad (\text{Eq. 3.8})$$

Where:

- $m$  mass flow rate [kg/s];
- $c$  heat capacity of the circulating fluid [J/kg·K];
- $\Delta T = |T_{wo} - T_{wi}|$  variation between inlet ( $T_{wi}$ ) and outlet ( $T_{wo}$ ) temperature [K].

In order to minimize the head losses and to avoid too expensive pumping system, a turbulent flow regime inside the pipes has to be ensured (Reynolds number higher than 2300). This can be achieved if the difference between the inlet ( $T_{wi}$ ) and outlet temperatures is:

$$|T_{wo} - T_{wi}| = 3 \div 5 \text{ } ^\circ\text{C} \quad (\text{Eq. 3.9})$$

The heat exchange is not an easy phenomenon: many parameters influence it and it is possible to study their influence by conducting parametric analyses.

Di Donna and Barla (2016) have conducted a parametric analysis in order to investigate the effect of ground temperature, groundwater flow velocity, and thermal conductivity on the heat exchange.

#### Ground temperature

The dimensioning of all the plant components is function of the fluid flowrate which, in turn, is function of the delta temperature between the heat carrier fluid temperature and the undisturbed ground temperature. Higher delta means smaller, cheaper geothermal plant but also a high impact on the thermal equilibrium of the ground and a reduction of heat pump

efficiency. Lower delta means good performance of the heat pump but a bigger and more expensive plant is needed.

The ideal deltas are:

$$|T_{wo} - T_g| = \begin{cases} 6 \div 11 \text{ }^\circ\text{C in heating regime} \\ 11 \div 17 \text{ }^\circ\text{C in cooling regime} \end{cases} \quad (\text{Eq. 3.10})$$

Where:

- $T_{wo}$  fluid outlet temperature;
- $T_g$  undisturbed ground temperature.

The authors concluded that the heat exchange improves by approximately 7%/°C of ground temperature, being more favourable in hot regions during winter and in cold regions during summer, *Figure 3.15*.

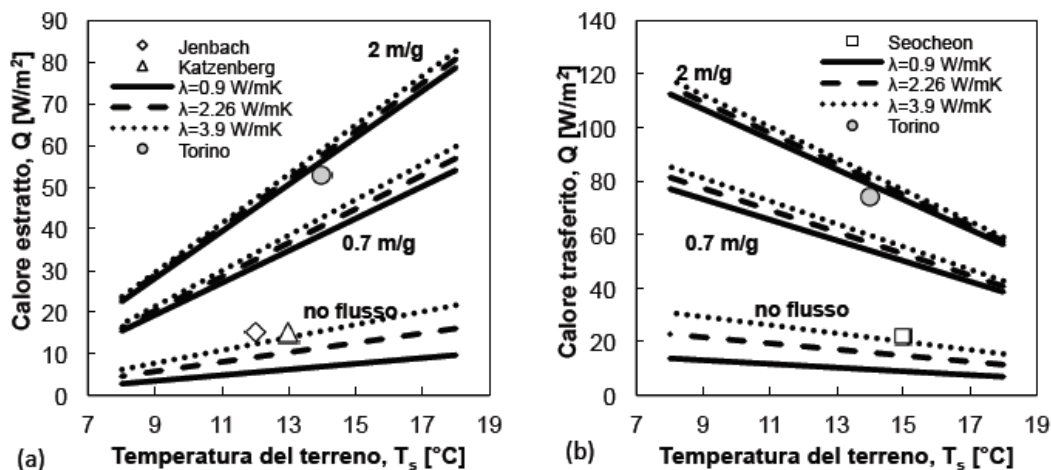


Figure 3.15. Effects of undisturbed ground temperature on the exchanged heat in a) winter and b) summer. (Di Donna & Barla, 2015)

### Groundwater flow

Groundwater flow can influence heat transfer by additional advection, which merely shifts the position of the underground thermal store.

Both in summer and winter, as shown in *Figure 3.16*, the exchanged heat increases with the groundwater flow rate.

With the groundwater flow, the heat exchange results from a combination of conduction and convection, and the most influencing factor is the velocity of groundwater flow. With an increase from 0 to 2 m/d, the exchanged heat improves by a factor of 3 to 8 times. However,

in the case of high groundwater flow velocity, the risk of thermal pollution should be assessed.

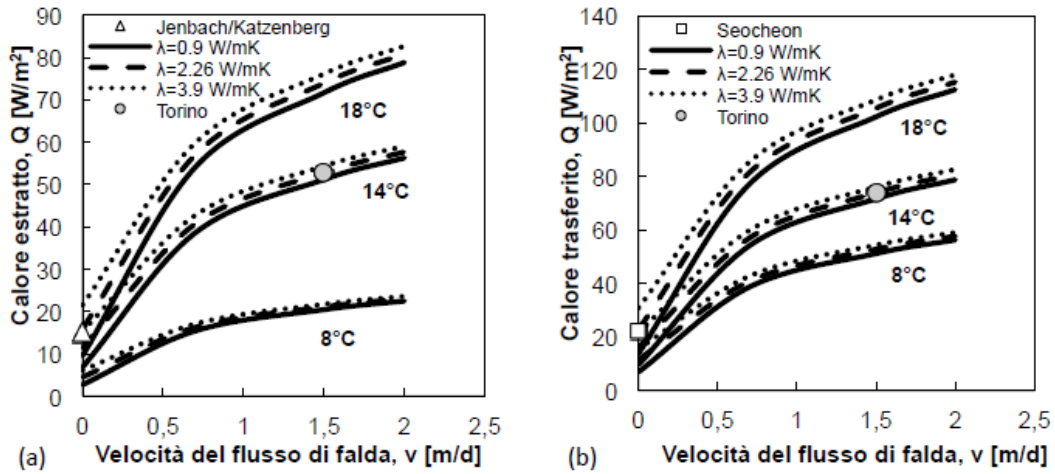


Figure 3.16. Effects of the groundwater rate on the exchanged heat in a) winter and b) summer (Di Donna & Barla, 2015)

Thermal conductivity

The exchanged heat increases with the thermal conductivity, but the effect is more significant with the reducing rate of groundwater flow, up to the case of static conditions, where the increase is the higher. In the absence of groundwater flow, when the heat exchange occurs essentially by conduction, the soil thermal conductivity plays a primary role and the exchanged heat is more than doubled, ranging from 0.9 to 3.9 W/(m·K) for both summer and winter operational modes, Figure 3.17.

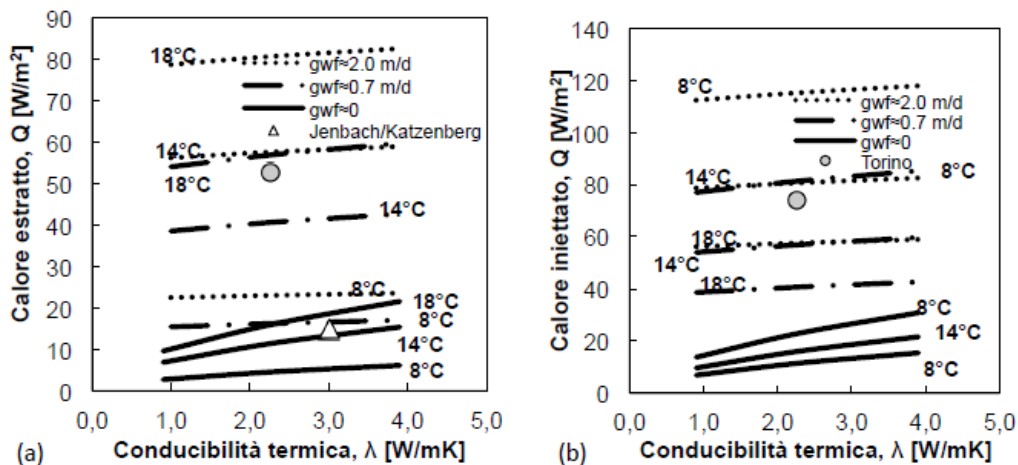
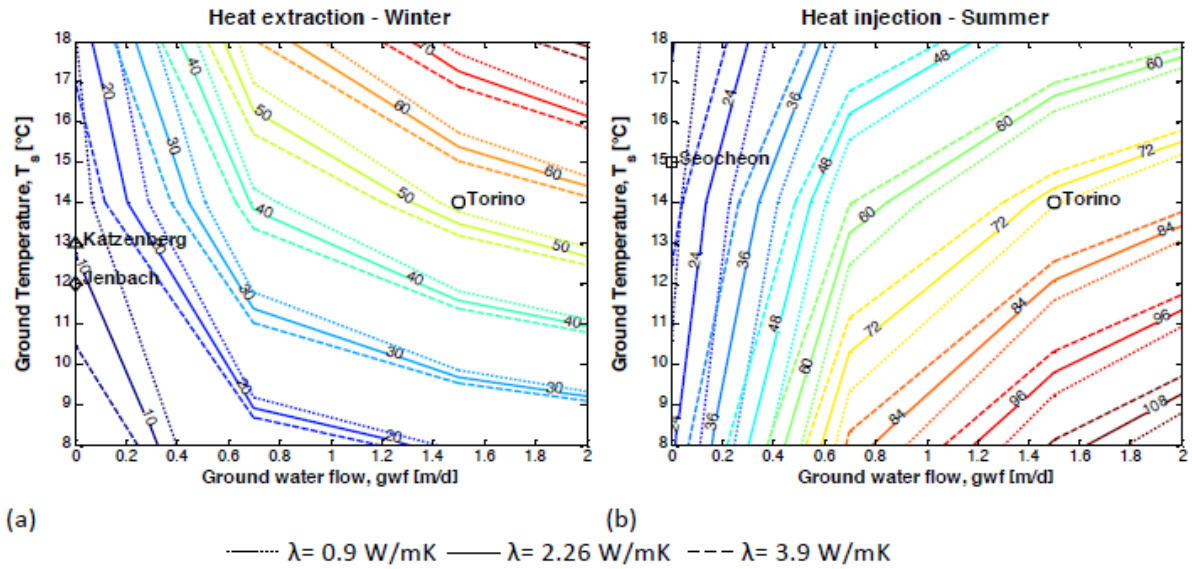


Figure 3.17. Effects of the thermal conductivity on the exchanged heat in a) winter and b) summer (Di Donna & Barla, 2015)

Based on the above-mentioned results, the authors have proposed two charts for the heat extraction and injection, in winter and summer respectively, which can be used in the

## Energy Tunnels design process

preliminary thermal design of an energy tunnel, *Figure 3.18*. The charts can be used for a preliminary assessment of the potential energy exploitation in both summer and winter based on the specific site conditions where the system is to be installed.



*Figure 3.18. Design charts for the heat exchange (extracted and injected heat in  $W/m^2$ ), function of the groundwater flow, the ground temperature and the thermal conductivity. (Di Donna & Barla, 2015)*

Assuming these requirements as a starting point, the plant can be designed in detail from both the geothermal and hydraulic point of view, including the choice of the appropriate heat pump, with the help of TH numerical analysis.

### **3.2.3 Key parameters – efficiency of the system**

The aim of the thermal design is to evaluate the performances of the system and it is done by the evaluation of the exploitable heat. It has been observed that the most influencing factors on the energy tunnel efficiency are the presence and velocity of the groundwater flow, the ground temperature and the thermal conductivity of soil.

The evaluation of the performances is the first step when designing an energy tunnel, if the results are positive and efficiency is advantageous, it is possible to continue the design sequence and consider the effects of the pipes system on the structure and the surrounding ground.

### **3.3 Structural design of a segmental lining**

The aim of this chapter is to describe how to design and size the structural components of a segmental lining, in particular a thermo-activated segmental lining. Segmental lining is the typical support system of mechanized excavation, the installation of several adjacent rings along the tunnel axis is made by the TBM. The lining is composed of multiple segmental rings, made of precast reinforced concrete segments. Segments are designed to provide structural capacity to resist to many actions: demoulding, storage, transportation, handling, erection and grouting pressures, permanent loads, ground loads, water pressure, TBM thrust, imposed loads (i.e. traffic) thermal loads and dynamic loads.

When dealing with energy tunnels, it is important to design not only the reinforcements cage inside the segments but also the pipes configuration and to study its effects on the global behaviour.

#### **3.3.1 Features of segments**

##### **3.3.1.1 Materials**

The segments forming the lining are commonly made of precast reinforced concrete (from C35/45 to C100/115 and C180/210 depending on the dimensions and loads – Fabozzi, 2017), but also the use of Fibre Reinforced Concrete (FRC) reflects the current state of the art. The latter consists of steel fibres mixed in the concrete to totally or partially replace the traditional reinforcements. In general, FRC and reinforcements cage are used together to assure the integrity of all the critical zones, such as the corners (Duretto, 2018).

##### **3.3.1.2 Geometry**

Rings are made of 5 to 7 segments, directly installed by TBM itself: the last segment is called the *key-segment*, smaller than the others, it closes the segmental ring. It has a trapezoidal shape which means that the two adjacent segments must have inclined sides to fit. At the end of the construction the ring is a cylinder with surfaces that could be parallel or not. The configuration only affects the installation process, not the performances. Three main types are available (*Figure 3.19*):

- Straight ring, with parallel sides, it fits well linear tracts;

- Tapered ring, with one side inclined, it fits well tracts with predefined curves;
- Universal ring, with two sides inclined (variable thicknesses), which is the most versatile, it fits both straight and curved path.

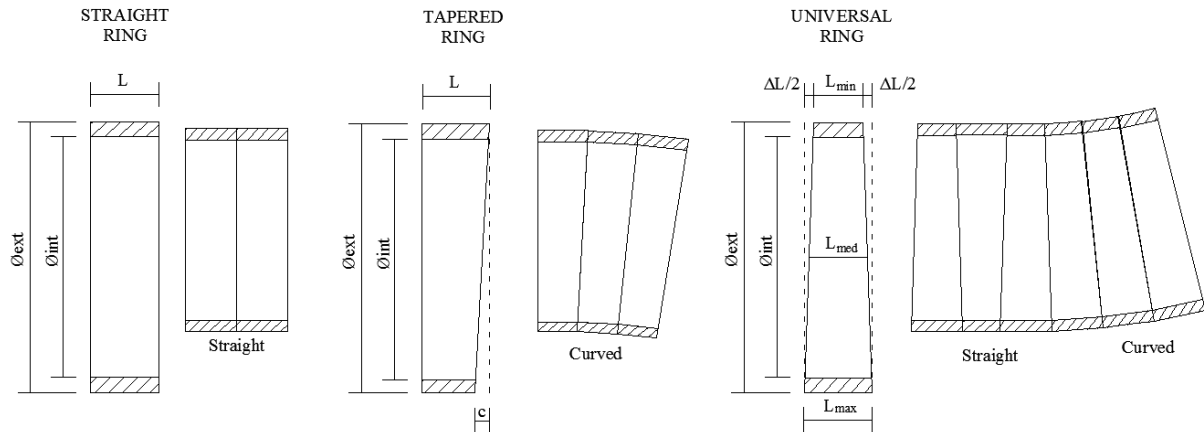


*Figure 3.19. Geometry of different types of ring*

The segments are commonly chosen as large as possible, in order to minimize the number of segments per ring, optimizing the advancing speed of the TBM. Thicknesses are in the order of 0.20 – 0.70 m, function of the structural characteristics (load-bearing capacity, bending moments, ...). For ordinary tunnel diameters, thickness is about 1/20 of tunnel diameter, but when a high strength concrete is used, it could be much smaller, up to 1/58 of tunnel diameter (Fabozzi, 2017). When the gasket is present, it is recommended to increase the thickness of 5 cm.

This kind of elements requires very strict geometric tolerances, in the range of 0.1 – 1 mm, given that the final ring must be as precise as possible. Controls are made in the initial phase before construction, checking the moulds, and also during the construction sequence.

To complete the geometrical description, in each segment, it is needed to design also “secondary” elements, such as the holes for the connectors, the holes for the erector of the TBM, the groove for the gasket and the groove for the guidance rod (*Figure 3.20*).

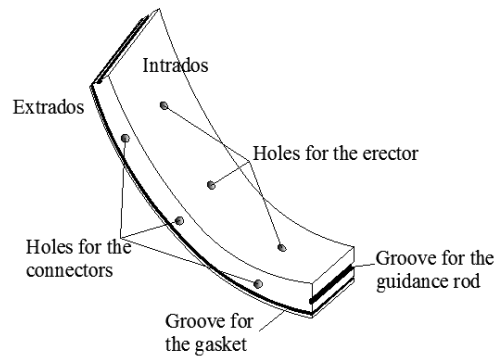


Figure 3.20. Secondary elements in the geometry of a segment

### 3.3.1.3 Connections

Inside a segmental tunnel lining it is possible to find two main types of connections: longitudinal, between the segments of the same ring, and transversal or circumferential, in the transverse direction, between different rings. To tie two adjacent elements, it is common to use joints with bolts, inserted during the construction phase of the segment, or with dowels, inserted in an automated way in special pockets of the segments during the installation phase. The first type of joints is suitable both for longitudinal and transversal connections, while the second is used only for connections between rings, between segments bars are inserted in the dedicated grooves (groove for the guidance rod).

### 3.3.1.4 Sealing

To avoid infiltration of water in the gallery, the entire tunnel support system has to be waterproof. To guarantee the functionality of the structure, attention must be paid to the constitutive materials, to the design details, to the transport/handling and installation of each segment. The construction sequence must be carefully monitored to have good results in sealing. Fractures and damages must be avoided, otherwise, filtration could occur. Gaskets are planned near the extrados of each segment to assure the hole lining to be impermeable, they are made of a gummy material and cover the joints. Their design follows some nomographs, given by the manufacturer (Duretto, 2018)

### 3.3.1.5 Legal framework

The current technical legislation in the building-civil field in Italy is represented by the D.M. 17-01-2018, better known as *NTC2018* (Norme Tecniche per le Costruzioni 2018), which

refers to the Eurocodes for detailed design of underground structures, such as tunnels. The most involved Eurocodes are:

- Eurocode 0 EN-1990 – Basis of structural design;
- Eurocode 1 EN-1991 – Actions on structures;
- Eurocode 2 EN-1992 – Design of concrete structures;
- Eurocode 7 EN-1997 – Geotechnical design.

### ***3.3.1.6 Design process***

With reference to the legal framework, it is possible to assume the design process of a segment as a sequence of structural verifications to be applied for each load scenarios that occur in the service life of a segment. Based on that, the first important step in each project is to carefully evaluate the load scenarios of the segments. A classification of these scenarios is adopted, based on the construction phase they refer to:

1. *Manufacturing phases*, they could include the lifting of the segment from the mould, the storage of the single segment during the curing phase, the transport, the in-situ handling of the segment.
2. *Installation phases*, such as the thrust of the advancing TBM or the injection pressure (grouting).
3. *Final phases (implementation)*, when the geostatic and water pressures act on the structure, the joints are subjected to bursting and potential additional strains could occur.

The structural verifications to be done are at Ultimate and Serviceability Limit State, ULS and SLS respectively:

- ULS verification against combined compressive and bending stress;
- ULS verification against shear;
- ULS verification against additional tension given by shear actions;
- SLS verification against cracking;
- SLS verification for the stress limitation.

Focusing on the lining, it is stated that the structural verifications of the reinforcement elements, of the segments, of the preliminary and final lining must be executed with characteristic values of geotechnical parameters, while the effects of the actions must be

increased with the partial coefficients  $A_1$  (NTC2018, 2018). When considering the soil-structure interaction in the design for the pre-dimensioning, the analysis must be run with characteristic values of geotechnical parameters, while the effects of the actions must be increased with the partial coefficients  $A_1$  (NTC2018, 2018).

The process includes a first approximation of reinforcement percentage for each load scenario: it is important to verify that the area of steel is sufficient to cover also the actions of the following load scenario.

### 3.3.2 TM design

Energy tunnels couple the structural role of geostructures with the energy supply by using the principle of shallow geothermal energy. For this reason, it is not possible to treat the structural behaviour and the thermal loads independently: they are related, and it is important to understand the thermo-mechanical behaviour of the ground in contact with the tunnel. Temperature changes during GHE operation can lead to the development of resulting changes in stresses and strains in the structure. These changes need to be evaluated to ensure that there is no detrimental impact on the structural performance of the energy geostructure.

Thermo-Mechanical analyses consider only conduction and thermal loads are coupled to the mechanical one at any time during a transient simulation, so that thermally induced stresses and strains can be evaluated. Only one-way coupling occurs, for example, when temperature varies, it may result in stress changes, but if a force is applied to the body, inducing mechanical changes, temperature is not affected. This restriction is acceptable, because the energy changes for quasi-static mechanical problems are usually negligible.

The magnitude of additional stresses and strains on the structure is function of several factors:

- Transient heat conduction parameters, because they determine the temperature gradient (input data taken from the energy performance analysis);
- The contrast between the volumetric elastic thermal expansion coefficients of concrete and of the phases of the soil (solid, liquid, gas);
- Saturation ratios;
- Permeability;
- Drainage conditions;
- Structure's boundary constraints.

Numerical methods provide an efficient tool for solving complicated partial differential equations such as those that govern the thermo-mechanical problem, because of their ability to integrate complexities arising from the geometry, thermo-mechanical loading, interaction between different rigidity bodies, etc.

In general, the thermal activation can be reproduced by building a numerical model simulating the excavation process, the installation of the lining and, at the end, the thermal activation.

The first step of the modelling sequence includes the setting of the geometry, the mechanical and thermal properties of the material, the initial and boundary conditions and the heat exchange model. Once all these features are set, it is possible to simulate the thermal activation of the lining, imposing a temperature variation law and by running two different analysis, winter and summer operational modes. Results in terms of stress variations can be extrapolated, with consequent determination of the new values of bending moment, normal and shear stresses, which are fundamental to compute all the structural verifications reported in *Chapter 3.3.1.6*.

### ***3.3.2.1 Background experience***

The most well studied geostructures under the TM point of view are the *energy piles*, well established results come from their projects. For energy piles, it is important to study the soil-structure interaction for correctly predicting the response of pile foundations in terms of displacement and lateral capacity.

When dealing with the effects of changes in temperature, they have a safety effect on the pile-soil interaction because, as reported in *Chapter 2.1.3.2*, in the case of sand no effects are produced by an increase of temperature and in the case of clay it improves the interface strength.

However, the thermo-elastic expansion and contraction of the piles induce an additional mechanically cyclic stress on the interface shear stress. The volumetric behaviour changes at each cycle due to the continual rearrangement of grains; the first contracting phase is followed by a dilating phase during each cycle and the combination of the two components results in a global contraction cycle after cycle. The effect is similar to the cyclic degradation phenomenon studied for piles subjected to cyclically axial loading in sandy ground. In the case of energy piles, this phenomenon happens even if the axial loading is static. It has been observed that the degradation phenomenon of piles in clay is less significant because of the reduced volumetric cyclic contraction of the interface with respect to the case of sand. In the case of NC clay, this volumetric cyclic contraction is even reduced by the increase in temperature, as

the soil first undergoes a thermal consolidation thus reducing the soil potential of collapse during shearing (Di Donna, Ferrari, Laloui, 2015).

It is possible to consider the numerical simulation of a pile conducted by Suryatriyastuti, Mroueha and Burlon (2012) with finite difference method under static thermal load for only cooling and only heating operation. Two different conditions of contact between soil and an energy pile have been taken into account: (1) perfectly contact and (2) sliding contact with frictional interface elements (both ends of the pile are freely restrained).

The results show that by the presence of interfaces at the zone of contact between soil and pile, the stresses and displacements obtained are lower than those with perfect contact. Cooling cycle in winter mode results in pile's contraction and shortening while summer mode operation leads to an uplift surface with expansion of pile, both produce surface's settlement (*Figure 3.21*). When in contraction, the tensile forces are induced at the pile, when dilating, compressive forces are applied to the pile. To be observed is that if interfaces are imposed at surface of contact, the values of temperature-induced normal forces produced are lower (*Figure 3.22.a*).

*Figure 3.22.b* shows frictions mobilised along interface soil–pile at model 2: cooling cycle increases frictions mobilised at the upper part of pile while reduces at the lower part of pile. On the contrary, a higher gradient temperature applied will possibly create negative friction at interface soil–structure. There is a node at the middle part of pile that is not influenced by temperature-induced friction mobilised, which is called null point.

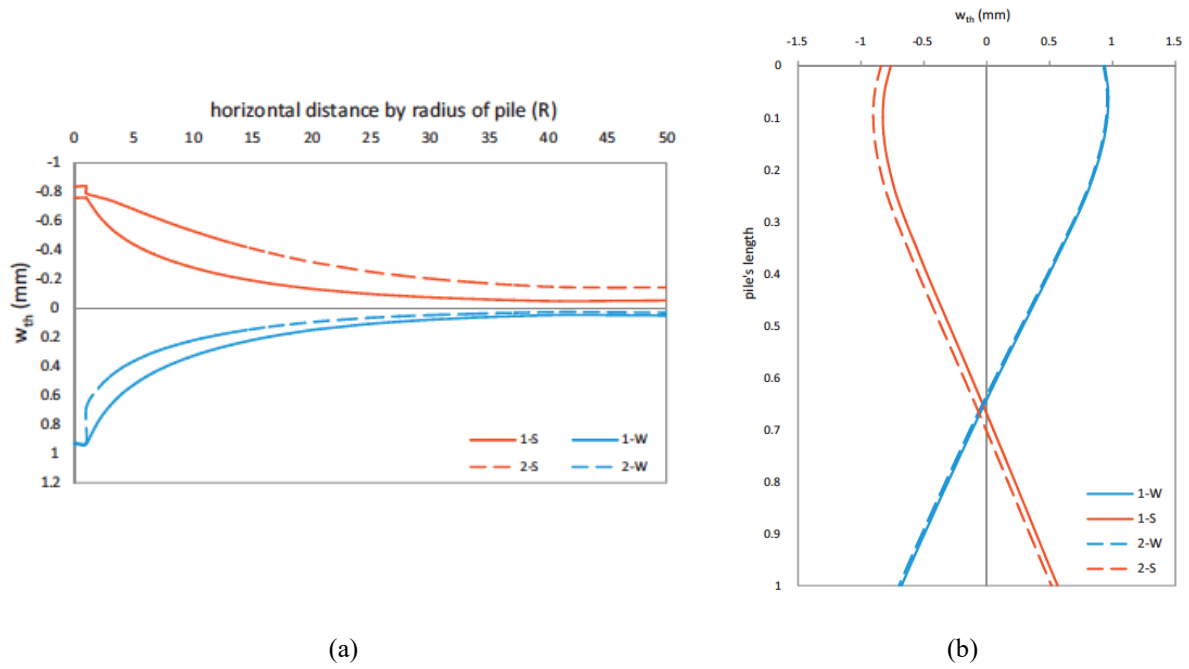


Figure 3.21. (a) Thermal surface displacements, (b) thermal vertical displacements of the pile (Suryatriyastuti, Mroueha and Burlon, 2012)

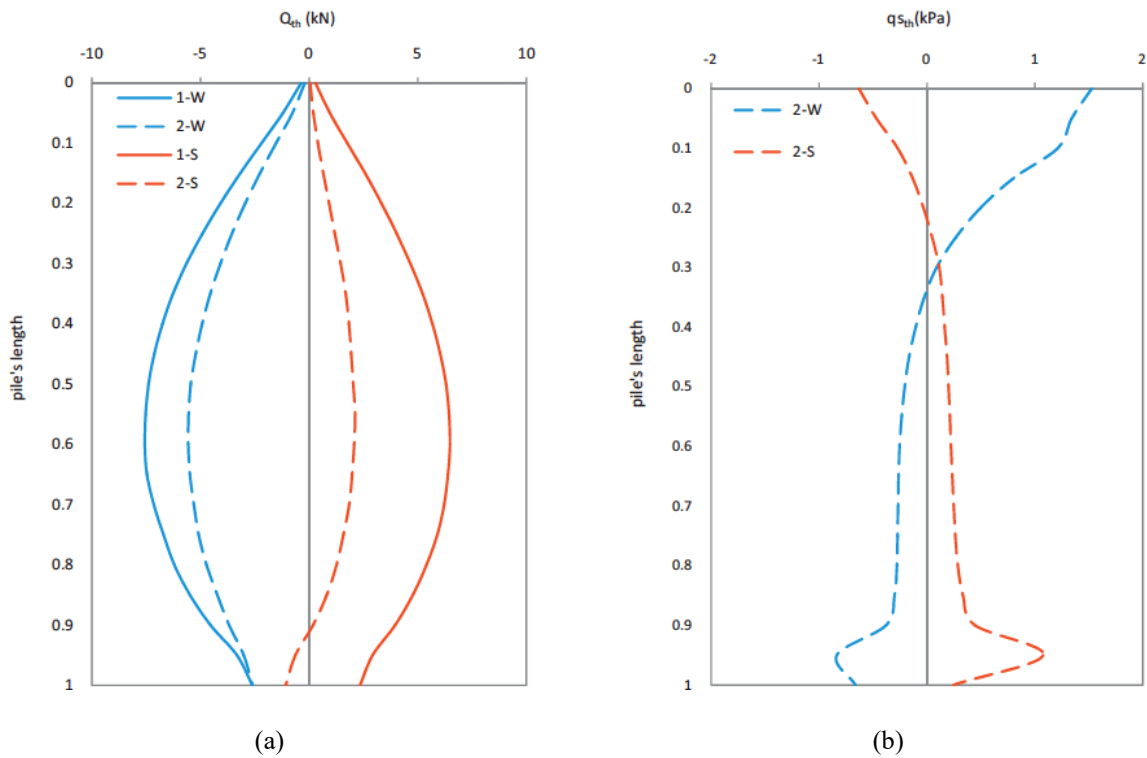


Figure 3.22. Pile under thermal loading (a) temperature induced normal forces in the pile, (b) temperature-induced frictions mobilised at interface soil-pile. (Suryatriyastuti, Mroueha and Burlon, 2012)

Coletti and Sterpo (2016) studied the structural and geotechnical response of an energy wall by sequentially coupled thermo-mechanical analyses: first, a thermal analysis of the soil-structure system permitted to investigate the energy performance and to calculate the cyclic temperature variations. Then, a thermo-mechanical analysis is carried out, simulating first the construction process and then the effects of the geothermal system, with the application of the cyclic temperature variations as thermal loads.

The authors stated that the behaviour is similar to the one observed in energy piles, but the complexity in the geometry (possible presence of anchors or slabs) and boundary conditions (the wall is fully embedded in the soil in its lowest part only, leaving an undetermined thermal condition on the face exposed to the excavation) of the wall make the results not easily predictable. The thermo-mechanical behaviour of energy walls has not yet been fully investigated. The possible detrimental action induced by cyclic thermal loads could be neglected, since the interface shear resistance is not a key factor in the structural behaviour of the wall, but variations of pressures induced by the materials thermal contraction or expansion could be of interest.

The conventional plane strain analysis has to be replaced by a three-dimensional scheme, due to temperature gradients arising the wall longitudinal plane.

In this study the temperature effects on the materials behaviour are limited to the thermal expansion and the hydro-mechanical coupling effects are neglected.

In *Figure 3.23.a*, it is possible to see how an increase in temperature is reflected in an increase of horizontal pressures and vice versa. In *Figure 3.23.b*, the top displacements are shown, they vary a lot with the presence of the heat exchangers in the wall with respect to the ordinary diaphragm walls and therefore they should be taken into account for the optimal design.

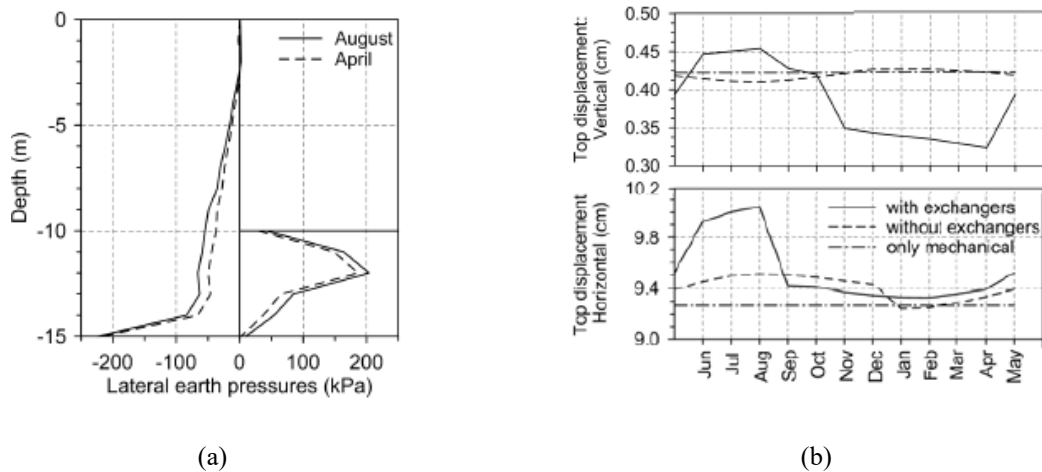


Figure 3.23 (a) Lateral earth pressures in two periods of the year; (b) Variation of the displacements at the wall top over the year ( $x=1.2m$ ), (Coletti, Sterpi, 2016)

The thermal loads can be considered not detrimental to the global stability and structural safety of the wall, since they affect mainly the axial elongation/contraction and mildly the flexural response. In *Figure 3.24*, it is clearly shown how the temperature affects the axial forces induced in the wall at different sections, while the thermal effect on the bending moment is negligible (*Figure 3.25*).

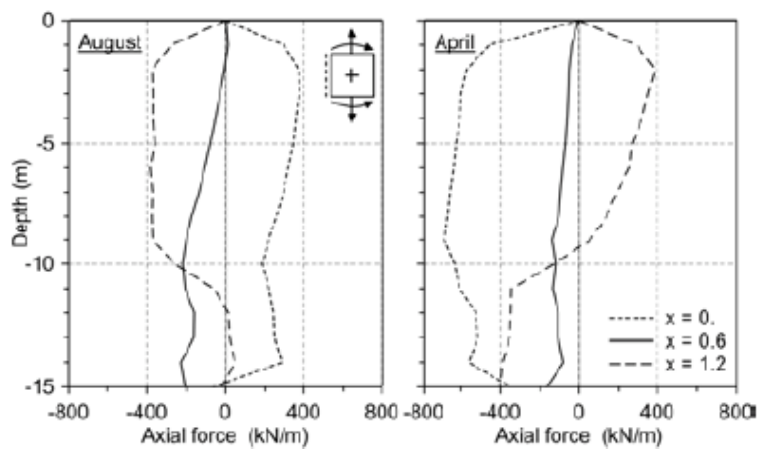


Figure 3.24. Axial load within the wall in two periods of the year and in three cross sections (Coletti, Sterpi, 2016)

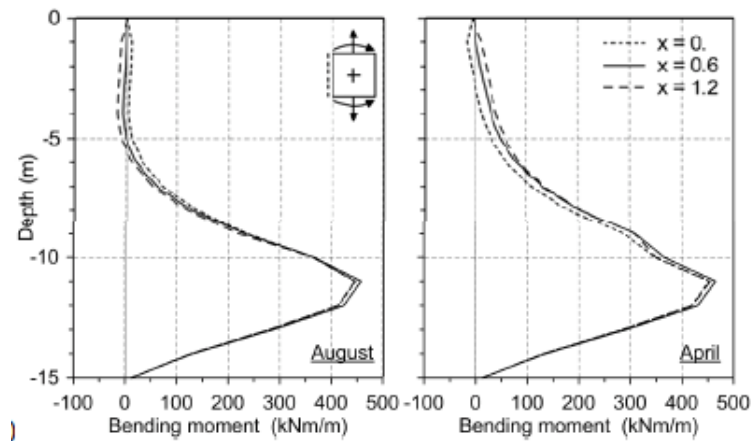


Figure 3.25. Bending moment within the wall in two periods of the year and in three cross sections (Coletti, Sterpi, 2016)

### 3.3.2.2 Energy tunnels

In the previous chapters, shallow structures have been taken in consideration, which are affected by the seasonal fluctuation of temperature, as explained in *Chapter 1*. When dealing with tunnels, they can be deeper than the “fluctuation depth” and, therefore, this phenomenon can have no effect on the structure.

Energy tunnels are the less investigated type of energy geostructure, they can be considered still at the beginning of their implementation compared to the energy piles; therefore, there still is a high need for research on their THM behaviour.

Barla and Di Donna (2018) simulated the activation of a thermal lining in order to investigate the effect of thermal loads on the structure. Pipes that are inside an energy tunnel are modelled with their real geometry and changes of temperature in them can be considered as boundary conditions at their contour.

A full summer-winter cycle was simulated with heat injection through the pipes in summer ( $T_i = 25.8^\circ\text{C}$ ) and heat extraction during winter ( $T_o = 4.5^\circ\text{C}$ ). Horizontal and vertical stresses decrease during heating with the segmental lining experiencing compression, while they increase during cooling, because of the experienced dilation. The stress change was in the order of less than 1 MPa, during the whole cycle for this specific application (*Figure 3.26*).

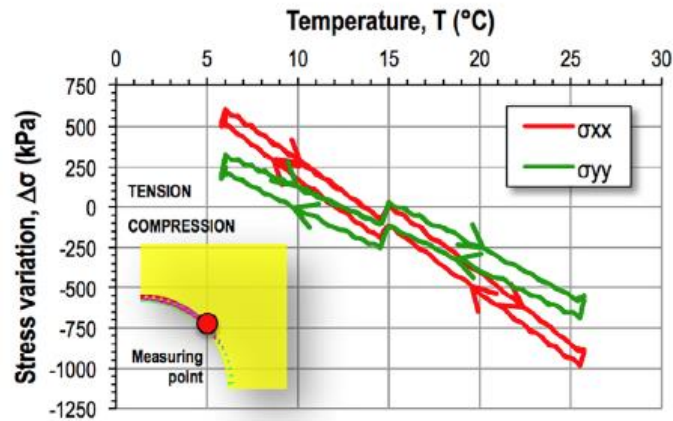


Figure 3.26. Horizontal ( $xx$ ) and vertical ( $yy$ ) stresses versus temperature variations computed by the TM analysis (Barla, Di Donna, 2018)

Based on that, the authors stated that the mechanical design of a tunnel lining, considering thermal loads, does not impose substantial variations with respect to normal procedures, thermal loads are negligible.

### 3.3.3 Key parameters – TM design of segments

Looking at the energy piles, an important observation that can be made is that contact conditions between structure and soil have a remarkable influence on the interface behaviour. The interface should be modelled in an appropriate way, such as its nodes can take into account the temperature transfer.

When dealing with tunnels, there is still a lack of information about the TM interface behaviour. In the previous chapter it has been reported that in the mechanical design of an energy tunnel, thermal loads have a very low impact on the stresses and so they can be neglected. However, those results have been carried for specific conditions of soil and structure, there could be differences when the types of soil or interface between the soil and the lining change.

### 3.4 Outcomes

In *Chapter 3*, attention has been paid to the input parameters, both geotechnical and thermal, with reference to the design stages and the numerical analyses.

Starting with the geotechnical design aspects of the tunnel, an analysis was made considering the structure, the surrounding ground and the soil-structure interaction. The site conditions, the strength parameters, the coefficient of earth pressure at rest, the permeability, the ground water level and the percentage of clay influence the design, the behaviour and the construction of the structure of the tunnel. The deformability parameters play a major role in the behaviour of the surrounding ground, in terms of amount of deformations, strain state and consequently of surface settlements that take place after the excavation of the tunnel. The soil-structure interaction behaviour is also function of one of the deformability parameters, the Young's Modulus.

The thermal design follows, in order to evaluate the performances of the system in terms of the exploitable heat. The performances of the system are function of the exploitable heat. The most influencing factors on the energy tunnel efficiency are the presence and velocity of the groundwater flow, the ground temperature and the thermal conductivity of soil.

The structural design of the lining, with particular attention to the TM behaviour has been then reported: to deepen the concepts, a comparison between the energy piles and the energy tunnels has been made, in terms of TM interface behaviour. In the first case, it is validated that contact conditions between structure and soil have a remarkable influence on the interface behaviour; on the contrary, when dealing with tunnels, there is still a lack of information about the TM interface behaviour. Some results from a model have been reported but with reference to very specific initial conditions, there could be differences when the types of soil or interface between the soil and the lining change.

Based on all the above contents of the previous chapters, it is possible to say that a lot of aspects regarding energy tunnels are still to be investigated, with respect to other types of energy geostructures, as the energy piles.

In *Table 3.4*, the most influencing parameters in the design of an energy tunnel are reported. In the next chapter, a 2D model of an energy tunnel will be presented and its aim is to

## Energy Tunnels design process

---

investigate, by parametric analyses, one of the missing aspects regarding its TM behaviour: how temperature, intended as the thermal activation of the lining, could affect the surface settlements.

*Table 3.4. Influencing parameters in the design of an energy tunnel - in bold letters the parameters for the parametric analysis*

| INFLUENCING PARAMETERS |   |
|------------------------|---|
| TM DESIGN              | Deformability parameters                              |
|                        | Strength parameters                                   |
|                        | Coefficient of Earth pressure at rest                 |
|                        | Permeability  |
|                        | <b>Thermal expansion coefficient</b>                  |
|                        | <b>Tunnel temperature (External, Fluid, Internal)</b> |
| TH DESIGN              | Groundwater flow                                      |
|                        | Ground temperature                                    |
|                        | Thermal conductivity                                  |



## **4 NUMERICAL ASSESSMENT OF THE ROLE OF THERMAL PARAMETERS**

### **4.1 Introduction**

In this chapter a numerical model of a cross section of a tunnel is described. The chosen software is FLAC. The final aim is to analyse how, after thermal activation of the lining, surface settlements could be affected.

First, the geometry is reproduced, and two main phases follow. The first one refers to the mechanical behaviour, initial and boundary conditions are applied only in terms of stresses and displacements, material properties do not include the thermal properties. The excavation is modelled, with the application of a relaxation factor, and the lining is installed. The surface settlements, without any influence by temperature, are analysed.

The second phase introduces temperature and its effects. The thermal properties are assigned to the materials and initial and boundary conditions in terms of temperature are applied. The

surface settlements are analysed both before and after the thermal activation of the lining, in order to make reasonable comparisons.

The analyses are made for winter, summer and mid-season conditions: temperatures vary for the external air, the tunnel air and the fluid in the pipes for each mode. In addition, a parametric analysis is conducted on the thermal linear expansion coefficient, which assumes three different values for each season.

## **4.2 FLAC – Fast Lagrangian Analysis of Continua**

### **4.2.1 General information**

FLAC, Fast Lagrangian Analysis of Continua, is a code intended for geotechnical engineering applications, for advanced analysis of soil, rock, groundwater, and ground support in two dimensions.

It is appropriate to design foundations, settlements, bearing capacities, slopes, tunnels, consolidation, thermal and creep problems. It allows to build plane-strain models with customized functions, procedures and constitutive laws. It has in memory some common constitutive laws of soils, from the very simple and widespread “Mohr-Coulomb” to the more sophisticated “Cam-Clay” model.

FLAC utilizes an explicit finite difference formulation that can model complex behaviours, the explicit, time-marching solution of the full equations of motion (including inertial terms) permits the analysis of progressive failure and collapse, which are particularly important phenomena for mine design and geotechnical construction.

With respect to the thermal analysis, FLAC includes both conduction and advection models. The conduction models allow simulation of transient heat conduction in materials, and the development of thermally induced displacements and stresses. The advection model takes into account the transport of heat by convection; it can simulate temperature-dependent fluid density and thermal advection in the fluid. In the model, different zones may have different thermal models and properties and they all can be used with any of the mechanical models. Several different thermal boundary conditions may be prescribed. The thermal option provides for one-way coupling to the mechanical-stress and pore-pressure calculations through the thermal expansion coefficients.

## 4.2.2 Finite Difference Method

The Finite Difference Method (FDM) is a numerical method used in continuum mechanics and it is considered as one of the oldest numerical techniques for the solution of boundary value problems. Every derivative in the set of governing equations is replaced directly by an algebraic expression written in terms of the field variables (e.g., stress or displacement) at discrete points in space; these variables are undefined within elements.

FLAC uses an explicit, time marching method to solve the algebraic equations. Explicit scheme is a function of time, which means that velocity and acceleration are different from zero and need to be considered. The explicit method works in timestep increments, variables are calculated as the time proceeds. Overall, explicit methods are better for non-linear, large-strain problems, while they are not efficient for modelling linear, small-strain problems.

The general calculation sequence embodied in FLAC is reported in *Figure 4.1*. First, new velocities and displacements are derived with the equations of motion from stresses and forces. Then, strain rates are derived from velocities, and new stresses from strain rates. The dynamic equations of motion are included in the formulation to ensure that the numerical scheme is stable when the physical system being modeled is unstable. Every cycle around the loop takes one timestep, which is chosen so small that information cannot pass from one element to another in that interval. After several cycles, disturbances can propagate across several elements, just as they would propagate physically.

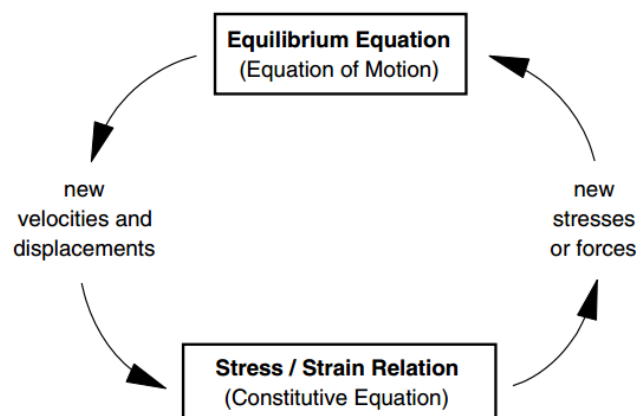


*Figure 4.1. Basic explicit calculation cycle (FLAC User's Manual)*

The most important advantage is that no iteration process is necessary when computing stresses from strains in an element, even if the constitutive law is wildly nonlinear. In an implicit method (which is commonly used in finite element programs), every element communicates with every other element during one solution step: several cycles of iteration are necessary before compatibility and equilibrium are obtained. Another difference from a finite element method is that matrices are never formed, with consequent minimum memory requirements and accommodating large displacements and strains without additional computing effort. A disadvantage is represented by the fact that small timestep means large numbers of steps to be taken to conclude the computation.

### 4.2.3 Thermo-Mechanical governing equations

The thermal option can be combined with the mechanical calculation to perform a thermo-mechanical analysis with FLAC. All the features of the thermal calculation, including transient and steady-state heat transfer, and thermal solution by either the explicit or implicit algorithm, are available in a thermo-mechanical calculation. FLAC includes both the conduction and advection models, in the model only conduction will be used, so only conduction formulations are reported.

#### 4.2.3.1 Conduction

Temperature and the two components of the heat flux are involved in heat conduction simulation in FLAC. They are related through the energy-balance equation and transport laws derived from Fourier's law of heat conduction.

##### Energy-Balance Equation

$$-\nabla \mathbf{q}^T + q_v^T = \frac{\partial \zeta_T}{\partial t} \quad (\text{Eq. 4.1})$$

In *Eq. 4.1* the differential expression of the energy balance is reported and the terms represent:

- $\mathbf{q}^T$  heat-flux vector [W/m<sup>2</sup>];
- $q_v^T$  volumetric heat-source intensity [W/m<sup>3</sup>];
- $\zeta_T$  heat stored per unit volume [J/m<sup>3</sup>].

As mentioned in the previous chapters, the assumed and valid hypothesis is that only temperature influences the mechanical behaviour and strains play a negligible role in influencing the temperature. It is possible to write:

$$\frac{\partial \zeta_T}{\partial t} = \rho C_v \frac{\partial T}{\partial t} \quad (\text{Eq. 4.2})$$

Where the terms are:

- $\rho$  mass density of the medium [kg/m<sup>3</sup>];
- $C_v$  specific heat at constant volume [J/kg°C];
- $\frac{\partial T}{\partial t}$  temperature rate.

Substituting Eq. 4.2 in Eq. 4.1, Eq. 4.3 is obtained:

$$-\nabla \mathbf{q}^T + q_v^T = \rho C_v \frac{\partial T}{\partial t} \quad (\text{Eq. 4.3})$$

#### Transport Law

The transport law, better known as the Fourier's law, defines the relationship between the heat-flux vector,  $\mathbf{q}^T$ , and the temperature gradient,  $\nabla T$ . For a stationary, homogenous, isotropic solid the connection is given by the thermal conductivity tensor,  $\mathbf{k}^T$  [W/m°C].

$$\mathbf{q}^T = -\mathbf{k}^T \nabla T \quad (\text{Eq. 4.4})$$

Substituting Eq. 4.4 in Eq. 4.3 yields the differential equation for heat conduction:

$$-\nabla(-\mathbf{k}^T \nabla T) + q_v^T = \rho C_v \frac{\partial T}{\partial t} \quad (\text{Eq. 4.5})$$

#### Mechanical Coupling: Thermal Strains

When temperature is present, the stress-strain rate formulation must be rewritten. Temperature changes induce a change in the total strain rate, while, for isotropic materials, the shearing-strain increments are unaffected. Considering  $\frac{\partial T}{\partial t}$  the temperature rate and a free thermal expansion situation, the associated thermal-strain rate is:

$$\frac{\partial \epsilon_{ij}^T}{\partial t} = \alpha_t \frac{\partial T}{\partial t} \delta_{ij} \quad (\text{Eq. 4.5})$$

Where:

- $\alpha_t$  coefficient of linear thermal expansion [ $1/^\circ\text{C}$ ];
- $\delta_{ij}$  Kroneker delta.

Fluid Coupling: Thermally Induced Pore Pressures

Thermal expansion of the constituents causes pore pressure changes, which can be considered the link between the heat transfer and the groundwater calculation.

$$\frac{\partial P}{\partial t} = M \left( \frac{\partial \zeta}{\partial t} - \alpha \frac{\partial \epsilon}{\partial t} + \beta \frac{\partial T}{\partial t} \right) \quad (\text{Eq. 4.6})$$

Where:

- $M$  Biot Modulus;
- $\alpha$  Biot coefficient;
- $\epsilon$  volumetric strain;
- $\beta$  volumetric thermal expansion, which in FLAC assumes the following form:

$$\beta = n\beta_f + (1 - n)\beta_g \quad (\text{Eq. 4.7})$$

Where  $n$  is the porosity,  $\beta_f$  and  $\beta_g$  are the volumetric thermal expansion coefficients of the fluid and the grains, respectively. In FLAC,  $\beta_g = 3\alpha_t$ .

Initial and Boundary Conditions

Initial conditions correspond to a given temperature field. Boundary conditions can be expressed in terms of temperature or the component of the heat-flux vector normal to the boundary.

In FLAC, five types of conditions are considered:

1. given temperature;
2. given component of the flux normal to the boundary;
3. convective boundaries;
4. radiative boundaries;

5. insulated (adiabatic) boundaries.

A convective boundary condition is expressed by:

$$q_n = h(T - T_c) \quad (\text{Eq. 4.8})$$

Where:

- $q_n$  component of the flux normal to the boundary in the direction of the exterior normal;
- $h$  convective heat-transfer coefficient [ $\text{W}/\text{m}^2 \text{ } ^\circ\text{C}$ ];
- $T$  temperature of the boundary surface [ $^\circ\text{C}$ ];
- $T_e$  temperature of the surrounding fluid [ $^\circ\text{C}$ ].

### 4.3 The numerical model

It has been chosen to analyse a tunnel hypothetically excavated in the Turin subsoil, by TBM EPB, with an excavation diameter of 8 m. The distance between the centre of the tunnel and the surface is assumed to be 20 m; if  $H < 5D$  (where  $D$  is the tunnel diameter) the structure is considered a *shallow tunnel*, it means that gravity plays an important role.

#### 4.3.1 Geometry

In order to build the numerical model, the first step is to determine the geometry. In *Table 4.1*, the most important geometric parameters are reported.

*Table 4.1. Geometry of the tunnel*

|   |       |
|---|-------|
| Tunnel diameter [m]                         | 8.00  |
| Distance centre of the tunnel – surface [m] | 20.00 |
| Thickness of the lining [m]                 | 0.30  |
| Distance pipes – segments' extrados [m]     | 0.05  |

FLAC organizes its zones (or “elements”) in a row-and-column fashion; however, the physical shape of a FLAC grid need not be rectangular: the rows and columns can be distorted so that the boundary fits arbitrary and more complicated shapes. The zones can vary in size across a grid.

With any numerical method, the accuracy of the results depends on the grid used to represent the physical system. In general, finer meshes (more zones per unit length) lead to more accurate results. Furthermore, the aspect ratio (ratio of height to width of a zone) also affects accuracy. When creating grids with FLAC, the greatest accuracy is obtained for a model with equal, square zones.

When deciding on the geometric extent of the grid and the number of elements to specify, it is needed to consider how the location of the grid boundaries will influence model results and what density of zoning is required for an accurate solution in the region of interest.

## Numerical assessment of the role of thermal parameters

Trying not to influence the results by imposing the boundary conditions, boundaries are located at a distance of 10 times the diameter from the excavation in the 3 possible directions, being a shallow tunnel on the top there is a fixed value, in this case 20 m from the centre of the tunnel. In *Figure 4.2 and 4.3* the model from FLAC is shown, general view and detailed respectively.

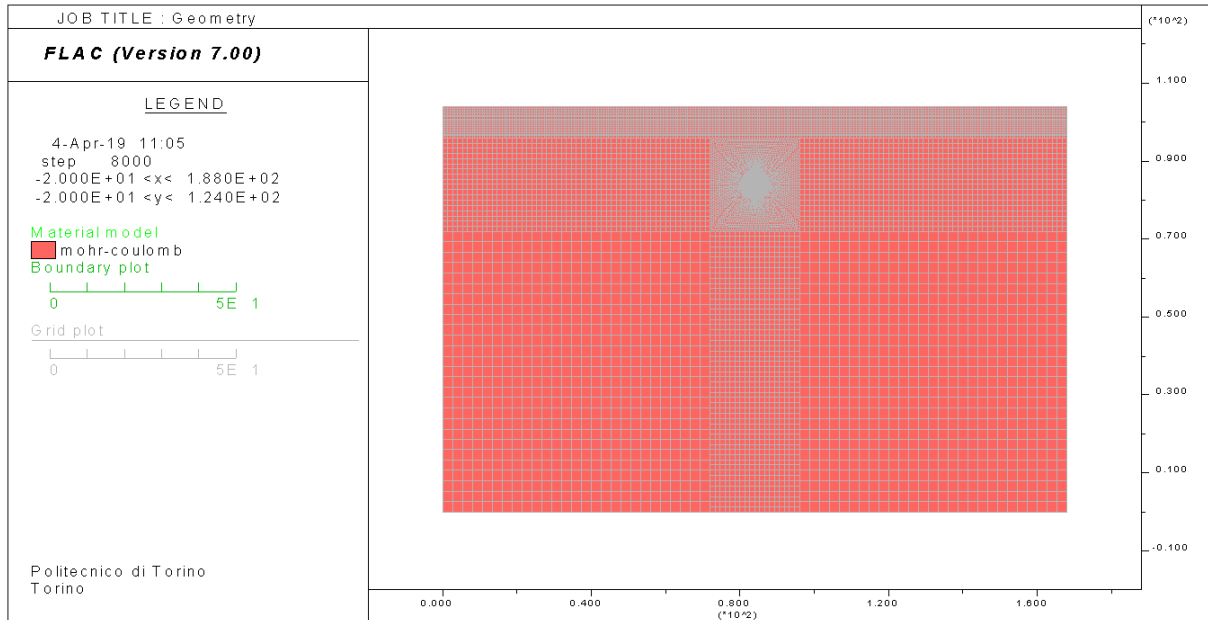


Figure 4.2. Geometry of the model

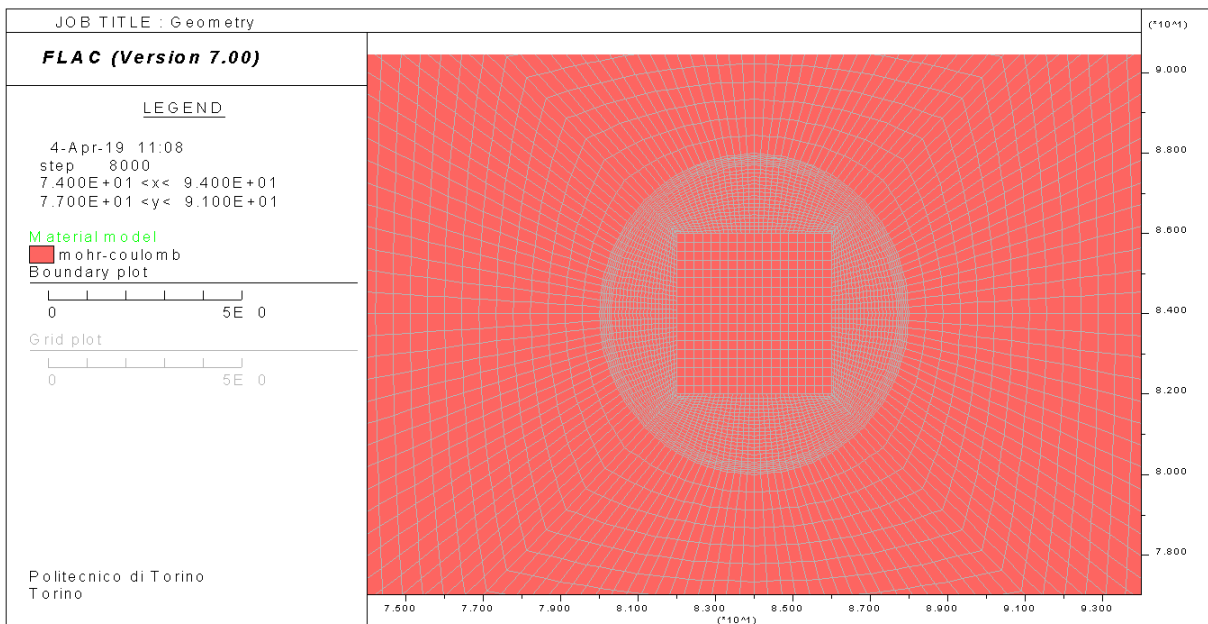


Figure 4.3. Detail of the mesh in the tunnel spot

## Numerical assessment of the role of thermal parameters

The mesh is denser around the tunnel and on the surface, since the purpose of the model is to analyse the surface settlements. The criterion applied to set the mesh is to approach elements not bigger or smaller than twice the adjacent ones.

The cross-section under study is taken at the half width of the segmental ring N° 179 of the extension of Turin Metro Line 1, made with ENERTUN segments, equipped with the “ground” pipes configuration (Barla & Insana, 2018).

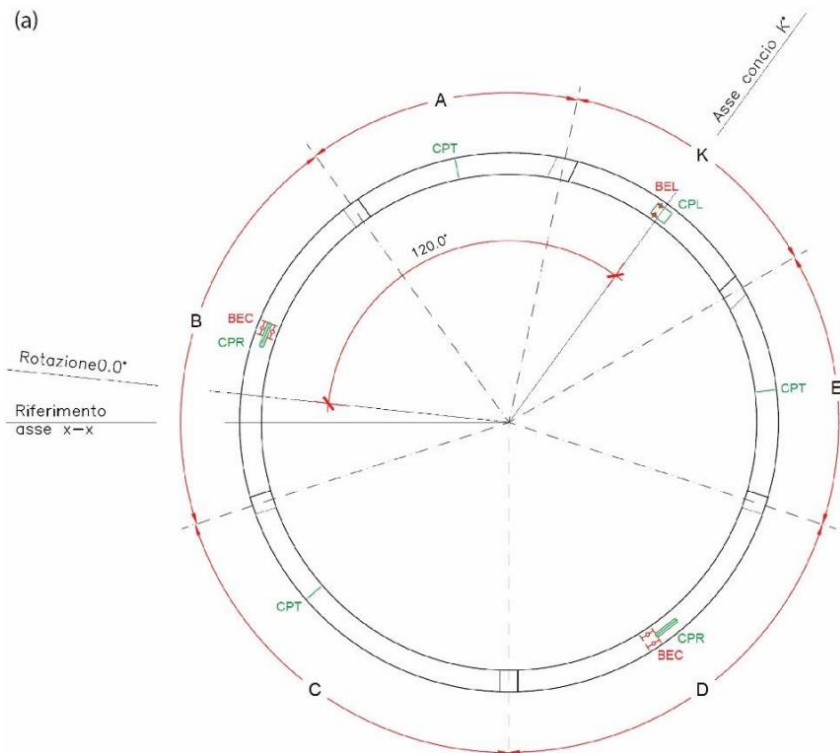


Figure 4.4. ENERTUN - Ring 179 - Extension of Turin Metro Line 1 (Barla & Insana, 2018)

### 4.3.2 Phase 1: Tunnel construction

#### 4.3.2.1 Material properties

In the whole model appear only two different types of material: the soil and the concrete used for the lining.

It has been supposed to model the tunnel in the Turin subsoil, which is usually classified by four different Geotechnical Units. A simplification was made: the ground is considered to be homogenous, no stratigraphy is present. The selected soil corresponds to the Geotechnical Unit 2 (Barla & Barla, 2012), its geotechnical parameters are written in *Table 4.2*.

*Table 4.2. Geotechnical parameters for the Geotechnical Unit 2 in Turin (Barla & Barla, 2012)*

| <b>G.U.</b>  | <b>%C</b>  | <b>D<sub>R</sub></b> | <b>γ</b>  | <b>E<sub>d</sub></b> | <b>v</b>   | <b>σ<sub>c</sub></b>  | <b>m</b>   | <b>c'</b>    | <b>φ'</b>  |
|--|------------|----------------------|---|----------------------|------------|---|------------|--------------|------------|
| <b>[-]</b>   | <b>[%]</b> | <b>[%]</b>           | <b>[kN/m<sup>3</sup>]</b>   | <b>[MPa]</b>         | <b>[-]</b> | <b>[MPa]</b>  | <b>[-]</b> | <b>[kPa]</b> | <b>[°]</b> |
| 2  | 0-25       | 50-70                | 18-21   | 190-240              | 0.3        | 0-0.03  | 3-4.8      | 0-30         | 37-39      |
| %C = Degree of cementation<br>D <sub>R</sub> = Relative density<br>γ = unit weight |            |                      | E <sub>d</sub> = Deformability modulus<br>v = Poisson's coefficient<br>σ <sub>c</sub> = Unconfined compressive strength |                      |            | m = Hoek & Brown constant<br>c' = cohesion<br>φ' = friction angle |            |              |            |

The constitutive model was chosen to be the Mohr-Coulomb model: it needed, as input parameters, the deformability parameters ( $E$ ,  $v$ ), the mass density ( $\gamma$ ) and the shear parameters ( $\phi'$ ,  $c'$ ). All these parameters were selected from *Table 4.2*, when a range is present the average value was selected, the used parameters are reported in *Table 4.3*.

*Table 4.3. Mohr-Coulomb input parameters for GU2 in FLAC*

| <b>G.U.</b> | <b>γ</b>                  | <b>E<sub>d</sub></b> | <b>v</b>   | <b>c'</b>    | <b>φ'</b>  |
|-------------|---------------------------|----------------------|------------|--------------|------------|
| <b>[-]</b>  | <b>[kg/m<sup>3</sup>]</b> | <b>[MPa]</b>         | <b>[-]</b> | <b>[kPa]</b> | <b>[°]</b> |
| 2           | 1988                      | 215                  | 0.3        | 15           | 38         |

As a general assumption, the value of the coefficient of earth pressure at rest in this model is assumed  $k_0 = 0.5$ .

For the lining, reinforced concrete precast segments are supposed. Their mechanical characteristics are reported in *Table 4.4*.

*Table 4.4. Mechanical parameters for reinforced concrete segments (Duretto, 2018)*

| <b>γ</b>                  | <b>f<sub>cd</sub></b> | <b>f<sub>ctd</sub></b> | <b>E</b>     | <b>v</b>   |
|---------------------------|-----------------------|------------------------|--------------|------------|
| <b>[kN/m<sup>3</sup>]</b> | <b>[kPa]</b>          | <b>[kPa]</b>           | <b>[MPa]</b> | <b>[-]</b> |
| 25                        | 23.5                  | 1.7                    | 28152        | 0.2        |

An elastic constitutive model is considered: in FLAC the bulk ( $K$ ) and shear ( $G$ ) modulus are required, they are computed from the deformability parameters  $E$  and  $\nu$ :

$$K = \frac{E}{3(1 - 2\nu)} \quad (\text{Eq. 4.5})$$

$$G = \frac{E}{2(1 + \nu)} \quad (\text{Eq. 4.6})$$

Table 4.5. Elastic input parameters for concrete in FLAC

| $\gamma$             | <b>E</b> | <b><math>\nu</math></b> | <b>K</b> | <b>G</b> |
|----------------------|----------|-------------------------|----------|----------|
| [kg/m <sup>3</sup> ] | [MPa]    | [-]                     | [MPa]    | [MPa]    |
| 2549                 | 28152    | 0.2                     | 15640    | 11730    |

#### 4.3.2.2 Initial and boundary conditions

In the first phase only conditions in terms of stresses and displacements are set.

When dealing with shallow tunnels, gravity ( $g = 9.81 \text{ m/s}^2$ ) must be imposed, because of its great impact on the behaviour of the model. Applying gravity, FLAC could be able to reach the equilibrium without any initial conditions on the stresses, however, in order to minimize the number of computational steps, it is better to impose the initial stress conditions on the model, both internal and on the boundary. In this case, the stresses along the x and z direction are half the ones in the y direction, because of the chosen  $k_0 = 0.5$ .

In addition, the following boundary conditions were set:

- Hinges (fixed X and Y displacements) on the lower boundary;
- Rollers (fixed X displacements) on the lateral boundaries;
- No displacements conditions on the surface, which is free to move.

All the above conditions are shown in *Figure 4.5*. Stresses on the boundaries appear as vectors, they are shown as forces and not as stresses. Force is derived from stress multiplied by a length: for example, on the lower boundary, a unique stress is applied, but vectors seem to be different; this is due to the mesh, which is denser in the middle part and the length between two adjacent gridpoints is shorter than the near ones, which means vectors are

smaller. In addition, also at the two ends of a range vectors are half the ones in the middle, since gridpoints at the end only receive load from one side.

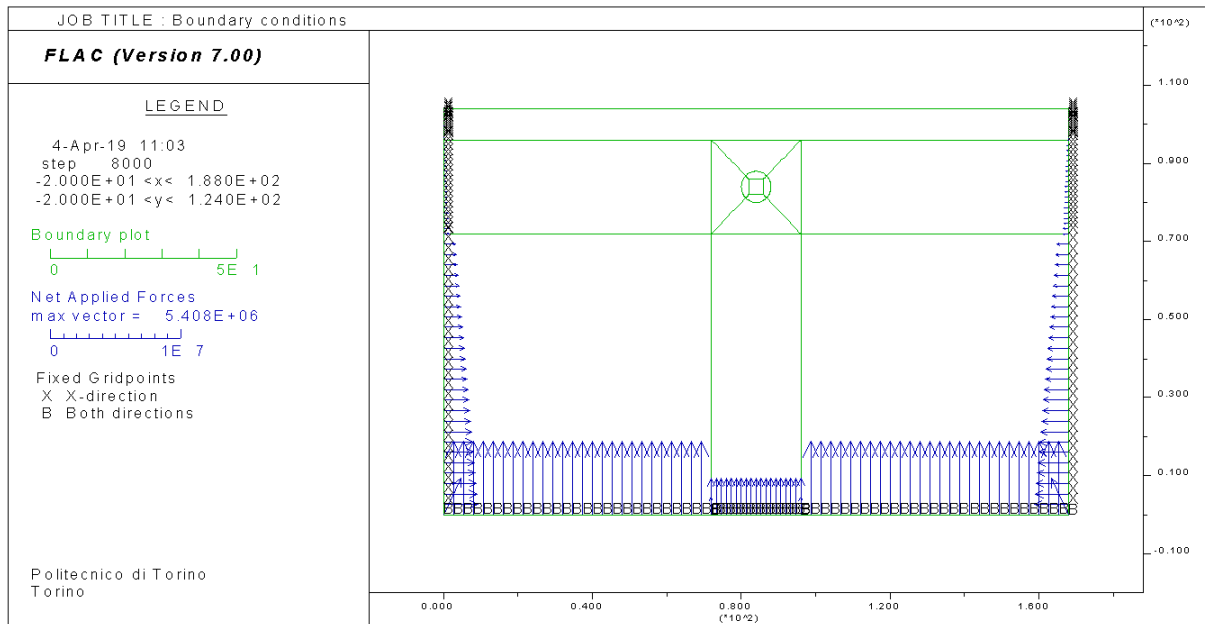


Figure 4.5. Boundary conditions - phase 1

The assumption of *free field* was made, there are no distributed loads on the surface.

### 4.3.2.3 Solving

The solving procedure is subdivided into 4 main stages:

1. Initial conditions;
2. Excavation, with relaxation factor (R.F.) of 0%
3. Excavation, with relaxation factor (R.F.) of 70%;
4. Lining installation, with relaxation factor of 100%.

#### Initial conditions

This stage includes only geostatic conditions, all the boundary and initial conditions in terms of stresses and displacements are set, no excavation (and no convergence) occurs and the analysis is run.

In *Figure 4.6*, the total stresses along the vertical direction are shown just to prove conditions are set in the right way: stresses increase with depth, following the well-known relationship

$$\sigma_{v0}[Pa] = \gamma \left[ \frac{kg}{m^3} \right] \cdot g \left[ \frac{m}{s^2} \right] \cdot z[m].$$

## Numerical assessment of the role of thermal parameters

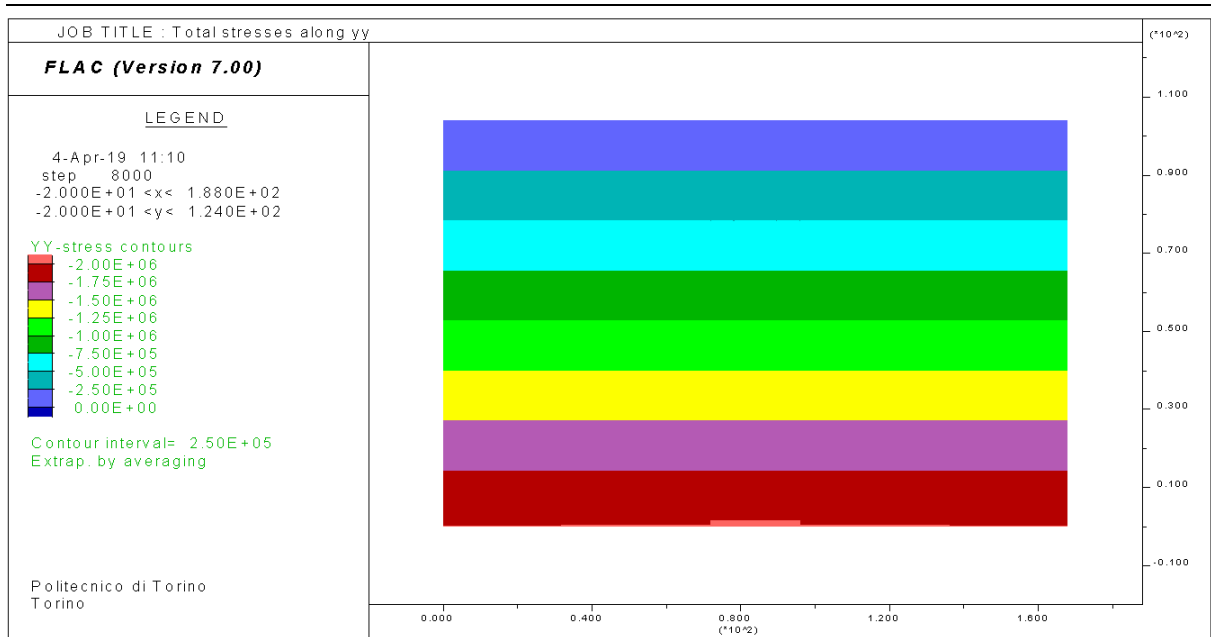


Figure 4.6. Total stresses along  $yy$  – initial condition

Surface displacements do not take place in the initial step.

### Excavation, $R.F. = 70\%$

The FLAC *null* material is assigned to the regions to be excavated, simulating the removal of the soil. Due to the tunnel advancement, before supports are installed, the load in the tunnel changes: this is due to some relaxation that occurs, function of the distance behind the face at which the supports are installed.

For this reason, simulating the excavation process in a 2D analysis is difficult, however, it is possible to consider the excavated volume initially filled with a fictitious radial pressure  $p$ , which gradually decrease from  $p_0$  to 0, depending on the relaxation factor.

$$p = (1 - R.F.) \cdot p_0 \quad (\text{Eq. 4.7})$$

The relaxation factor is not a constant, but it assumes values between 0 and 1 and is function of the position of the advancing face with respect to the studied section. This procedure is commonly known as the stress reduction method.

In this second step a  $R.F. = 0\%$  is assigned, in order to validate the FISH function that is used to simulate the relaxation. When  $R.F. = 0\%$ , it means that the tractions applied to the tunnel boundary reproduce the geostatic stress state, simulating no excavation.

## Numerical assessment of the role of thermal parameters

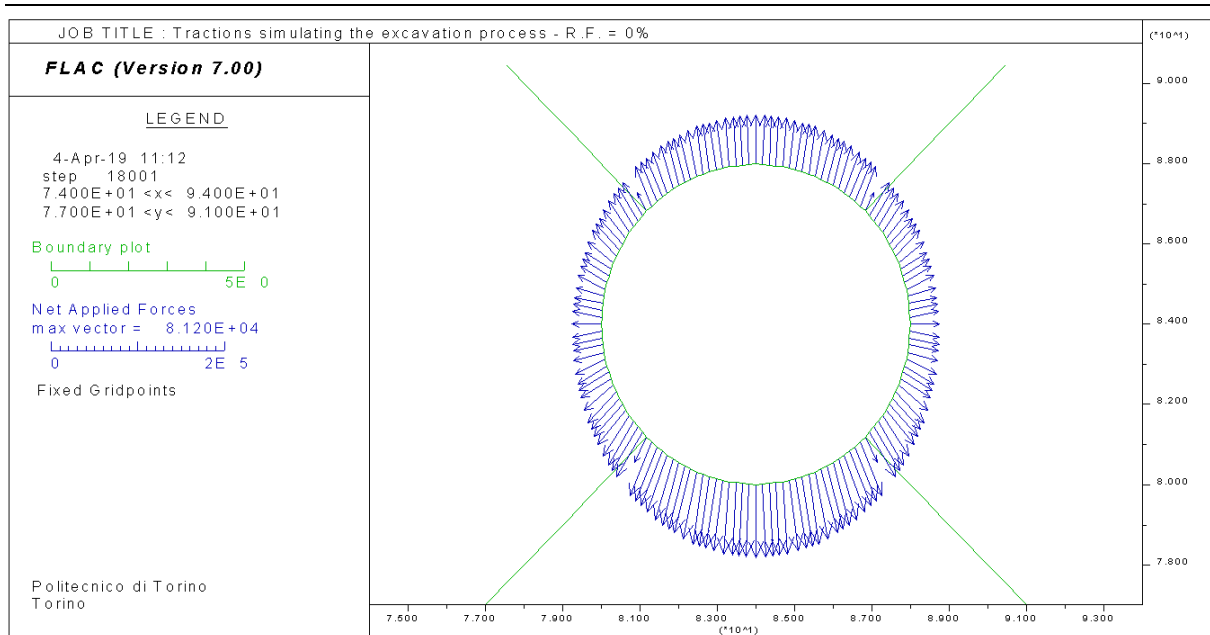


Figure 4.7. Fictitious tractions on the tunnel boundary to simulate the excavation process – R.F.=0%

### Excavation, R.F.=70%

In this stage, the excavation occurs. In the model a relaxation factor of 70 % has been imposed in the third stage before the lining installation. In *Figure 4.8*, the fictitious tractions are applied on the tunnel boundary:

$$p = (1 - 0.7) \cdot p_0 = 0.3 \cdot p_0 \quad (\text{Eq. 4.7})$$

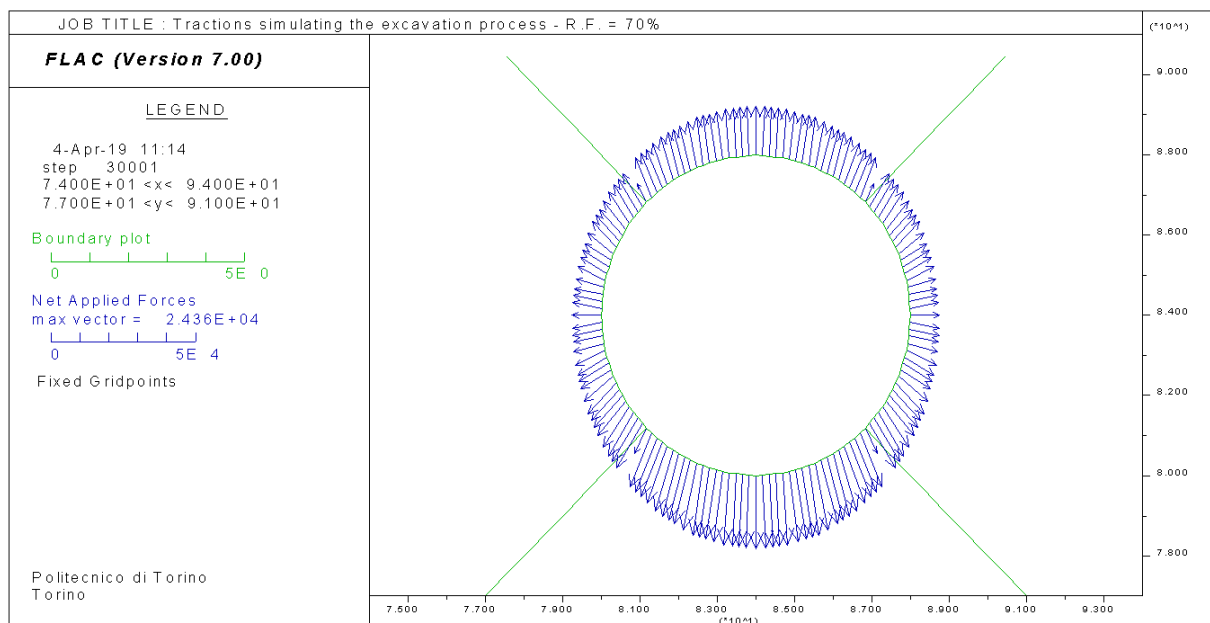


Figure 4.8. Fictitious tractions on the tunnel boundary to simulate the excavation process – R.F.=70%

## Numerical assessment of the role of thermal parameters

In the following *Figure 4.9*, the total stresses along the vertical direction after the excavation, with the fictitious tractions applied, is reported.

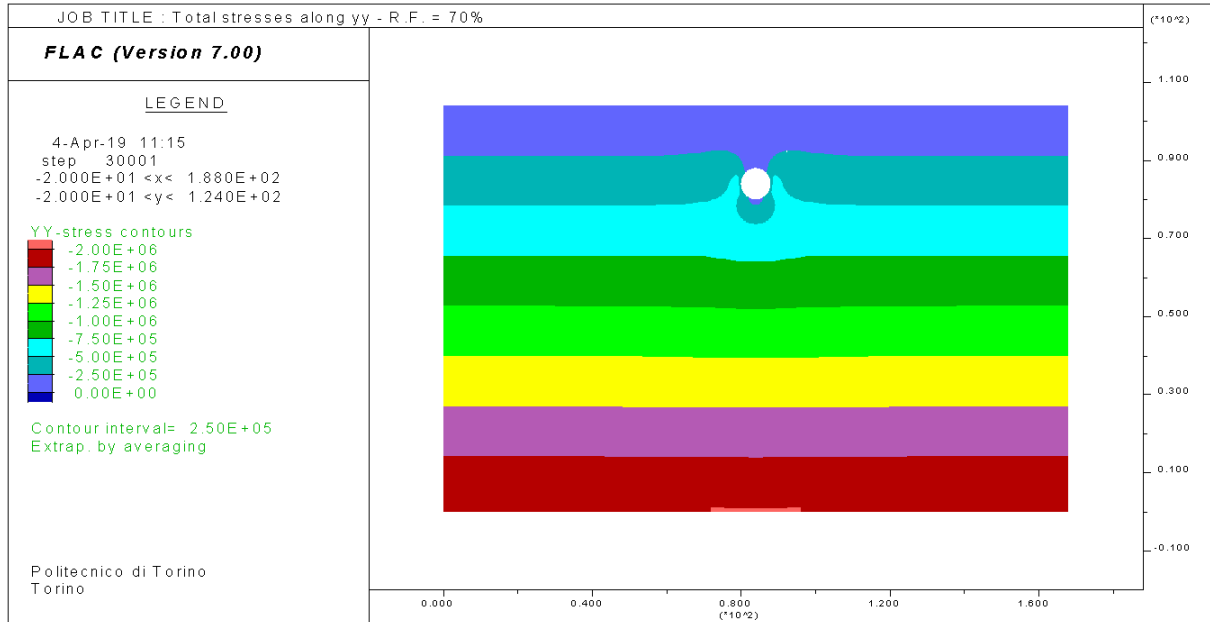


Figure 4.9. Total stresses along yy – Excavation, R.F.=70%

### Lining installation

In this last mechanical computational stage, the lining is installed at the relaxation state of 70%, then the total relaxation is set. The installation of the lining is modelled by assigning to the appropriate regions the *Concrete material*, as shown in *Figure 4.10*.

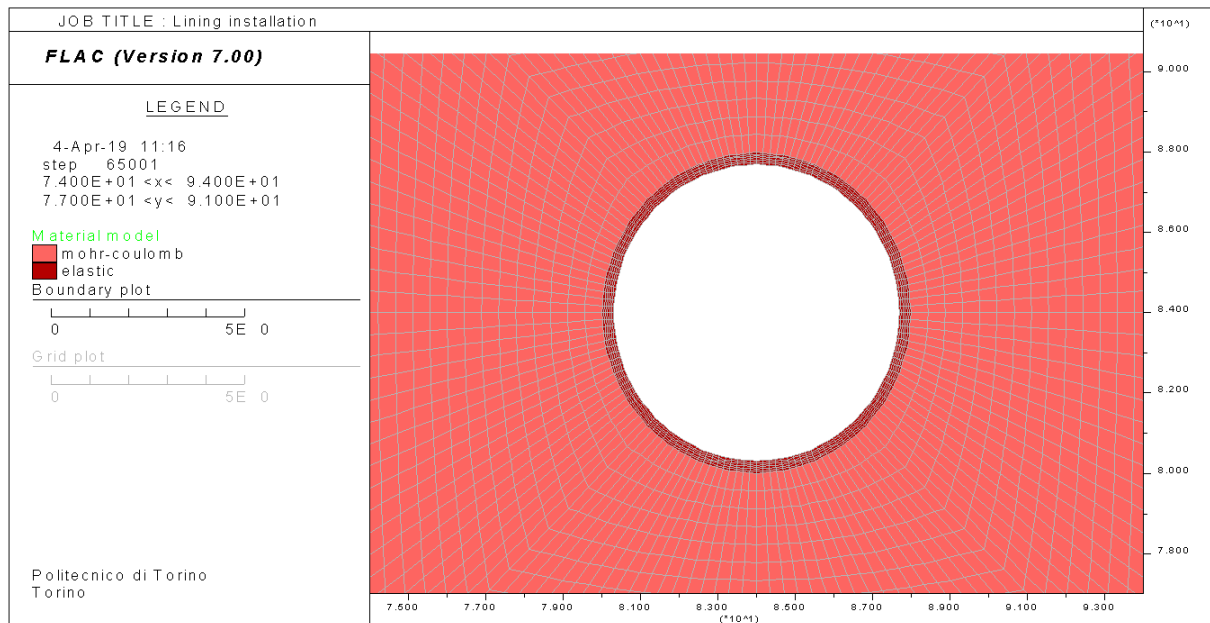


Figure 4.10. Lining installation – detail

## Numerical assessment of the role of thermal parameters

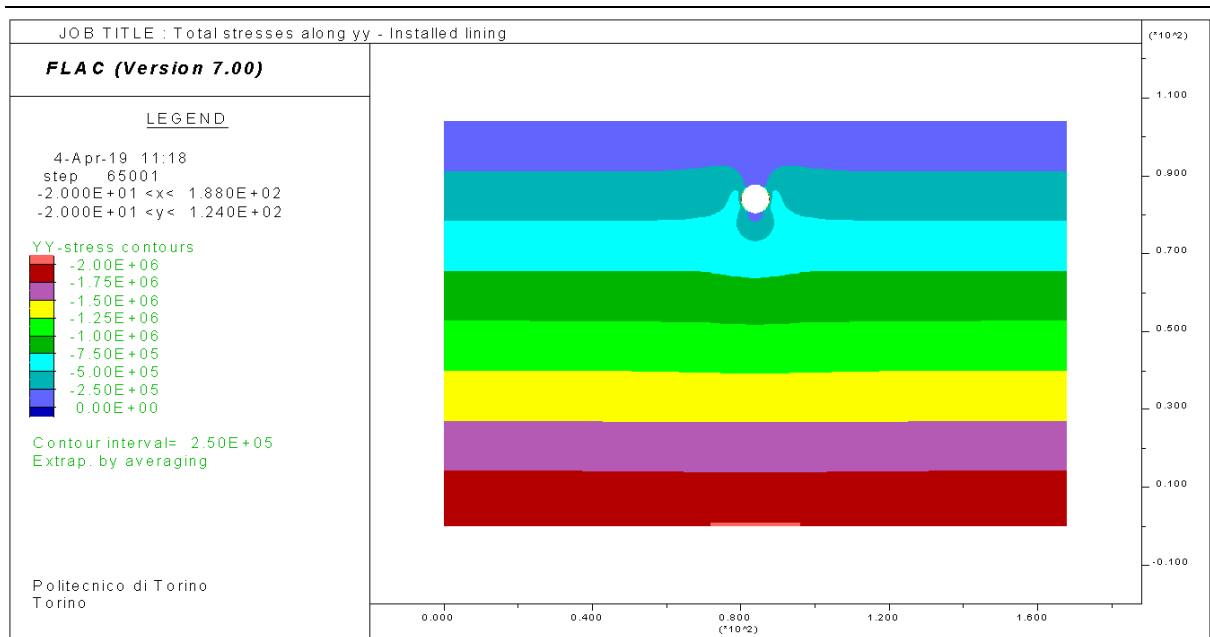


Figure 4.11. Total stresses along yy – Lining installed, R.F.=100%

### 4.3.2.4 Model validation

In order to validate the model, the same geometry and computational stages have been reproduced on RS2, a 2D finite element software for soil and rock application (RocScience suite).

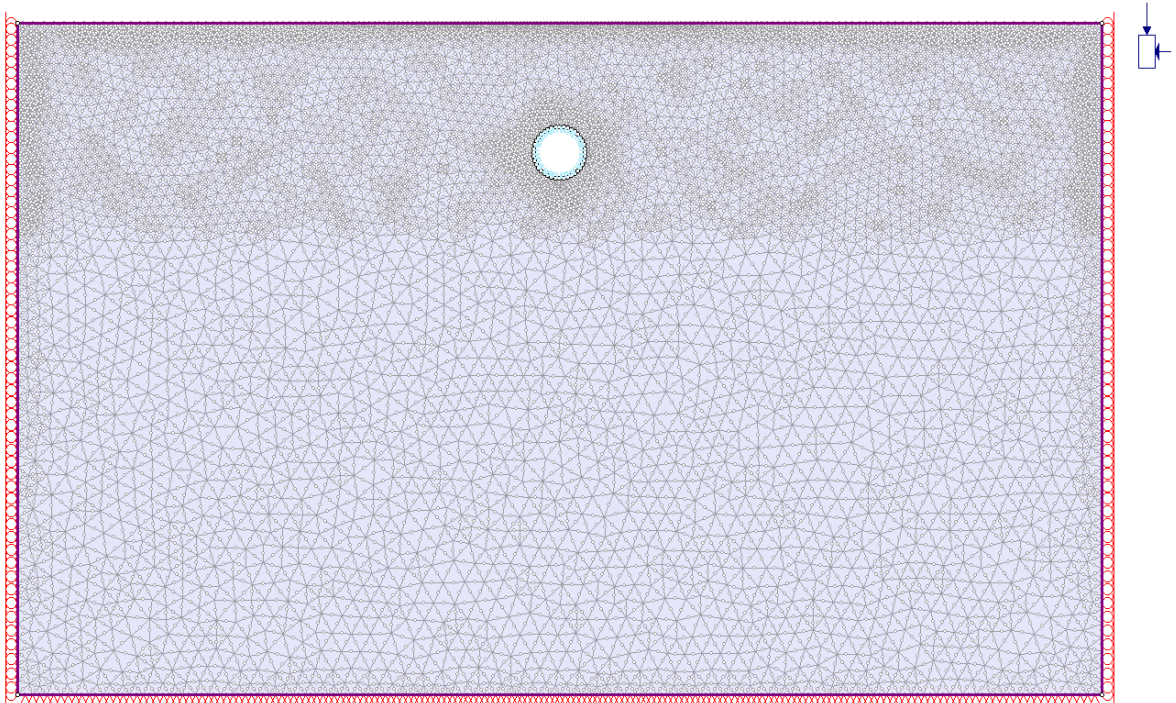


Figure 4.12. Finite Element model of the tunnel in RS2

Boundary conditions and field stress properties correspond to the ones of the FLAC model, the only difference lies in the discretization: a graded mesh with 6 noded triangles has been adopted, with an increase in density in the shallow portion.

The construction sequence follows the FLAC one, with computation stages simulating from the geostatic conditions to the installation of the lining.

### 4.3.2.5 Surface settlements

A comparison between the FLAC and RS2 results is now possible, in terms of surface settlements. They assume the typical configuration of a gaussian curve, with the maximum value above the tunnel centre and a negligible difference of less than 1 mm between the two software. The FLAC model is reliable. *Table 4.6* shows the maximum values of surface settlements in FLAC and RS2, with reference to the R.F.=70% and R.F.=100%.

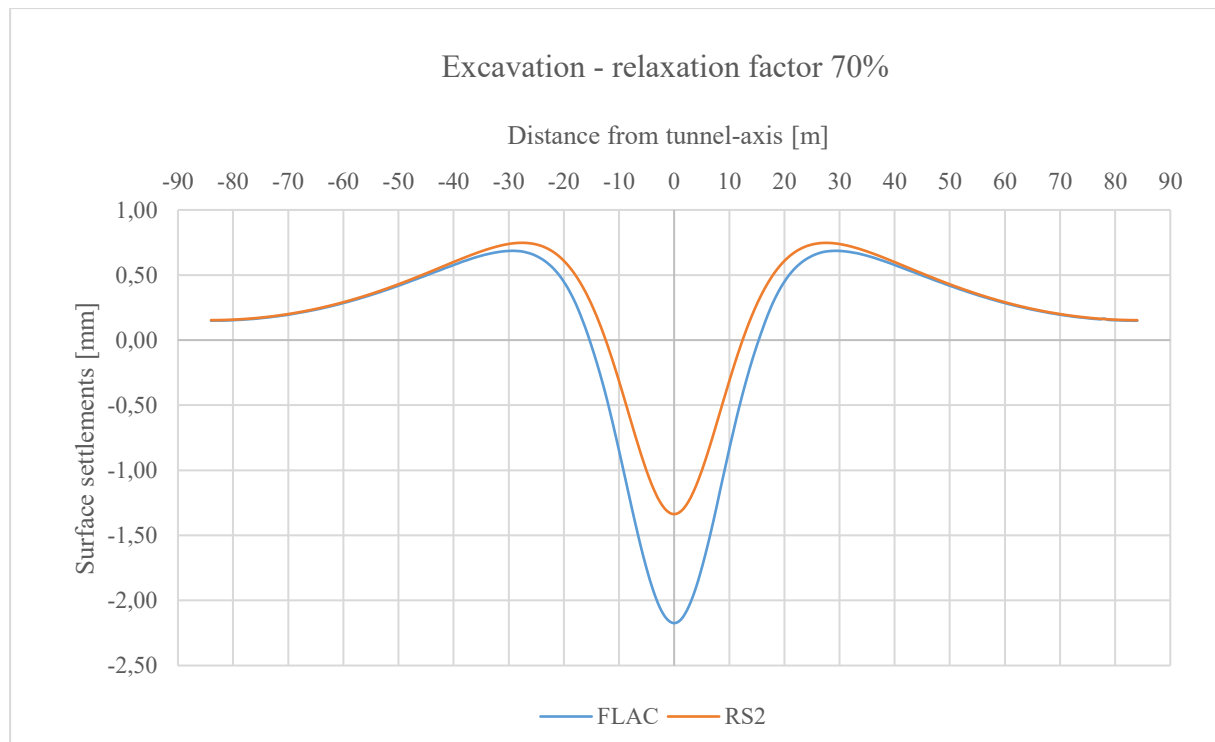


Figure 4.13. Surface settlements – Excavation R.F.=70% - FLAC vs. RS2 results

## Numerical assessment of the role of thermal parameters

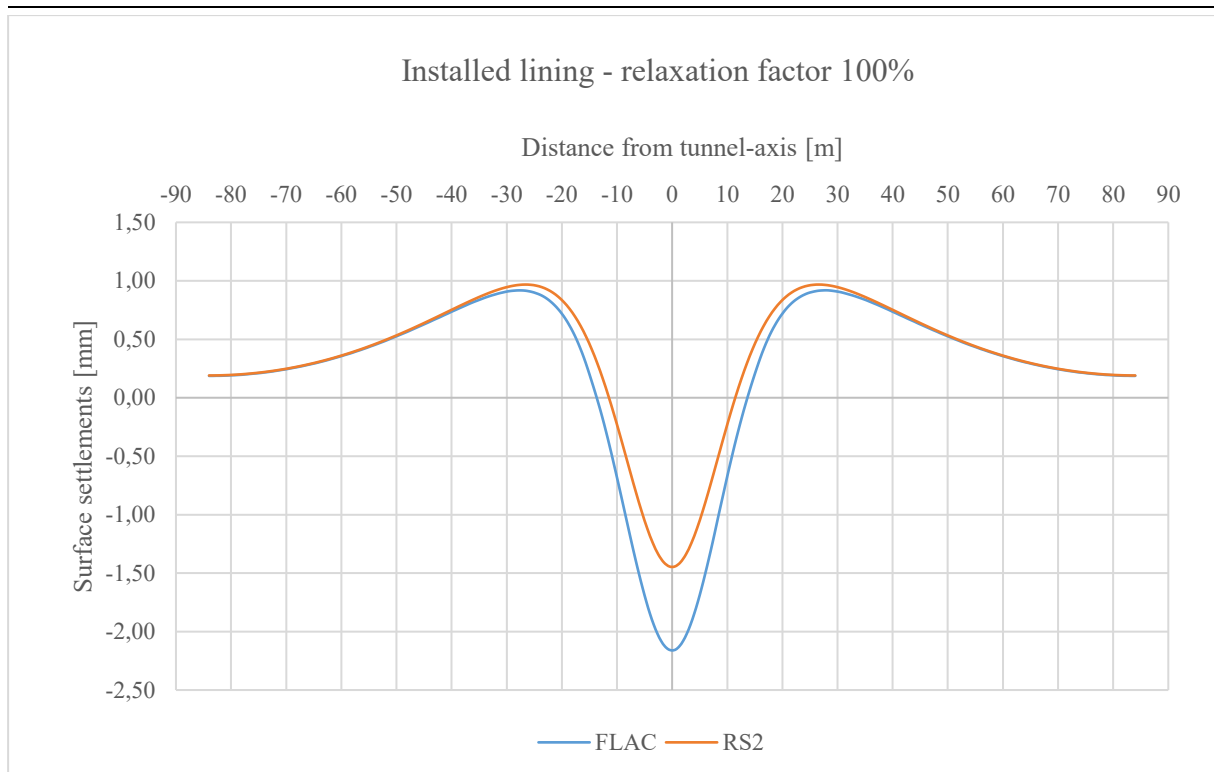


Figure 4.14. Surface settlements - Installed lining R.F.=100% - FLAC vs. RS2 results

Table 4.6. Maximum surface settlements - FLAC vs. RS2 results

|             | FLAC<br>[mm] | RS2<br>[mm] | $\Delta S_{\max}$<br>[mm] |
|-------------|--------------|-------------|---------------------------|
| R.F. = 70%  | 2.174        | 1.333       | 0.841                     |
| R.F. = 100% | 2.161        | 1.443       | 0.718                     |

Considering only FLAC, a comparison between the surface settlements before and after the lining installation is made, *Figure 4.15*. After the support is installed, the maximum displacement is of 2.161 mm.

## Numerical assessment of the role of thermal parameters

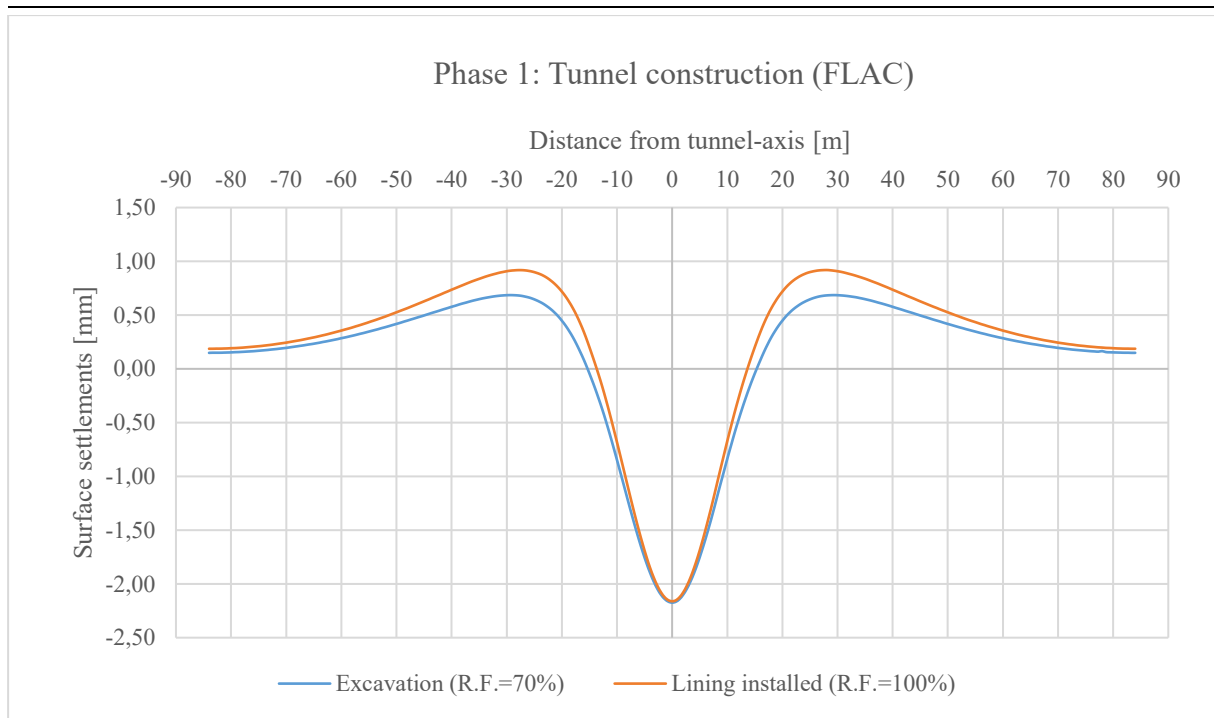


Figure 4.15. Surface settlements – R.F.=70% vs. R.F.=100% - FLAC

### 4.3.3 Phase 2: Thermo-Mechanical analysis

This section includes the thermal activation. Steady-state analyses are run, with fixed temperatures. *Figure 4.16* shows the adopted geometry for the pipes in the segmental ring. *Figure 4.17* shows the FLAC model with marked points, corresponding to the pipes.

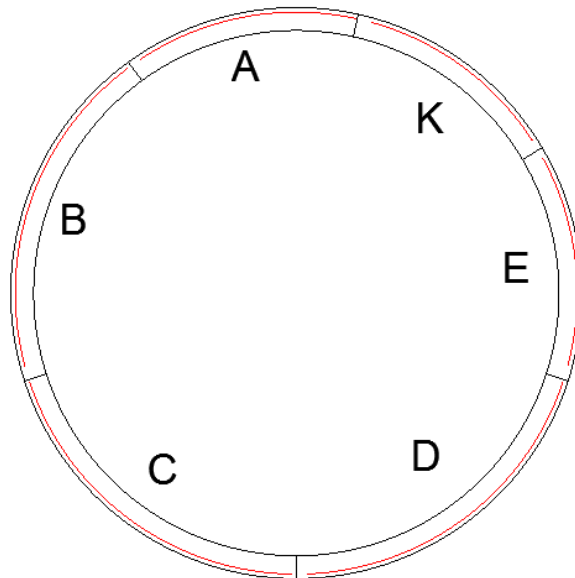


Figure 4.16. Autocad view - Positions of the ground configuration pipes - ring 179 extension Turin Metro Line 1

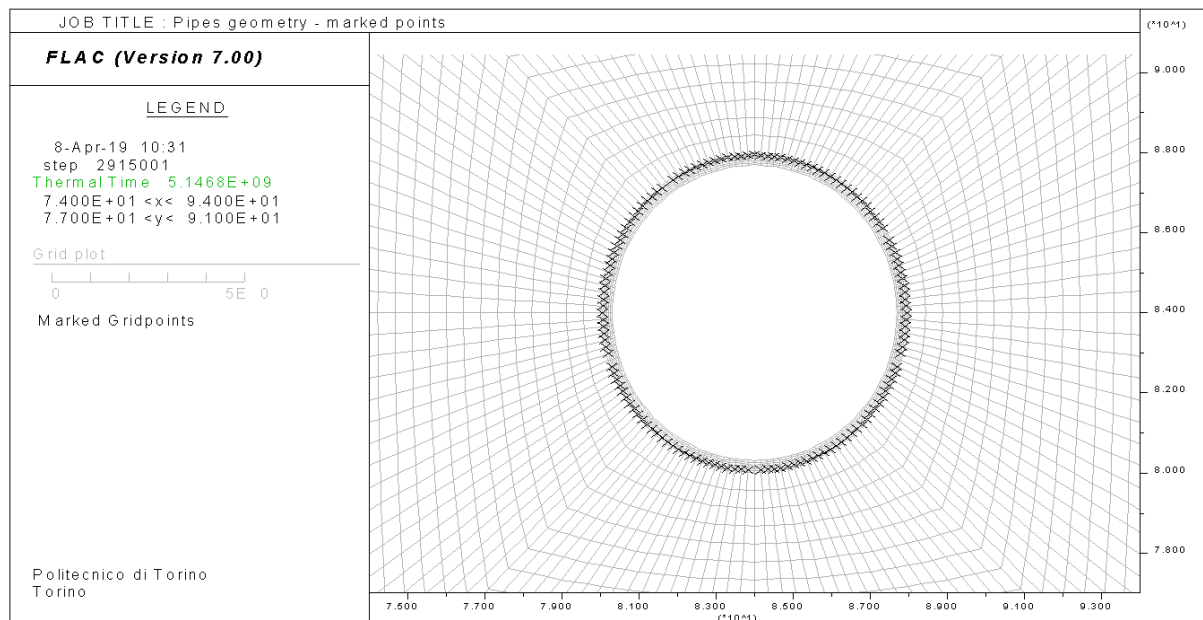


Figure 4.17. Marked points corresponding to the pipes' configuration - FLAC

### 4.3.3.1 Material properties

Input thermal parameters need to be added to the mechanical ones, in order to run a TM analysis. In this model, an isotropic conduction model is assigned both to the soil and concrete. Three main properties are required:

1. Thermal conductivity [W/mK];
2. Specific heat [J/kgK];
3. Coefficient of linear thermal expansion [ $K^{-1}$  or  $^{\circ}C^{-1}$ ].

For the soil and the concrete, the values of the thermal conductivity and the specific heat reported in *Table 4.6*, have been derived from Duretto (2018). The third parameter is not taken as a constant for the soil, but it varies in order to study its influence on the amount of surface settlements: the parametric analysis provides for three different values, as shown in *Table 4.7*, choices based on literature values for different types of soil (McKinstry, 1965).

Regarding the concrete, the coefficient of linear thermal expansion could assume a value between  $6\div 13 \cdot 10^{-6} \text{ }^{\circ}C^{-1}$ , its variation is consequence of the mix design of the concrete. To have precise information it is always better to test the material (Bertolini, 2010). In this model a value of  $1 \cdot 10^{-5} \text{ }^{\circ}C^{-1}$  has been chosen.

*Table 4.7. Thermal properties for isotropic conductive materials (Duretto, 2018)*

| <b>Material</b> | <b><math>\lambda</math><br/>[W/mK]</b> | <b>c<br/>[J/kgK]</b> | <b><math>\alpha</math><br/>[<math>^{\circ}C^{-1}</math>]</b> |
|-----------------|--|----------------------|--|
| GU2 – soil      | 2.8                                    | 1053                 | <i>Table 4.7</i>   |
| Concrete        | 1.12                                   | 876                  | 1.00E-05   |

*Table 4.8. Coefficients of linear thermal expansion - parametric analysis*

|  | <b>Case Study 1</b> | <b>Case Study 2</b> | <b>Case Study 3</b> |
|--|---------------------|---------------------|---------------------|
| <b><math>\alpha</math> [<math>^{\circ}C^{-1}</math>]</b> | 1.00E-05            | 2.00E-05            | 0.50E-05            |

### 4.3.3.2 Initial and boundary conditions

In addition to the initial and boundary conditions in terms of stresses and displacements, several temperature conditions are set:

- External air temperature on the upper boundary;
- Tunnel internal air temperature on the tunnel boundary;
- Ground initial temperature on the whole soil.

All the temperatures set in the model are based on the assumption of locating the structure in Turin.

First, the annual air temperature of Turin has been studied: its trend is shown in blue in *Figure 4.18*, however, for a steady-state analysis, a constant value of temperature is required. Three main seasons have been identified, and the mean constant temperature is used in the analyses.

Table 4.9. Mean external air temperatures - Turin

| Seasons    | Temperature [°C] |
|------------|------------------|
| Winter     | 2.5              |
| Mid-Season | 12.0             |
| Summer     | 21.0             |

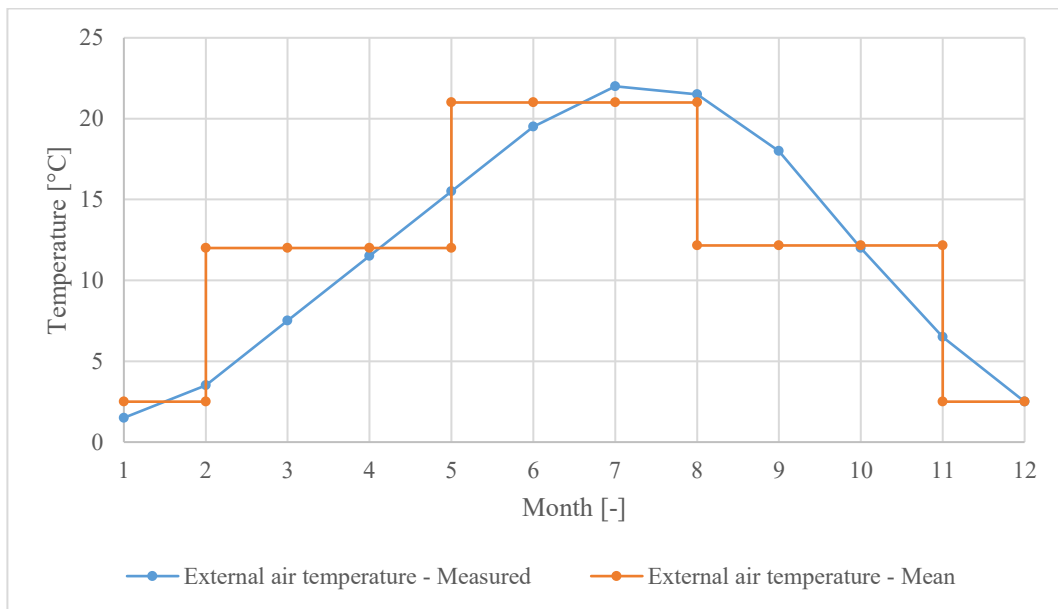


Figure 4.18. Turin air temperature trends - data from Torino Caselle station (ilmeteo.it)

Figure 4.19 shows the trend of the tunnel air temperatures for a year period. The same procedure of the external temperatures is adopted: three mean values, one for each season, were extrapolated (see Table 4.10 and Figure 4.20).

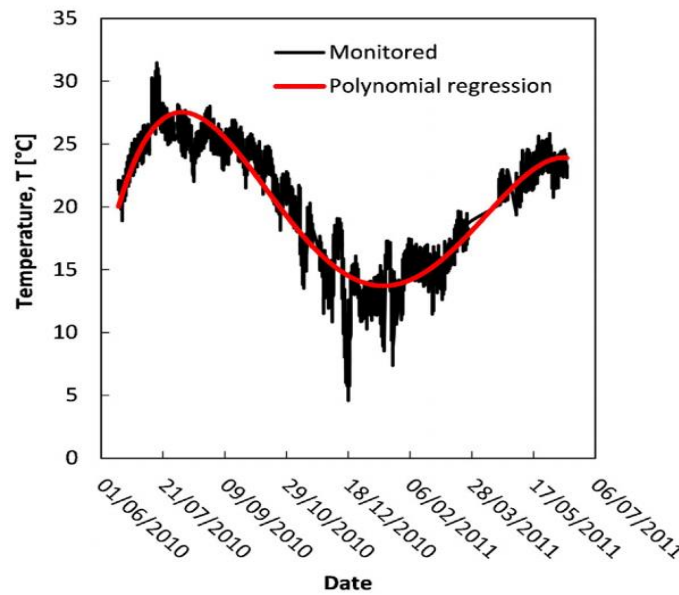


Figure 4.19. Monitored tunnel internal temperature in the Metro (Barla et al., 2016)

Table 4.10. Mean tunnel air temperatures – Metro Turin (from Barla et al., 2016)

| Seasons    | Temperature [°C] |
|------------|------------------|
| Winter     | 12.0             |
| Mid Season | 18.0             |
| Summer     | 24.0             |

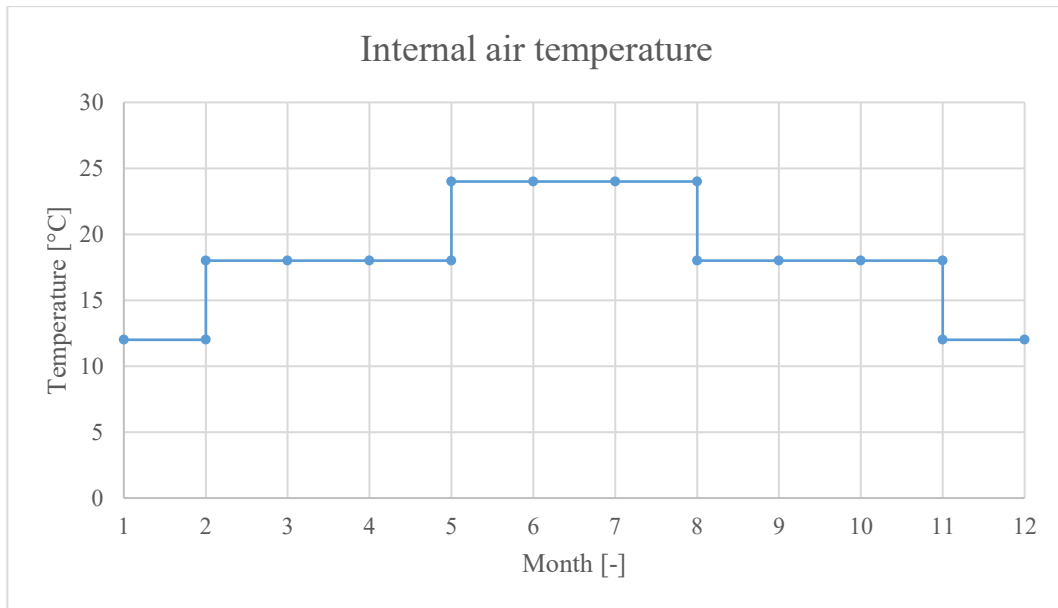


Figure 4.20. Mean season values of the tunnel air temperature, derived from Barla et al. (2016)

Regarding the initial temperature in the whole ground, it is assumed a constant initial temperature of 14 °C, which surely gradually varies once all the above-mentioned conditions are set.

In the following pictures, to fully understand the new applied conditions, it is possible to see how the temperature distribution appears for each season. Figures refer to the first case study, with  $\alpha_T = 1.00E - 05 \text{ } ^\circ\text{C}^{-1}$ , before the thermal activation of the lining is modelled.

Table 4.11. Winter - Temperature boundary conditions

|                        |                 |         |
|------------------------|-----------------|---------|
| External temperature   | Upper boundary  | 2.5 °C  |
| Tunnel air temperature | Tunnel boundary | 12.0 °C |

## Numerical assessment of the role of thermal parameters

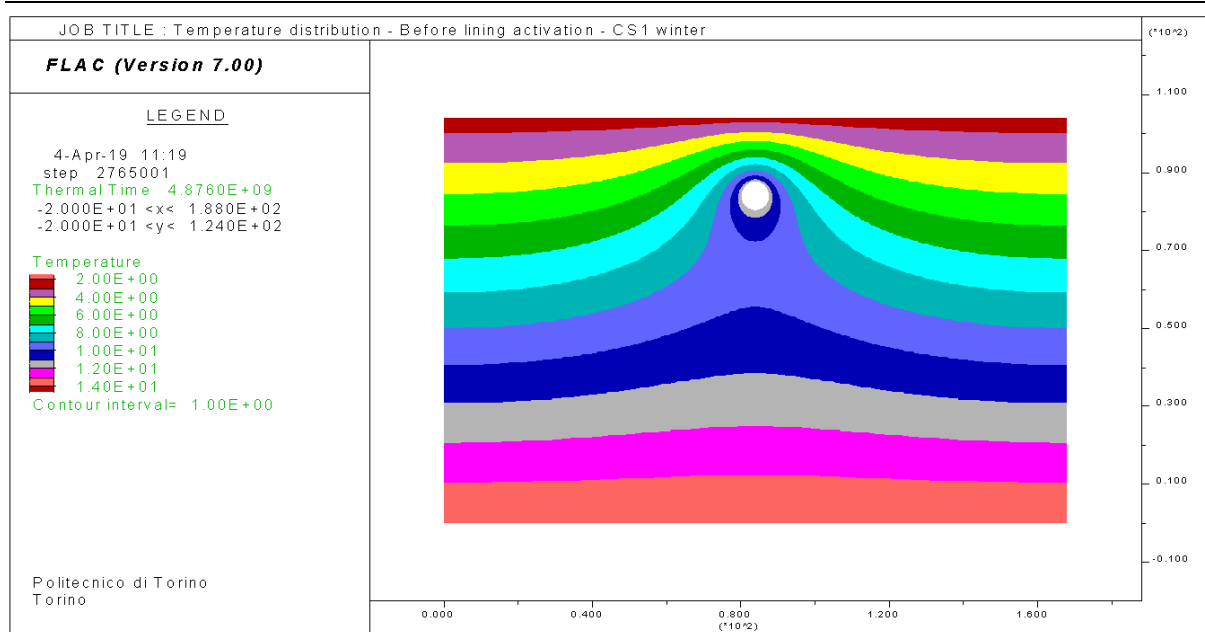


Figure 4.21. Winter - temperature distribution before activation of the lining - CS1

Table 4.12. Mid-season - Temperature boundary conditions

|                        |                 |         |
|------------------------|-----------------|---------|
| External temperature   | Upper boundary  | 12.0 °C |
| Tunnel air temperature | Tunnel boundary | 18.0 °C |

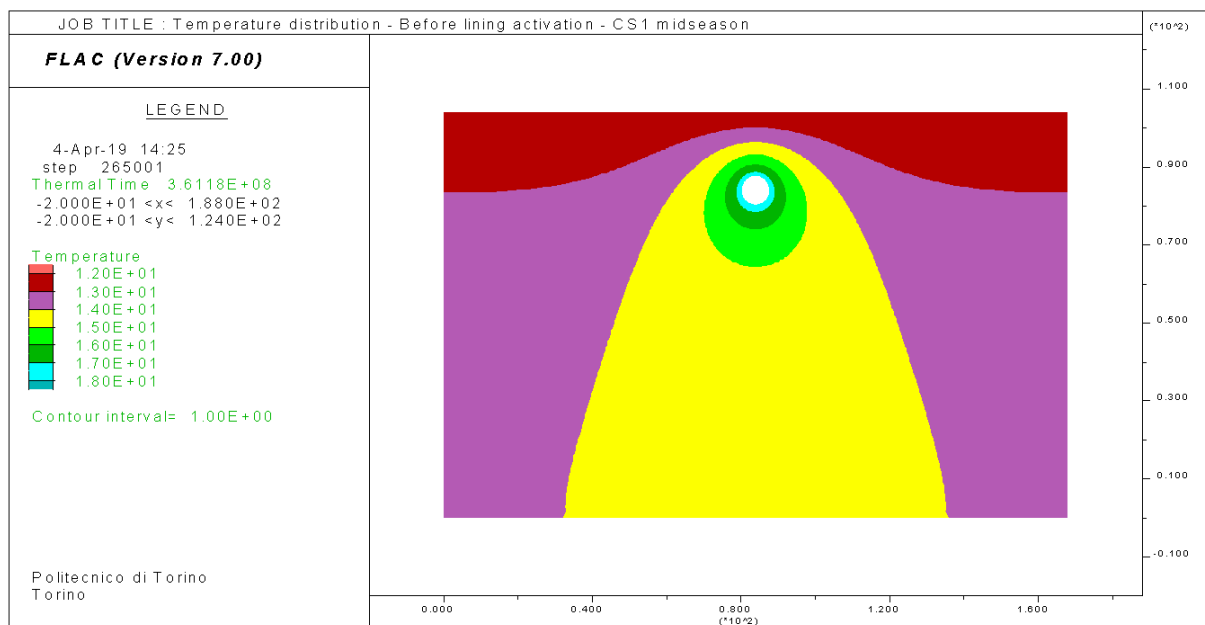
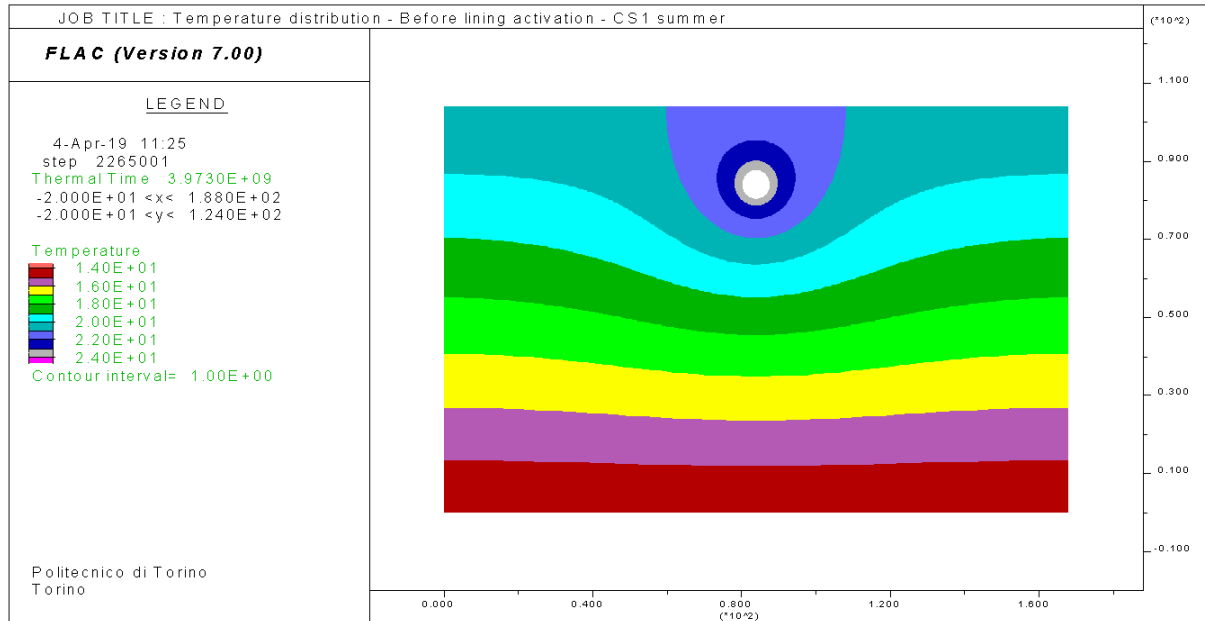


Figure 4.22. Mid-season - temperature distribution before activation of the lining - CS1

## Numerical assessment of the role of thermal parameters

*Table 4.13. Summer - Temperature boundary conditions*

|                        |                 |         |
|------------------------|-----------------|---------|
| External temperature   | Upper boundary  | 21.0 °C |
| Tunnel air temperature | Tunnel boundary | 24.0 °C |



*Figure 4.23. Summer - temperature distribution before activation of the lining - CS1*

### 4.3.3.3 Solving

Once the temperature conditions are set, the lining can be thermally activated. Practically speaking, the activation in FLAC is simulated by imposing to the gridpoints, geometrically corresponding to the red lines in *Figure 4.17*, a fixed temperature. This temperature is the inlet fluid temperature of the ground configuration pipes: values vary with seasons and are resumed in *Table 4.14*. For example, the Case Study 1 with  $\alpha_T = 1.00E - 05 \text{ } ^\circ\text{C}^{-1}$  is considered: figures with temperature distribution after thermal activation of the lining are shown in the following pages.

*Table 4.14. Different fluid temperatures imposed in the analyses*

|            | T [°C] |
|------------|--------|
| Winter     | 3.0    |
| Mid Season | 15.0   |
| Summer     | 30.0   |

## Numerical assessment of the role of thermal parameters

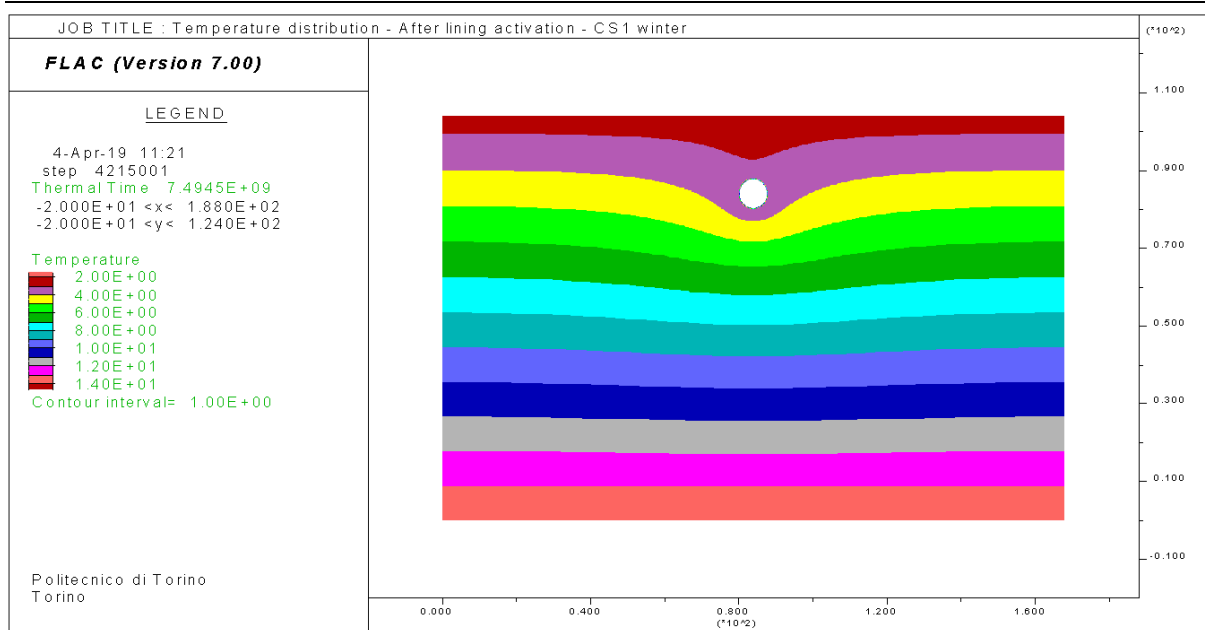


*Figure 4.24. Winter - temperature distribution after thermal activation of the lining - CS1*

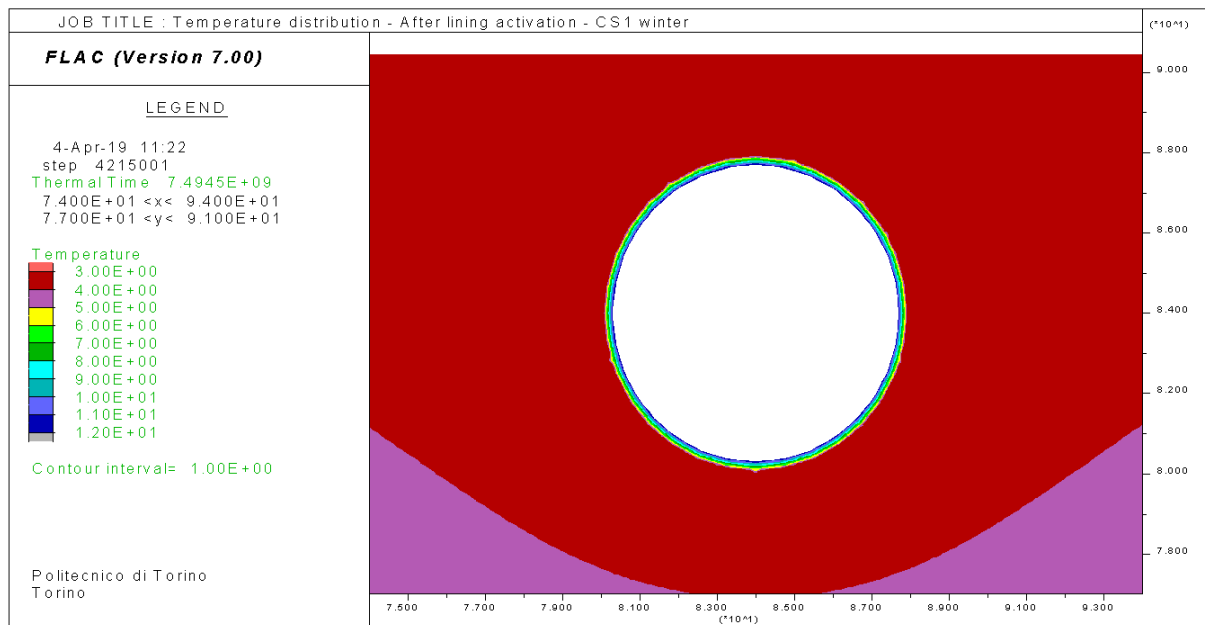


*Figure 4.25. Winter - DETAIL - temperature distribution after thermal activation of the lining - CS1*

## Numerical assessment of the role of thermal parameters

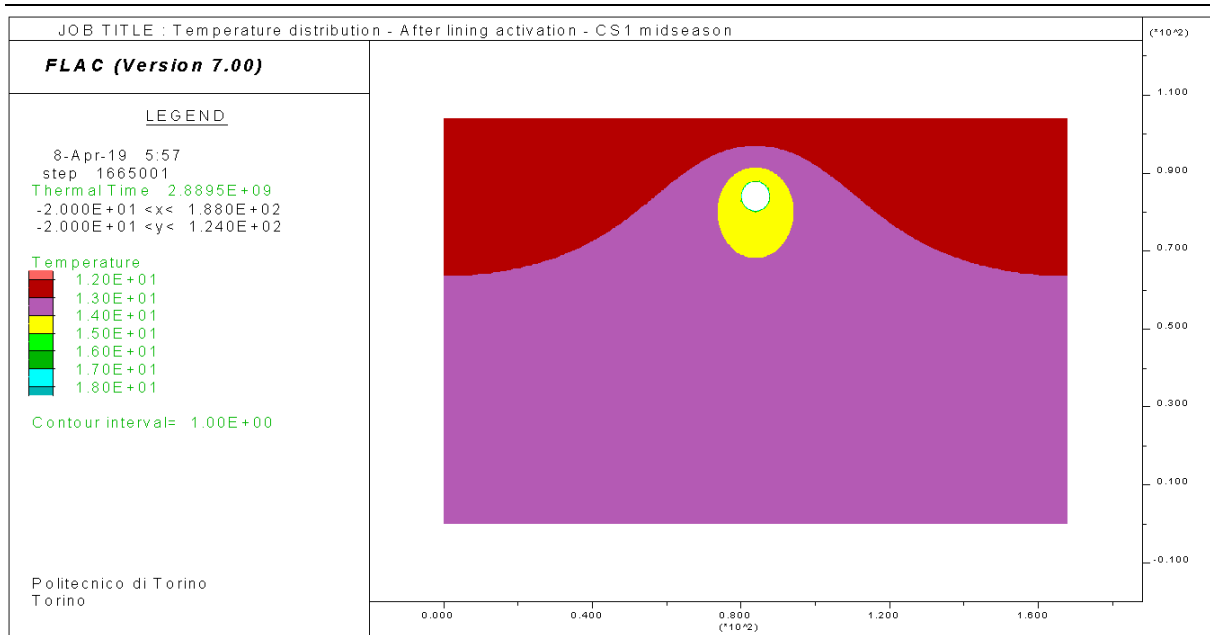


Figure 4.26. Mid-season - temperature distribution after thermal activation of the lining - CS1

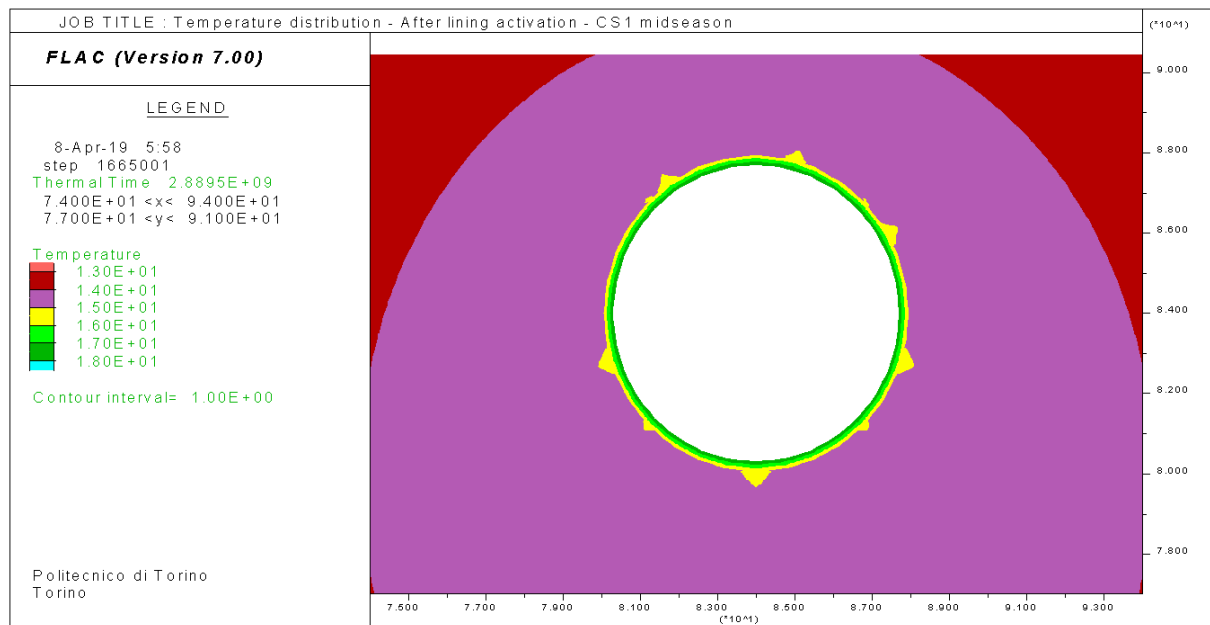
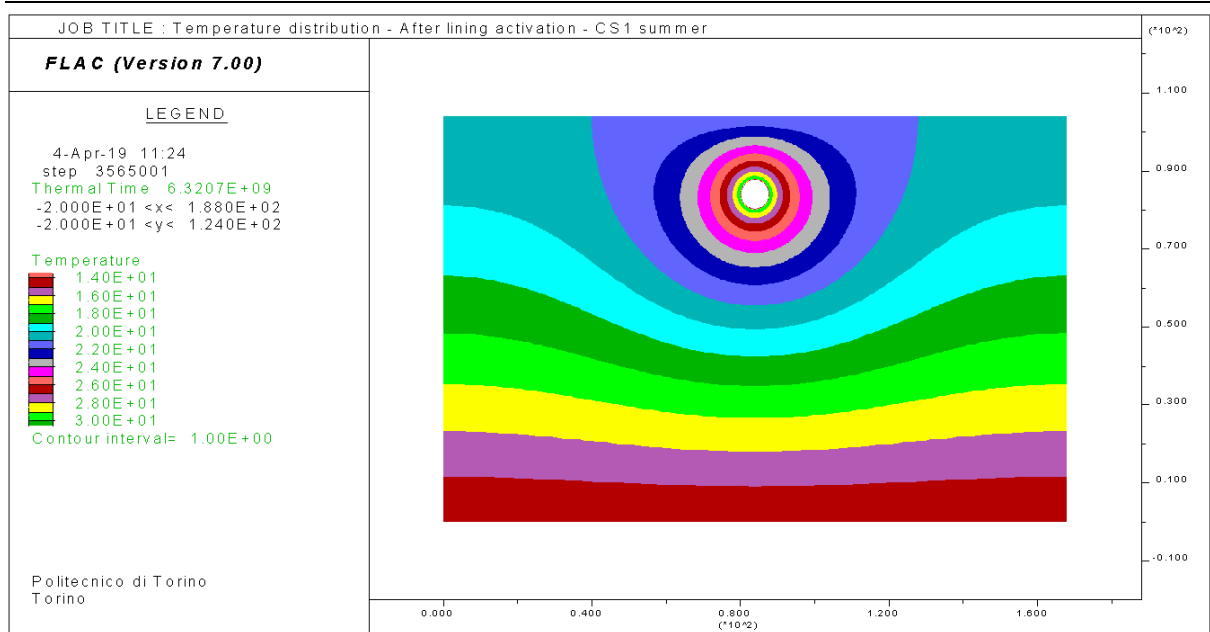
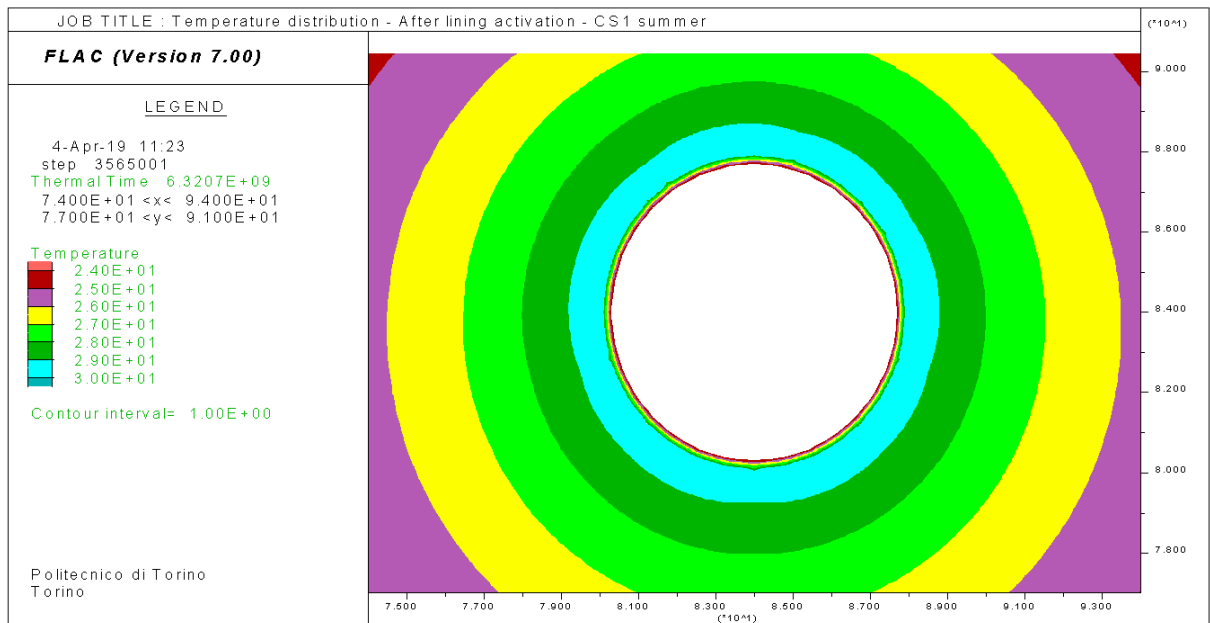


Figure 4.27. Mid-season - DETAIL - temperature distribution after thermal activation of the lining - CS1

## Numerical assessment of the role of thermal parameters



*Figure 4.28. Summer - temperature distribution after thermal activation of the lining - CS1*



*Figure 4.29. Summer - DETAIL- temperature distribution after thermal activation of the lining - CS1*

**4.3.3.4 Parametric analysis – results**

Focusing on the aim of the analysis, in this chapter, the results in terms of surface settlements are reported. In *Table 4.15*, all the case studies are described: three values of linear thermal expansion coefficient were chosen and for each one the three seasonal conditions are set.

In the end, it has been decided not to analyse the conditions related to the mid-seasons for case study 2 and 3; only 7 case studies have been studied.

Results are plotted in terms of surface settlements that occur because of the lining activation.

*Table 4.15. Description of case studies*

| <b>CASE STUDY 1</b>                                  |            |                |            |
|--|------------|----------------|------------|
| $\alpha_T [^{\circ}\text{C}^{-1}] = 1.00\text{E-}05$ |            |                |            |
|  | 1A: Winter | 1B: Mid-season | 1C: Summer |
| Fluid T[ $^{\circ}\text{C}$ ]                        | 3.0        | 15.0           | 30.0       |
| External air T[ $^{\circ}\text{C}$ ]                 | 2.5        | 12.0           | 21.0       |
| Tunnel air T[ $^{\circ}\text{C}$ ]                   | 12.0       | 18.0           | 24.0       |

| <b>CASE STUDY 2</b>                                  |            |                           |            |
|--|------------|---------------------------|------------|
| $\alpha_T [^{\circ}\text{C}^{-1}] = 2.00\text{E-}05$ |            |                           |            |
|  | 2A: Winter | <del>2B: Mid-season</del> | 2C: Summer |
| Fluid T[ $^{\circ}\text{C}$ ]                        | 3.0        | <del>15.0</del>           | 30.0       |
| External air T[ $^{\circ}\text{C}$ ]                 | 2.5        | <del>12.0</del>           | 21.0       |
| Tunnel air T[ $^{\circ}\text{C}$ ]                   | 12.0       | <del>18.0</del>           | 24.0       |

| <b>CASE STUDY 3</b>                                  |            |                           |            |
|--|------------|---------------------------|------------|
| $\alpha_T [^{\circ}\text{C}^{-1}] = 0.50\text{E-}05$ |            |                           |            |
|  | 3A: Winter | <del>3B: Mid-season</del> | 3C: Summer |
| Fluid T[ $^{\circ}\text{C}$ ]                        | 3.0        | <del>15.0</del>           | 30.0       |
| External air T[ $^{\circ}\text{C}$ ]                 | 2.5        | <del>12.0</del>           | 21.0       |
| Tunnel air T[ $^{\circ}\text{C}$ ]                   | 12.0       | <del>18.0</del>           | 24.0       |

4.3.3.4.1 Case Study 1,  $\alpha = 1.00E - 05 \text{ } ^\circ\text{C}^{-1}$

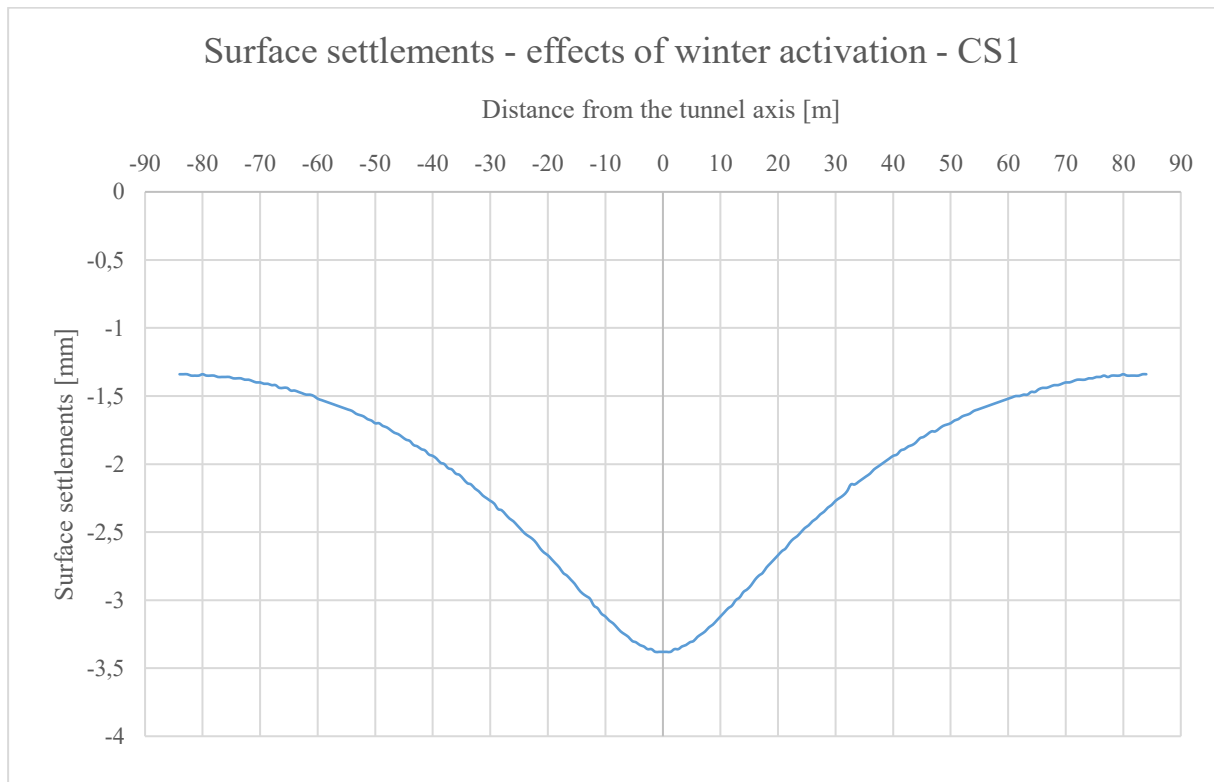


Figure 4.30. Winter - Surface settlements - CS1

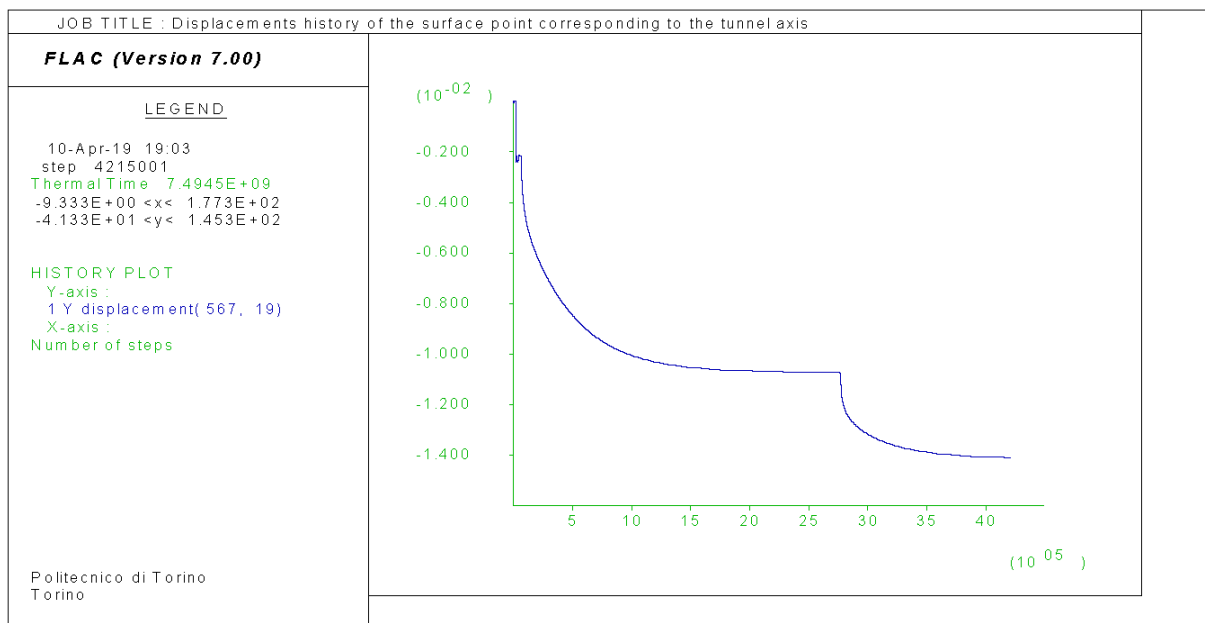
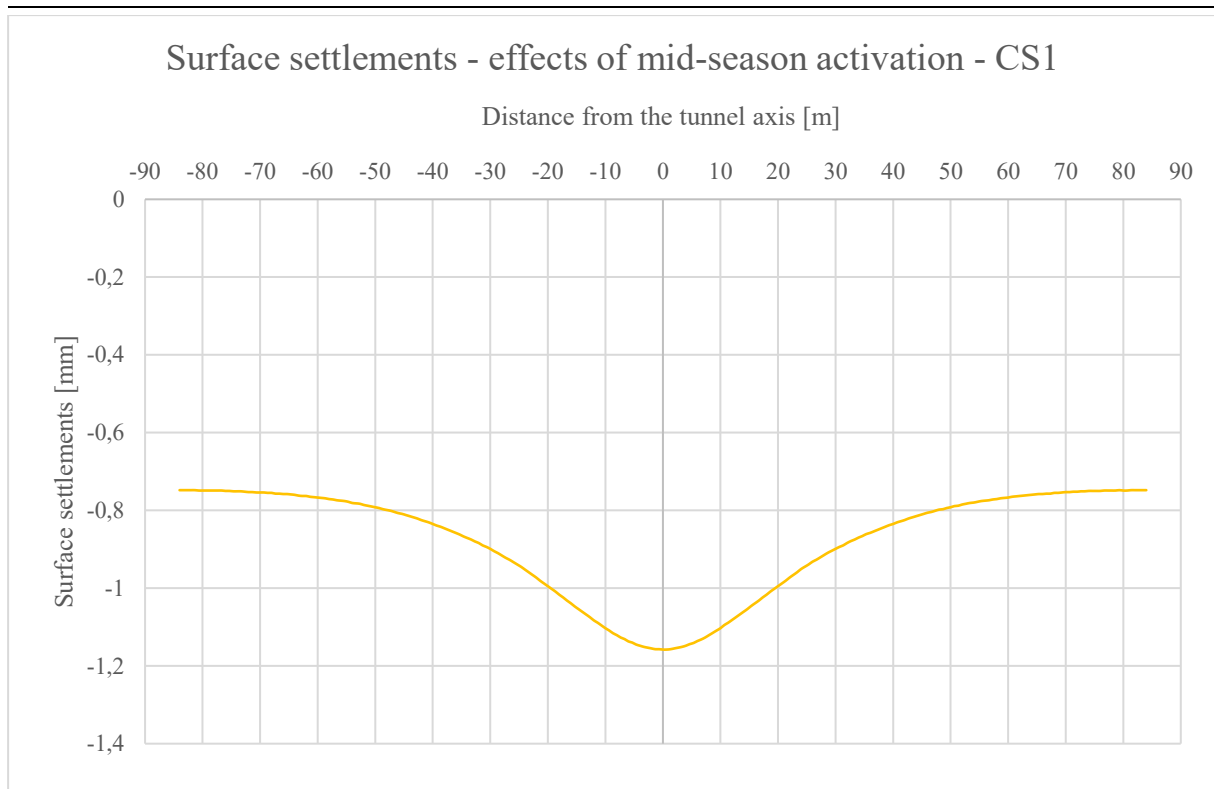
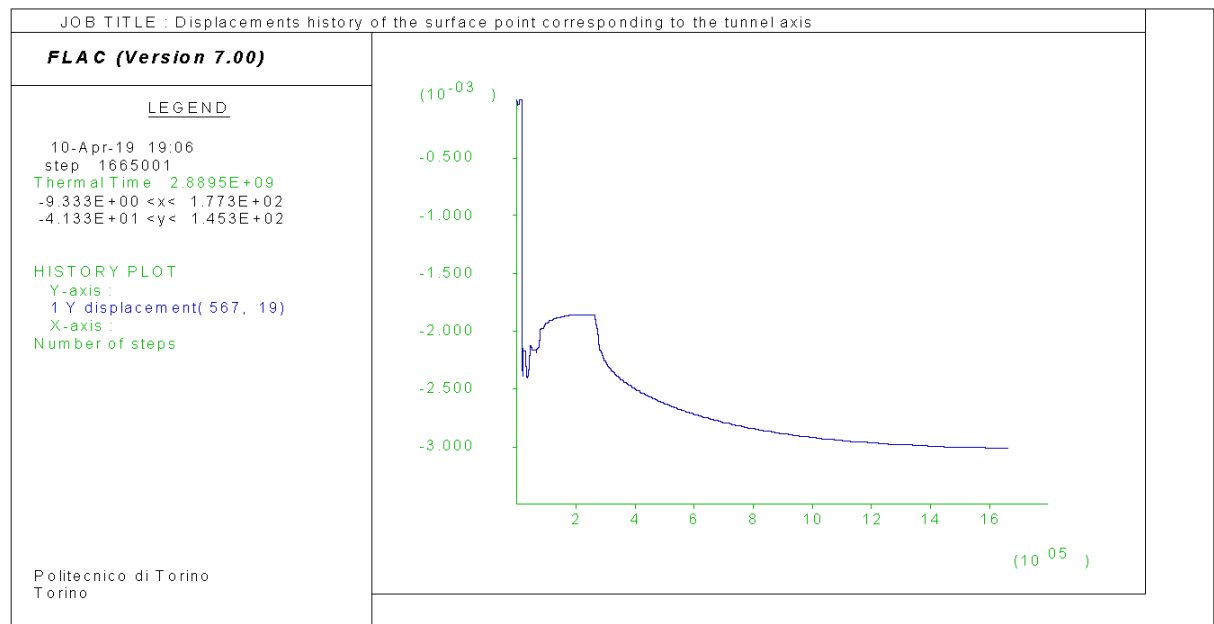


Figure 4.31. Displacements history of the surface point corresponding to the tunnel axis – Winter CS1

## Numerical assessment of the role of thermal parameters



*Figure 4.32. Mid-season - Surface settlements - CS1*



*Figure 4.33. Displacements history of the surface point corresponding to the tunnel axis – Mid-season CS1*

## Numerical assessment of the role of thermal parameters

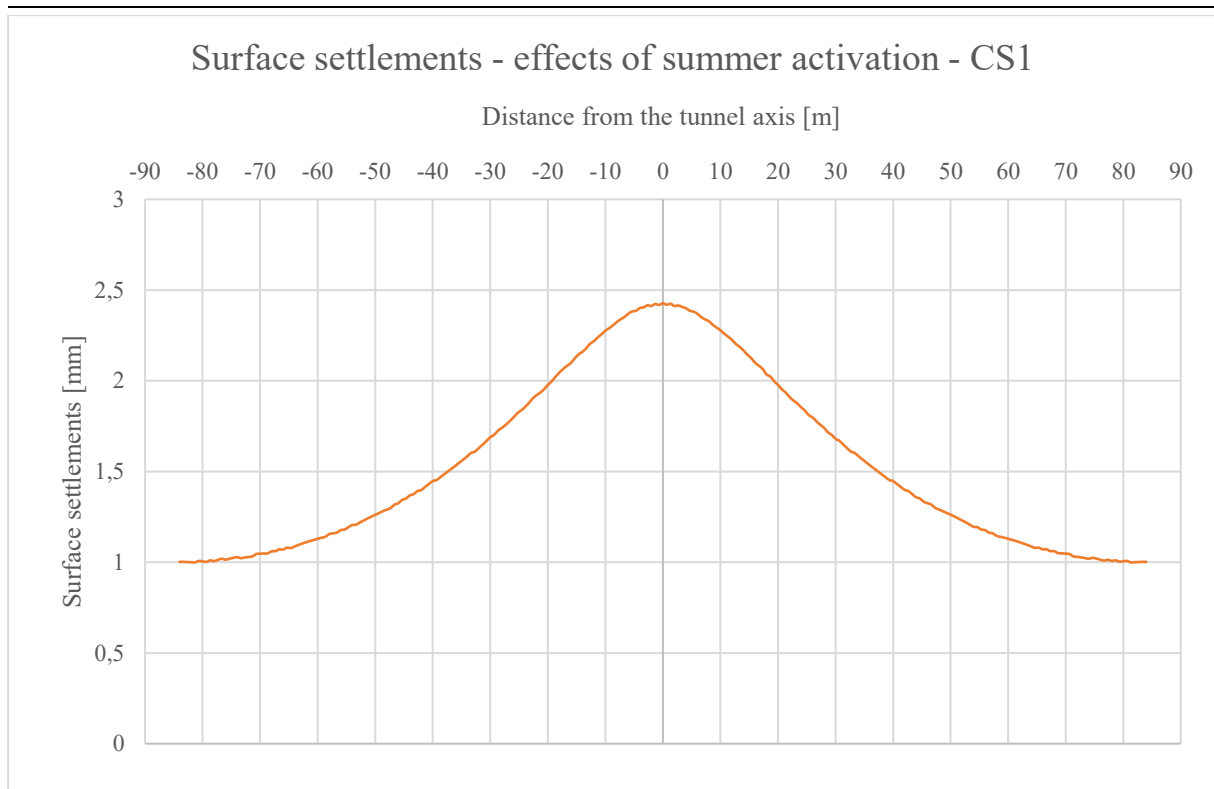


Figure 4.34. Summer - Surface settlements - CS1

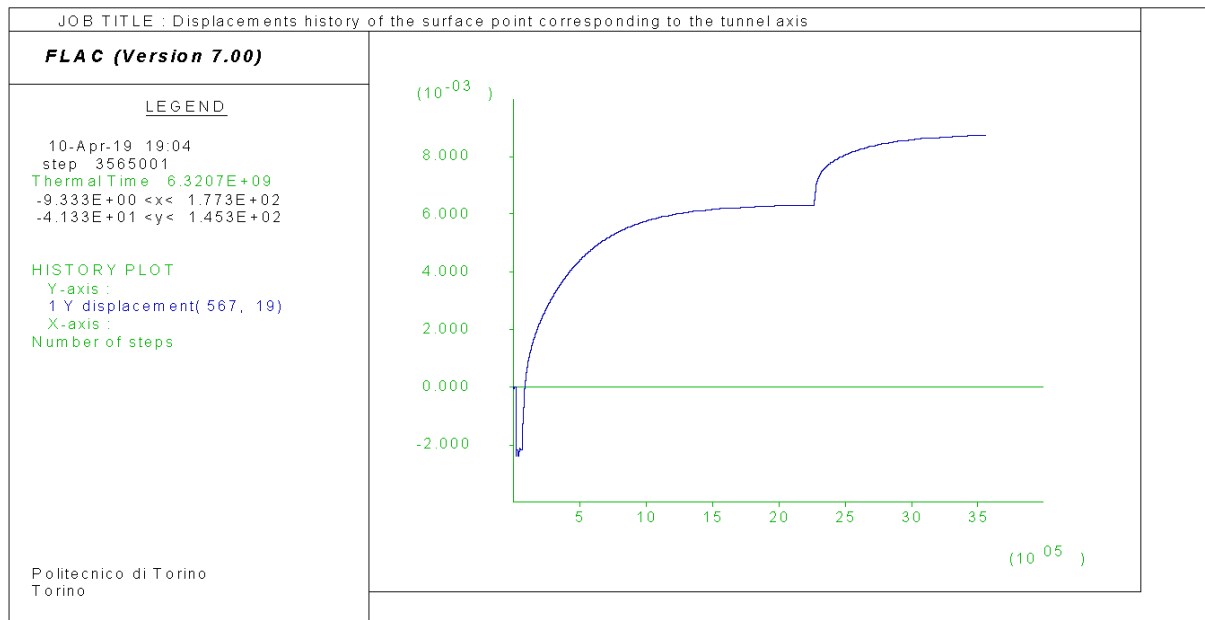


Figure 4.35. Displacements history of the surface point corresponding to the tunnel axis – Summer CS1

## Numerical assessment of the role of thermal parameters

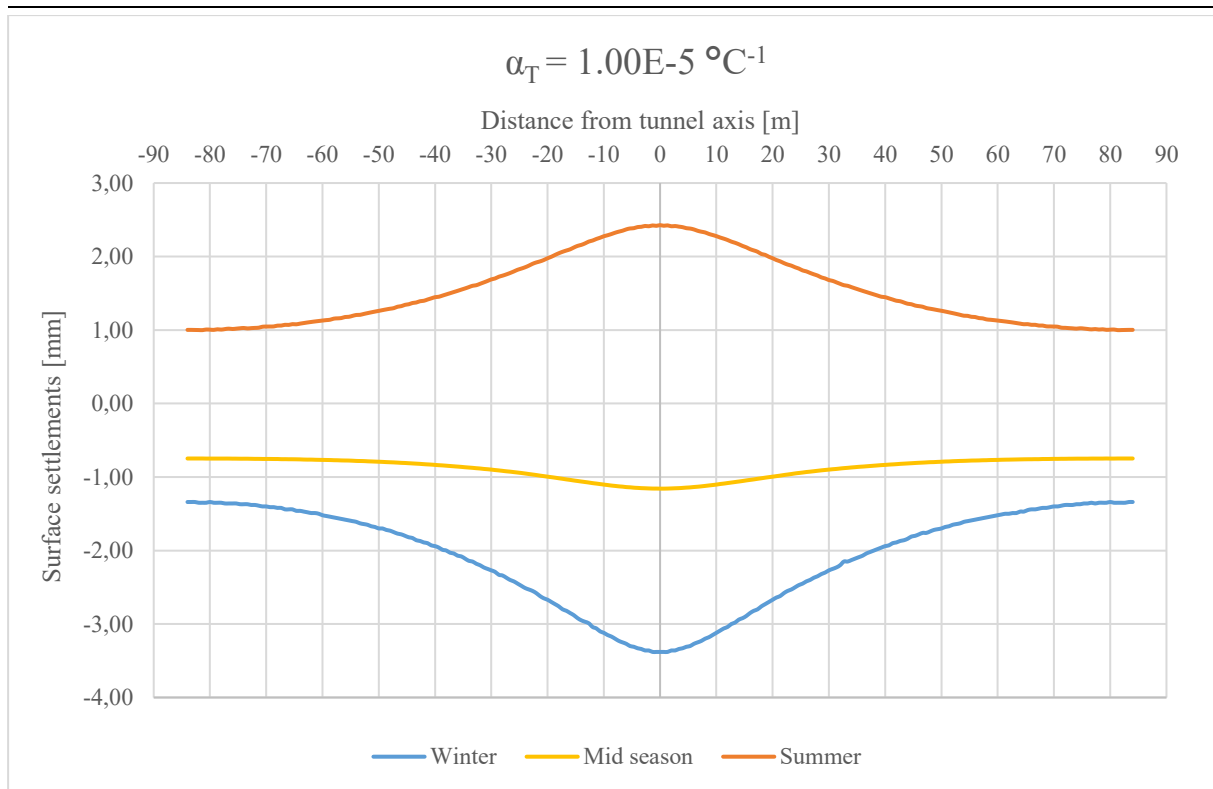


Figure 4.36. CSI - Surface settlements during the year

It is possible to observe that the variation between the surface settlements of the point corresponding to the centre of the tunnel, before and after the activation of the lining, is in the order of 1-3 mm, depending on the season. Table 4.16 shows the precise values.

Table 4.16. Values of surface settlements corresponding to the tunnel axis - CSI ( $x=0$ )

|            | $s(x=0)$<br>[mm] |
|------------|------------------|
| Winter     | -3.380           |
| Mid-season | -1.158           |
| Summer     | 2.297            |

4.3.3.4.2 Case Study 2,  $\alpha = 2.00E - 05 \text{ } ^\circ\text{C}^{-1}$

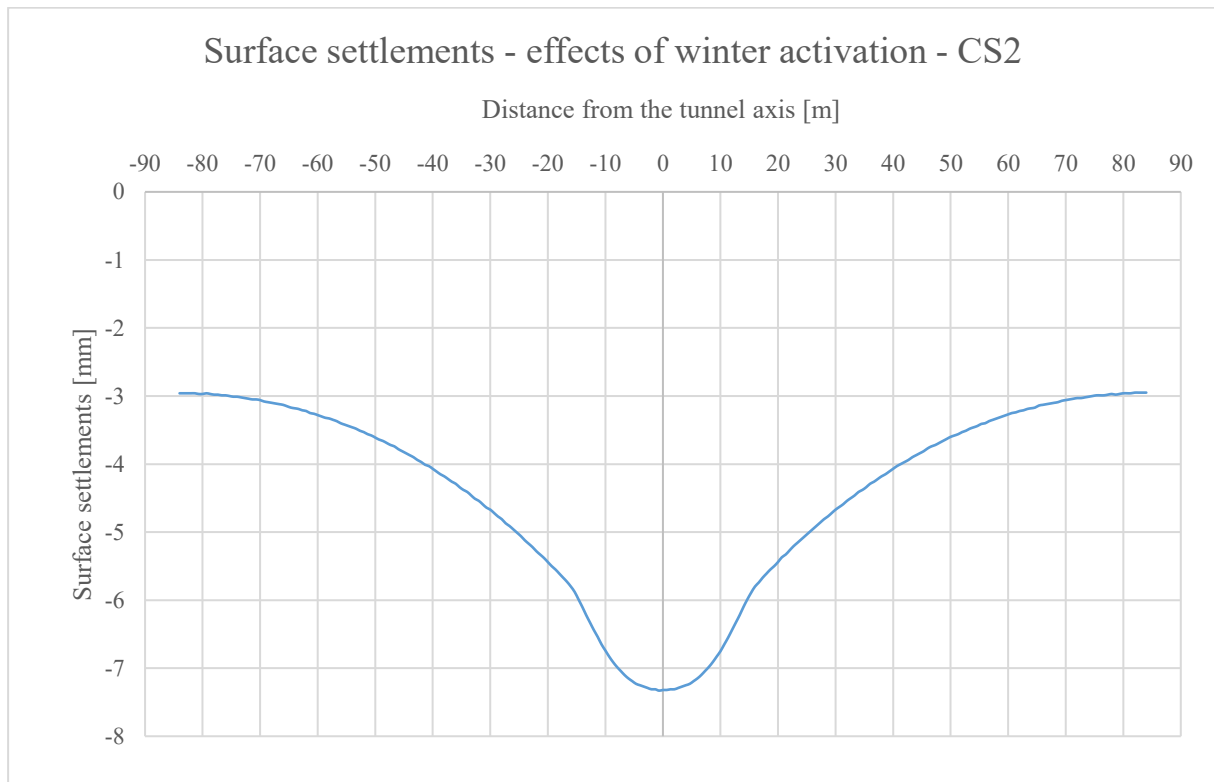


Figure 4.37. Winter - Surface settlements - CS2

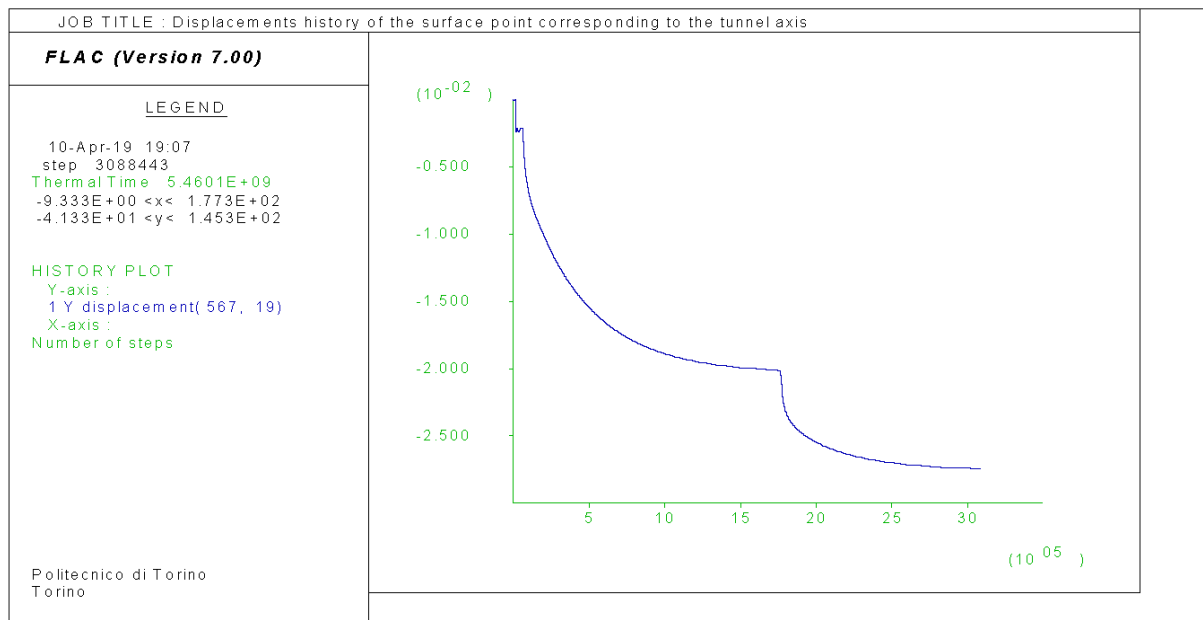


Figure 4.38. Displacements history of the surface point corresponding to the tunnel axis – Winter CS2

## Numerical assessment of the role of thermal parameters

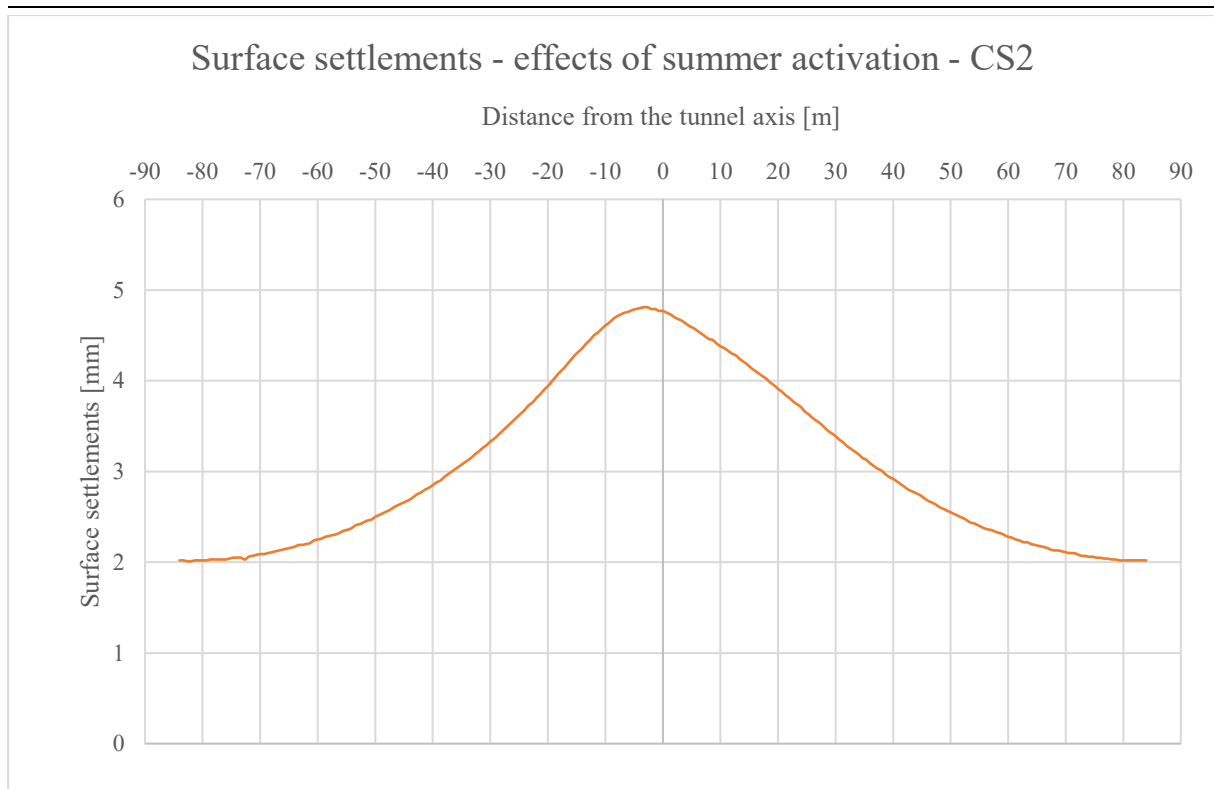


Figure 4.39. Summer - Surface settlements - CS2

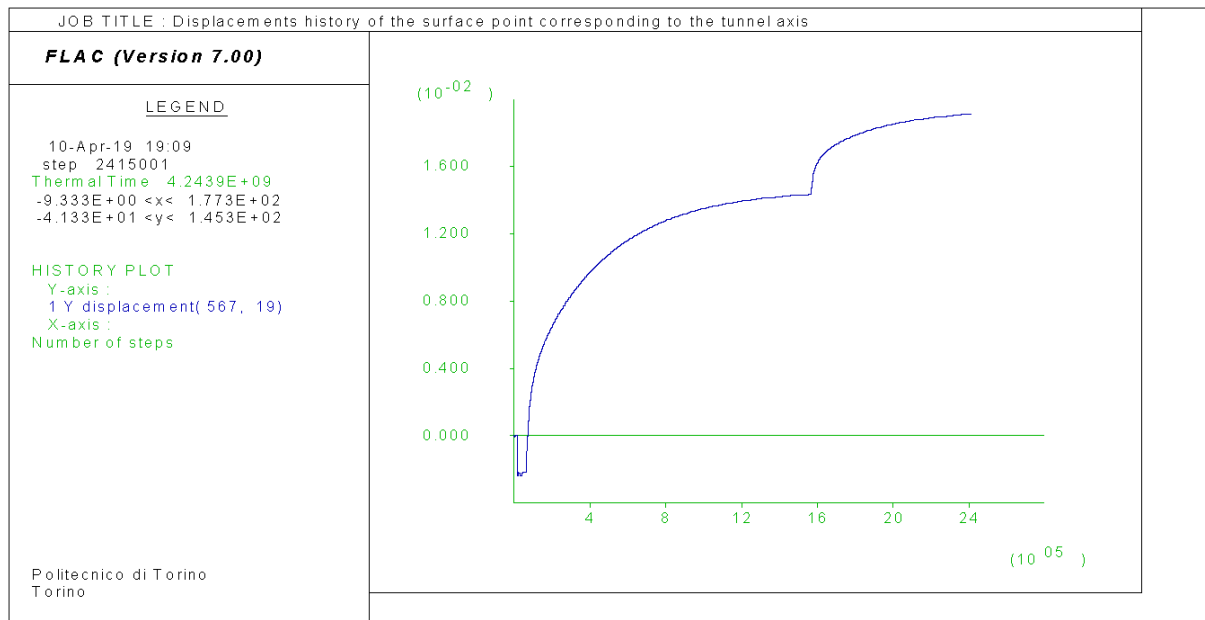


Figure 4.40. Displacements history of the surface point corresponding to the tunnel axis – Summer CS2

## Numerical assessment of the role of thermal parameters

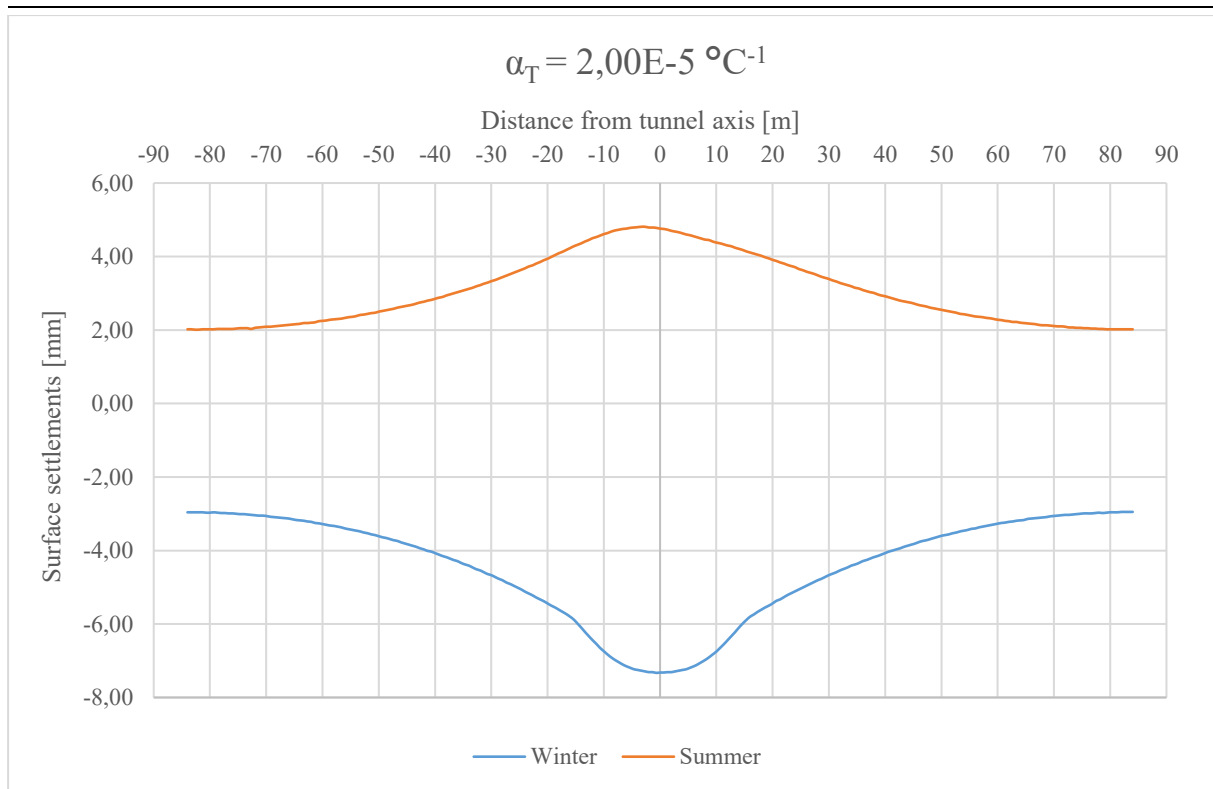


Figure 4.41. CS2 - Surface settlements during the year

It is possible to observe that the variation between the surface settlements of the point corresponding to the axis of the tunnel, before and after the activation of the lining, is in the order of 4-7 mm, depending on the season. Table 4.17 shows the precise values.

Table 4.17. Values of surface settlements corresponding to the tunnel axis – CS2 ( $x=0$ )

|            | $s(x=0)$<br>[mm]  |
|------------|-------------------|
| Winter     | -7.320            |
| Mid-season | - Not simulated - |
| Summer     | 4.770             |

4.3.3.4.3 Case Study 3,  $\alpha = 5.00E - 06 \text{ } ^\circ\text{C}^{-1}$

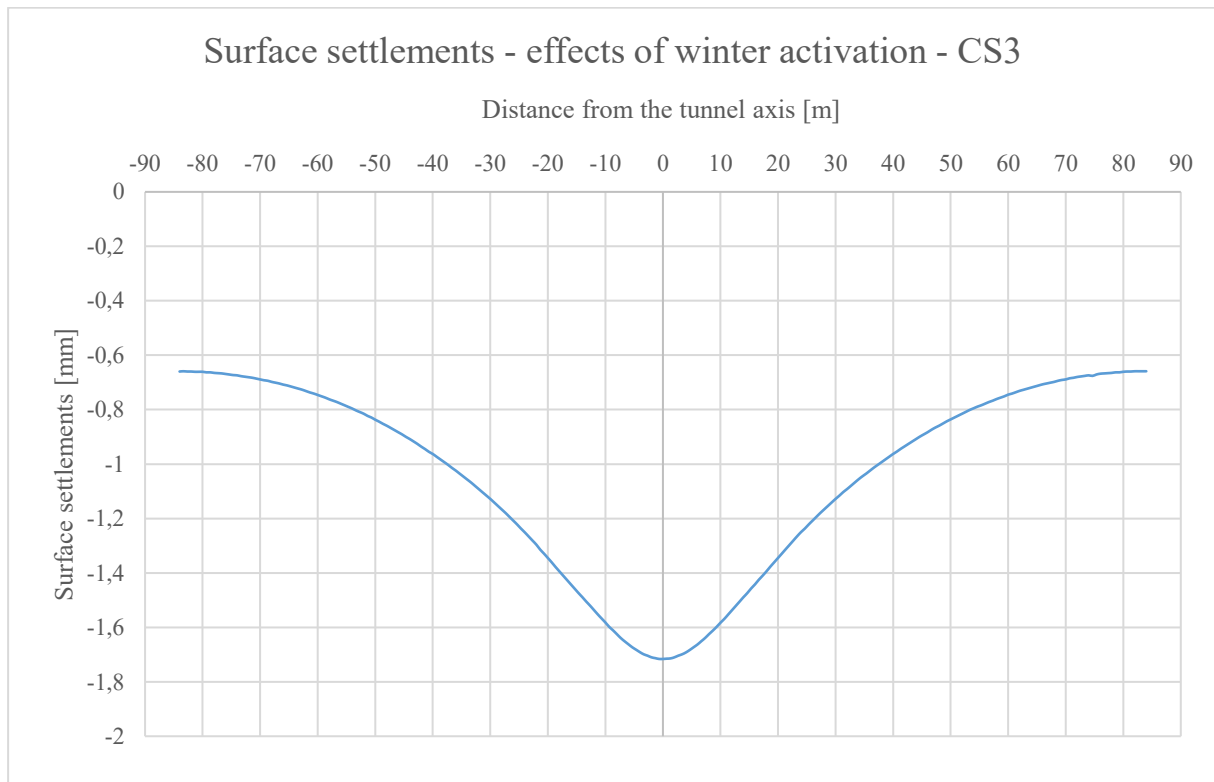


Figure 4.42. Winter - Surface settlements - CS3

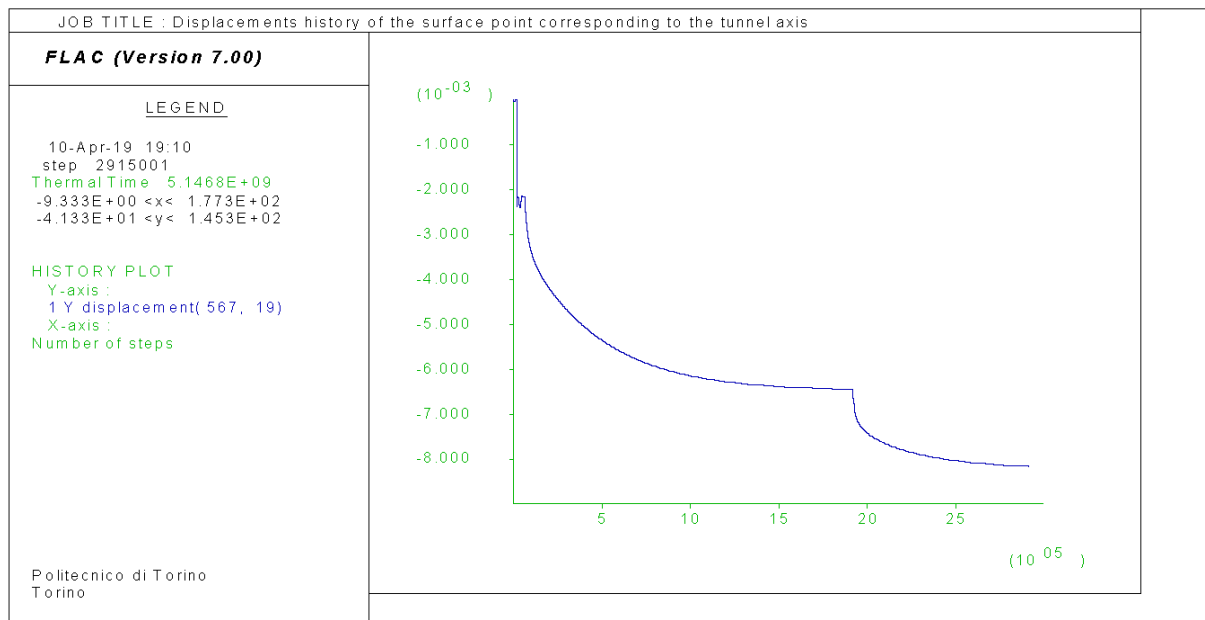


Figure 4.43. Displacements history of the surface point corresponding to the tunnel axis – Winter CS3

## Numerical assessment of the role of thermal parameters

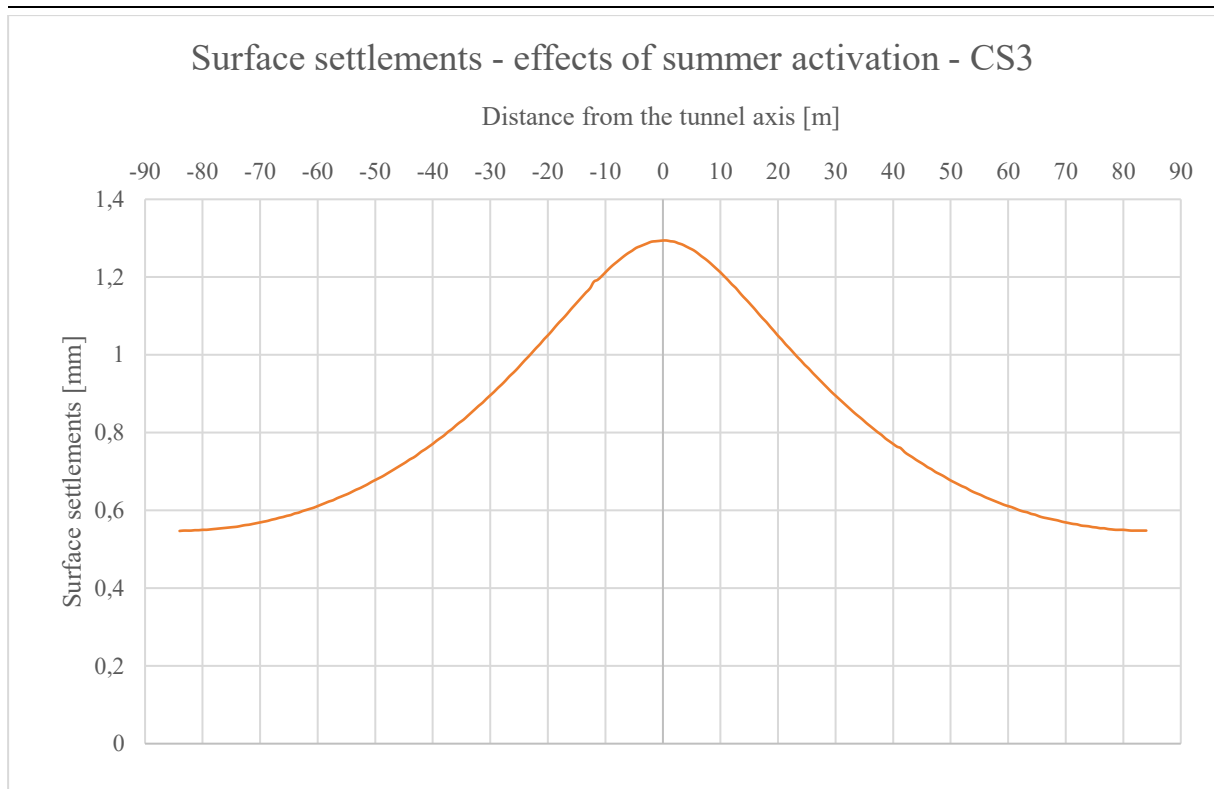


Figure 4.44. Summer - Surface settlements - CS3

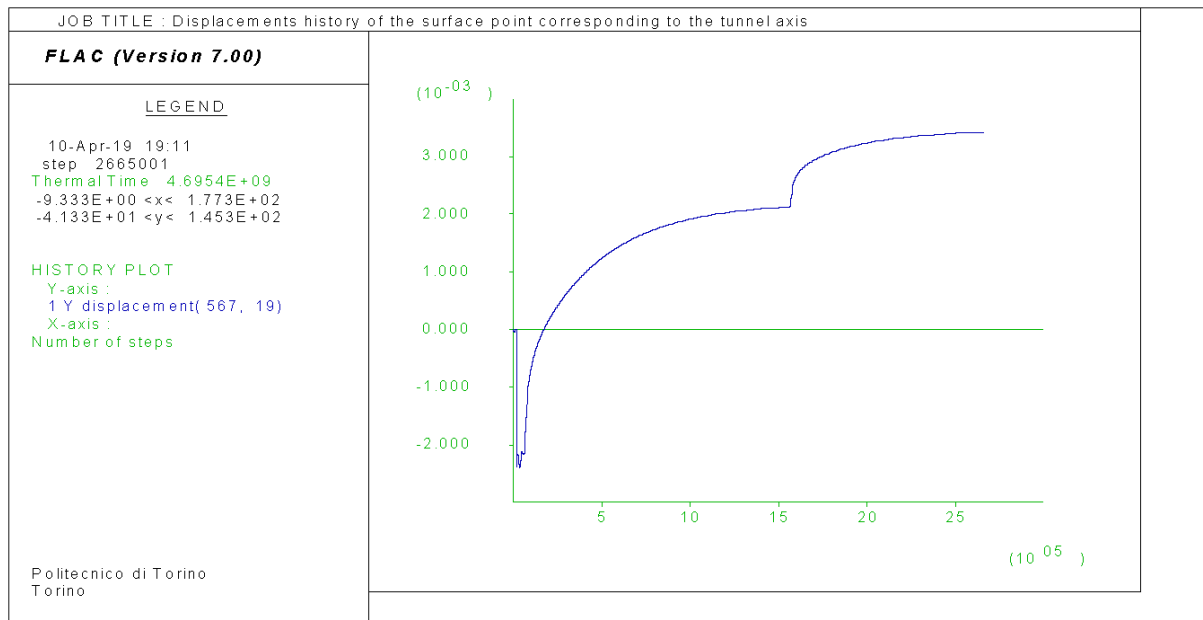


Figure 4.45. Displacements history of the surface point corresponding to the tunnel axis – Summer CS3

## Numerical assessment of the role of thermal parameters

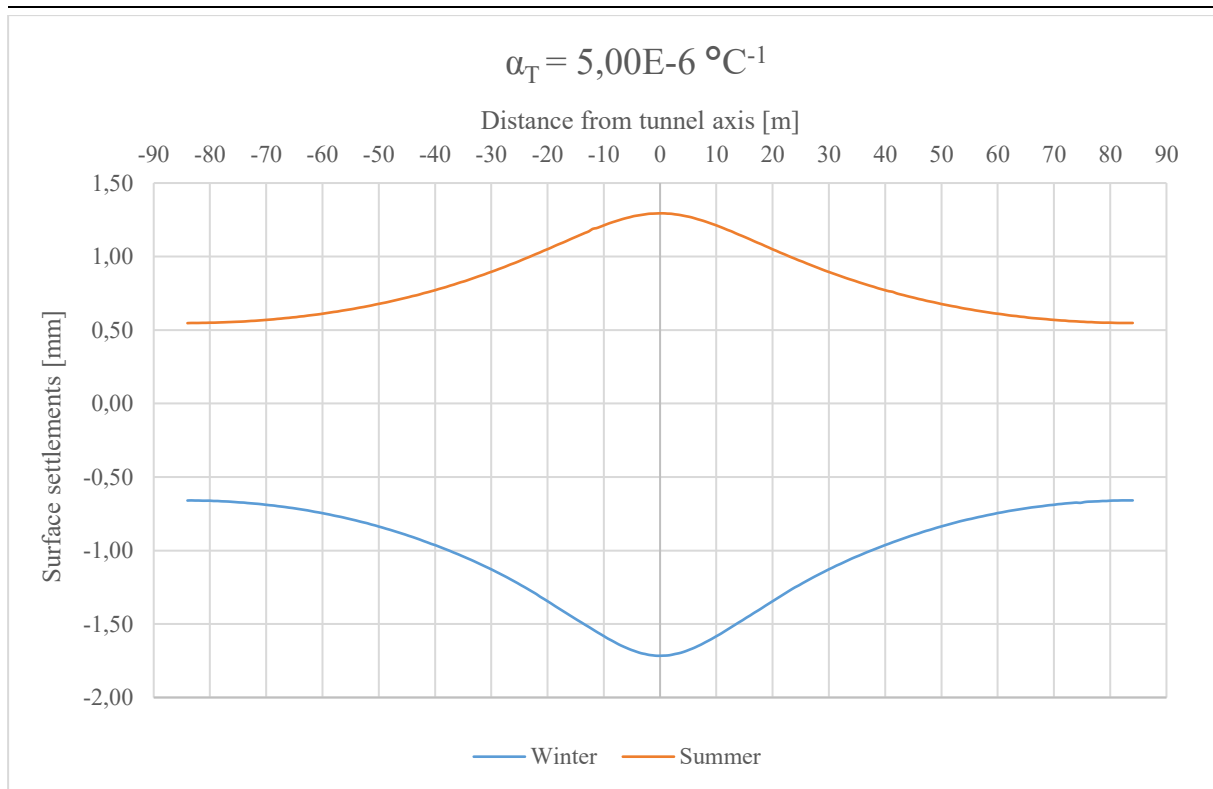


Figure 4.46. CS3 - Surface settlements during the year

It is possible to observe that the difference between the surface settlements of the point corresponding to the centre of the tunnel, before and after the activation of the lining, is in the order of 1.2-1.7 mm, depending on the season. Table 4.18 shows the precise values.

Table 4.18. Values of surface settlements corresponding to the tunnel axis – CS3 ( $x=0$ )

|            | $s(x=0)$<br>[mm]  |
|------------|-------------------|
| Winter     | -1.716            |
| Mid-season | - Not simulated - |
| Summer     | 1.249             |

#### 4.3.3.4.4 Comparisons

It is now possible to compare the results.

The situation after the thermo-activation of the lining is analysed, the variations of the surface settlements of the point corresponding to the tunnel axis are collected in *Table 4.19*, they vary depending on the fluid temperature (seasonal operational mode) and on the linear thermal expansion coefficient.

*Table 4.19. Comparison between surface settlements (x=0) after the activation of the lining*

| Case study | Fluid Temperature [°C] | $\alpha_T$ [°C <sup>-1</sup> ] | s (x=0) [mm] |
|------------|------------------------|--------------------------------|--------------|
| 1A         | 3                      | 1.00E-05                       | -3.380       |
| 1B         | 15                     |                                | -1.158       |
| 1C         | 30                     |                                | 2.427        |
| 2A         | 3                      | 2.00E-05                       | -7.320       |
| 2C         | 30                     |                                | 4.770        |
| 3A         | 3                      | 5.00E-06                       | -1.716       |
| 3C         | 30                     |                                | 1.294        |

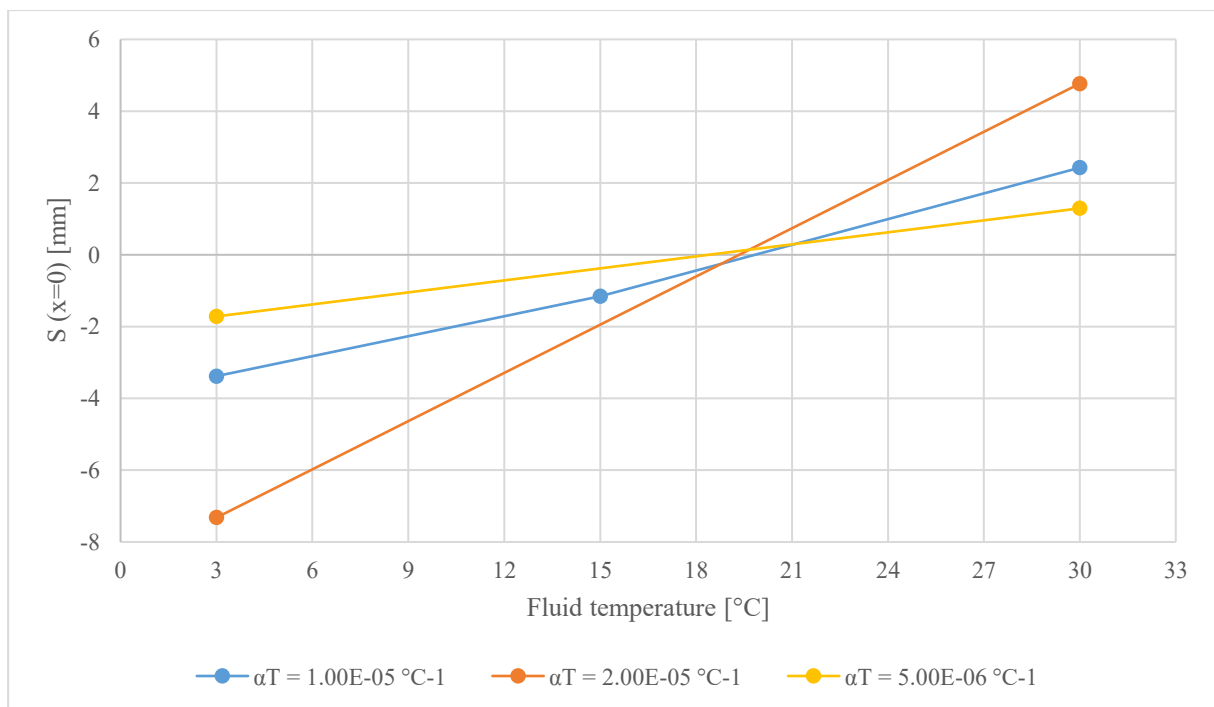


*Figure 4.47. Comparison between surface settlements (x=0) after the activation of the lining*

## Numerical assessment of the role of thermal parameters

Depending on  $\alpha$ , the trends have different slopes: the higher the value, the higher the slope. This is important to be observed, meaning that different values bring to different surface settlements: it is an aspect that needs to be deeper investigated. It is possible to observe that the surface settlements tends to be directly proportional to the value of the expansion coefficient: if a given expansion coefficient is considered and the related settlements are calculated, when then value of the coefficient is half the first, also the value of settlements is reduced by half. In *Figure 4.41* the variation of the seasonal settlements (winter and summer) with the expansion coefficient are represented.

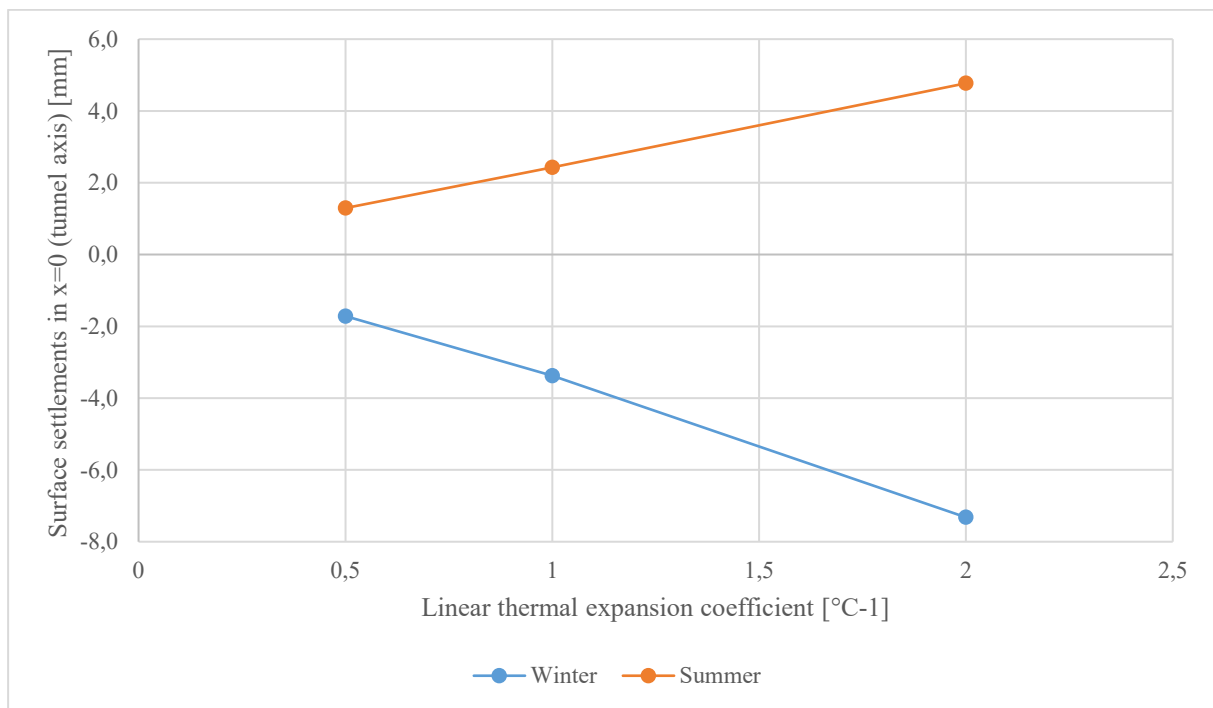


Figure 4.48. Variation of the seasonal settlements (winter and summer) with the expansion coefficient

#### 4.3.3.4.5 Improvement of the model

The results obtained seem to be not realistic, because the activation of the lining seems to have a comparable effect to the excavation, with relatively large settlements.

From the analysis of the previous results, it has been observed that it could be possible to add some improvements to the model, in order to evaluate if the results are representative.

Considering only  $\alpha = 1.00E - 05 \text{ } ^\circ\text{C}^{-1}$ , in winter and summer conditions, the model is modified, with the addition of temperature conditions on the lateral boundaries. A temperature of  $14^\circ\text{C}$  is fixed from the depth of 10 m to the lower boundary of the model.

The equilibrium in terms of temperature should be more consistent with the observations made in *Chapter 1.1.1*, regarding the depth of seasonal effects.

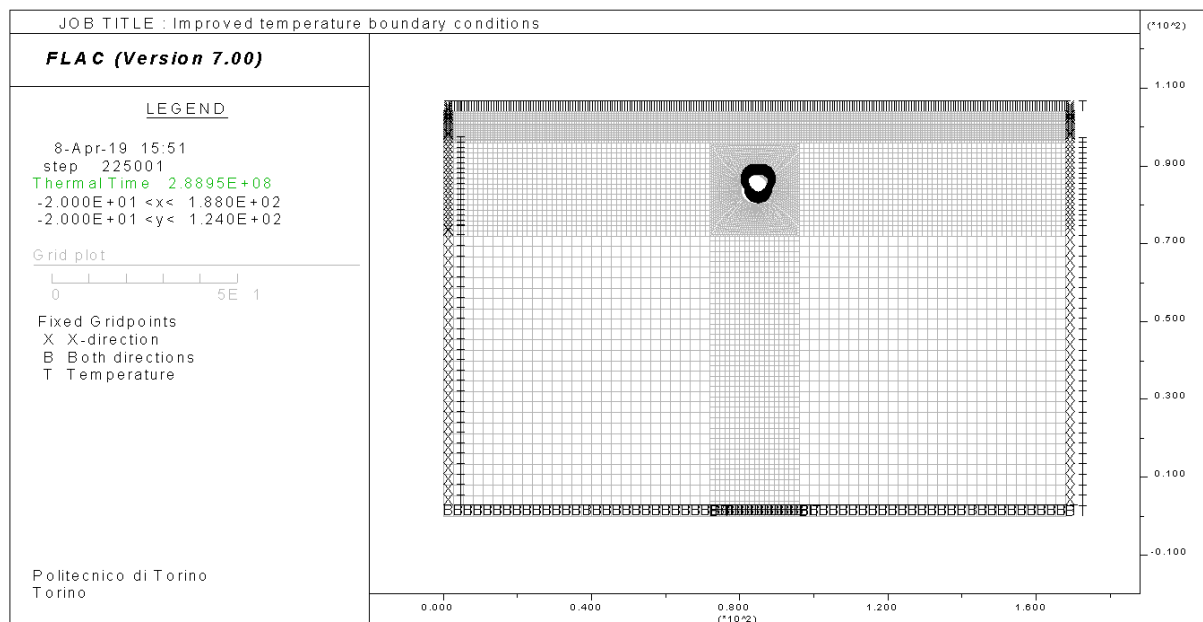
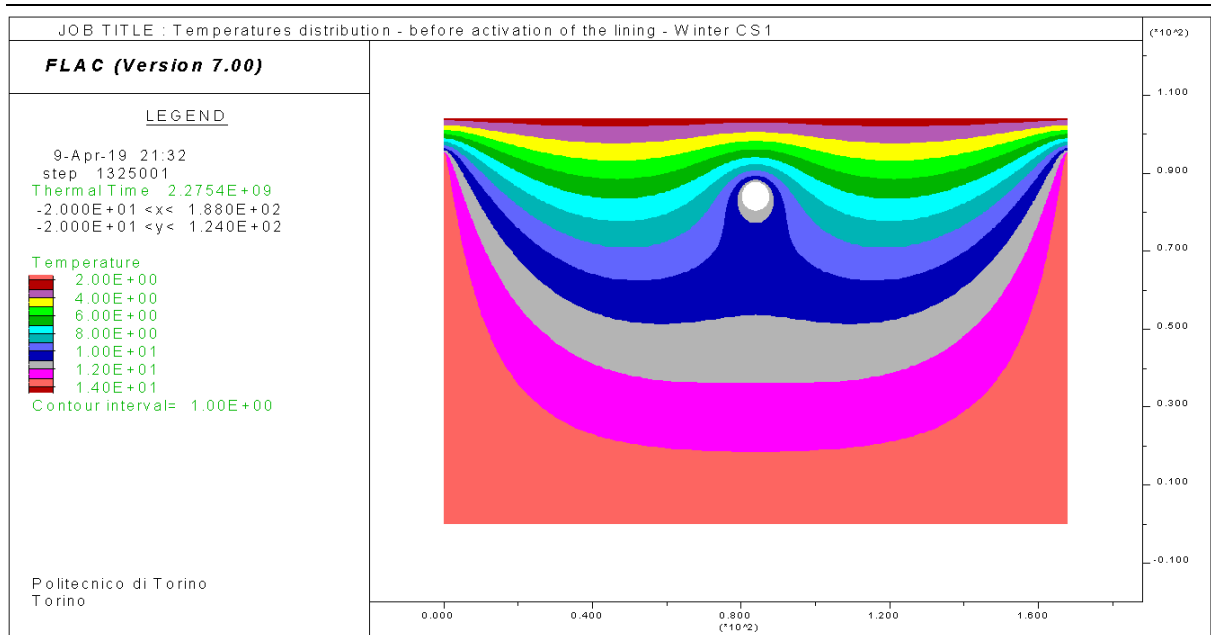


Figure 4.49. Improved temperature boundary conditions

In the following *Figures* the new temperatures distributions are reported: it is clearly visible the effect of the new thermal boundary conditions.

## Numerical assessment of the role of thermal parameters



*Figure 4.50. Temperatures distribution - before activation of the lining - Winter CS1*

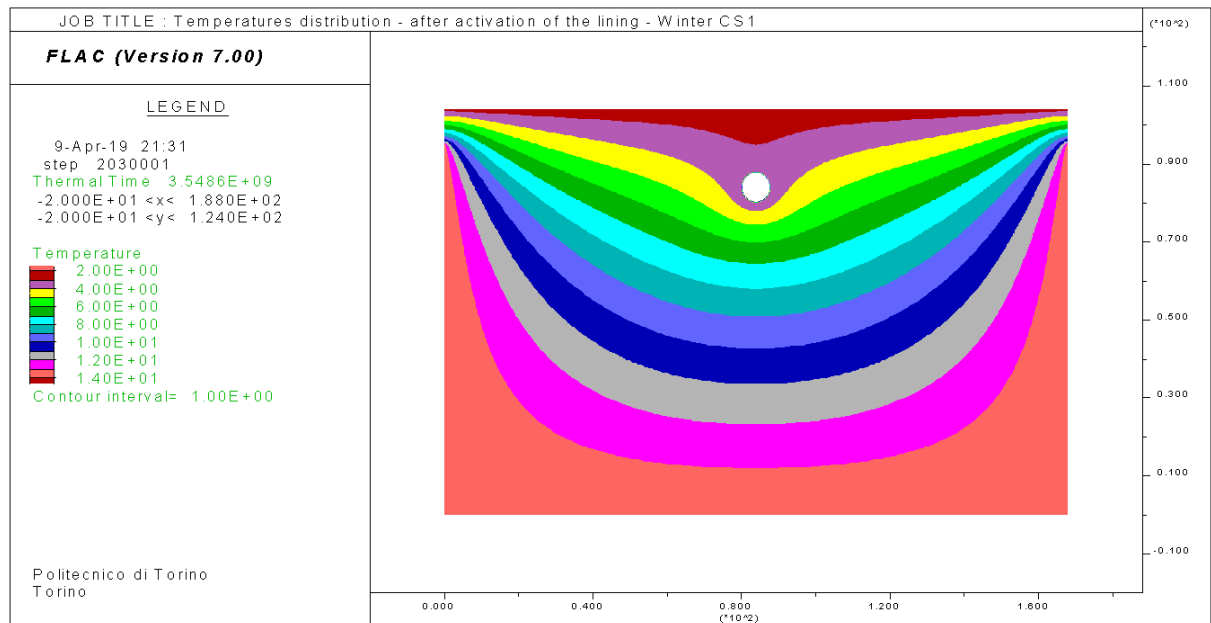


*Figure 4.51. Temperatures distribution - after activation of the lining - Winter CS1*

## Numerical assessment of the role of thermal parameters

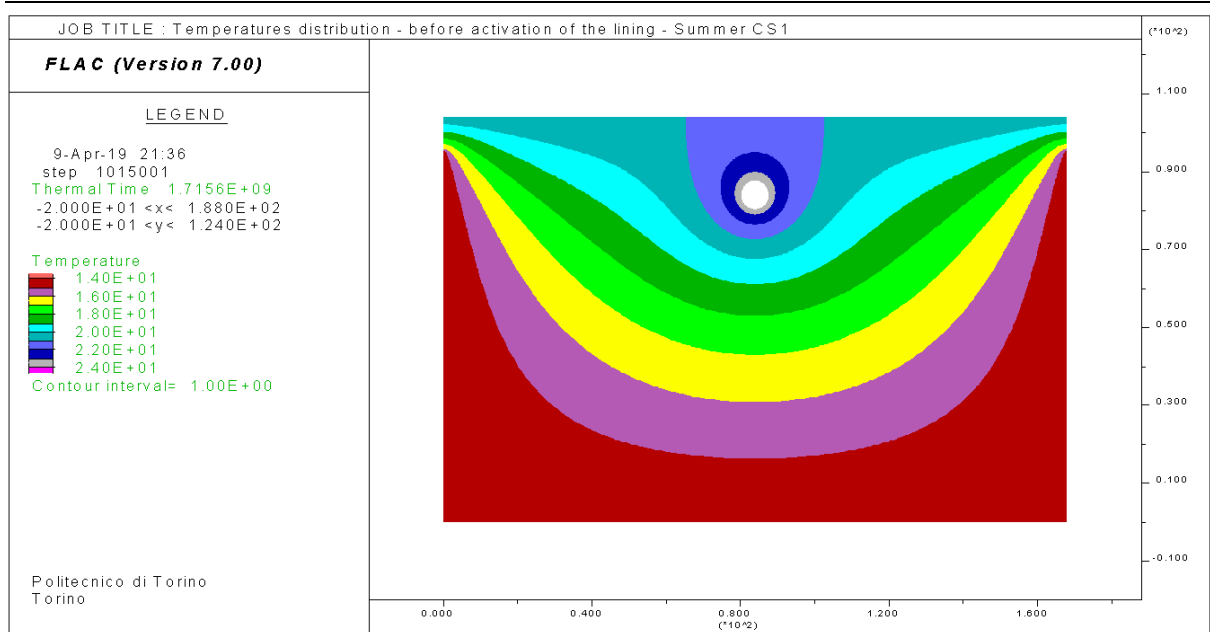


*Figure 4.52. Temperatures distribution - before activation of the lining - Summer CS1*

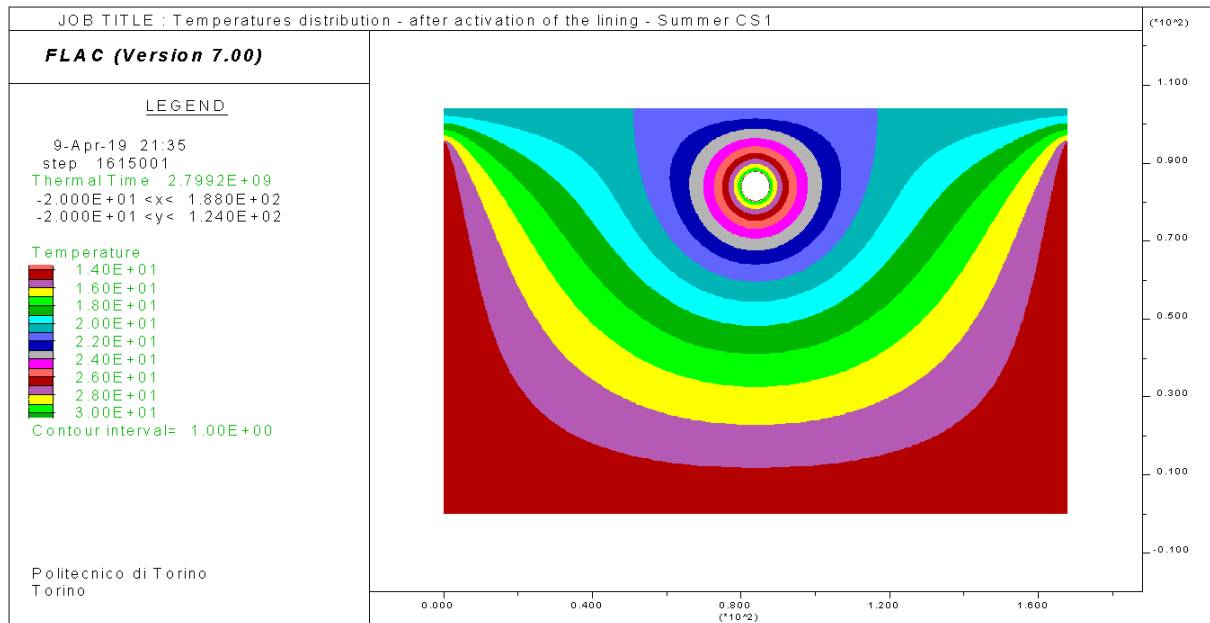


*Figure 4.53. Temperatures distribution - after activation of the lining - Summer CS1*

## Numerical assessment of the role of thermal parameters

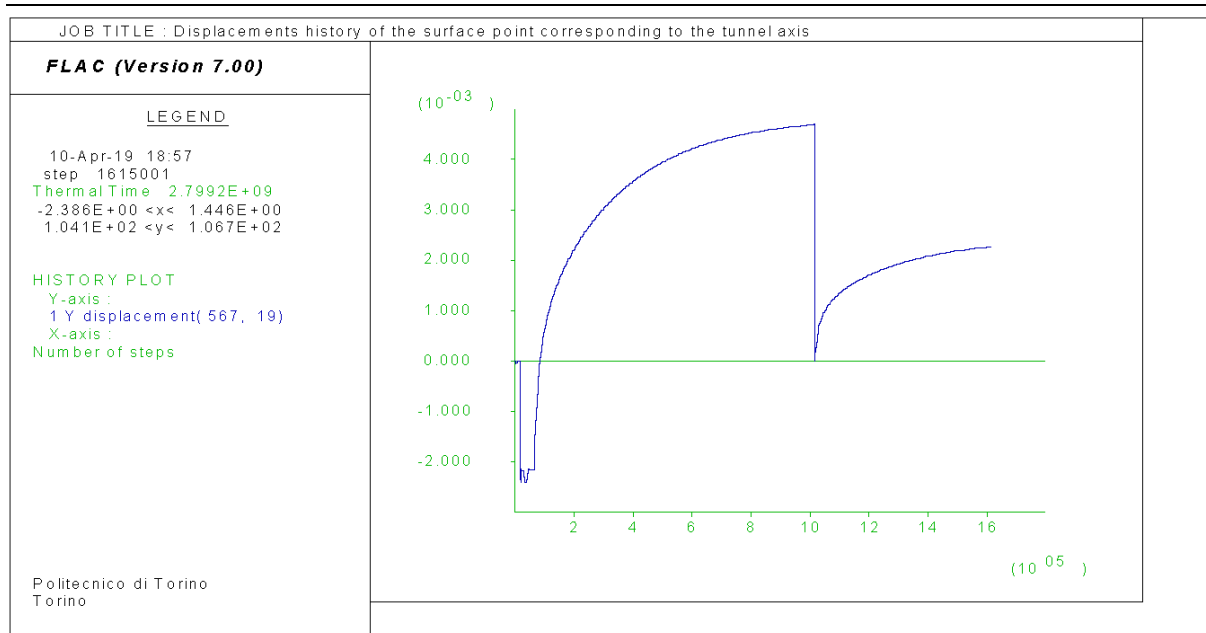


*Figure 4.54. Displacements history of the surface point corresponding to the tunnel axis – Summer CSI*

Results are plotted in terms of surface settlements that occur because of the lining activation, then compared with the previous ones.

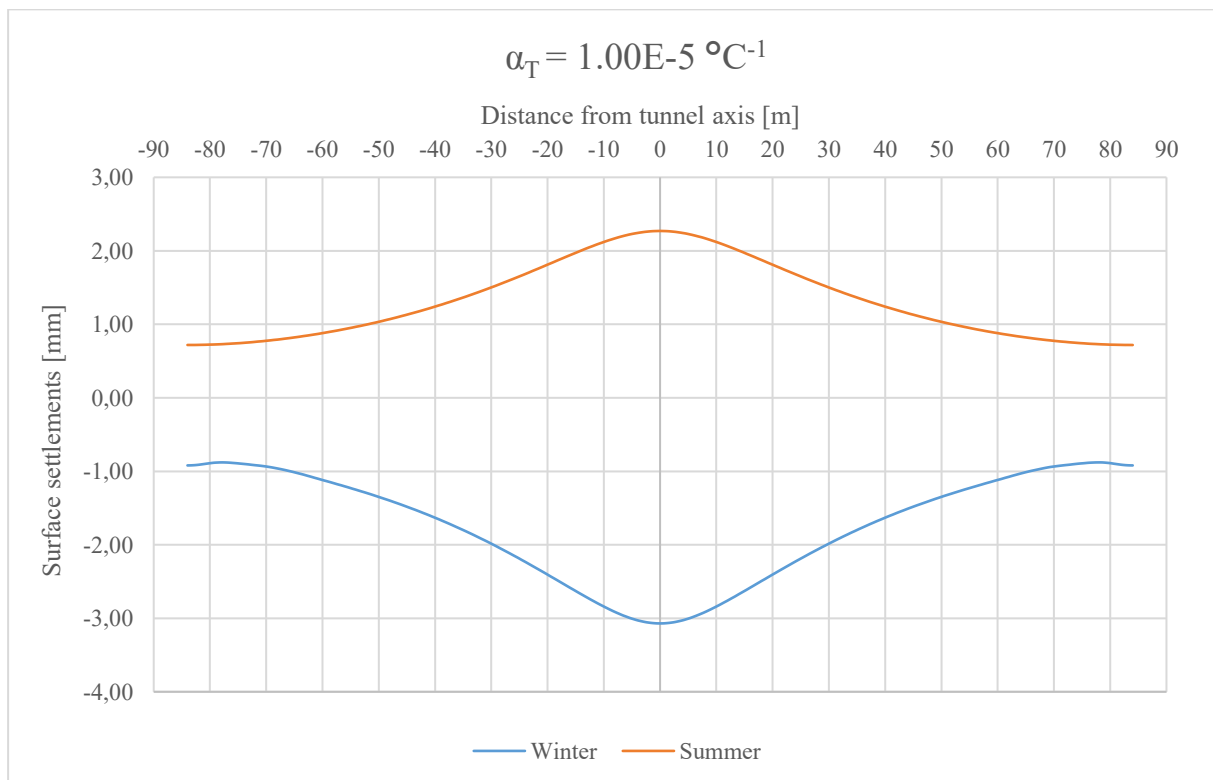


*Figure 4.55. Surface settlements after lining activation - in winter and summer conditions with new temperature conditions-CSI*

## Numerical assessment of the role of thermal parameters

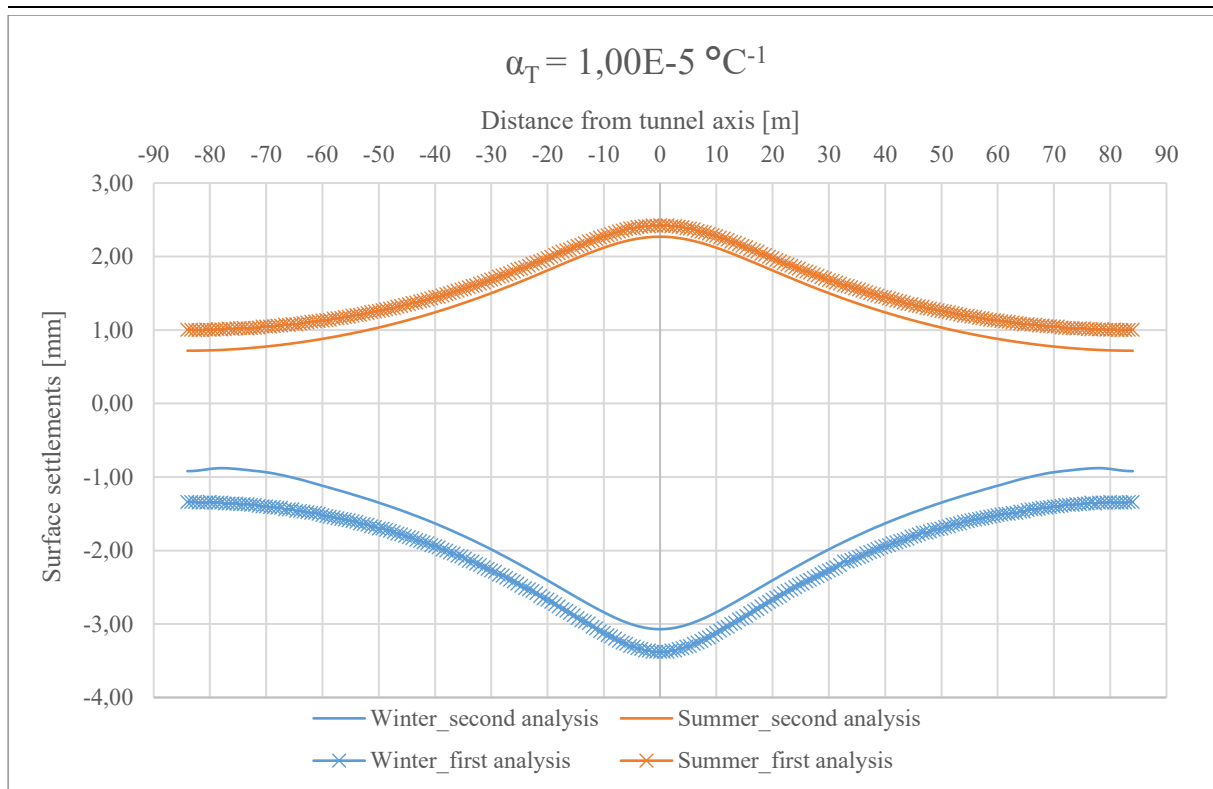


Figure 4.56. Comparisons of the surface settlements between the two analyses - CSI

It is possible to see how the settlements are slightly reduced after the imposition of the new temperature conditions. However, there is still influence of the phenomenon also very far from the tunnel. More improvements could be helpful in reaching reliable results.

Below, the representations of the displacements' vectors are reported.

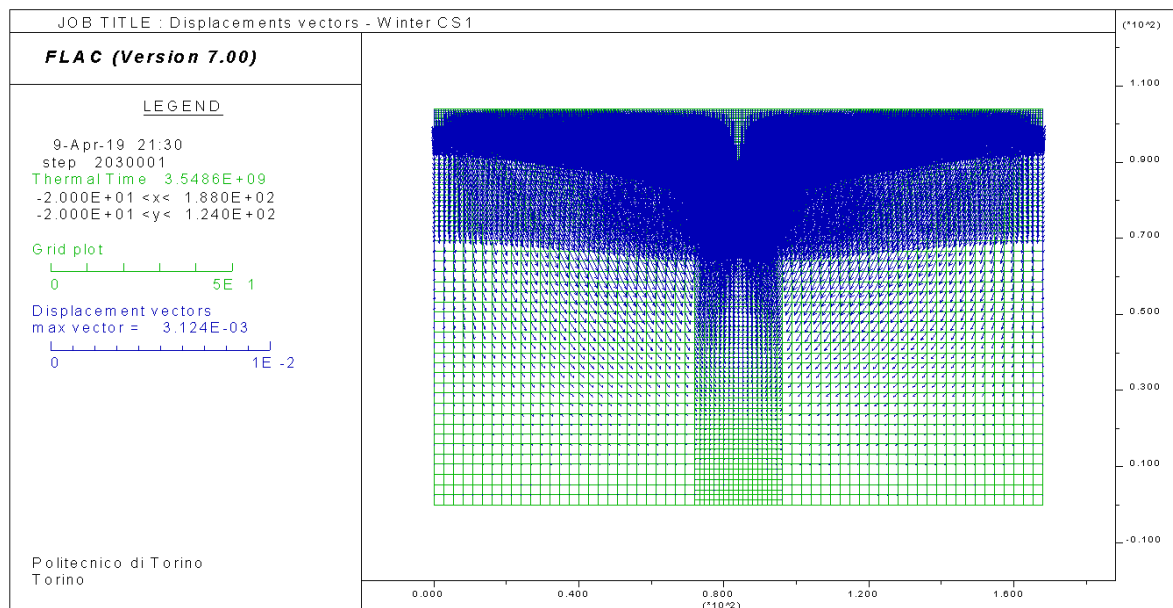


Figure 4.57. Displacements vectors - Winter CSI

## Numerical assessment of the role of thermal parameters

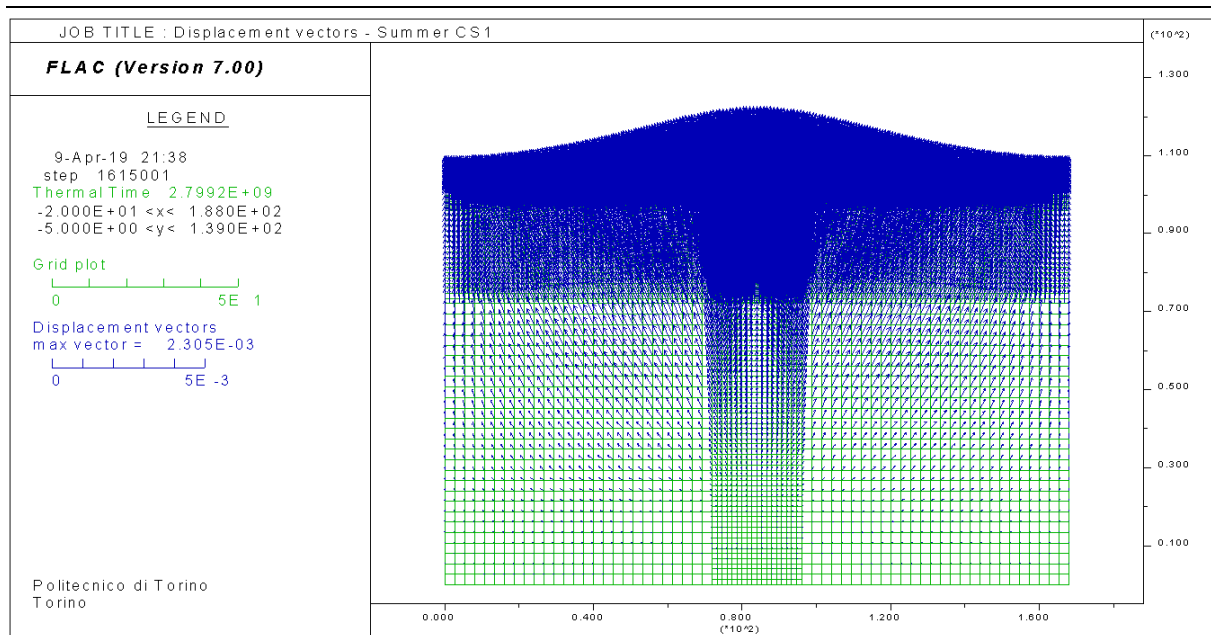


Figure 4.58. Displacements vectors - Summer CS1

An observation that could be done is that all the previous analyses were run in order to reach an equilibrium in the model, i.e. looking at the displacements of a point, after a certain number of steps, the value remains constant. This implied that the thermal computational time of the simulations exceeded 70 years. This is absolutely not realistic: temperatures do not remain constant for such a long time; they vary cyclically during the year. From this perspective, another improvement could be building a unique model, where temperature boundary conditions are no more represented by fixed values but by an annual cyclic trend.

In order to see more realistic results with the previous modelled situations, the analyses were rerun in order to simulate 2 months:

- 1 month = no activated pipes;
- 1 month = after the activation of the pipes.

**Winter CS1**

*First month: no activated pipes*

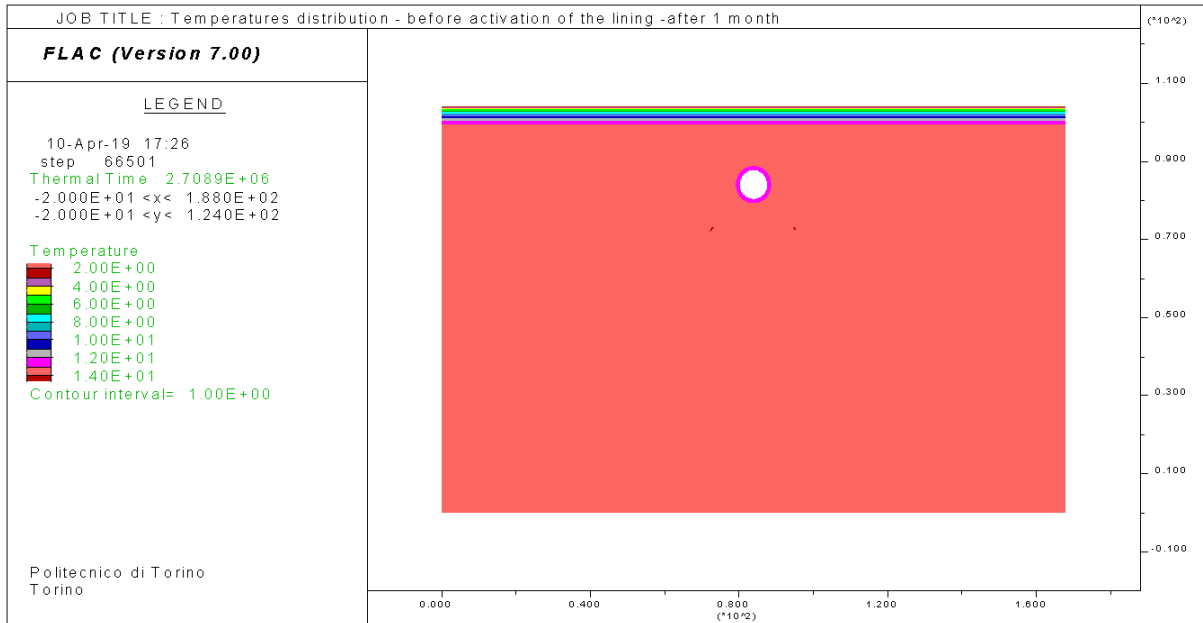


Figure 4.59. Winter conditions CS1 - 1 month of simulation - before the activation of the lining

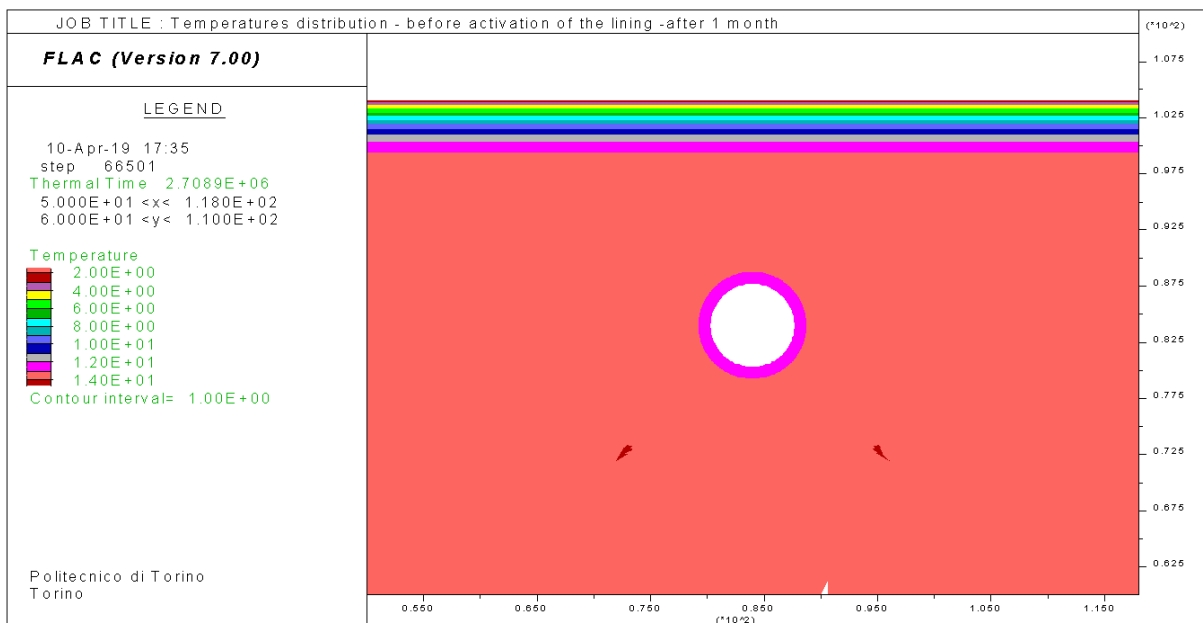


Figure 4.60. Winter conditions CS1 - 1 month of simulation - before the activation of the lining – detail

*Second month: activation of the pipes*

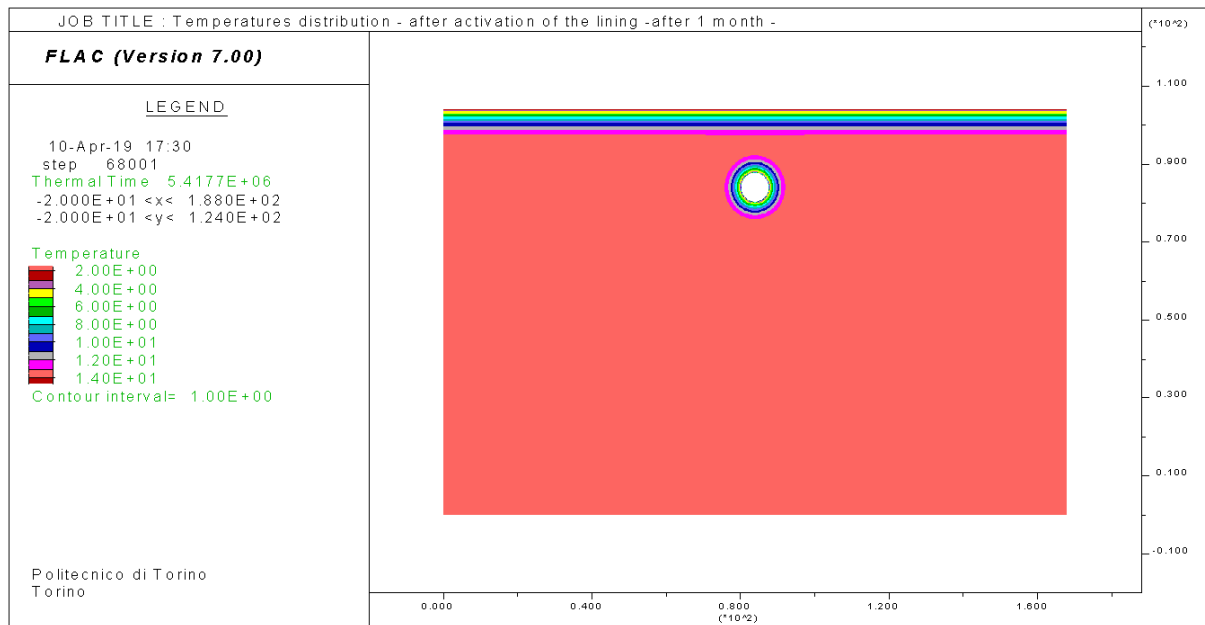


Figure 4.61. Winter conditions CSI - 1 month of simulation - after the activation of the lining

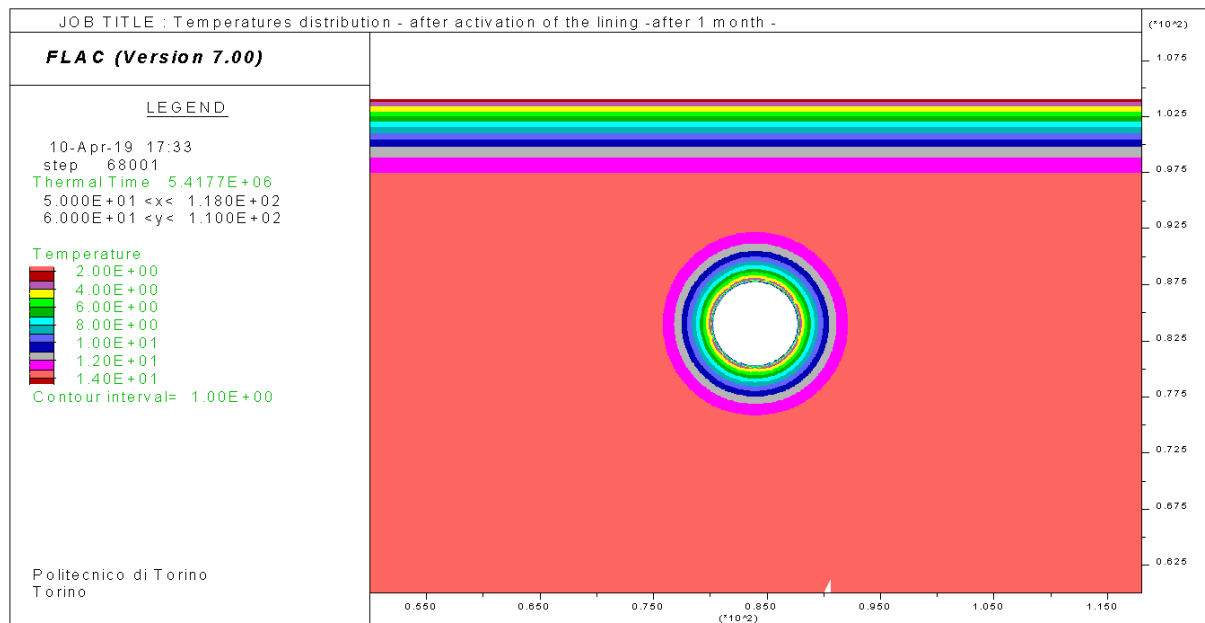


Figure 4.62. Winter conditions CSI - 1 month of simulation - after the activation of the lining – detail

## Numerical assessment of the role of thermal parameters

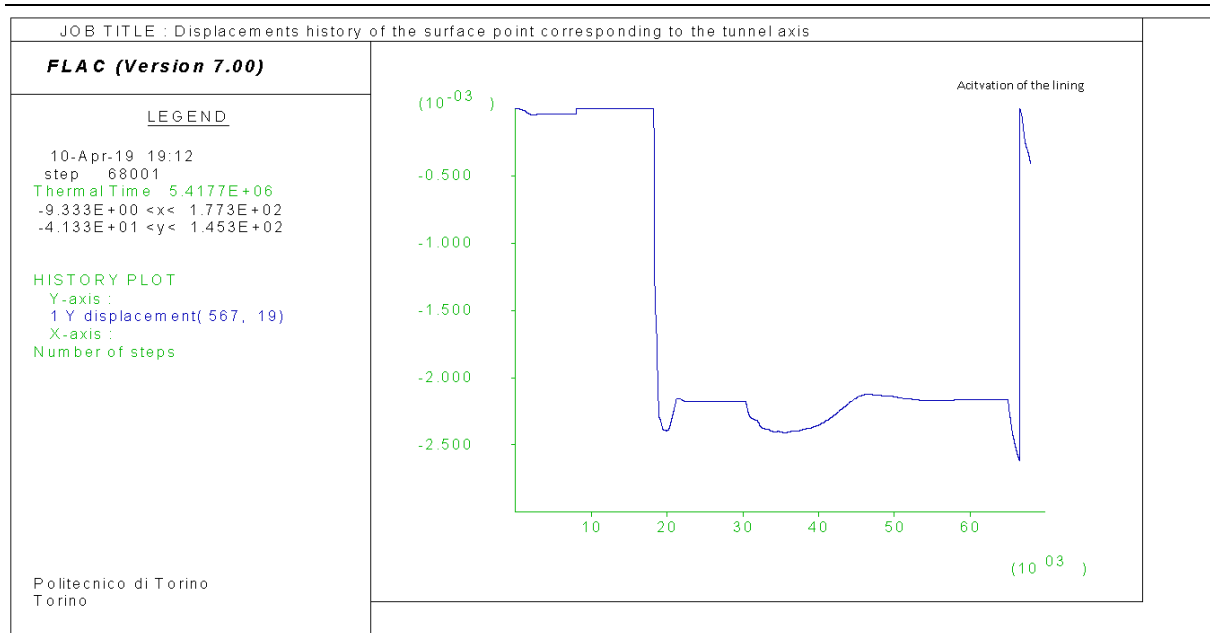


Figure 4.63. Displacements history of the surface point corresponding to the tunnel axis – Winter CSI

### Summer CSI

First month: no activated pipes

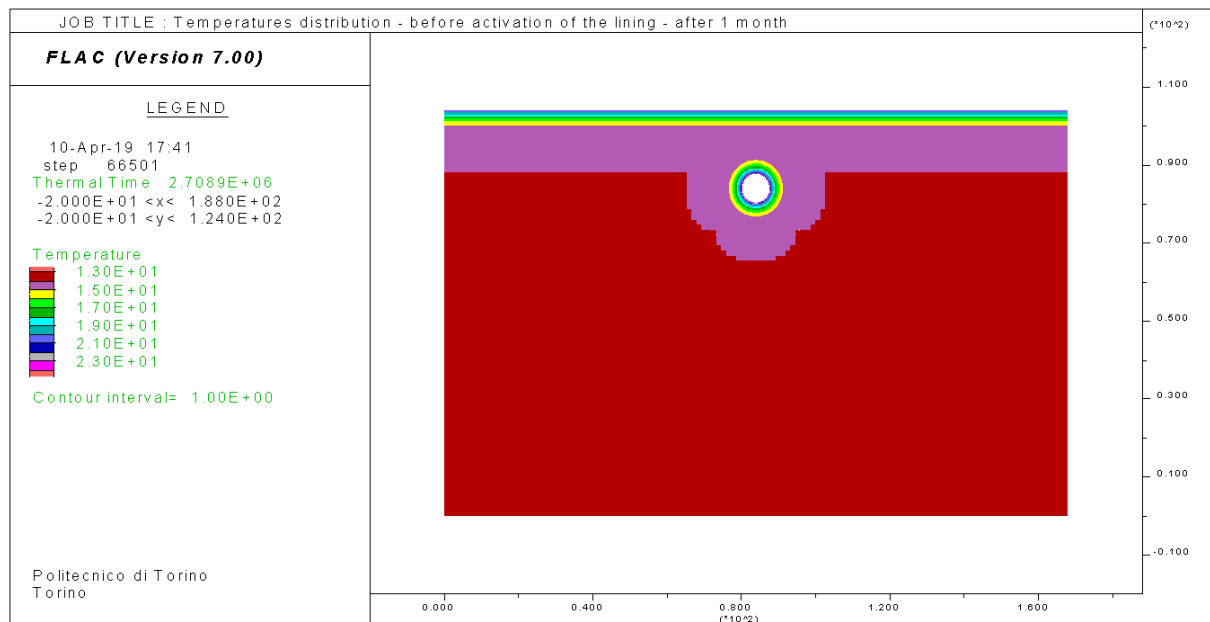


Figure 4.64. Summer conditions CSI - 1 month of simulation - before the activation of the lining

## Numerical assessment of the role of thermal parameters

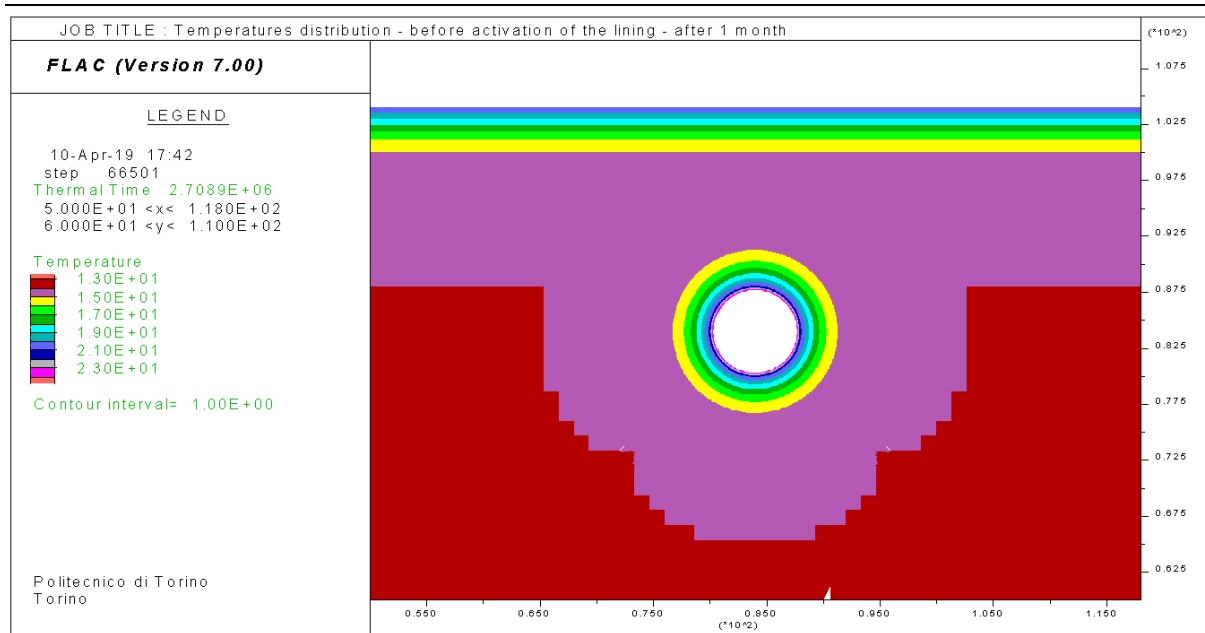


Figure 4.65. Summer conditions CSI - 1 month of simulation - before the activation of the lining - detail

### Second month: activation of the pipes

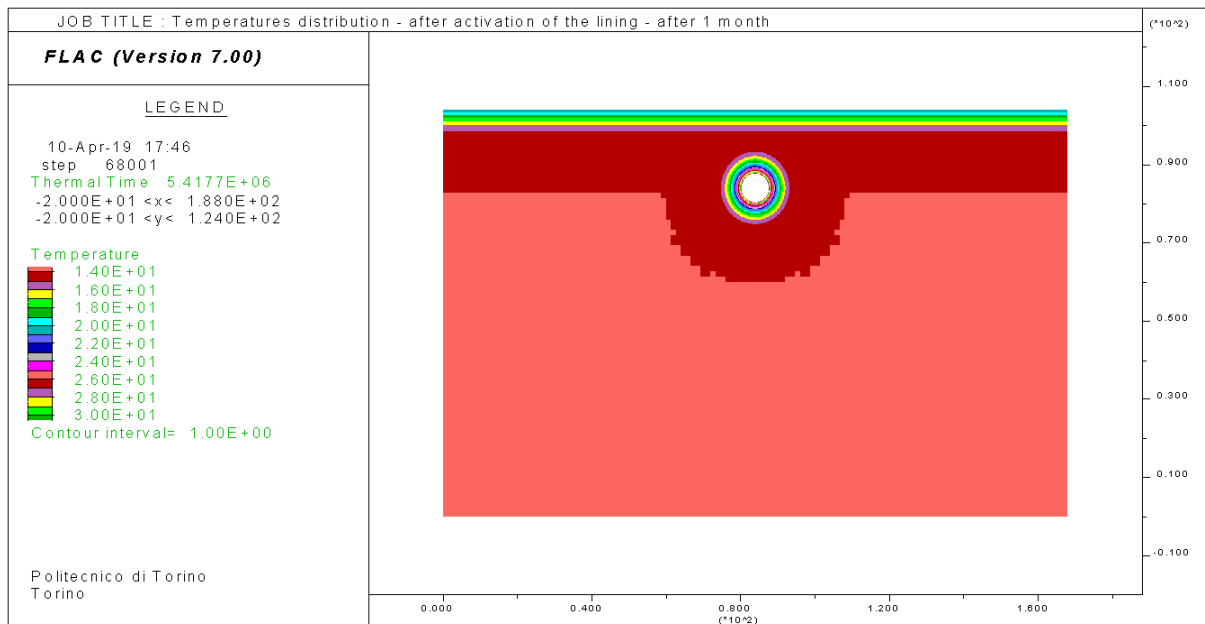


Figure 4.66. Summer conditions CSI - 1 month of simulation - after the activation of the lining

## Numerical assessment of the role of thermal parameters

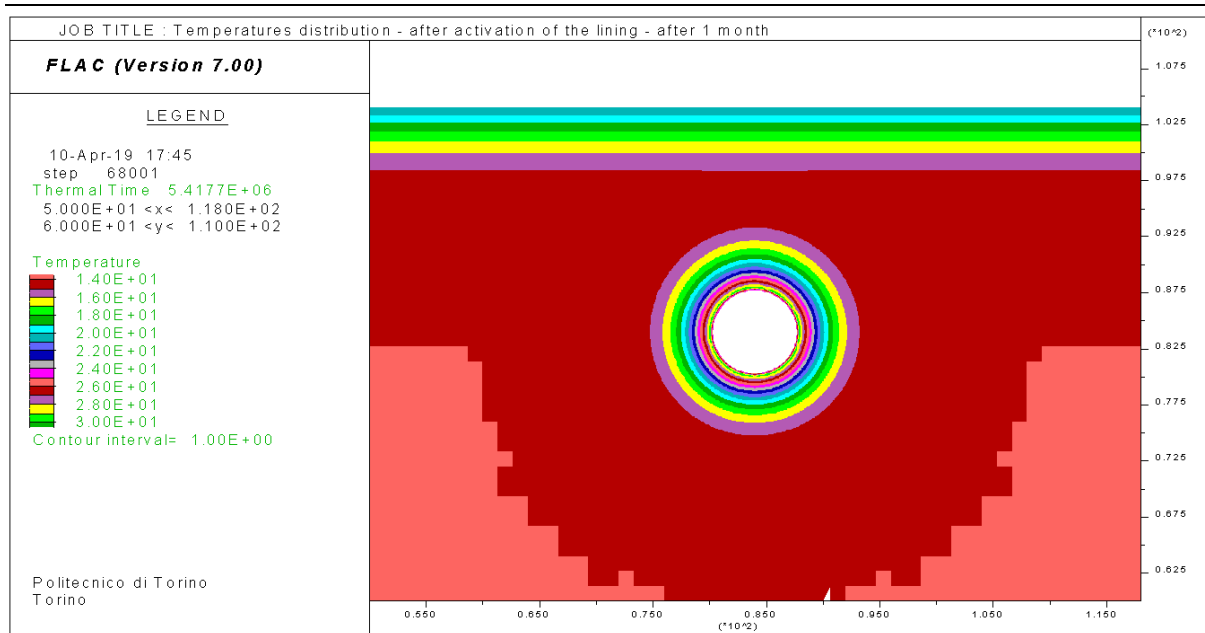


Figure 4.67. Summer conditions CSI - 1 month of simulation - after the activation of the lining - detail

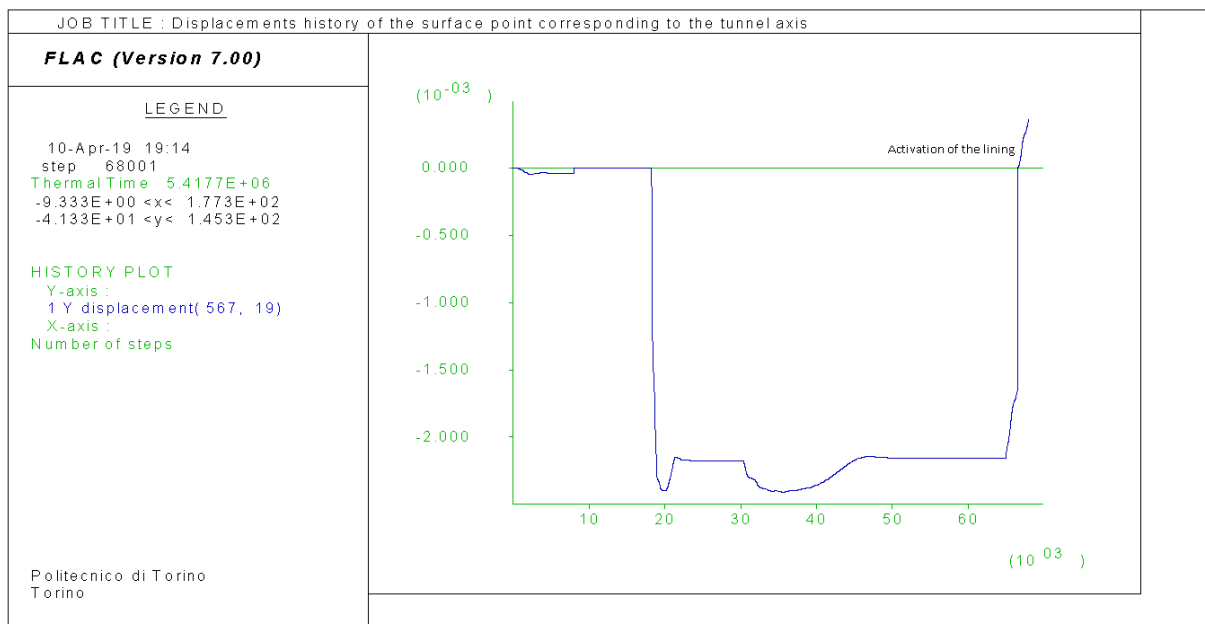


Figure 4.68. Displacements history of the surface point corresponding to the tunnel axis – Summer CSI

The temperature distributions are now very consistent with the considerations made in the first chapter. Surface settlements too went through a significant modification, as shown in the *Figure* below. The maximum values are now in the range between -0.4075 mm (winter) and 0.3607 mm (summer).

## Numerical assessment of the role of thermal parameters

Table 4.20. Comparison of surface settlements in  $x=0$  - 70+ years vs. 1 month of activation

|        | Surface settlements ( $x=0$ ) [mm] |         |            |
|--------|------------------------------------|---------|------------|
|        | 70+ years                          | 1 month | Reduction  |
| Winter | -3,07                              | -0,4075 | <b>87%</b> |
| Summer | 2,27                               | 0,3607  | <b>84%</b> |

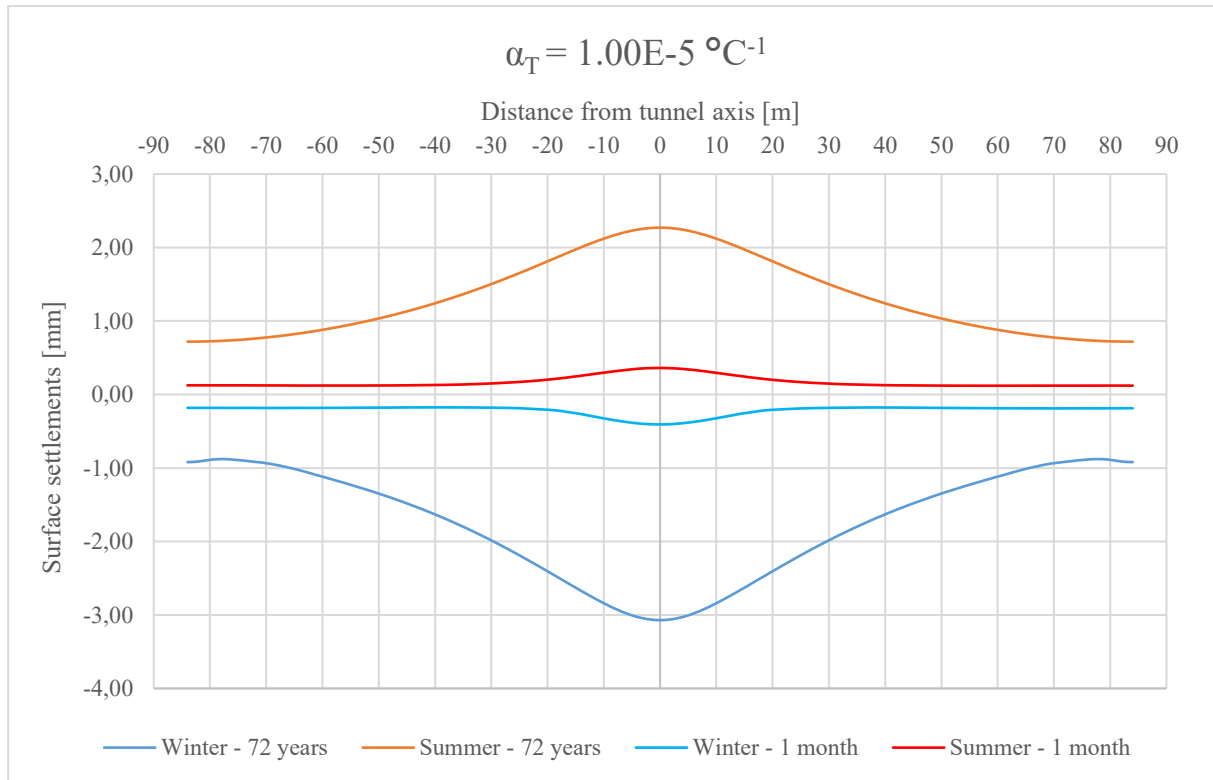


Figure 4.69. Surface settlements - comparison between 1 month of activation vs. 70+ years of activation

Results related to 70+ years of activation could be regarded as *limit* values, related to situations where temperatures do not vary during the years; while results related to 1 month of activation can be considered as a starting point to go deeper in the investigation of this behaviour, for example, running a similar parametric analysis in view of all the above-mentioned considerations.



### 5 CONCLUSIONS

Parameters assessing represents one of the most important steps when designing an energy tunnel. Input parameters play a major role in the process and their investigation is central. With a parametric analysis it has been possible to state how the behaviour changes when parameters vary.

In the first part of the work an introduction on geothermal energy and its traditional exploitation was presented, introducing the concept of “energy geostructure” and its intrinsic sustainability. The work mainly focused on the energy tunnels, which were deepened in the third chapter, describing the design process aspects.

The whole thesis focuses on the input parameters, geotechnical and thermal: they are described, paying attention to the investigation methods used to determine them. The idea is that when dealing with a structure of huge dimensions and very few implementations as an energy tunnel, there is still lack of a standard procedure in planning the investigations. A quick voyage on the traditional investigation methods, for the geotechnical parameters, and on the new tests, THM tests or for thermal parameters, was took.

A brief discussion on the future of the in situ thermal investigation has been presented, focusing on the need of having a fast, simple and cheap way to test the thermal properties of

## Conclusions

---

soils for structures with a large extent. The TCT was proposed, a device that, compared with the TRT, reduces a lot the duration of the investigation, with economic benefits. The TCT is born based on the idea that the cone of the CPT, in the past, has been equipped with a lot of different devices, in order to obtain specific characteristics and parameters, i.e. seismic waves sensors. A thermocouple is attached to the CPT device to measure the temperature at the contact between the rod and the surrounding soil. The penetration of the device in the ground produces heat, which dissipates with time and the measured dissipation is used to determine the thermal parameters of the soil (conductivity, diffusivity, etc.) over the test interval, using proper empirical curves.

Referring to the tunnel design procedure, the intention was to highlight the parameters playing an important role in each step of the design. To sum up, the design, the behaviour and the construction of the structure of the tunnel is function of the site conditions, the strength parameters, the coefficient of earth pressure at rest, the permeability, the ground water level and the percentage of clay. The deformability parameters control the behaviour of the surrounding ground, in terms of amount of deformations, strain state and consequently of surface settlements that take place after the excavation of the tunnel. The soil-structure interaction behaviour is influenced by the Young's Modulus. The most influencing factors on the energy tunnel efficiency are the presence and velocity of the groundwater flow, the ground temperature and the thermal conductivity of soil. Dealing with the structural design of the lining, in particular the TM aspects, there is still a lack of information about the TM interface behaviour. Some results from a model (Barla, Di Donna, 2018) were presented but with reference to very specific initial conditions, there could be differences when the types of soil or interface between the soil and the lining change.

In this scenario, with the aim of adding some of the missing information of the TM behaviour of a thermo-activated tunnel, a parametric analysis with FLAC was run. The final scope was to understand how the surface settlements could be influenced when the temperatures of the system and the coefficient of linear thermal expansion vary. At the beginning, no big results were expected, anyway it has been observed that something happened. The first analyses showed up a not negligible influence of the thermal activation of the lining on the surface settlements. The values of the point on the surface corresponding to the tunnel axis were similar to the ones that occur when the excavation process was run. This aspect raised many doubts on the results and there was the necessity to make an analysis on the model

## Conclusions

---

construction sequence and the adopted simplifications. Since many of them were made, the results are representative of a very general condition. More realistic simulations could be run, for example assuming the real stratigraphy of the ground, considering the presence of the groundwater, or using a more sophisticated constitutive model. Another option could be running a 3D analysis, since the surface settlements is a phenomenon that is influenced also by the distance of the excavation front from the studied section, more accurate results could be found.

Also, the imposition of the temperature conditions could have been more accurate and realistic, in the first model, for example, on the lateral boundaries no conditions were imposed, but only after many computational steps a gradient of temperatures was observed. From this perspective, a second analysis was run, with an improvement related to the temperature boundary conditions. The obtained outcomes have a little variation with respect to the first ones.

Another aspect related to the temperature conditions is that in the models only fixed temperatures were imposed, without taking in consideration that they cyclically vary during the year. This brought to results at equilibrium, but the equilibrium was reached with a computational time of more than 70 years, not realistic condition. For this reason, another analysis was performed and stopped after one month of activation, a relatively realistic situation for this type of geostructure: surface settlements went through a reduction of more than 80%, with maximum values in the order of less than 0.5 mm. These outcomes can be considered as a starting point to go deeper in the investigation of this behaviour.

To conclude, the outcomes of the thesis suggest including the assessment of the linear thermal expansion coefficient, when the investigation plan is designed. First analyses show its influence on long-term results. In the future, if the assessment on several types of soil will be performed, a detailed database could be built, since in literature most rock information is available.

## Conclusions

---

## ***Acknowledgements***

*It just does not seem real. It cannot be real. After many years passed daydreaming about this achievement, it is finally time to live it and, above all, share it, with the most important people of my life. Like any other long-awaited moment, also this one, in no time, will become a joyful and dense with satisfaction memory. In any case, I'd like to try, with some emotion, to retrace the past years and to express my gratitude to all the people, who were essential to reach this destination. Or to reach the new life that is waiting for me.*

*I would like to thank my supervisors Prof. Ing. Marco Barla and Ing. Alessandra Insana from Politecnico di Torino and my external supervisor Ing. Iulia Prodan, from Technical University of Cluj-Napoca. They offered me the great opportunity to work on this project for two months in Cluj-Napoca (Romania), which was an unexpected experience. I had the chance to take part to the "C65 International Conference", which took place in Cluj-Napoca to celebrate the 65 years of higher education in Civil Engineering in Transilvania. The participation to the conference gave me the opportunity to meet many personalities working in the civil engineering field, above all Professor Heinz Brandl, a distinguished personality of the international scientific community in the field of Geotechnics.*

*The most precious words of thanks are for my Family, for its support and presence in the brightest but especially the darkest moments of this journey. Every time I intended to give up, someone was there to remind me I could reach my objectives. Every time I had to take difficult choices, which included great distances and absences, I always felt supported and understood. Every time a challenge showed up, I found someone ready to bet I would get over it. Few words cannot explain how big my gratitude and love are.*

*Special thanks to the world of Villa San Giuseppe, which welcomed me for almost five years. Fratelli and Villici, you have been essential, leaving to me so many great lessons that I will always bring in my heart and memories that will never stop to give rise to strong emotions and a bit of melancholy.*

*I would like to thank also my colleagues, Manu, Marco, Caros, Nicolas, Jacopo, Albi e Albi, in the past years we've shared joy and sorrow of this dark Politecnico world, but positivity never left us alone and now we can finally see the light at the end of the tunnel.*

*Thanks to all the people I met in Cluj, Nina and Lia, my personal guides, friends far from home and gossip girls; Razvan and Bianca, the nature-lovers that made me discover the beautiful Romanian woods and all the others that helped me feel at home.*

*Andre, Giuli, Lidia and Alessandro: I can't remember exactly when this unbreakable bond was born, maybe when you were eating carrots sitting on the stairs in Casapрати and I was hiding behind my aunt's trousers, but I perfectly remember all the summer times we lived as brothers and sisters. This is one of the reasons why I never wanted to grow up.*

*Cori, irreplaceable Cori, my remote support and best confidant, you are unique. Eri, from the crib until today: we are crossing different roads with destinations that are far away from each other, however, we always stay close. Sweet Giuli, laughing with you is one of the things I prefer. Lisa, Stefi and little Teresa, we are linked by something so strong that makes us share every important moment of our life, we cannot do without each other. Lu, Cinci and Debbi, we are living all over the North of Italy, however, whenever we are together, it is home.*

*In the end, during this journey, there have been some lucky days, but one, in particular, made me meet the greatest joy of my life. To Stefano, a million times thank you, for your constant patience, care and love.*

## **Ringraziamenti**

*Non mi sembra vero. Non può essere vero. Dopo anni passati a sognare questo traguardo, è finalmente giunto il momento di viverlo e soprattutto dividerlo, con le persone più importanti della mia vita. Come ogni istante tanto atteso, anche questo, in un lampo, resterà un ricordo, sicuramente di gioia e denso di soddisfazione. In ogni caso, vorrei provare, con non poca emozione, a ripercorrere gli ultimi anni e a esprimere la mia gratitudine verso tutti coloro che sono stati fondamentali nel raggiungimento di questa meta. O del nuovo inizio che mi aspetta.*

*Vorrei rivolgere i miei sentiti ringraziamenti ai Relatori Prof. Ing. Marco Barla e all'Ing. Alessandra Insana, del Politecnico di Torino, oltre che all'Ing. Iulia Prodan, che ha supervisionato il mio lavoro durante la mia permanenza presso l'Università Tecnica di Cluj-Napoca. La grande opportunità che mi è stata offerta di lavorare su questo progetto per due mesi a Cluj-Napoca (Romania) è stata un'inaspettata esperienza del mio percorso formativo che ricorderò piacevolmente e a lungo. Ho avuto la possibilità di partecipare alla "C65 International Conference", svoltasi per celebrare i 65 anni della facoltà di ingegneria civile in Transilvania. La partecipazione a un evento di questo calibro mi ha permesso di incontrare, per la prima volta al di fuori del contesto universitario in cui sono cresciuta, grandi personalità del mondo dell'ingegneria civile con cui altrimenti non avrei avuto modo di entrare in contatto, in particolare il Professore Heinz Brandl, una distinta personalità della comunità scientifica internazionale nel campo della geotecnica.*

*I ringraziamenti più preziosi li rivolgo alla mia Famiglia, per il supporto e la presenza nei momenti di gioia ma soprattutto in quelli più bui di questo percorso. Ogni volta che ho pensato di rinunciare, c'era sempre qualcuno pronto a ricordarmi che avrei potuto raggiungere i miei obiettivi. Ogni volta che ho dovuto prendere scelte difficili, che comprendevano grandi distanze e lunghe assenze, mi sono sempre sentita supportata e compresa. Ogni volta che una sfida mi si poneva davanti, ho trovato qualcuno con cui scommettere che l'avrei superata. Poche parole non possono esprimere quanto la mia gratitudine e il mio amore nei vostri confronti sia incommensurabile.*

*Un ringraziamento speciale al mondo di Villa San Giuseppe, che mi ha accolto per quasi cinque anni. Fratelli e Villici siete stati fondamentali: mi avete lasciato insegnamenti*

*che mi porterò nel cuore per sempre e ricordi che non smetteranno mai di suscitarmi forti emozioni e un po' di malinconia.*

*Vorrei ringraziare anche i miei colleghi, Manu, Marco, Caros, Nicolas, Jacopo, Albi e Albi, negli ultimi anni abbiamo condiviso gioie e dolori di questo oscuro mondo che è il Politecnico, ma "sempre positivi!" siamo finalmente arrivati a vedere la luce in fondo al tunnel.*

*Grazie a tutte le persone conosciute a Cluj, Nina e Lia, le mie guide personali, amiche lontano da casa e "gossip girls"; Razvan e Bianca, gli amanti della natura che mi hanno fatto scoprire le bellezze dei boschi della Romania e a tutti coloro che mi hanno aiutato a sentirmi a casa.*

*Andre, Giuli, Lidia e Alessandro: non riesco a ricordare con precisione quando è iniziato questo legame indissolubile, forse mentre mangiavate carote per merenda a Casapratì e io mi nascondevo dietro ai pantaloni della zia, ma ricordo perfettamente tutte le estati passate a vivere e rincorrerci come fratelli ed è uno dei motivi che mi fa dire con ancora più convinzione "non voglio diventare grande".*

*Cori, insostituibile Cori, Amica di sempre, il mio supporto a distanza e presenza costante, sei unica. Eri, chi lo avrebbe mai detto, dalla culla ad oggi, la vita ci ha costruito strade diverse che portano in posti tra loro lontani, ma noi, comunque, non ci allontaniamo mai. Dolce Giuli, ridere insieme a te è da sempre una delle cose che preferisco. Lisa, Stefi e piccola Teresa, siamo legate da qualcosa di così forte che ci porta a condividere ogni momento importante della nostra vita, non potendo fare a meno l'una delle altre. Lu, Cinci e Debbi, siamo sparse tra le province del Nord Italia eppure, quando siamo insieme, è casa.*

*Per concludere, durante questo percorso, ci sono stati alcuni momenti in cui mi sono un po' sentita "baciata dalla fortuna", ma uno in particolare mi ha fatto conoscere la mia gioia più grande. A Stefano, un milione di volte grazie, per la tua costante pazienza, le tue attenzioni e il tuo amore.*

## REFERENCES

- Adam, D., Markiewicz, R., *Energy from earth-coupled structures, foundations, tunnels and sewers*, Geotechnique, Volume 59 (3), 2009.
- Akrouch, G. A., et al., *Thermal Cone Test to Determine Soil Thermal Properties*, Journal of Geotechnical and Geoenvironmental Engineering, Volume 142(3), 2016.
- Balasubramanian, A., *Geotechnical investigation for tunnelling*, Technical report, 2016.
- Baldi, G., Hueckel, T., Pellegrini R., *Thermal volume change of the mineral-water system in low-porosity clay soils*. Can. Geot. J., 25, 807-825, 1988.
- Banks, D., *An Introduction to Thermogeology: Ground Source Heating and Cooling*, John Wiley & Sons, 2012.
- Barpi, F., Barbero, M., Peila, D., *Numerical modelling of ground-tunnel support interaction using bedded-beam-spring model with fuzzy parameters*, 2011.
- Barla, M., *Elementi di Meccanica e Ingegneria delle Rocce*, Celid, 2011.
- Barla, M., Di Donna, A., Insana, A., *Energy Tunnel Experimental Site in Turin Metro*, 15th IACMAG, Wuhan, China, 2017.
- Barla, M., Di Donna, A., Perino, A., *Application of energy tunnels to an urban environment*, Geothermics, Volume 61, 2016.
- Barla, M., Di Donna, A., *Energy tunnels: concept and design aspects*, Underground Space 2018.
- Barla, M., Insana A., *Energy Tunnel Segmental Lining: an Experimental Site in Turin Metro*, WTC Dubai, 2018.
- Barla, M., Perino, A., *Energy from geo-structures: a topic of growing interest*. Environmental Geotechnics 2(1): 3-7, 2014.
- Bertolini, L., *Materiali da costruzione-Volume I-Struttura, Proprietà e Tecnologie di Produzione* – Seconda edizione. CittàStudi edizioni, 2010.
- Bodas Freitas, T. M., Cruz Silva, F., and Bourne-Webb, P. J., *The response of energy foundations under thermo-mechanical loading*, Proceedings of the 18<sup>th</sup> International

- Conference on Soil Mechanics and Geotechnical Engineering, Paris, Conference paper, 2013.
- Bourne-Webb, P., Burlon, S., Javed, S., Kürten, S., Loveridge, F., *Analysis and design methods for energy geostructures*, Renewable and Sustainable Energy Reviews, Volume 65, 2016.
- Brandl, H., *Energy foundations and other thermo-active ground structures*, Géotechnique, Vol. 56, No. 2, 2006.
- Brandl, H., *Geothermal Geotechnics for Urban Undergrounds*, 15th International scientific conference “Underground Urbanisation as a Prerequisite for Sustainable Development”, Procedia Engineering (165), 2016.
- Burkhard, S., *Shallow geothermal energy*, International summer school on direct application of geothermal energy, 2003.
- Campanella, R. G., Mitchell, J. K., *Influence of temperature variations on soil behavior*. ASCE J. Soil Mech. and Fdtn. Div., ASCE, 94, 709-734, 1968.
- Chakeri, H., Unver, B., *A new equation for estimating the maximum surface settlement above tunnels excavated in soft ground*, Environmental Earth Sciences, 2013.
- Cekerevac, C., *Thermal Effects on the Mechanical Behaviour of Saturated Clays: An Experimental and Constitutive Study*. Ph.D. Thesis, École Polytechnique Federal de Lausanne, Lausanne, Switzerland, 2003.
- Cekerevac, C., Laloui, L., *Experimental study of thermal effects on the mechanical behaviour of a clay*. Int. J. Numer. Anal. Meth. Geom. 28, 209–228, 2004.
- Church, R., *At-rest Earth Pressure Relationships*, Theoretical Geomechanics Winter Quarter, 2003
- Cianci, S., Garbin, F. et al., *La caratterizzazione geotecnica mediante prove di laboratorio*, Professione geologo.
- Coletti, A., Sterpi, D., *Structural and geotechnical effects of thermal loads in energy walls*, Procedia Engineering, Volume 158, 2016.
- Di Donna, A., Barla, M., *Il ruolo delle condizioni geotecniche sull’efficienza delle gallerie energetiche*, IARG Cagliari, 2015.

- Di Donna, A., Ferrari, A., Laloui, L., *Experimental investigations of the soil–concrete interface: physical mechanisms, cyclic mobilization, and behaviour at different temperatures*, NRC Research Press, 2015.
- Dickson, M. H., & Fanelli, M., *Cos'è l'energia geotermica?*, Pisa, 2004.
- Duretto, A., *Progettazione strutturale delle gallerie energetiche*, Tesi di Laurea Magistrale, Politecnico di Torino, 2018.
- Fabozzi, S., *Behaviour of segmental tunnel lining under static and dynamic loads*, Doctoral Thesis, University of Naples Federico II, 2017.
- FLAC – Fast Lagrangian Analysis of Continua, Online Manual, version 7.0.
- François, B., Laloui, L., *An Oedometer for Studying Combined Effects of Temperature and Suction on Soils*, Geotechnical Testing Journal, 2010.
- Frodl, S., Franzius, J.N., Bartl, T., *Design and construction of the tunnel geothermal system in Jenbach*, Geomechanics and Tunnelling, Volume 3, 2010.
- Guglielminetti, V., Grasso, P., Mahtab A., Xu, S., *Mechanized Tunneling in Urban Areas: Design methodology and construction control*, Taylor & Francis Group, 2008.
- Hähnlein, S., Bayer, P., Ferguson, G., Blum, P., *Sustainability and policy for the thermal use of shallow geothermal energy*, Energy Policy, Volume 59, 2013.
- Kova Ceci, C. et al., *Possibilities of underground engineering for the use of shallow geothermal energy*, Scientific Figure on ResearchGate, 2013.
- Langmaack, L., Feng, Q., *Soil Conditioning for EPB Machines: Balance of Functional and Ecological Properties*, 2005
- Laloui, L., Di Donna, A., *Energy geostructures. Innovation in Underground Engineering*, John Wiley & Sons, 2013.
- Laloui, L. et al., *Issues involved with thermoactive geotechnical systems: characterization of thermomechanical soil behavior and soil-structure interface behavior*, DFI Journal - The Journal of the Deep Foundations, 2014.
- Lines, S., Williams, D. J., Galindo-Torres, S., *Determination of Thermal Conductivity of Soil Using Standard Cone Penetration Test*, 2<sup>nd</sup> International Conference on Advanced on Clean Energy Research, ICACER, 2017.

- Martin, J.R., Abdelaziz, S.L., Olgun, C.G., *Renewable energy applications using thermo-active deep foundations*, International Scientific Conference, 2010.
- Manzella, A., *Geothermal energy*, EPJ Web of Conferences, Volume 148 00012, 2017.
- Moldovan, A. R., *Considerații privind influența structurilor subterane asupra terenului înconjurător (Considerations regarding the influence of underground structures on the surrounding soil)*, UTCN, 2013.
- Nicholson, D.P. et al., *The design of thermal tunnel energy segments for Crossrail, UK*, Engineering Sustainability, Volume 167, 2014.
- Norme Tecniche per le Costruzioni 2018, NTC2018, D.M. 17/01/2018.
- Olgun et al., *Long-term performance of heat exchanger piles*, Scientific Figure on ResearchGate, 2015.
- Oreste, P., *The Convergence-Confinement Method: Roles and Limits in Modern Geomechanical Tunnel Design*, American Journal of Applied Science 6, 2009.
- Pahud, D., Hubbuch, M., *Measured thermal performances of the energy pile system of the Dock midfield at Zurich Airport*, Proceedings of European Geothermal Congress, Unterhaching, Germany, 2007, pp.1-7.
- Panet, M., Guenot, A., *Analysis of convergence behind the face of a tunnel*, Tunnelling 82 (Brighton, 1982), The Institution of Mining and Metallurgy, London, 1982.
- Parker, H. W., *Planning and site investigation in tunnelling*, 1º Congresso Brasileiro de Túneis e Estruturas Subterrâneas Seminário Internacional South American Tunnelling, 2004.
- Piemontese M., *Sensitivity analysis on the geothermal potential of energy walls*, Tesi di Laurea, Politecnico di Torino, Italy, 2018.
- Raines, G., *Geotechnical Site Investigations For Tunnelling*, Breakthroughs in Tunnelling, 2016.
- Santamarina, J.C., Park, J., *Geophysical properties of soils*, Australian Geomechanics Society, 2016.
- Schlosser, T., et al., *Potenzial der Tunnelbaustrecke des Bahnprojektes Stuttgart 21 zur Wärme- und Kältenutzung*, 2007.

- Schwartz, C. W., Einstein, H. H., *Improved design of tunnel supports: volume 1 – simplified analysis for ground-structure interaction in tunnelling*, MIT, 1980.
- Suryatriyastuti, M.E., Mroueha, H., Burlon, S., *Understanding the temperature-induced mechanical behaviour of energy pile foundations*, Renewable and Sustainable Energy Reviews, 2012.
- Vardon, P. J., Baltoukas, D., Peuchen, *Interpreting and validating the thermal cone penetration test (T-CPT)*, Géotechnique, 2017.
- Vardon, P. J., Baltoukas, D., Peuchen, *Thermal Cone Penetration Test (T-CPT)*, Delft University of Technology (Netherlands), 2018.
- Vieira, A., Prodan, I., et al., *Characterisation of ground thermal and Thermo-Mechanical behaviour for shallow geothermal energy applications*, Energies, 2017.
- Zacco F., *Sfruttamento geotermico della galleria della Linea 2 della metropolitana di Torino*, Tesi di Laurea Magistrale, Politecnico di Torino, Italy (in Italian), 2017.
- Zhang, G., et al., *A new model and analytical solution for the heat conduction of tunnel lining ground heat exchangers*, Cold Regions Science and Technology, Volume 88, 2013.